# Investigating fungal cellular processes involved in early colonisation of wheat by *Zymoseptoria tritici*

**Harry Child**


Submitted by Harry Child to the University of Exeter
as a thesis for the degree of
Doctor of Philosophy in Biological Sciences in March 2021



I certify that all material in this thesis which is not my own work has been identified and that no material has previously been submitted and approved for the award of a degree by this or any other University.

Signature: 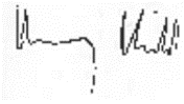

## Thesis Abstract

The fungal pathogen *Zymoseptoria tritici* causes the most economically important disease of wheat in Europe. Despite recent advances in our understanding of its molecular host-pathogen interaction, fundamental questions remain about the cellular processes underlying plant colonisation by this fungus. The work presented in this thesis uses both reverse and forward genetic techniques to further understand the molecular determinants of *Z. tritici* virulence. To address questions about the source of nutrients utilised by *Z. tritici* to support symptomless colonisation of the leaf, this thesis explores cellular pathways utilised by other plant pathogenic fungi to access stored macromolecules. While autophagy is crucial for the infection-related development of many fungal plant pathogens, this study reveals that autophagy is dispensable for *Z. tritici* pathogenicity, and points towards a potential autophagy-independent function of *ZtATG8* in virulence. The mitochondrial fatty acid β-oxidation pathway was however found to support the switch to hyphal growth on the leaf surface, providing strong evidence that catabolism of stored lipids is required for early host invasion by *Z. tritici*.

Forward genetic investigation identified enzymes within the cell wall integrity (CWI) and cyclic adenosine monophosphate (cAMP) signalling pathways as playing a key role in *Z. tritici* virulence. *In planta* transcriptomic analysis revealed that the CWI pathway regulates the expression of infection-related secreted proteins, including the characterised LysM effectors required for host defence evasion, suggesting that *Z. tritici* may co-regulate virulence gene expression with the response to cell wall perturbation. Findings presented here also suggest that cAMP signalling regulates transcription during the switch to necrotrophic growth, providing insights into the elusive mechanisms controlling this infection cycle transition. Finally, genomic and transcriptomic analysis of a spontaneous *Z. tritici* mutant revealed the potential function of the light responsive transcription factor white collar 1 in controlling *Z. tritici* morphological development and infection.

These novel findings advance our understanding of the cellular pathways contributing to *Z. tritici* infection and inform the development of future strategies to control this devastating pathogen.

## Table of Contents

## List of Figures

## List of Tables

## List of Accompanying Material

Table S5.1 Differentially expressed *Z. tritici* genes during infection by *Δztbck1* and *Δztcyr1* compared to IPO323 at 6 and 9 dpi, and between the time points for each strain (Supplementary Excel file)

Table S5.2 Differentially expressed wheat genes during infection by *Δztbck1* and *Δztcyr1* compared to IPO323 at 9 dpi, and between 6 and 9 dpi for each strain (Supplementary Excel file)

Table S6.2 Results of RNA sequencing differential expression analysis between IPO323 and IPO323_SSV (Supplementary Excel file)

Supplementary data files can be found at https://doi.org/10.24378/exe.3505

# Abbreviations

| | |
|---|---|
| % | Percentage |
| ANOVA | Analysis of variance |
| bp | Base pairs |
| cDNA | Complementary DNA |
| chr | chromosome |
| d | Day(s) |
| DNA | Deoxyribonucleic acid |
| dpi | Days post infection |
| g | Grams |
| GFP | Green fluorescent protein |
| h | Hour(s) |
| kb | Kilobase pairs |
| kDa | Kilodaltons |
| L | Litre |
| M | Molar |
| Mb | Megabase |
| mg | Milligram |
| min | Minute(s) |
| ml | Millilitre |
| mm | Millimetre |
| mM | Millimolar |
| mRNA | Messenger RNA |
| ng | Nanogram |
| nm | Nanometre |
| nM | Nanomolar |
| $^{o}C$ | Degree Celsius |
| $OD_{600}$ | Optical density at 600 nm measured by spectrophotometry |
| PCR | Polymerase chain reaction |
| R | A free software environment for statistical computing and graphics |
| RNA | Ribonucleic acid |

RNase Ribonuclease

rpm Revolutions per minute

rRNA Ribosomal RNA

SE Standard error

T-DNA Transfer DNA transferred to the host from the tumor-inducing plasmid of *Agrobacterium tumefaciens*

UV Ultra-violet radiation

v/v Volume/volume ratio

w/v Weight/volume ratio

x G Times gravity

µg Microgram

µL Microlitre

µm Micrometre

µM Micromolar

# Acknowledgments

This work was funded by the BBSRC through the SWBio Doctoral Training Partnership.

Firstly I need to thank Ken Haynes, to whom I am grateful for the opportunity to carry out this exciting research. Despite his passing early during my PhD, I hope he would be proud of what I have achieved with this project that he conceived. Equally, I would like to thank Steven Bates for taking the reins in Ken's absence. I am sure you did not expect to contribute so much to my degree at the start, but your continued support, advice and encouragement has been greatly appreciated. I also thank Jason Rudd for his guidance, not only during my time at Rothamsted, but throughout my PhD. He also must hold the record for fastest reading of a thesis chapter first draft, having received it at 9.12pm and returned it with helpful comments at 8.14am the next morning. Meetings with Steve and Jason have always provided me with confidence in myself and my work, and I am glad to say I have always left happier than when I went in.

Thank you to Mike Deeks for stepping in as my supervisor after Ken's passing, and for his ideas and advice, especially with microscopy.

Many thanks to members of the Haynes group for their support, including Graham Thomas, Yogesh Chaudhari, Jane Usher and Nicolas Helmstetter. Special thanks go to Graham and Nico for their friendship and entertainment along with the help and advice they kindly provided in the lab.

Thank you to all the technical staff who have helped over the years in the 3rd Floor and Mezzanine labs, particularly Sheera Abdulla, Nicola Wood, Dagmara Kolak, Keith Ansell, Chris Milne and Rich Webb. I would also like to thank Karen Moore, Paul O'Neill and Audrey Farbos from the Exeter Sequencing service, as well as Ryan Ames and Stuart Cannon, for their help and advice with sequencing and bioinformatics analysis.

I have made many great friends during my PhD who I thank for their support, both in and out of work. Particular thanks to Guy, Roland, Jahcub, Tom, Josh, Cam, Hazel and Georgie for the countless entertaining coffee breaks.

Finally, I would like to thank my family for their emotional and financial support over the years, and my wonderful partner Harriet, who has been by my side and kept me smiling.

# Chapter 1
# **General Introduction**

## 1.1 Fungal plant pathogens: a threat to modern agriculture

Pests and pathogens pose a major threat to global agriculture, causing estimated losses of 20-30% in the world's major food crops (Oerke, 2006; Savary et al., 2019). Fungal diseases contribute significantly to this devastation, causing crop yield reductions and contamination of food products with harmful mycotoxins (Dean et al., 2012; Fisher et al., 2012). The threat from existing and emerging fungal plant pathogens is ever increasing with the impacts of climate change, modern agricultural practices and the global food system (Bebber et al., 2013; Fisher et al., 2012; McDonald & Stukenbrock, 2016). Increasing global temperatures as a result of anthropogenic climate change are predicted to enable the spread of fungal plant pathogens poleward (Bebber et al., 2013). Indeed, it has been reported that changing climatic conditions in the UK could facilitate the spread of stem rust caused by *Puccinia graminis f. sp. tritici*, which has recently re-emerged in Europe (Lewis et al., 2018). This is compounded by the spread of plant pathogens to new regions facilitated by global distribution of crops and plant material, such as the recent spread of the devastating wheat blast pathogen *Magnaporthe oryzae Triticum* to Bangladesh from South America in 2016 (Islam et al., 2019). The planting of genetically uniform crops, which has increased since the Green Revolution (van de Wouw et al., 2009), can also increase susceptibility to disease epidemics (McDonald & Stukenbrock, 2016). For example, this has enabled the spread of *Fusarium oxysporum f. sp. cubense* tropical race 4 (TR4) in populations of the globally cultivated Cavendish banana cultivar (Dita et al., 2018), which comprises 99% of the world's exported bananas (Scheerer et al., 2018). This genetic uniformity is often accompanied by higher planting densities, facilitating disease transmission, driving increases in pathogen populations and enhancing competition, all of which drives the evolution of increased virulence (McDonald & Stukenbrock, 2016).

Considering current projections for the global population to reach 9.7 billion by 2050 (United Nations, 2019), and the estimated 60% increase in global food production required to feed this burgeoning population (Alexandratos & Bruinsma, 2012), mitigating the impacts of fungal crop diseases is key to the maintenance of global food security. This is particularly relevant considering the evidence that yield losses due to crop diseases and the impact of disease

epidemics on the food system are most detrimental to developing countries (Godfray et al., 2016; Savary et al., 2019).

Current control strategies rely heavily on fungicide inputs, with the estimated value of the global fungicide market ranging from $13.4-16 billion (statistica.com). Agricultural fungicide inputs are dominated by six main chemistries which inhibit ergosterol biosynthesis, microtubule assembly and mitochondrial processes, resistance to which has built up rapidly in major pathogens (Fisher et al., 2018). The sequential use of newly discovered active compounds and subsequent spread of resistance in pathogen populations has rendered many of these chemical inputs ineffective over time (Lucas et al., 2015). This represents an ever increasing threat, with slow development and registration of new active compounds, the increasingly strict regulation of chemical inputs by the European Union and concerns of fungicide resistance accumulating in human opportunistic pathogens in the environment (Fisher et al., 2018). Strategies for prolonging the efficacy of fungicides are currently focused on effective tracking of resistance emergence (R4P Network, 2016), tailoring seasonal fungicide application depending on disease pressure (Jørgensen et al., 2017), and the combination of active compounds to increase the heterogeneity of selection (Bourguet et al., 2013).

Similarly, the vulnerability of resistant crop varieties to pathogen evolution is evident from recent emerging fungal pathogens. For example, after successful breeding for resistance to *P. graminis f. sp. tritici* during the Green Revolution (Ellis et al., 2014), the majority of global wheat cultivars have now been found to be susceptible to the recently emerged Ug99 strain (Singh et al., 2008), including 80% of the cultivars currently planted in the UK (Lewis et al., 2018). This threat is compounded by the time taken to breed new resistant varieties (Ashkani et al., 2015), as well as the constant trade-off between yield and disease resistance (Summers & Brown, 2013). Strategies for preserving the longevity of resistant crops in the face of pathogen evolution are based around increasing the heterogeneity of selection, through spatiotemporal deployment of different resistant varieties or pyramiding of resistance loci in crops (Bourguet et al., 2016). There is also interest in the increased durability provided by quantitative resistance loci, which exert reduced selection pressure on the

pathogen and require the co-evolution of multiple traits in the pathogen to be overcome (Pilet-Nayel et al., 2017).

Mounting an effective response to the threat of fungal plant diseases requires coordinated and collaborative efforts from the agricultural and scientific communities across the world. This has been exemplified by the recent formation of international research collaborations in response to recent emerging fungal diseases, such as the Borlaug Global Rust Initiative (Mcintosh & Pretorius, 2011) and Open Wheat Blast (http://openwheatblast.net/), promoting significant investment into research on epidemiology, genomics, crop breeding and agronomy related to fungal pathogens, as well as coordinating the economic and societal responses to these threats. Furthermore, these collaborations highlight the importance of fundamental research into the biology of these fungal pathogens to drive the development of effective control strategies (Konopka et al., 2019).

## 1.2 Plant pathogen infection strategies

### 1.2.1 The diversity of fungal-plant interactions

Fungal associations with plants are extremely diverse at an ecological level. These range from saprotrophs crucial for the degradation of senescent plant material, to mutually beneficial symbioses and devastating pathogens (Naranjo-Ortiz & Gabaldon, 2019). Fungal symbionts provide diverse benefits to their hosts, including the improved access to inorganic nutrients and water from the soil which characterise the interaction with root-associated mycorrhizal fungi (Brundrett, 2004), and the enhanced tolerance of abiotic stressors and resistance to attack by pathogens and herbivores provided by other endophytes (Rodriguez et al., 2009). At the opposite end of the spectrum, plant pathogens are commonly defined by their trophic interaction with the host, with biotrophs obtaining nutrients from living host tissue and necrotrophs killing the host and feeding on the resulting dead tissue (Rodriguez-Moreno et al., 2018). Other pathogens exhibit a combination of these lifestyles during infection, which have been termed hemibiotrophs. These pathogens display an initial infection phase resembling biotrophic invasion, before switching to necrotrophic colonisation of the host (Horbach et al., 2011). Despite this variety, all fungal associations with plants follow the same basic principle of gaining an advantage from their

interaction with the host, usually by accessing nutrients, without succumbing to the resistance mounted by the plant's defences.

Biotrophic interactions with plant hosts offer a lucrative niche for fungi, with reliable access to nutrients and reduced competition than that observed between saprotrophic microorganisms in the soil (Spanu & Panstruga, 2017). Biotrophic infection by fungi often involves development of specialised feeding structures, known as haustoria or intracellular invasive hyphae, by breaching the plant cell wall and forming intimate associations with invaginations of the host cell membrane (De Silva et al., 2017; Voegele & Mendgen, 2003). These are similar to the arbuscules developed by mycorrhizal fungi in the *Glomeromycota* (Parniske, 2000). Other biotrophic pathogens reside exclusively in the apoplast of the host, similar to endophytic fungi (Christensen et al., 2008; Joosten & De Wit, 1989). Nutrient acquisition in these interactions involves manipulation of host metabolism, induction of host nutrient efflux and subsequent uptake by the fungus (Chen et al., 2010; Kretschmer et al., 2017; Sutton et al., 2007; Voegele et al., 2001). Conversely, necrotrophic colonisation is supported by nutrients released from host cell lysis and tissue degradation, typically enabled through production of toxins and hydrolytic enzymes. Genomic analyses have revealed that necrotrophic and some hemibiotrophic pathogens have maintained many of the genes encoding plant cell wall degrading enzymes (PCWDEs) from their saprotrophic ancestors (Zhao et al., 2013). This allows them to acquire nutrients from degradation of host cell walls within dying tissue.

Discrete classification of fungal species based on trophic association and their impact on plant fitness may represent an oversimplification of pathogen lifestyles, which would be better viewed as a continuous spectrum (Rodriguez et al., 2009). Recent studies suggest that some fungal species generally accepted to be pathogens may display asymptomatic endophytic colonisation depending on host species, genotype and tissue-type (Lofgren et al., 2018; Shaw et al., 2016; Van Kan et al., 2014). For example, *Botrytis* species, which are typically considered as broad host range necrotrophic pathogens, have recently been identified to commonly undergo symptomless endophytic colonisation of host plants (Shaw et al., 2016). These studies suggest that our misconceptions of fungal-plant interactions may be caused by overrepresentation of studies into associations with artificially selected crop hosts (Van Kan et al., 2014). This

plasticity in fungal lifestyle has been recognised in mycorrhizal fungi for some time (Brundrett, 2004). Further understanding of these complex and flexible fungal-plant interactions will improve our ability to combat destructive pathogens, for example through elucidating what host and environmental conditions induce and reduce pathogenicity (Van Kan et al., 2014). For diseases of crops, this may involve studying the relationships of pathogens with wild relatives (Lofgren et al., 2018).

### 1.2.2 Barriers to infection: The plant defence system

The ability of plants to resist exploitation by microorganisms has evolved into multiple layers of defence, formed of both constitutive and inducible elements. The first effective barrier to plant colonisation by invading microbes is physical, consisting of the waxy cuticle located on the epidermis of above-ground tissues, and the cell wall which covers all plant cells (Malinovsky et al., 2014; Reina-Pinto & Yephremov, 2009). Although these surface polymers serve mechanical and protective functions, such as against desiccation and abiotic stressors, they invariably limit the access to nutrients by microorganisms through forming a physical barrier to penetration. Furthermore, there is increasing evidence that both the cell wall and cuticle are dynamic structures contributing to inducible plant defence, through roles in pathogen recognition and structural reinforcement during immune responses (Underwood, 2012; Ziv et al., 2018). Constitutive defence is also contributed to by antimicrobial compounds present in plant tissues regardless of pathogen presence, known as phytoanticipins (Soledade et al., 2015; VanEtten et al., 1994). These chemical defences are distinct from those produced upon recognition of microbial invasion, which are termed phytoalexins (Jeandet, 2015).

The inducible elements of the plant immune system are formed in response to recognition of molecular signals from invading microorganisms, which are elegantly summarised in the zig-zag model (Fig. 1.1; Jones & Dangl, 2006). The first layer of this model involves detection of molecules that are both essential and conserved in microbial classes, known as pathogen- or microbe-associated molecular patterns (PAMPs/MAMPs), by cell surface receptor-like proteins,

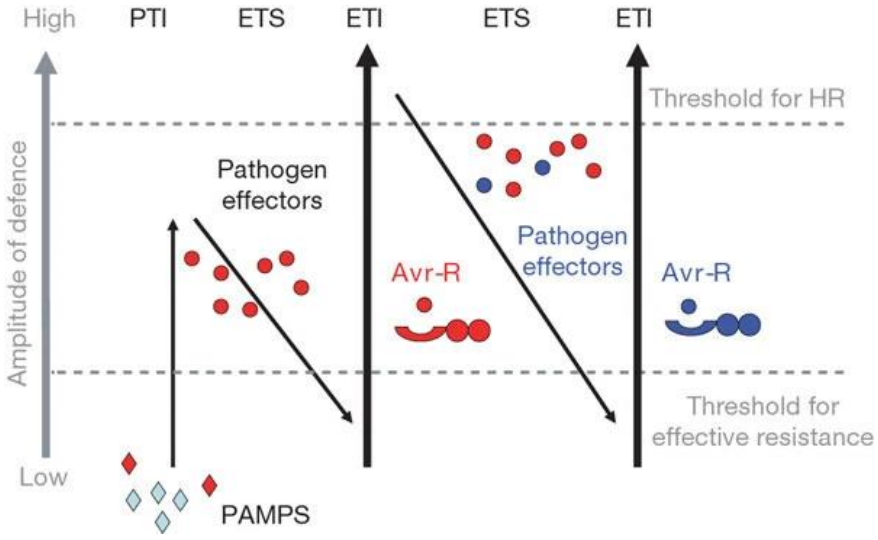


**Figure 1.1 The zig-zag model of plant immunity and pathogen arms race.** Pathogen- or microbe-associated molecular patterns (PAMPs) induce PAMP triggered immunity (PTI). Pathogens effectors lead to effector triggered susceptibility (ETS). Plants recognise avirulence (Avr) effectors through receptors encoded by resistance (R) genes, leading to effector triggered immunity (ETI), which often manifests as a hypersensitive response (HR). Taken from Jones and Dangl, (2006).

termed pattern-recognition receptors (PRRs; Jones & Dangl, 2006). For fungal pathogens, this mainly encompasses recognition of complex polysaccharide components of the fungal cell wall, including β-glucans, mannan and chitin, as well as the cell membrane component ergosterol (Barre et al., 2019; Khoza et al., 2019; Oliveira-Garcia & Deising, 2013; Sanchez-Vallet et al., 2014). Several widespread PCWDEs have also been proposed to act as PAMPs in eliciting plant defences (Ma et al., 2015; Zhang et al., 2014). Furthermore, plants are able to recognise the signs of direct attack on the plant cell wall by fungal hydrolytic enzymes, detecting the presence of breakdown products in the apoplast known as damage-associated molecular patterns (DAMPs; Lotze et al., 2007). Detection of PAMPs and DAMPs leads to generalised host defence responses, termed PAMP-triggered immunity (PTI; Fig. 1.1; Jones & Dangl, 2006). This includes the induction of an extracellular oxidative burst, $Ca^{2+}$ influx and activation of intracellular kinase cascades, which in turn regulates the expression of defence related genes and the synthesis of plant hormones leading to further transcriptional reprogramming (Boller & Felix, 2009).

As the majority of PAMPs recognised by host plants are indispensable to microbial survival and fitness, pathogens have evolved to counteract PTI through evading recognition of these molecules, or suppression of the resulting

defence responses. This is largely facilitated by the activity of effectors, which are broadly defined as molecules secreted by pathogens to enable host colonisation (Rovenich et al., 2014). Many of these effectors interfere with PTI, leading to effector-triggered susceptibility (ETS; Fig. 1.1; Jones & Dangl, 2006). The second layer of the plant immune response is composed of specific recognition of these pathogen effectors, known as effector-triggered immunity (ETI; Fig. 1.1). According to the zig-zag model, this typically involves direct recognition of pathogen effectors secreted into the host cell, or indirect recognition of their influence on host targets, by nucleotide binding-leucine rich repeat (NB-LRR) domain proteins (Dodds & Rathjen, 2010). Discovery of this second layer of induced defence was instrumental in understanding the gene-for-gene resistance proposed in the 1940s (Person et al., 1962), with the presence of a specific effector encoded by the avirulence (*Avr*) gene recognised by a receptor encoded by a resistance (*R*) gene (Fig. 1.1; Jones & Dangl, 2006). Defence responses associated with ETI are often rapid and drastic, involving the induction of localised host cell death at the infection locus to inhibit pathogen spread, known as the hypersensitive response (Balint-Kurti, 2019; HR). This provides strong resistance against biotrophic and hemibiotrophic pathogens which rely on living host cells.

Several limitations to the zig-zag model have been recognised since its initial widespread acceptance, leading to the proposal of alternative models. Firstly, many effectors are secreted into the apoplast, especially by pathogens which live all or part of their life cycles in the intercellular space (Catanzariti & Jones, 2010). Apoplastic effectors can induce defence responses through recognition by receptor-like proteins at the plant cell surface, many of which are structurally related to the PRRs involved in PTI (Schellenberger et al., 2019). This mechanism has recently been termed effector-triggered defence (ETD), which is proposed to entail a slower host response than ETI, limiting the growth and reproduction of the pathogen without necessarily directly impacting on its viability (Stotz et al., 2014). However, recognition of some apoplastic effectors causes a strong HR, such as those secreted by *Cladosporium fulvum* (Stergiopoulos & de Wit, 2009), while others induce slower responses reminiscent of PTI (Thomma et al., 2011). Cases of HR induced by PAMPs also lead to limitations in the definition of PTI as a weak defence response.

Furthermore, many effectors have been found to belong to conserved families and some PAMPs have restricted taxonomic distribution, leading to difficulty assigning defence-eliciting molecules to these classes (Thomma et al., 2011). This has led to the emergence of a new 'Invasion model' for the plant immune system, in which host defence responses are induced by recognition of invasion patterns, which encompasses any pathogen- or host-derived molecules that result from microbial colonisation (Cook et al., 2015). This was recently refined to the 'Spatial Invasion model', which differentiates intracellular and extracellular recognition of invasion patterns, which entail distinct signalling mechanisms and efficacies against intracellular and apoplastic pathogens (Kanyuka & Rudd, 2019).

### 1.2.3 Fungal pathogens manipulate plant defence

Plant pathogenic fungi with different lifestyles have evolved multiple strategies for dealing with these layers of host defence. Biotrophic pathogens generally rely on evading recognition and suppressing host defence responses, to enable successful colonisation whilst maintaining living host tissue. This strategy is analogous to that employed by symbiotic mycorrhizal and endophytic fungi. Effectors are secreted across the interface between pathogen and host and supress host defence responses through a plethora of mechanisms (Rovenich et al., 2014). Pathogenic fungi have evolved effectors which inhibit host defence through masking of cell wall polysaccharide elicitors (de Jonge et al., 2010), inhibition of downstream immune signalling components (Irieda et al., 2019), and modulating defence-related hormones (Djamei et al., 2011; Rabe et al., 2013). Other effectors protect the pathogen from antimicrobial host responses through inhibition and destruction of host hydrolytic and reactive oxygen species (ROS)-generating enzymes (Hemetsberger et al., 2012; Mueller et al., 2013; Naumann et al., 2011), detoxification of fungicidal secondary metabolites (Ökmen et al., 2013), and direct protection of fungal cell wall components (Van Esse et al., 2007). Furthermore, the reduced complement of PCWDE in biotrophic and symbiotic fungi has been suggested to represent a strategy to avoid recognition of these enzymes and their hydrolysis products as invasion patterns by the host (Balestrini & Bonfante, 2014; Zhao et al., 2013). The remaining PCWDEs in the genomes of fungi with biotrophic lifestyles may be involved in host penetration and nutrient acquisition from limited host cell wall

degradation, as has been suggested by the affinity of monosaccharide transporters from endophyte and mycorrhizal fungi for plant cell wall monosaccharides (Helber et al., 2011; Rasmussen et al., 2012).

Necrotrophic pathogens have evolved a distinct strategy for overcoming host defence based around secretion of an extensive armoury of toxins to kill host cells. Necrotrophs have long been known to secrete phytotoxic secondary metabolites which induce cell death in their hosts. This includes broad spectrum toxins, such as the sesquiterpene botrydial synthesised by *B. cinerea* (Colmenares et al., 2002; Reino et al., 2004), as well as host-specific toxins, such as the polyketide T-toxin from *Cochliobolus heterostrophus* (Baker et al., 2006). More recently, many necrotrophs have been found to produce host-specific toxic effector proteins (Oliver & Solomon, 2010). Functional analysis of these effectors found them to target plant immune receptors to induce host cell death and enable colonisation. For example, the *Stagonospora nodorum* necrotrophic effector SnTox1 was found to promote host cell death by interacting with the wheat wall-associated kinase Snn1, a member of a receptor family which confers resistance to biotrophic pathogens (Liu et al., 2012; Shi et al., 2016). Similar induction of host defence is seen in the activity of some host-specific toxins, such as the activation of the *Arabidopsis thaliana* NB-LRR protein LOV1 by the *Cochliobolus victoriae* cyclic peptide victorin (Lorang et al., 2012; Lorang et al., 2007). In this way, these necrotrophs co-opt the defence response induced by effector recognition, typically seen in effective resistance to biotrophs, to confer host susceptibility.

Although induction of host defence is a common strategy of necrotrophic colonisation, some elements of host defence can be effective against necrotrophic pathogens (Liu et al., 2013; Veronese et al., 2006; Wan et al., 2008; Zhang et al., 2013). The genomes of necrotrophic pathogens typically contain large repertoires of small secreted proteins with the hallmarks of effector proteins (Derbyshire et al., 2017; Guyon et al., 2014; Van Kan et al., 2017), and recent reports have demonstrated immune suppression by necrotrophs through effector expression and cross-kingdom RNAi (Sexton et al., 2009; Weiberg et al., 2013; Xu & Chen, 2013; Zhu et al., 2013). For example, the broad host range necrotroph *Sclerotinium sclerotiorum* produces oxalic acid, which was recently found to suppress the plant defence response

through inhibition of the host-induced oxidative burst (Williams et al., 2011), before carrying out its previously described function in inducing apoptotic cell death (Kim et al., 2008). In the absence of oxalic acid, *S. sclerotiorum* colonisation is inhibited by a host response reminiscent of the HR to biotrophs, involving autophagic cell death and callose deposition (Kabbage et al., 2013). This has led to suggestions that *S. sclerotiorum* has a lifestyle more akin to that of hemibiotrophs, with initial host defence suppression followed by induction of cell death (Kabbage et al., 2015).

These recent advances in our understanding of the plant immune system, and the strategies used by pathogens to overcome it, have further challenged the rigid definitions previously used to classify fungal-plant interactions. The role of necrotroph effectors in precise activation and suppression of host defences presents a far more complex model for their lifestyle than the previous 'smash and grab' image (Kabbage et al., 2015; Oliver & Solomon, 2010). Furthermore, the so-called 'biotrophic phase' of hemibiotroph infection may function more in suppression of host defences than in nutrient acquisition (Kabbage et al., 2015). This calls into question the relevance of the definition 'hemibiotrophic' pathogen, which may be better thought of as necrotrophic pathogens requiring a period of host defence evasion to successfully complete their life cycle. However, if treated as flexible lifestyle traits, the definitions of endophytic, biotrophic and necrotrophic interactions are useful in understanding what elements of host defence will mount an effective response. Furthermore, elucidating the strategies used by plant pathogens to evade and suppress host defence response, as well as the components of the plant immune system which are successful in combatting pathogen invasion in non-host plants and resistant varieties, is crucial for effective development of control strategies against agricultural diseases. Indeed, understanding the evolutionary processes behind this arms race in plant-pathogen interactions will inform us on how to enhance the plant immune response in a way that will avoid subsequent evolution of pathogen evasion strategies.

### 1.2.4 Developmental transitions in fungal pathogenesis

Developmental transitions are key to the infection of humans and plants by pathogenic fungi, playing crucial roles in colonisation, adaptation to the host

environment and reproduction (Brand, 2012; Gauthier, 2015; Mendgen et al., 1996). Many fungal pathogens display the ability to switch between growth morphologies from filamentous hyphal growth to yeast-like budding (Lin et al., 2015; Nadal et al., 2008). In general, hyphal growth in these pathogens enables colonisation of host tissues in search of nutrients, while yeast-like growth facilitates efficient proliferation and dispersal, either within the host or during transmission between hosts (Lin et al., 2015). Exceptions include thermally dimorphic fungi that grow as hyphae in the environment and switch to pathogenic yeast-like growth in response to increased temperature in the human host, for which invasion of host cells occurs passively through endocytosis (Gauthier, 2015; Wang & Lin, 2012). Other human pathogens, exemplified by *Candida albicans*, switch to hyphal growth for invasion of host tissues and cells (Brand, 2012). In fungal plant pathogens, hyphal growth is required for the colonisation of host tissues (Mendgen et al., 1996). The directional growth of fungal hyphae and their ability to orientate in relation to external stimuli (tropism) is important to this invasive process (Brand & Gow, 2009). For example, this allows root-associated fungi to grow towards the host through the soil following chemical gradients (Turrà et al., 2015; Turrà & Di Pietro, 2015). This also enables hyphae of some foliar pathogens to grow across the leaf surface towards the stomata through which they invade, displaying thigmotropism to follow architectural characteristics of the epidermal cells (Vaz Patto & Niks, 2001; Wynn, 1976).

Fungal pathogens overcome the physical barriers to invasion at the plant surface either by exploiting natural openings into host tissues, including natural wounds and stomatal apertures, or penetrating directly through the cuticle and epidermal cell surface. Fungal pathogens display varying levels of differentiation during host penetration, including development specialised structures called appressoria (Mendgen et al., 1996). These unicellular dome-shaped structures use the build-up of turgor pressure and secretion of hydrolytic enzymes to drive a penetration hypha into the host tissue (Ryder & Talbot, 2015). Appressoria are often heavily melanised to generate enough turgor pressure to physically breach the host epidermis without losing cell integrity (Howard & Ferrari, 1989). Appressorium development requires complex cellular differentiation, involving remodelling of the cell wall and cytoskeleton triggered through the combination

of multiple signalling pathways (Ryder & Talbot, 2015). Differentiation of appressoria is observed in both direct penetration and invasion of stomata in different pathogens, and occurs in response to physical and chemical properties of the host surface (Gilbert et al., 1996; Hoch et al., 1987). Intriguingly, the differentiation of appressoria-like cells was recently identified in many saprotrophic species from across the *Dikarya* (Demoor et al., 2019). Furthermore, detailed investigation of appressorium development in the saprotroph *Podospora anserina* identified common elements in the genetic control of appressorium development with plant pathogens (Brun et al., 2009; Lambou et al., 2008). This suggests that homologous penetration structures may be a more basal trait in fungi than previously thought (Demoor et al., 2019).

The cellular mechanisms supporting infection-related morphogenesis in fungal plant pathogens have been extensively studied. Over the past two decades, autophagy has emerged as a key process for the developmental transitions of fungal plant pathogens (Khan et al., 2012). Autophagy is the cellular pathway by which eukaryotic cells transport organelles and cytosolic contents to the vacuole/lysosome for degradation, which plays diverse roles in cellular nutrient recycling, homeostasis and development (Reggiori & Klionsky, 2013). This process has been shown to function in the starvation response and cellular differentiation of filamentous fungi (Pinan-Lucarré et al., 2003; Richie et al., 2007). Subsequent studies have found autophagy to contribute to pathogenicity on plants through its involvement in conidial germination, vegetative growth and appressorial development (Asakura et al., 2009; Josefsen et al., 2012; Kershaw & Talbot, 2009; Ren et al., 2017). Autophagy also has a crucial function in asexual and sexual reproduction in these pathogens, representing another major developmental transition in their infection cycles (Asakura et al., 2009; Liu et al., 2007; Lv et al., 2017; Ren et al., 2017).

Considering the lack of available nutrients on the surface of above-ground plant organs, utilisation of stored nutrients in the form of lipid droplets within spores is often required during the early development of fungal pathogens (Divon & Fluhr, 2007). Indeed, fatty acid β-oxidation has been shown to contribute to virulence through functions in conidial germination and appressorium formation in *F. graminearum* and *M. oryzae*, respectively (Patkar et al., 2012; Tang et al., 2019), while lipid catabolic processes were upregulated during pre-penetration

development in *Blumeria graminis* (Both et al., 2005; Pham et al., 2019). Furthermore, a complex relationship between lipid droplet dynamics and autophagy has recently been elucidated in yeast and mammalian cells (Maeda et al., 2017; Shpilka & Elazar, 2015; Singh et al., 2009; van Zutphen et al., 2014). This relationship has been demonstrated in filamentous fungal pathogens by the impact of autophagy disruption on conidial lipid droplet content and breakdown (Josefsen et al., 2012; Liu et al., 2007; Ren et al., 2017), indicating the potential interplay between these cellular processes during infection-related development.

Research has also focused on the signalling pathways regulating developmental transitions during infection. The mitogen-activated protein kinase (MAPK) FUS3 has been shown to be ubiquitously required for appressorium development in plant pathogens (Jiang et al., 2018; Xu & Hamer, 1996). FUS3 signalling was also found to be required for host penetration by pathogens without appressoria (Cousin et al., 2006; Jenczmionka et al., 2003; Jenczmionka & Schäfer, 2005; Mey et al., 2002), and in the recognition of host surface signals (Doehlemann et al., 2006; Liu et al., 2011). Given these findings, it has been proposed FUS3 plays a conserved role in controlling host penetration across varied invasion strategies (Turrà et al., 2014). The cell wall integrity (CWI) pathway involving the MAPK SLT2 has been found to contribute to pathogenicity in many fungal plant pathogens, with involvement in regulating vegetative growth and appressorium differentiation (Hou et al., 2002; Kojima et al., 2002; Xu et al., 1998). Disruption of *SLT2* also leads to defects in host tissue colonisation and increased sensitivity to antimicrobial plant defences (Joubert et al., 2011; Mehrabi, Van Der Lee, et al., 2006; Mey et al., 2002; Rui & Hahn, 2007), leading to suggestions of its function in regulating pathogen resistance to host defence (Turrà et al., 2014). Cyclic adenosine monophosphate (cAMP) signalling via protein kinase A (PKA) is also required for development during infection by many fungal pathogens, having crucial roles in host surface recognition, hyphal morphogenesis and appressorium development (Choi & Dean, 1997; Doehlemann et al., 2006; Yamauchi et al., 2004). Finally, cAMP signalling and the aforementioned MAPK pathways are required for asexual and sexual reproductive morphogenesis in different pathogens (Choi & Dean, 1997; Jenczmionka et al., 2003; Nguyen et al., 2012;

Xu et al., 1998). These pathways therefore represent a conserved signalling network regulating key aspects of infection-related development in fungal plant pathogens.

Common cellular pathways required for the development of fungal pathogens present an important potential target for intervention in disease, especially those involved in the initial steps of host penetration and colonisation. The proper functioning of pathways such as autophagy, lipid metabolism, MAPK cascades and cAMP signalling, are emerging as potential prerequisites for fungal pathogenicity on plants. This is especially intriguing considering the apparent conservation of some elements of these pathways between fungal pathogens (Turrà et al., 2014). For example, FUS3 homologs have been shown to complement the deletion of native alleles in various pathogens (Di Pietro et al., 2001; Guo et al., 2011; Mey et al., 2002; Takano et al., 2000), and this gene has shown promise as a target for RNAi-based control across different rust species using identical constructs (Panwar et al., 2013). Furthermore, elucidating the downstream components and transcriptional targets of these signalling pathways is crucial in furthering our understanding of the mechanisms behind morphogenesis in fungal pathogens.

## 1.3 *Zymoseptoria tritici*

### 1.3.1 Septoria tritici blotch: impacts and control

Wheat is currently the second most important global crop, estimated to provide 18.3% of global calorie intake (FAOSTAT, 2018). Global wheat production is under threat from yield losses caused by various biotrophic and necrotrophic fungi, which has increased due to the intensification of wheat growing and emergence of highly virulent pathogen strains (Singh et al., 2016). This includes the devastating ascomycete fungus *Zymoseptoria tritici*, which causes the disease Septoria Tritici Blotch (STB; Fig. 1.2; Eyal et al., 1987). STB causes necrosis in the foliar tissue of the host (Fig. 1.2), reducing its capacity to photosynthesise and subsequently leading to reduction in grain yields. Severe STB epidemics have been reported to lead to crop losses of up to 50% (Eyal et al., 1987). This disease remains of huge economic importance, particularly in Europe where STB has the highest impact of any disease on the intensive production of bread or common wheat *Triticum aestivum* (Jørgensen et al.,

2014). The host range of *Z. tritici* also includes *Triticum turgidum subsp. durum* (durum wheat). This is a particularly important crop in Middle Eastern and North African countries such as Tunisia, which has the highest wheat consumption per capita globally (FAOSTAT, 2018; Slim et al., 2019). The potential for large yield losses remains high in these regions, such as in recurring STB epidemics in Tunisia causing yield reductions of up to 40% (Berraies et al., 2014).

**Figure 1.2 Wheat leaf displaying typical STB symptoms.**
Leaves develop widespread necrosis and the formation of melanised pycnidia (*Z. tritici* asexual fruiting bodies) in stomata. Image from Ponomarenko et al., (2011).

Current strategies for combating *Z. tritici* are largely based on the application of fungicides. In recent years, 70% of fungicide input in Europe is attributed to STB control, costing an estimated $1.2 billion annually (Torriani et al., 2015). This is combined with major investment in the development of cultivars with STB resistance (Brown et al., 2015). This effort has faced significant challenges from the genetic association of resistance loci with those reducing yield potential (Torriani et al., 2015). This is thought to have been the source of widespread susceptibility to STB resulting from selection for increased yield during the Green Revolution (Arraiano & Brown, 2017). A total of 22 *Stb* (disease resistance) genes have been mapped in the wheat genome conferring qualitative resistance to specific *Z. tritici* genotypes (Brown et al., 2015; Yang et al., 2018), although their durability has been poor in the field (Brown et al., 2015; Cowger et al., 2000). The accumulation of quantitative resistance through breeding is thought to have provided the majority of field resistance (Torriani et al., 2015), and many of the contributing quantitative trait loci (QTL) have been mapped (Brown et al., 2015). The results of these efforts to control STB are evident; average yields losses in the UK can reach 20% when susceptible wheat varieties are planted, but can be reduced to 5-10% with the combined

use of resistant cultivars and fungicide application (Fones & Gurr, 2015). However, *Z. tritici* remains a moving target for control strategies, having shown the ability to rapidly evolve resistance to fungicides and virulence on resistant wheat cultivars (Torriani et al., 2015).

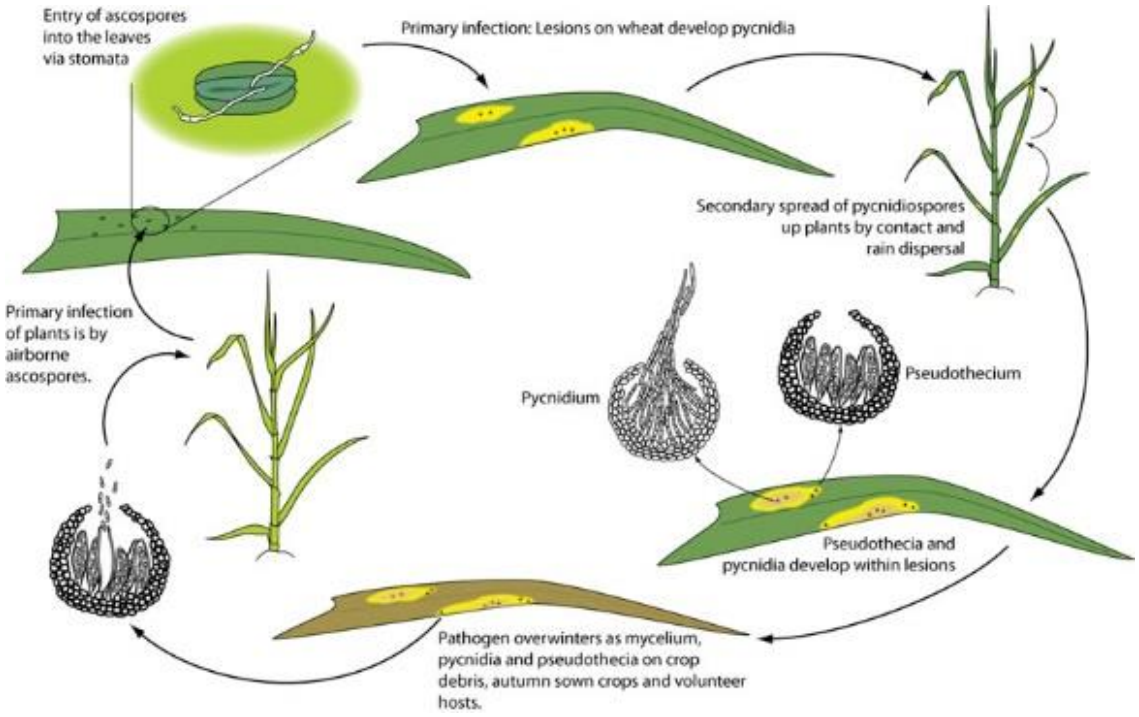


**Figure 1.3 The *Z. tritici* polycyclic infection cycle (Ponomarenko et al., 2011)**

The erosion in efficacy of control strategies against STB is attributed largely to the genomic population structure observed in *Z. tritici*, arising from elements of its life cycle (Fig. 1.3). *Z. tritici* has an active sexual cycle which leads to high levels of recombination in the population (Stukenbrock & Dutheil, 2018). Sexual reproduction results in the production air-borne ascospores which can spread on a continental scale (Fig. 1.3), leading to a high rate of gene flow (Shaw & Royle, 1989; J. Zhan et al., 2003). This is compounded by the high levels of genome diversity in *Z. tritici*, caused by transposable elements (TEs) and chromosomal instability (Badet et al., 2020). These factors lead to extremely high levels of genetic diversity even at a local scale, with one study reporting that 90% of the global genetic variation in *Z. tritici* can be found within a single field of wheat (Zhan et al., 2003). Furthermore, *Z. tritici* goes through many generations of asexual sporulation within a growing season (Fig. 1.3), leading to intra-annual selection for aggressiveness (Suffert et al., 2018). This causes high population sizes in the field, which is exacerbated by high cropping densities of genetically uniform hosts (Fones & Gurr, 2015). These life cycle traits give *Z.*

*tritici* a high capacity to rapidly overcome fungicides and host resistance, and increase the chances of highly virulent strains arising (Fones & Gurr, 2015).

This has had dire consequences on the durability of control strategies to date (Brown et al., 2015; Torriani et al., 2015). Widespread use of Quinone outside Inhibitors (QoIs) to control *Z. tritici* has now been rendered almost redundant in many European countries with widespread evolution of resistance (Blake et al., 2018; Cheval et al., 2017; Fraaije et al., 2005), Furthermore, genotypes providing resistance against the demethylation inhibitor (DMI) and succinate dehydrogenase inhibitor (SDHI) fungicides, currently used for STB control, are arising rapidly in Europe (Cools & Fraaije, 2013; Kildea et al., 2019; Rehfus et al., 2018; Steinhauer et al., 2019). The level of diversity seen in isolates *of Z.* tritici has also left qualitative resistance, offered by previously identified *Stb* genes, vulnerable to coevolution of their fungal counterparts in the gene-for-gene relationship (Brown et al., 2015). This is evident in the findings that resistance to STB in the field is a quantitative trait despite the presence of *Stb* genes (Stewart et al., 2018; Stewart & McDonald, 2014). Furthermore, the majority of *Z. tritici* strains are virulent in most *Stb* host backgrounds, calling into question the durability of qualitative resistance against a diverse field population, even with *Stb* gene pyramiding (Brown et al., 2015).

Looking forward, ongoing management of STB epidemics will require the complex integration of available control strategies (Jørgensen et al., 2014; Torriani et al., 2015), and is the subject of ongoing research efforts with four main goals. The first aims to identify new resistance loci in wheat and understand the underlying mechanisms of the resistance they confer, in order to breed for durable resistance (Brown et al., 2015). This is increasingly focusing on bolstering downstream host defences without relying on gene-for-gene resistance and stacking of quantitative resistance loci (Brown et al., 2015; Torriani et al., 2015). As well as identifying new resistance traits, a recent study found that introducing resistant varieties into cultivar mixes can dramatically reduce disease severity in durum wheat, which may also benefit the durability of resistance through reduced selection pressure on the pathogen (Ben M'Barek et al., 2020). The second aims to improve the management of fungicide resistance to currently available chemistries (Torriani et al., 2015). This encompasses monitoring of the spread of fungicide resistant genotypes in the

population (Garnault et al., 2019), optimising the dose and timing of spraying regimes (van den Berg et al., 2013, 2016) and the modelling of *Z. tritici* epidemics in an effort to intelligently inform spatiotemporal deployment of fungicide inputs (Savary et al., 2015).

The third goal focuses on the development of novel compounds with activity against *Z. tritici* (Torriani et al., 2015). Two recent studies have reported identification of fungicides with novel target sites on mitochondrial complex III which are active against QoI resistant *Z. tritici* strains (Owen et al., 2017; Suemoto et al., 2019). The final aims to identify alternative strategies for controlling STB, including the identification of novel biocontrol agents such as endophytic fungi (Latz et al., 2020) and bacteria (Lynch et al., 2016; Mejri et al., 2018). This also includes techniques based on RNA-interference, such as host-induced gene silencing (HIGS; Qi et al., 2019) and spray-induced gene silencing (SIGS; Cagliari et al., 2019). However, a recent trial of HIGS against essential *Z. tritici* genes was unable to inhibit infection, possibly due to the inability of the fungus to take up double-stranded RNA (Kettles et al., 2019).

Advancement in our understanding of the molecular determinants of *Z. tritici* infection will be valuable to the effective development of these control strategies. This includes the identification of cellular processes and specific proteins that are indispensable to *Z. tritici* pathogenicity, which could present novel molecular targets for fungicides. This can also increase the efficiency of fungicide discovery by informing the use of known inhibitor compounds or development of assays for identifying compounds with activity against specific cellular processes.

### 1.3.2 Molecular tools for studying *Z. tritici*

Despite the importance of STB in global wheat agriculture, relatively little is known about the molecular host-pathogen interactions and cellular development of *Z. tritici* compared to model pathogens like *M. oryzae* (McDonald et al., 2015; Steinberg, 2015). However, recent advances in the development of molecular tools for studying *Z. tritici* have enabled rapid progress in our understanding of its interaction with wheat. The initial breakthrough came with the development of an *Agrobacterium tumefaciens*-mediated transformation (*A*tMT) protocol for efficient genetic manipulation of *Z. tritici* (Zwiers & De Waard, 2001), allowing

functional characterisation of genes through reverse genetics. These techniques for targeted insertion of transgenic elements are based around homologous recombination, the efficiency of which has recently been enhanced by the development of strains deficient in the non-homologous end-joining pathways (Bowler et al., 2010; Sidhu, Cairns, et al., 2015). These capabilities have been advanced by the development of suites of transformation vectors containing different selective markers, designed for functional analysis through gene knockout, overexpression and fluorophore fusion protein expression (Cairns et al., 2015; Sidhu, Chaudhari, et al., 2015). This is complemented by the generation of *Z. tritici*-optimised fluorescent proteins and strains containing a range of labelled organelles to improve imaging of *Z. tritici* cell biology (Kilaru et al., 2017; Kilaru, Schuster, et al., 2015).

The next major breakthrough enabling our understanding of *Z. tritici* biology came with the sequencing of the reference isolate IPO323 genome published in 2011 (Goodwin et al., 2011). This enabled detailed functional genomic analysis, including the characterisation of the *Z. tritici* secretome (Morais do Amaral et al., 2012), candidate small secreted effector proteins (Mirzadi Gohari et al., 2015) and PCWDEs (Brunner et al., 2013; Goodwin et al., 2011). The use of RNA-sequencing technologies has also furthered our understanding of *Z. tritici* infection at a molecular level, with multiple studies analysing the host and pathogen transcriptomes across different time points during infection (Kellner et al., 2014; Ma et al., 2018; Palma-Guerrero et al., 2016; Rudd et al., 2015; Yang et al., 2013). These genomics studies have facilitated functional characterisation of genes through reverse genetics, by enabling informed selection of gene targets for analysis (Rudd et al., 2015).

Forward genetics approaches have also recently been applied to identify key genes in *Z. tritici* development and pathogenicity (King et al., 2017; Motteram et al., 2011; Yemelin et al., 2017). These studies utilised random integration of T-DNA through *At*MT and subsequent identification of insertion loci through nested PCR techniques. With recent advances in next generation sequencing technologies and the reductions in the associated costs, identification of genotypic variations associated with interesting phenotypes is becoming easier. Indeed, this, along with the ability to perform sexual crosses in *Z. tritici* (Kema, Verstappen, et al., 1996), has increased the efficiency of QTL mapping and

genome wide association studies (GWAS) in identifying loci associated with *Z. tritici* virulence, fungicide sensitivity and development (Hartmann et al., 2017; Lendenmann et al., 2015; Stewart et al., 2018; Zhong et al., 2017)) and wheat resistance (Odilbekov et al., 2019; Yates et al., 2019).

### 1.3.3 The *Z. tritici* infection cycle

#### 1.3.3.1 Host penetration and the asymptomatic phase

Both the sexual and asexual spores of *Z. tritici* are able to initiate infection of the wheat leaf (Fig. 1.4A; Eyal et al., 1987). Primary inoculum for *Z. tritici* infection at the start of the growing season comes predominantly from airborne ascospores dispersed from infected wheat debris (Shaw & Royle, 1989; Suffert & Sache, 2011). After completion of the initial infection cycle, asexual reproduction produces abundant pycnidiospores which are dispersed locally by rain splash. These pycnidiospores provide a secondary inoculum, leading to the polycyclic infection that characterises STB epidemics across each growing season (Suffert et al., 2018).

After landing on the leaf surface, *Z. tritici* spores undergo a key morphological switch to form hyphal filaments, which grow over the leaf surface and colonise the apoplast through stomata (Fig. 1.4; Kema, Yu, et al., 1996). Some studies have reported evidence of thigmotropic growth of epiphytic *Z. tritici* hyphae, observing orientation of germ tubes towards stomata (Duncan & Howard, 2000). However, other authors have observed failure of hyphae to penetrate despite crossing stomatal apertures, and high proportions of germ tubes growing away from stomata, suggesting that epiphytic growth is likely to be random (Kema, Yu, et al., 1996; Shetty et al., 2003). Indeed, Fones et al., (2017) found that the rate of stomatal penetration over early infection was consistent with that predicted by their model of random growth across a simulated leaf surface. Stomatal penetration has been reported to occur as early as 12-24h post inoculation (Duncan & Howard, 2000; Kema, Yu, et al., 1996). However, recent evidence suggests that penetration events at this early stage may be rare, with over 95% of hyphae remaining entirely epiphytic up until 10 days post infection (dpi; Fones et al., 2017). The authors proposed that the frequency of early penetration events may have been overestimated in earlier studies due to the

increased likelihood of epiphytic hyphae being washed off the leaf during staining procedures, compared to hyphae that had already penetrated stomata (Fones et al., 2017).

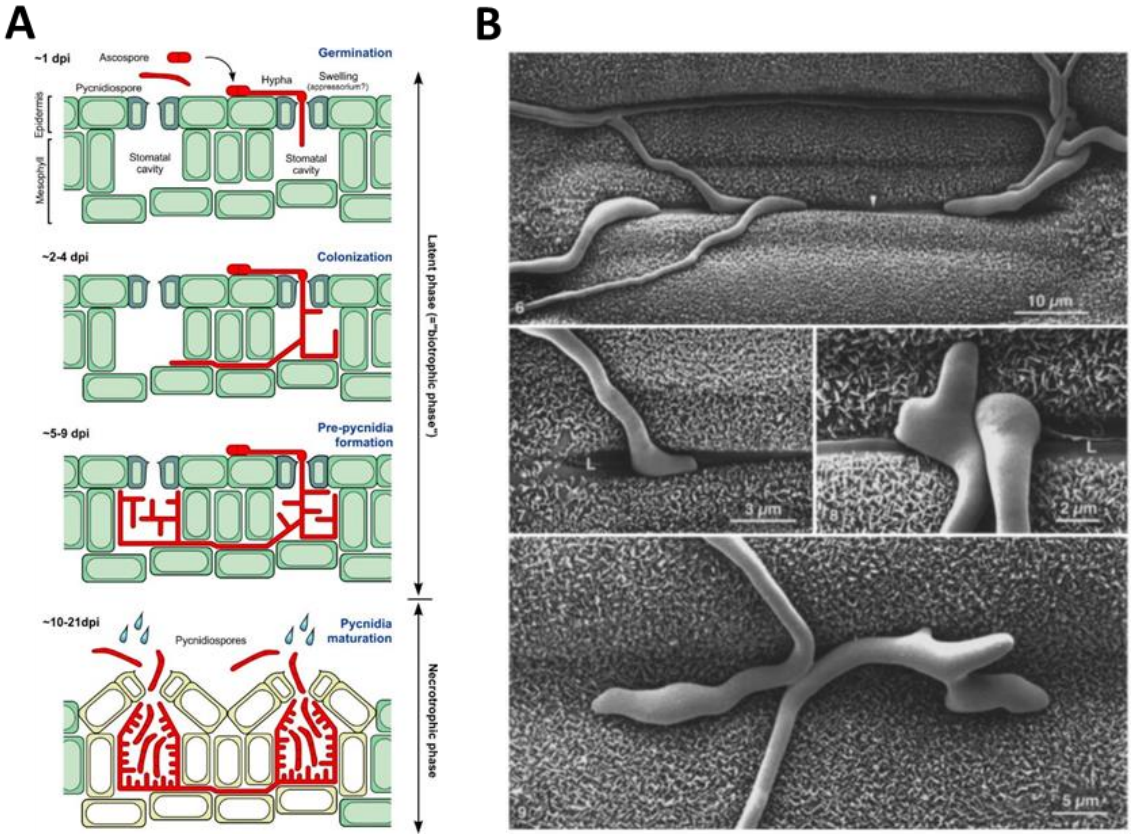


**Figure 1.4 Host colonisation by *Z. tritici***
(A) Stages of typical wheat infection by *Z. tritici* (Steinberg, 2015). (B) Cryo-scanning electron microscopy of *Z. tritici* germ tubes entering host stomata (top), germ tube apices swelling over stomata possibly primitive appressoria (middle), and development of hyphal swellings over anticlinal cell wall of epidermal cells (Duncan and Howard, 2000).

The mode of leaf penetration by *Z. tritici* has been the subject of some debate. Although there is no evidence for the development of a melanised unicellular appressorium in *Z. tritici,* swellings have been observed at the hyphal tip before penetration (Fig. 1.4; Cohen & Eyal, 1993; Duncan & Howard, 2000; Kema, Yu, et al., 1996; Siah et al., 2010). These may represent the differentiation of primitive invasion or appressoria-like structures, as observed broadly in the *Dikarya* (Demoor et al., 2019). Although the consensus is that *Z. tritici* invades the wheat leaf through stomata (Kema, Yu, et al., 1996), observations of these swellings forming over the anticlinal cell wall between epidermal cells have been made (Fig. 1.4; Duncan & Howard, 2000; Rohel et al., 2001). This may

result from *Z. tritici* cells mistaking the depression at the epidermal cell junction for a stomatal aperture (Duncan & Howard, 2000). Furthermore, two studies have reported observations of direct penetration of the epidermis resulting in hyphal growth into the mesophyll (Rohel et al., 2001; Siah et al., 2010), although data demonstrating this was not shown by Siah et al., (2010). Epidermal penetration events have been reported at varying frequencies, and may represent a strain-specific invasion strategy (Cohen & Eyal, 1993; Siah et al., 2010). However these observations may also be the result of utilisation of microscopic wounds in the leaf surface by *Z. tritici*.

Following stomatal penetration, *Z. tritici* hyphae colonise the mesophyll tissue asymptomatically for 7 days or more (Fig. 1.4A), depending on the strain-cultivar combination (Duncan & Howard, 2000; Kema, Yu, et al., 1996; Keon et al., 2007; Palma-Guerrero et al., 2017) and environmental conditions (Chungu et al., 2001; Suffert & Thompson, 2018). Growth during the symptomless phase is extremely slow, with increases in biomass undetectable using ELISA assays (Kema, Yu, et al., 1996) and real-time polymerase chain reaction (RT-PCR; Keon et al., 2007). Furthermore, leaf colonisation by *Z. tritici* is strictly extracellular throughout infection (Kema, Yu, et al., 1996), unlike many plant pathogens which develop haustorial feeding structures and penetrative invasive hyphae (De Silva et al., 2017; Kankanala et al., 2007; Voegele & Mendgen, 2003). This has major implications on the *Z. tritici* infection strategy, with molecular host-pathogen interactions occurring exclusively within the apoplast (Kettles & Kanyuka, 2016). Moreover, extensive epiphytic and intercellular growth during colonisation limits *Z. tritici* to the nutrients available on the leaf surface and in the apoplast during symptomless growth (Rudd et al., 2015).

Dramatic transcriptional changes have been identified at this early stage of infection, with over 1000 *Z. tritici* genes showing differential expression after 24h on the leaf (Rudd et al., 2015). During symptomless early infection, the fungus shows upregulation of genes involved in lipid metabolism and downregulation of hexose and nitrate transporters, suggesting the fungus is predominantly relying on internal nutrients at this stage (Palma-Guerrero et al., 2016; Rudd et al., 2015). However, upregulation of a small set of PCWDEs during this period has been suggested to indicate some use of host derived nutrition during early colonisation (Brunner et al., 2013; Palma-Guerrero et al.,

2016; Rudd et al., 2015; Sánchez-Vallet et al., 2015). In general, the complement of PCWDEs in the *Z. tritici* genome is significantly reduced compared to other pathogens with necrotrophic life cycle stages (Goodwin et al., 2011; Ohm et al., 2012). This, along with the general downregulation of PCWDEs during early infection (Rudd et al., 2015), could represent a strategy to avoid host recognition during colonisation, which has been termed 'stealth pathogenesis' (Goodwin et al., 2011). Additionally, secretion of aspartic proteases and secreted lipases during early infection may contribute to acquisition of leaf surface and apoplastic nutrients (Palma-Guerrero et al., 2016).

Stomatal penetration occurs regardless of whether the host is susceptible or resistant (Shetty et al., 2003; Siah et al., 2010). During infection of resistant wheat cultivars, arrest of hyphal colonisation is associated with the accumulation of $H_2O_2$ in the apoplast, indicating a role of ROS in a successful host defence response to *Z. tritici* (Shetty et al., 2003). In contrast, initial colonisation of susceptible hosts is accompanied by downregulated expression of host defence-related genes and minimal $H_2O_2$ accumulation, indicating successful evasion and/or suppression of the host defence response by the fungus during early infection (Rudd et al., 2015; Shetty et al., 2003; Yang et al., 2013). *Z. tritici* shows early upregulation of many genes encoding secreted proteins, including many putative cysteine-rich effectors thought to suppress host immune responses (Mirzadi Gohari et al., 2015; Palma-Guerrero et al., 2016; Rudd et al., 2015). Also upregulated at this stage are the secreted chloroperoxidases, an expanded gene family in *Z. tritici* (Morais do Amaral et al., 2012), which may act to detoxify host defence-related ROS generation (Palma-Guerrero et al., 2016; Rudd et al., 2015). The subset of proteases expressed during symptomless infection may also contribute to hydrolysing host defence proteins (Palma-Guerrero et al., 2016; Stotz et al., 2014). Contrary to the hypothesis of successful evasion of host recognition by *Z. tritici,* Ma et al., (2018) reported upregulation of receptor-like kinase (RLK) and senescence-related genes associated with defence during the symptomless phase of infection by virulent *Z. tritici* strains. However, as all these strains went on to successfully colonise the leaf, any defence response triggered in the host was

successfully suppressed or endured by *Z. tritici*, presumably facilitated by the armoury of fungal secreted proteins.

### 1.3.3.2 The transition to necrotrophy

Following this extended latent phase, *Z. tritici* undergoes a switch to necrotrophy (Fig. 1.4A; Fig. 1.5). This is characterised by host cell death and lysis, release of nutrients into the apoplast and a rapid increase in fungal growth rate (Kema, Yu, et al., 1996; Keon et al., 2007; Rudd et al., 2015). This transition coincides with an increase in cytosolic cytochrome c, loss of genomic DNA integrity and the accumulation of ROS, strongly suggesting that host cells are undergoing programmed cell death (PCD) reminiscent of the HR (Keon et al., 2007). Furthermore, transcriptome analysis at this stage identified upregulation of genes related to host defence responses, including pathogenesis-related (PR) proteins and biosynthesis of defence-related hormones (Rudd et al., 2015). This is accompanied by upregulation of host peroxidases which may contribute to ROS production, as well as cell death-related subtilases and plastocyanin-like proteins (Rudd et al., 2015). There is evidence that this host PCD response is controlled by the upregulated expression and activation of TaMPK3, a homolog of MAPKs involved in HR-mediated resistance in other plant-pathogen interactions (Rudd et al., 2008). These findings suggest that *Z. tritici* triggers host cell death through induction of HR-like defence pathways to facilitate colonisation, similar to other necrotrophic pathogens (Hammond-Kosack & Rudd, 2008).

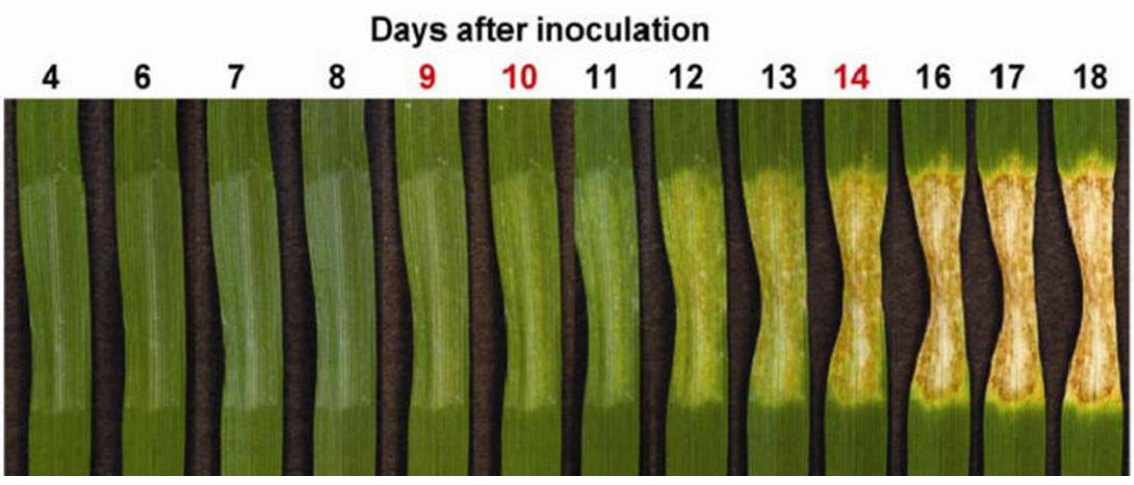


**Figure 1.5 Transition between symptomless and necrotrophic phases during *Z. tritici* infection**
Time course of symptom development in wheat leaf infected with *Z. tritici* (Keon et al., 2007).

Transcription analyses have attempted to elucidate how *Z. tritici* controls this transition to necrotrophy. These studies have identified upregulated expression of small cysteine-rich proteins and a set of secondary metabolite gene clusters during this transition (Mirzadi Gohari et al., 2015; Palma-Guerrero et al., 2016; Rudd et al., 2015). These effectors are proposed to trigger necrosis through direct activation of plant HR and provide protection from the induced plant defence (Rudd et al., 2015). However, functional characterisation is yet to confirm their individual contribution to virulence, suggesting the presence of functional redundancy (Mirzadi Gohari et al., 2015; Rudd et al., 2015; Stergiopoulos et al., 2003). While genes involved in fatty acid metabolism show reduced expression at the transition to necrotrophy, the fungus upregulates production of secreted proteases as well as ammonium, amino acid and MFS transporters (Palma-Guerrero et al., 2016). This indicates a switch from use of internal lipid stores to the uptake of nutrients released from host cell lysis, especially extracellular proteins (Rudd et al., 2015).

#### 1.3.3.3 Necrotrophic growth and sporulation

After the transition to necrotrophy, the fungus continues to grow rapidly in the collapsing wheat leaf tissue (Kema, Yu, et al., 1996; Keon et al., 2007). Rudd et al., (2015) observed a general reduction in the expression of secreted effectors by the fungus during late necrotrophic growth, with only a small group of putative effectors peaking at this stage. Conversely, another study reported the peak expression of a large group of candidate effectors during necrotrophy (Mirzadi Gohari et al., 2015). However, this discrepancy is likely due to variation in sampling time-points, with expression of most of these genes peaking around the transition at 8 or 12 dpi and subsequently declining (Mirzadi Gohari et al., 2015). The late necrotrophic phase also sees a downregulation in secreted proteases and simultaneous upregulation of the majority of secreted PCWDEs and α-amylases, indicating a shift in fungal nutrient acquisition towards host cell wall polysaccharides and starch (Brunner et al., 2013; Palma-Guerrero et al., 2016; Rudd et al., 2015). Concurrent with the abundant host cell death, the plant further increases its expression of defence-related genes while reducing its investment in photosynthesis (Rudd et al., 2015).

During necrotrophic colonisation, asexual reproduction begins through development of melanised fruiting bodies called pycnidia in the substomatal cavities (Fig. 1.4A; Kema, Yu, et al., 1996). This occurs after between 14-40 days in the field depending on host cultivar and environmental factors (Ponomarenko et al., 2011). *Z. tritici* produces two types of conidia, multicellular macropycnidiospores and unicellular micropycnidiospores, which are exuded through the stomata in a mass called a cirrus (Eyal et al., 1987). Pseudothecia appear in infected leaf lesions long after the first development of pycnidia (29-95 days), and continue to produce ascospores on senescent leaf tissue and crop debris (Eriksen & Munk, 2003; Hunter et al., 1999). This produces a peak in airborne ascospore densities in late autumn, which provide inoculum to infect emerging seedlings (Hunter et al., 1999; Suffert & Sache, 2011). *Z. tritici* was also recently shown to develop chlamydospores with thick cell walls, capable of maintaining viability under heat, cold and desiccation stress (Francisco et al., 2019). The authors proposed that these cells may enhance pathogen survival between growing seasons (Francisco et al., 2019).

### 1.3.4 Beyond the reference strain – diversity in *Z. tritici* infection strategies

Along with the immense genetic diversity in the field, significant variability in virulence and infection strategy has been observed between *Z. tritici* strains. As described above, the broadly defined infection stages of host penetration, symptomless colonisation, transition to necrotrophy and colonisation of necrotic host tissue are consistent (Haueisen et al., 2019). However, some elements of the infection cycle vary considerably between *Z. tritici* genotypes, such as the timing of host penetration and the length of latent period before symptom development and asexual reproduction (Haueisen et al., 2019; Palma-Guerrero et al., 2016). These infection checkpoints can even vary considerably between cells of the same genotype (Fones et al., 2017; Haueisen et al., 2019). This is unlike fungal pathogens with strictly coordinated developmental programs such as *Magnaporthe oryzae*, which displays incredible synchronicity in its infection cycle (Kankanala et al., 2007; Osés-Ruiz & Talbot, 2017; Soanes et al., 2012). In a recent study, detailed microscopic investigation of infection by three *Z. tritici* isolates revealed diversity in their colonisation strategies, despite similar disease severity after the necrotrophic transition (Haueisen et al., 2019). This

included variation in the extent of epiphytic growth and the pattern of mesophyll colonisation during the symptomless phase. Elucidating the causes of this variation in infection phenotypes is crucial to our understanding of infection by diverse *Z. tritici* genotypes in the field (Haueisen et al., 2019).

Recent genomic and transcriptomic analysis has focused on the genetic basis for this variation in development and virulence between *Z. tritici* isolates (Badet et al., 2020; Francisco et al., 2019; Haueisen et al., 2019; Ma et al., 2018; Palma-Guerrero et al., 2017). Analysis of the recently constructed pangenome of *Z. tritici* has revealed the genomic plasticity of the species, displaying around 40% accessory gene content (Badet et al., 2020; Plissonneau et al., 2018). Furthermore, eight of the 21 chromosomes the *Z. tritici* genome are dispensable, showing presence-absence variation and substantial rearrangements within the population driven by meiosis (Croll et al., 2013; Fouché et al., 2018). Fungal pathogens often display two-speed genomes, with genomic regions rich in transposable elements and repeat sequences acting as a “cradle for adaptive evolution” (Dong et al., 2015). Indeed, transposable elements (TEs) are associated with chromosomal size variation and rearrangements (Badet et al., 2020; Croll et al., 2013) as well as gene presence-absence polymorphisms (Hartmann & Croll, 2017), and accessory genes are located in close proximity to TEs (Plissonneau et al., 2018).

To elucidate the causes of the observed variation in virulence, these studies have revealed interesting patterns in the conservation and expression of genes involved in pathogenicity between *Z. tritici* strains. On top of the aforementioned genetic diversity, expression of the ‘core’ genes identified across isolates can also be highly divergent, with one study reporting differential expression of 20% of the genes shared by three isolates across infection (Haueisen et al., 2019). However, enzymes thought to be involved in the degradation of host tissue, including PCWDEs, proteases and secreted lipases, are highly conserved in their gene content and expression patterns across infection amongst *Z. tritici* strains (Badet et al., 2020; Palma-Guerrero et al., 2017). Siah et al., (2010) reported an observed correlation between pycnidia density and xylanase activity during late infection, proposing that these PCWDEs represent an important pathogenicity factor influencing virulence. However, this correlation could result from co-expression of xylanases with other virulence factors during infection,

meaning more detailed functional characterisation is required. Conservation in content and regulation of genes encoding secreted peroxidases and proteases has also been observed, with these enzymes predicted to function in detoxification of ROS and defence proteins generated by the host (Palma-Guerrero et al., 2017). However, higher expression levels of two chloroperoxidases was reported for the most virulent strain in this study, suggesting that regulation of these enzymes may have some impact on virulence (Palma-Guerrero et al., 2017).

Converse to the apparent conservation of these enzyme classes, the majority of putative effector proteins are encoded by accessory genes (Badet et al., 2020), and these are frequently located in TE-enriched regions (Hartmann et al., 2017; Meile et al., 2018; Zhong et al., 2017). Similarly, 40% of secondary metabolite gene clusters show presence-absence polymorphism across strains (Badet et al., 2020). Although the overall pattern of putative effector gene expression is consistent between strains, with peaks in small secreted protein expression during symptomless growth and the transition to necrotrophy, strain-specific expression profiles of these genes have been frequently observed (Haueisen et al., 2019; Palma-Guerrero et al., 2016, 2017). Those effector genes found to have consistent expression profiles between strains have been proposed to represent “core” effectors with important infection-related functions across the species (Haueisen et al., 2019). Effectors displaying variation in gene presence–absence and regulation between isolates are thought to contribute significantly to variation in virulence. Indeed, structural rearrangements and gene polymorphisms associated with TE-rich regions have been shown to contribute to *Z. tritici* virulence evolution through their influence on adaptation, loss and differential regulation of avirulence effectors (Brunner & McDonald, 2018; Fouché et al., 2020; Hartmann et al., 2017; Meile et al., 2018).

The diversity in effectors deployed by *Z. tritici* strains during infection represents a varied molecular armoury used to colonise the host. This is thought to contribute to the flexibility in infection strategies employed by *Z. tritici* (Haueisen et al., 2019), and the maintenance of pathogen virulence shaped by co-evolutionary responses to the host environment (Palma-Guerrero et al., 2017). Considering this, the relevance of studying the importance of virulence factors in single isolate-cultivar interactions to field populations has been questioned

(Haueisen et al., 2019). This highlights the importance of identifying conserved infection-related processes, required for the virulence of all *Z. tritici* genotypes, to the development of effective control strategies.

### 1.3.5 Understanding the molecular determinants of *Z. tritici* virulence

Aiming to identify crucial molecular factors that contribute *Z. tritici* infection, many studies have carried out detailed investigation of putative effector proteins. Genomic and transcriptomic analysis has identified candidates for effectors involved in the manipulation of the host at different stages of wheat infection, including defence suppression and necrosis induction (Haueisen et al., 2019; Mirzadi Gohari et al., 2015; Palma-Guerrero et al., 2017; Rudd et al., 2015). However, subsequent functional characterisation of these effectors has revealed that many are dispensable to virulence (Mirzadi Gohari et al., 2015; Rudd et al., 2015). Similarly, although the identity of three *Z. tritici* avirulence genes has been elucidated, the functions of the encoded effectors during infection of susceptible hosts, and the mechanisms by which they induce host defence (Fig. 1.6), has not been determined (Hartmann et al., 2017; Kettles & Kanyuka, 2016; Meile et al., 2018; Zhong et al., 2017). Along with high variation in effector content and expression between strains, this indicates a high level of functional redundancy and host specificity in their contribution to infection (Rudd et al., 2015).

Although it is typical for protein effectors to possess no homology to functionally characterised proteins, members of several conserved effector families have been investigated in *Z. tritici*. Three chitin-binding Lysin (LysM) domain proteins were identified in *Z. tritici*, which are highly expressed during the symptomless and transition phases of infection (Marshall et al., 2011; Palma-Guerrero et al., 2017). Mg3LysM was confirmed to inhibit chitin recognition by the pattern receptors CEBiP and CERK1 and protect hyphae from host chitinases (Fig. 1.6), and is essential for *Z. tritici* virulence (Lee et al., 2014; Marshall et al., 2011). The remaining two LysM effectors were recently shown to display partial functional redundancy with Mg3LysM, and also contribute to *Z. tritici* virulence (Tian et al., 2021). Other effectors have been investigated as potential triggers of host cell death during the transition to necrotrophy. The Necrosis and Ethylene-inducing Peptide 1 (NEP1)-like proteins (NLPs) are a family known to

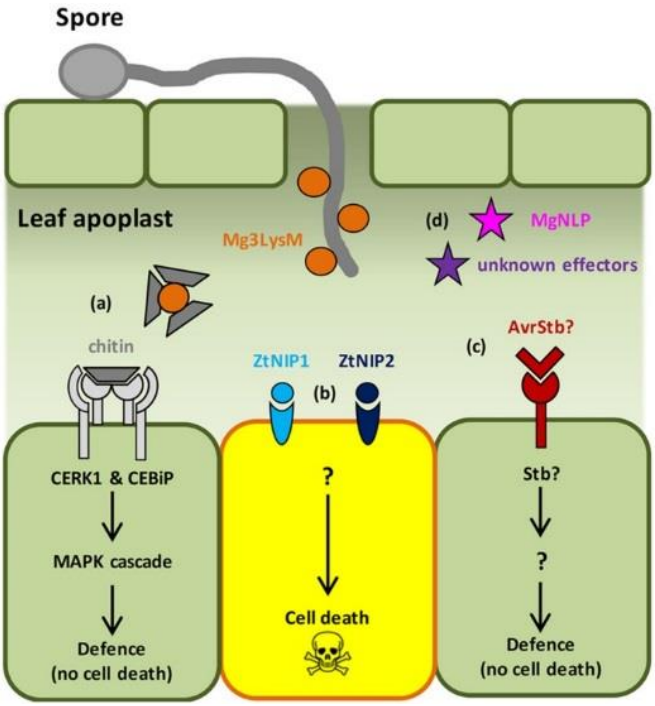


**Figure 1.6 Characterised molecular interactions between wheat and *Z. tritici***
(a) LysM domain effectors suppress the recognition of fungal PAMP chitin by wheat Chitin Elicitor Binding Protein (CEBiP) and Chitin Elicitor Receptor Kinase 1 (CERK1). (b) *Z. tritici* effectors (e.g. necrosis-inducing proteins (ZtNIP1/2)) induce programmed cell death. (c) *Z. tritici* avirulence genes (e.g. AvrStb6) induce host defence via wheat R proteins (e.g. Stb6) without host cell death. (d) Many *Z. tritici* effectors of unknown function (Kettles and Kanyuka, 2016).

induce necrosis in dicots (Gijzen & Nürnberger, 2006). However, MgNLP from *Z. tritici* caused no necrosis in wheat leaves and was dispensable for virulence (Motteram et al., 2009). Similar findings have recently been reported for *M. oryzae* MoNLP effectors, leaving the question of the role of these effectors in monocot pathogens open (Fang et al., 2017). An alternative method of necrotrophic effector discovery is to identify necrosis-inducing proteins in culture filtrates (Bailey, 1995). Using this approach, two necrosis inducing proteins (ZtNIP1/2) were identified in *Z. tritici* culture filtrates which trigger cell death in wheat (Fig. 1.6). However, this effect varied between host genotypes, and elucidation of their impact on virulence through gene deletion has not yet been reported (Ben M'Barek et al., 2015).

The *Z. tritici* effector Zt6 was recently characterised as a potent ribonuclease with cytotoxicity to wheat, suggesting that it may contribute to the induction of host cell death (Kettles et al., 2018). However, Zt6 was also shown to have toxicity to bacteria and fungi, and display two peaks in expression during symptomless phase and after the transition to necrotrophy. This prompted

authors to suggest that Zt6 functions in niche protection against competing microorganisms in the leaf (Kettles et al., 2018). This type of antimicrobial effector may be responsible for the observed suppression of *Blumeria graminis f. sp. tritici* powdery mildew when co-inoculated with *Z. tritici* (Orton & Brown, 2016). Effectors with such antimicrobial functions remain relatively unexplored (Snelders et al., 2018). Intriguingly, one study has recently demonstrated the importance of the antimicrobial effectors VdAMP2 and VdAve1 from *Verticillium dahlia*e for the colonisation of plant hosts and soil in competition with bacteria (Snelders et al., 2020). This paves the way for similar studies into *Z. tritici* effector function. Interest in the interaction of *Z. tritici* with the wheat microbiome has focused on identifying antagonistic interactions which may lead to novel biocontrol agents (Kerdraon et al., 2019; Kildea et al., 2008). Understanding the mechanisms of these microbial interactions is important for understanding *Z. tritici* infection in a field context.

Despite these advances in our understanding of *Z. tritici* effector function, detailed functional analysis of many effector candidates remains to be done (Fig. 1.6; Rudd et al., 2015). This includes those identified to be conserved among *Z. tritici* isolates and display consistent expression at crucial time points during infection (Haueisen et al., 2019; Palma-Guerrero et al., 2017). For example, multiple hydrophobins have been hypothesised to have important functions in *Z. tritici* virulence, with cases of conserved expression patterns across virulent isolates (Haueisen et al., 2019) and differential expression correlated with variation in virulence between strains (Palma-Guerrero et al., 2017). Hydrophobins are known to contribute to virulence of multiple other plant pathogens through their involvement in infection-related development and surface adhesion (Quarantin et al., 2019; Talbot et al., 1996). Furthermore, characterisation of putative necrosis-inducing effectors could assist in breeding of *Z. tritici* resistance in wheat, through screening of germplasm for sensitivity to these proteins (Kettles & Kanyuka, 2016).

Investigation into the molecular determinants of *Z. tritici* virulence has also focused on the mechanisms of infection-related development. Given that filamentous growth is required for host colonisation by *Z. tritici*, studies have explored the regulation of the dimorphic switch and hyphal growth. *Z. tritici* is usually propagated *in vitro* in its ‘yeast-like’ form, which results from budding of

multicellular blastospores formed of 2-8 elongate cells separated by septa (Fig. 1.7A). However, hyphal germination can be induced *in vitro* through the application of various stressors, including oxidative stress, high temperature and nutrient deprivation (Fig. 1.7B; Francisco et al., 2019; Steinberg, 2015). This facilitates characterisation of the molecular processes involved in morphogenesis (Mehrabi, Zwiers, et al., 2006; Motteram et al., 2011). Interestingly, cell stress was recently shown to induce de-repression of regions rich in TEs, and lead to expression of many co-localised effector genes (Fouché et al., 2020). This provides a possible explanation for the mechanisms behind effector gene regulation during infection, and the observed co-regulation of these genes with *in vitro* mycelial growth (Francisco et al., 2019). Germination of *Z. tritici* spores during infection is likely triggered by starvation stress, as the leaf surface represents a nutrient-poor environment (Francisco et al., 2019).

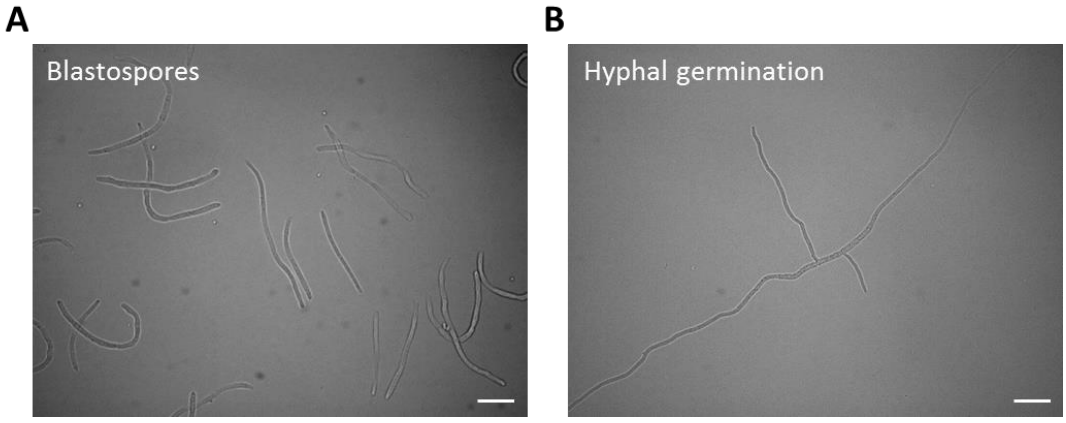


**Figure 1.7 *In vitro* growth morphologies of *Z. tritici***
(A) *Z. tritici* IPO323 blastospores grown on rich media (YPD) at 19$^{o}$C for 5 days, (B) Blastospore germinating hyphal growth from the spore apex and laterally after 24h on 2% water agar. Scale bars = 20 µm.

Functional investigation of major signalling pathways in *Z. tritici* has revealed regulatory elements controlling developmental transitions, hyphal growth and adaptation to the host environment. The MAPK MgHog1 was found to be required for germination under nutrient-limitation *in vitro* and on the leaf surface, and is therefore a necessary signalling component for pathogenicity (Mehrabi, Zwiers, et al., 2006). Similarly, deletion of MgSTE7 and MgSTE11, homologs of upstream components in the FUS3 MAPK pathway in *S. cerevisiae* (Chen & Thorner, 2007), led to defects in filamentation and loss of pathogenicity (Kramer et al., 2009). Interestingly, deletion of MgFUS3 had no impact on germination and hyphal growth, with loss of pathogenicity in this strain attributed to impaired

stomatal penetration (Cousin et al., 2006). This is consistent with the conserved role of the fungal FUS3 pathway in plant colonisation (Turrà et al., 2014), and suggests that *Z. tritici* stomatal penetration requires some level of cellular differentiation triggered by stomatal recognition. This also indicates that MgSTE7 and MgSTE11 may act in the regulation of alternate signalling pathways than through FUS3 (Kramer et al., 2009). The *Z. tritici* homolog of the MAPK Slt2, part of the *S. cerevisiae* cell wall integrity (CWI) pathway, was also found to be required for pathogenicity (Mehrabi, Van Der Lee, et al., 2006). Although germination and stomatal penetration was unperturbed in *mgslt2* mutants, subsequent colonisation of the mesophyll tissue was limited. This led authors to hypothesise that MgSlt2 regulates cell wall-remodelling required to evade and withstand the host defence response, as has been proposed for other plant pathogens (Turrà et al., 2014).

In addition to MAPK pathways, cAMP signalling has also been implicated in the regulation *Z. tritici* development during infection (Mehrabi et al., 2009; Mehrabi & Kema, 2006). The heterotrimeric guanine nucleotide-binding protein (G protein) subunits MgGpb1 and MgGpa3 were demonstrated to positively regulate cAMP production, and deletion of the encoding genes led to aberrant hyphal growth *in vitro* and abolished pathogenicity (Mehrabi et al., 2009). However, the protein kinase A (PKA) subunits MgBcy1 and MgTpk2, putatively regulated by cAMP signalling, were dispensable for development of invasive hyphae *in planta* (Mehrabi & Kema, 2006). Loss of pathogenicity in *MgBcy1* and *MgTpk2* deletion mutants was instead attributed to reduced capacity to induce necrosis and develop pycnidia in sub-stomatal cavities (Mehrabi & Kema, 2006). Furthermore, *MgGpb1* deletion led to different *in vitro* growth phenotypes to these PKA mutants, developing wavy hyphae which underwent frequent hyphal fusion (anastomosis), suggesting the involvement of this subunit in separate signalling pathways (Mehrabi et al., 2009).

Forward genetic screens have also identified genes involved in *Z. tritici* morphogenesis and hyphal growth. The alpha-1,2-mannosyltransferase MgAlg2, involved in protein N-glycosylation, was found to be required for hyphal growth on the leaf surface and therefore pathogenicity. Authors hypothesised that this enzyme is crucial for the post-translational modification and localisation of proteins involved in morphogenesis (Motteram et al., 2011). Disruption of the

glycosyltransferase gene *ZtGT2* also inhibited hyphal growth across solid surfaces, including the wheat leaf, leading to loss of pathogenicity (King et al., 2017). It was proposed that *ZtGT2* is required for the synthesis of an extracellular polysaccharide which enables *Z. tritici* to overcome frictional forces exerted on hyphae during growth on solid surfaces (King et al., 2017). Furthermore, Yemelin et al., (2017) conducted a mutagenesis screen for loci involved in hyphal morphogenesis, identifying a number of genes involved in various cellular processes. This included another member of the Hog1 MAPK pathway ZtSSK1, as well as the *de novo* purine biosynthesis enzyme Ade5,7p (Yemelin et al., 2017).

Many of the genes found to be crucial for *Z. tritici* development have conserved functions across the fungal plant pathogens (Turrà et al., 2014; Yemelin et al., 2017), and likely between *Z. tritici* isolates. They therefore represent promising targets for novel control strategies against STB and other fungal diseases. However, many gaps still remain in our understanding of the regulation of cellular development and infection in *Z. tritici*. This includes the identity of downstream targets of the cAMP and MAPK signalling cascades that have been identified as important to infection. Moreover, investigation of further components of these pathways is required, in order to build a coherent model of this complex signalling network and how it contributes to development during *Z. tritici* infection.

### 1.3.6 Current knowledge gaps in *Z. tritici* infection

Despite dramatic advances in our understanding of *Z. tritici* infection at a molecular level, fundamental questions still remain about the infection strategy of this pathogen (Brennan et al., 2019; Sánchez-Vallet et al., 2015). The first of these ponders what causes the transition to necrotrophic growth, and what adaptive advantage is gained from such a long symptomless phase? Despite the identification of many genes upregulated during the transition to necrotrophy (Haueisen et al., 2019; Rudd et al., 2015), functional characterisation of these genes is yet to confirm the requirement of any effectors, metabolites or cellular processes in triggering this important infection checkpoint (Mirzadi Gohari et al., 2015; Rudd et al., 2015). Although three *Z. tritici* effectors have been shown to induce necrosis in wheat (Ben M'Barek et al., 2015; Kettles et al., 2018), none

have been shown to confer a quantitative contribution to virulence. This is likely a result of high functional redundancy between factors inducing necrosis (Rudd et al., 2015). Considering the resemblance of the necrosis induced by *Z. tritici* to the HR characteristic of gene-for-gene resistance to biotrophic pathogens (Keon et al., 2007; Rudd et al., 2008), the existence of an effector or toxin which specifically interacts with defence-related host receptor to hijack the host defence response has been suggested (Hammond-Kosack & Rudd, 2008). Future characterisation of the conserved effectors and secondary metabolite clusters may elucidate the existence of such a factor. Furthermore, little is understood about the regulation of this switch to necrotrophy, both in terms of the stimuli causing this transition and the intracellular pathways controlling the dramatic transcriptional shift observed.

It has been speculated that the long symptomless phase represents a lasting remnant of the previous endophytic lifestyle of *Z. tritici* (Sánchez-Vallet et al., 2015). One hypothesis for the adaptive function of the latent phase postulates that symptomless colonisation maximises fitness by allowing the fungus to achieve a “critical biomass” before inducing necrosis in the leaf (Brennan et al., 2019; Lee et al., 2015). Indeed, truncation of the latent phase through silencing of host homeodomain protein, TaR1, led to reduced pycnidiospore production (Lee et al., 2015). However, other studies have found that inter-strain variation in the length of the latent period and the extent of mesophyll colonisation during symptomless infection, does not necessarily correlate with reproductive fitness (Haueisen et al., 2019), although this may be a result of the high inoculum densities used in this study. It is feasible that some degree of colonisation whilst suppressing host defence is required for *Z. tritici* to establish a foothold in the leaf, before hijacking the wheat PCD response to complete its reproductive cycle. Subsequent variation in this latent period may represent the results of complex life history trade-offs. For example, the ability to spread extensive invasive hyphae in the mesophyll layer from the point of penetration may increase the number of accessible stomata for asexual sporulation, which may be particularly important during early stages of an epidemic when inoculum levels are low. Furthermore, genotypes showing reduced latent phases may produce fewer asexual spores per infection cycle, but have the ability to undergo more infection cycles in a growing season.

The second major unanswered question regards the source of nutrients utilised by *Z. tritici* during symptomless colonisation, and its controversial classification as a hemibiotroph (Sánchez-Vallet et al., 2015). The lack of specialised intracellular feeding structures, as well as the low expression of secreted hydrolytic enzymes and upregulation of genes involved in lipid metabolism during early infection, suggests that *Z. tritici* relies on internal nutrient stores rather than extracellular plant-derived nutrients during the symptomless phase (Rudd et al., 2015; Sánchez-Vallet et al., 2015). It has been proposed that the few secreted PCWDEs, proteases and lipases that are expressed during symptomless colonisation could contribute to accessing nutrients in the apoplast (Goodwin et al., 2011; Palma-Guerrero et al., 2016; Sánchez-Vallet et al., 2015). However, these enzymes do have other potential functions. Cutinases and lipases could assist in spore adhesion and surface sensing, as demonstrated in other plant pathogens (Deising et al., 1992; Skamnioti & Gurr, 2007), or could facilitate access to the epidermal cell surface for secreted *Z. tritici* effectors (Kettles et al., 2017). Secreted proteases may function in detoxification of plant defence proteins (Palma-Guerrero et al., 2016), such as those identified in *Fusarium sp.* (Jashni et al., 2015; Naumann et al., 2011), while PCWDEs may facilitate apoplastic growth of *Z. tritici* hyphae, as has been proposed for the function of such enzymes expressed by biotrophic pathogens (Spanu & Kämper, 2010).

Moreover, considering the extent of hyphal growth observed *in vitro* without external nutrient sources (Francisco et al., 2019; King et al., 2017), it is unlikely that degradation of host tissues is required for invasive hyphal growth. Neutral lipid staining has demonstrated the high content of lipid droplets in *Z. tritici* spores, which is reduced in hyphae (Francisco et al., 2019), suggesting that the breakdown of these storage molecules occurs during hyphal germination. However, although the expression profiles of various genes related to lipid metabolism has been reported (Rudd et al., 2015), direct evidence for the requirement of lipid metabolism in *Z. tritici* infection has not been demonstrated. Furthermore, investigation is required into the cellular mechanisms involved in remobilising stored macromolecules in the *Z. tritici* spore during early infection.

## 1.4 The scope of the thesis

The work in this thesis aims to further elucidate the cellular processes involved in *Z. tritici* infection of wheat. In order to understand the mechanisms involved in *Z. tritici* nutrient acquisition during symptomless colonisation, the role of autophagy in recycling stored macromolecules during development and infection was investigated (Chapter 3). Also to this end, various components of the lipid metabolism machinery in *Z. tritici* were functionally characterised, including enzymes involved in fatty acid β-oxidation, to assess the importance of utilising lipids for host colonisation (Chapter 4).

To complement these reverse genetics analyses, a forward genetic approach was also taken to identify genetic elements contributing to *Z. tritici* development and virulence. Investigation of T-DNA insertion mutants with attenuated virulence revealed disruption of the CWI pathway MAPK kinase kinase gene *ZtBCK1* and the adenylate cyclase gene (*ZtCYR1*) responsible for cAMP synthesis (Chapter 5). Subsequent transcriptomic analysis of knockout mutants in these genes was implemented to advance our understanding of infection-related signalling in *Z. tritici*. Finally, this thesis presents genomic and transcriptomic characterisation of a spontaneous laboratory mutant, which displays an unusual cellular morphology, aberrant filamentation and reduced virulence (Chapter 6).

# Chapter 2
# **Materials and Methods**

## 2.1 Microbial strains and growth conditions

All growth media for microbial cultures was prepared with MilliQ water using the recipes detailed in Table 2.1. Media was sterilised by autoclaving for 15 min at 121$^{o}$C and 0.1MPa and antibiotics were filter sterilised before being added to cooled media.

**Table 2.1 Growth media recipes**

| *Growth Medium* | *Component* | *Concentration* |
|---|---|---|
| *Yeast Extract–Peptone–Dextrose (YPD)* | Yeast extract | 10 g/L |
| | Bacteriological peptone | 20 g/L |
| | Glucose | 20 g/L |
| | Agar | 20 g/L |
| *Aspergillus minimal medium (AMM) (pH 6.5 with KOH)* | $NaNO_3$ | 6 g/L |
| | KCl | 0.52 g/L |
| | $MgSO_4.7H_2O$ | 0.52 g/L |
| | $KH_2PO_4$ | 1.52 g/L |
| | $ZnSO_4.7H2O$ | 2.2 mg/L |
| | $H_3BO_3$ | 1.1 mg/L |
| | $MnCl_2.4H2O$ | 0.5 mg/L |
| | $FeSO_4.7H2O$ | 0.5 mg/L |
| | $CoCl_2.5H2O$ | 0.16 mg/L |
| | $CuSO_4.5H2O$ | 0.16 mg/L |
| | $(NH_4)_6Mo_7O_{24}.4H2O$ | 0.11 mg/L |
| | $Na_4EDTA$ | 5 mg/L |
| | Glucose | 10 g/L |
| | Agar (for solid) | 20 g/L |
| *Basal medium (BM) (pH 6 with $Na_2HPO_4$)* | Asparagine | 2 g/L |
| | Yeast nitrogen base w/o amino acids or $NH_4SO_4$ | 1.7 g/L |
| | $NH_4NO_3$ | 1 g/L |
| | Glucose | 10 g/L |
| | Agar | 20 g/L |
| *Induction medium (IM) (pH 5.6 with NaOH)* | $K_2HPO_4$ | 10 mM |
| | $KH_2PO_4$ | 10 mM |
| | NaCl | 2.5 mM |
| | $MgSO_4.7H_20$ | 2 mM |
| | $CaCl_2$ | 0.7 mM |
| | $FeSO_4$ | 10 µM |
| | $(NH_4)_2SO_4$ | 4 mM |
| | Glucose | 10 mM |
| | Glycerol | 0.5% (w/v) |
| | MES buffer | 40 mM |
| | Agar (for solid) | 20 g/L |
| *Synthetic complete without uracil (SC-URA)* | Yeast nitrogen base w/o amino acids (Formedium, UK) | 6.9 g/L |
| | Complete amino acid supplement w/o Uracil (Formedium, UK) | 790 mg/L |
| | Glucose | 20 g/L |
| | Agar (for solid) | 20 g/L |
| *Potato dextrose broth/agar (PDA/PDB)* | Potato dextrose broth (Sigma-Aldrich, UK) | 24 g/L |
| | Agar (for soild) | 20 g/L |
| *Lysogeny broth (LB)* | LB Broth (Miller) (Sigma-Aldrich, UK) | 25 g/L |
| | Agar (for solid) | 15 g/L |

| | | |
|---|---|---|
| *V8 juice (V8)* | V8® Original vegetable juice (clarified by centrifugation) | 200 ml/L |
| | $CaCO_3$ | 3 g/L |
| | Agar | 20 g/L |

The reference *Z. tritici* strain IPO323 was used in this study, isolated from a Dutch field of wheat (cultivar Arminda) in 1984 and subject of the first fully assembled genome sequence of the species (Goodwin et al., 2011). Additionally, a minority of mutants were generated in the strain *Δku70* (Bowler et al., 2010), generated from IPO323 through deletion of the gene *KU70* (ZtritIPO323_04g07374) involved in the non-homologous end joining pathway for repairing double stranded breaks in DNA. Blastospores of *Z. tritici* strains were stored long-term in suspensions of 50% glycerol at -80$^{o}$C. *Z. tritici* blastospores were routinely cultured on YPD agar at 19$^{o}$C under darkness for 5 days before use in transformations, infection experiments and *in vitro* phenotypic assays.

The *Saccharomyces cerevisiae* strain BY4741 was used for plasmid construction, and was cultured on YPD or SC-URA at 30$^{o}$C, with 180 rpm shaking for liquid cultures. Plasmid amplification was carried out using the *Escherichia coli* strain DH5α, which was cultured using LB broth or agar at 37$^{o}$C, with 180 rpm shaking for liquid cultures. *Z. tritici* transformations were carried out using *Agrobacterium tumefaciens* strain EHA105, which contains chromosomal resistance to rifampicin and the tumour-inducing plasmid pTiBo542DT-DNA, containing the virulence genes required for transfer of T-DNA to hosts during transformation (Hellens et al., 2000). *A. tumefaciens* was grown at 28$^{o}$C on LB supplemented with 100 µg/ml rifampicin, with 220 rpm shaking for liquid cultures.

## 2.2 Plasmid construction and amplification

### 2.2.1 Plasmid backbones and selective markers

Transformation vectors were constructed using the suite of plasmids developed previously by Sidhu et al., (2015). These vectors contain the required components for selection and amplification in *S. cerevisiae*, *E.coli* and *A. tumefaciens* (Fig. 2.1). They also contain selective marker cassettes between T-DNA border repeats that confer resistance to hygromycin B (pC-HYG-YR;

Addgene ID – 61765), sulfonylurea (pC-SUR-YR; Addgene ID – 61768) and glufosinate ammonium (pC-BAR-YR; Addgene ID – 61766) when transformed into *Z. tritici*. Using this range of selective markers allowed for consecutive transformations of *Z. tritici*, enabling generation of multiple gene deletion, knockout complementation and fusion protein expression within the same strain.

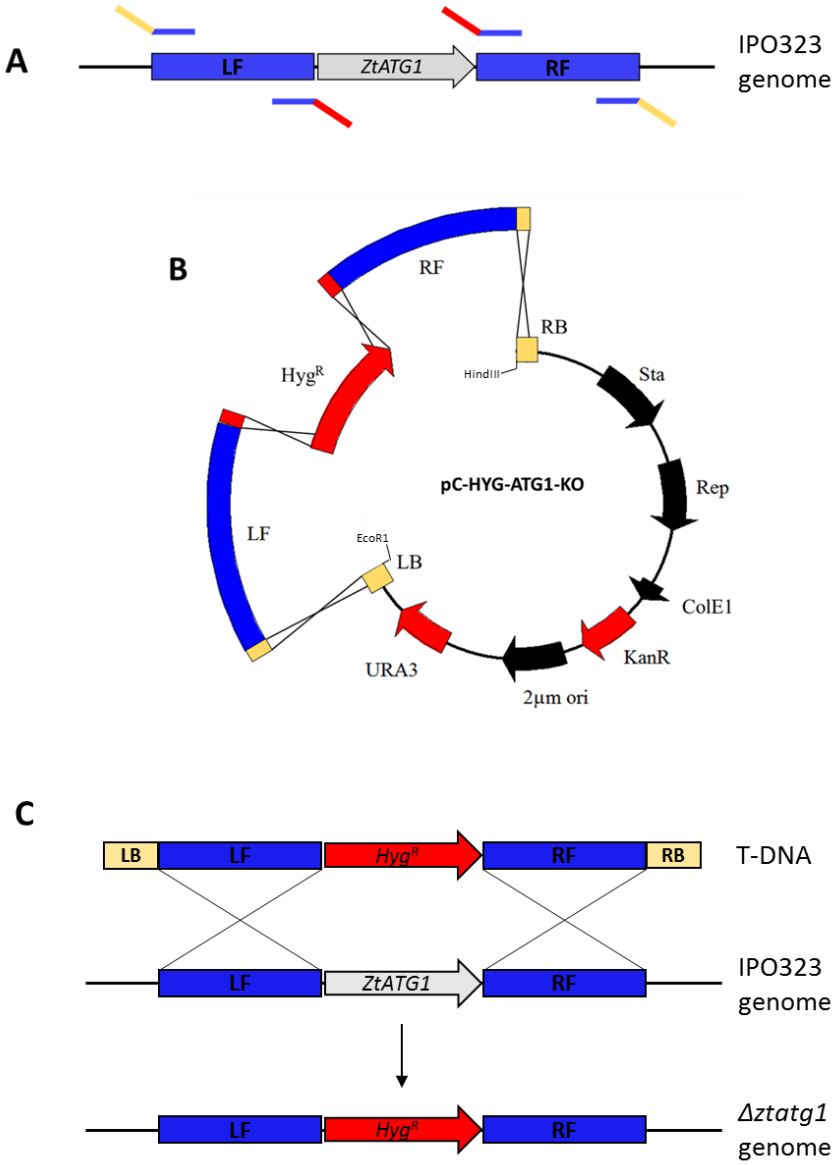


**Figure 2.1 Construction of plasmids by recombination in yeast for targeted insertion into the *Z. tritici* genome, using deletion of *ZtATG1* as an example.**
(A) Amplification of flanking regions (LF and RF) from *Z. tritici* genomic DNA used to target T-DNA to the desired locus. Primers used contain 5' extensions overlapping with the T-DNA border sequences (yellow) and selective marker region (red) (B) Insertion of flanking sequences into the digested plasmid backbone by homologous recombination in yeast. Plasmid contains ColE1 origin of replication, *RepA* replication protein, *StaA* stability protein and *KanR* kanamycin resistance marker for bacterial propagation, and *URA3* selective marker and 2µ origin of replication for *S. cerevisiae* propagation (C) Insertion of the hygromycin resistance ($Hyg^R$) selective marker by homologous recombination after transfer of T-DNA into *Z. tritici* nuclei by *Agrobacterium*-mediated transformation.

Selective markers were delivered to specific loci within the *Z. tritici* genome through insertion of T-DNA sequences by homologous recombination (Fig. 2.1). To achieve this, flanking sequences complimentary to regions up- and downstream of the target locus were cloned on either side of the selective marker within the T-DNA repeats of the chosen vector (Fig. 2.1A-B). Upon insertion of the T-DNA into *Z. tritici* nuclei, these flanking sequences anneal to complementary sequences in the genome and instigate insertion of the selective marker by homologous recombination (Fig. 2.1C).

### 2.2.2 Yeast recombinational cloning

Plasmid vectors for transformation of *Z. tritici* were constructed by recombinational cloning in *S. cerevisiae*, using methods similar to those described previously (Collopy et al., 2010; Sidhu, Cairns, et al., 2015). Flanking sequences to be incorporated into plasmids were amplified by PCR using primers with 5' extensions of 29 bp (Fig. 2.1A). These 5' extensions were designed to overlap with the terminal sequences of fragments to be inserted at adjacent positions in the vector (Fig. 2.1B). PCR amplified fragments were co-transformed into *S. cerevisiae* alongside the aforementioned plasmid vectors which had been linearised by restriction digestion with EcoR1 and HindIII. Upon co-transformation, these overlapping fragments assembled by homologous recombination to yield the complete plasmid (Fig. 2.1B).

### 2.2.3 Transformation of *S. cerevisiae*

Transformation of *S. cerevisiae* was achieved using a protocol adapted from Gietz & Woods (2002). An overnight culture was prepared by inoculating 5 ml of YPD broth with a single colony of *S. cerevisiae*. After incubation for 12 h, 2 ml of the overnight culture was diluted in 48 ml YPD broth in a sterile conical flask and incubated for a further 5 h. *S. cerevisiae* cells were harvested by centrifugation in a 50 ml falcon tube at 3000 x G for 5 min, before being washed with 50 ml sterile deionised water (SDW). After repeating the centrifugation, the cell pellet was washed with 1 ml of sterile 0.1M lithium acetate (LiOAc) and transferred to a 1.5 ml centrifuge tube. Cells were pelleted at 13,000 rpm for 15 s, the supernatant was removed, and the pellet resuspended in 400 µl sterile 0.1M LiOAc.

DNA fragments to be transformed into *S. cerevisiae* were combined in a 1.5 ml centrifuge tube at a final volume of 34 µl. This included 200 ng of the linearised plasmid and 500 ng of each purified PCR product. This DNA mix was combined with 50 µl of single-stranded salmon sperm DNA (2 mg/ml in Tris-EDTA (TE) buffer pH 8; denatured for 5 min at 95ºC and cooled on ice), 50 µl *S. cerevisiae* cell suspension, 36 µl of sterile 1M LiOAc and 240 µl of sterile 50% (w/v) polyethylene glycol 3000, and the resulting suspension was mixed by pipetting. The transformation mix was incubated for 30 min at 30ºC before being transferred to a 42ºC water bath for 15 min. Following heat shock, the transformation mix was centrifuged at 6000 rpm for 15 s, the supernatant was removed and the cell pellet was resuspended in SDW. The cell suspension was plated on SC-URA agar plates and incubated for 3 days at 30ºC.

### 2.2.4 Plasmid extraction from yeast

*S. cerevisiae* colonies were screened for correct assembly of fragments by colony PCR using alkaline lysis. A small amount of cells was harvested from a colony using a 10 µl pipette tip and suspended in 20 µl of 20 mM NaOH. Cells were lysed by incubation at 96ºC for 20 min, before the cell debris was pelleted by centrifugation and 1 µl of the supernatant was used in a 25 µl PCR reaction.

Once identified, a colony containing a fully assembled plasmid was inoculated into 10 ml SC-URA broth and incubated overnight. Plasmid DNA was extracted using a QAIprep spin miniprep kit (Qaigen, UK) in combination with lyticase enzymatic digestion of the cell wall (Singh and Weil 2002). In brief, a 5 mg/ml lyticase solution was prepared using lyticase from Arthrobactor luteus (Sigma-Aldrich, UK) in 100 mM sodium phosphate buffer (pH 7.4) containing 1.2M sorbitol. Cells were harvested by centrifugation at 3000 x G for 5 min and cell pellet was suspended in 200 µl of Buffer P1 and 100 µl lyticase solution. After incubation for 30 min at 37ºC, 300 µl Buffer P2 was added and the suspension was incubated for 10 min at room temperature. Following addition of 420 µl Buffer N3, the plasmid was isolated following the QAIprep spin miniprep kit protocol and eluted in 30 µl TE buffer.

### 2.2.5 Amplification of plasmids in *E. coli*

In order to amplify the plasmids constructed in *S. cerevisiae*, they were transformed into *E. coli* chemically competent cells. Competent *E. coli* cells

were prepared by washing cells with $CaCl_2$. An overnight culture of *E. coli* was prepared by inoculating 5 ml of LB with *E. coli* straight from glycerol stock. The overnight culture was diluted 100-fold in 100 ml LB in a conical flask and grown until the $OD_{600}$ reached 0.48. Reagents and cell cultures were cooled on ice for 20 min before cells were pelleted by centrifugation at 4$^{o}$C and 3000 x G for 5 minutes. The supernatant was discarded and the cells were resuspended in 20 ml ice-cold 100mM $CaCl_2$, before incubating on ice for 20 min. Centrifugation was repeated and the resulting pellet was resuspended in 5 ml ice-cold 100mM $CaCl_2$ amended with 15% glycerol. Competent cells were stored at -80$^{o}$C.

For transformation, competent *E coli* cells were thawed on ice and a 50 µl aliquot was mixed with 10 µl of plasmid isolated from *S. cerevisiae*. After incubation on ice for 30 min, cells were submitted to heat shock at 42$^{o}$C for 30 sec in a water bath and replaced on ice for 5 min. *E. coli* cells were allowed to recover by addition of 200 µl LB and incubation for 2 h at 37$^{o}$C with 180 rpm shaking. Cell suspensions were plated out on LB agar plates amended with 100 µg/ml kanamycin and incubated overnight. A single colony was inoculated into 5 ml LB containing 100 µg/ml kanamycin incubated overnight, before plasmid DNA was extracted using QAIprep spin miniprep kit (Qaigen, UK) following the manufacturers protocol. The fidelity of flanking sequence cloning was confirmed by Sanger sequencing through the Eurofins Genomics Mix2Seq service, using Seq1-F/Seq2-R and HYF-F/Seq-4-R for the left and right flanks of pC-HYG-YR-based vectors, Seq1-F/Seq2-R and BAR_END_F/Seq-4-R for the left and right flanks in pC-BAR-YR-based vectors and Seq1-F/ SUR_INT_R and SUR_END_F/Seq-4-R for the left and right flanks in pC-SUR-YR-based vectors.(Table 2.2).

### 2.2.6 Transformation of *A. tumefaciens*

Constructed plasmids were transformed into *A. tumefaciens* prior to *Agrobacterium*-mediated transformation of *Z. tritici*. To prepare competent cells, *A. tumefaciens* was grown overnight in 5 ml LB. A 2 ml aliquot of this overnight culture was diluted in 48 ml of the same media in a sterile conical flask and incubated until the $OD_{600}$ reached 0.6. After cooling on ice for 5 min, the cells were pelleted by centrifugation at 3000 x G for 5 min at 4$^{o}$C. The pellet was resuspended in 1 ml of 20mM $CaCl_2$ and 50 µl aliquots were stored at -80$^{o}$C.

For transformation, 50 µl aliquots of competent *A. tumefaciens* cells were thawed on ice before 10 µl of plasmid DNA was added and mixed gently. Transformation mixtures were then snap frozen in liquid nitrogen before undergoing heat shock in a water bath at 37$^{o}$C for 5 min. Cells were then allowed to recover by addition of 500 µl LB and incubation at 28$^{o}$C for 3 h with 220 rpm shaking, before plating onto LB agar amended with 100 µg/ml rifampicin and 100 µg/ml kanamycin and incubation for 2 days.

## 2.3 *Agrobacterium tumefaciens*-mediated transformation of *Z. tritici*

*Agrobacterium tumefaciens*-mediated transformation (*At*MT) was carried out following a protocol adapted from Zwiers & De Waard (2001). A single colony of *A. tumefaciens* was inoculated into 5 ml LB containing 100 µg/ml rifampicin and 100 µg/ml kanamycin and grown overnight. The overnight culture was diluted to an $OD_{600}$ of 0.09 in 10 ml induction medium (IM) amended with 40 µg/ml acetosyringone and 100 µg/ml kanamycin, and grown for 2-3 h until the $OD_{600}$ reached 0.2-0.24. *Z. tritici* cells were harvested from YPD agar and suspended in water, before being filtered through a 100 µm sterile cell strainer and diluted to a concentration of $5x10^5$ spores/ml. Equal volumes of *A. tumefaciens* and *Z. tritici* cells were mixed by gentle pipetting before 150 µl of the mixture was inoculated onto an IM agar plate covered by a nitrocellulose disc and incubated at 19$^{o}$C for 2 days. Following co-incubation of *A. tumefaciens* and *Z. tritici*, nitrocellulose discs were transferred onto either AMM containing 200 µg/ml hygromycin B or 200 µg/ml glufosinate ammonium or BM containing 10 µg/ml sulfonylurea, depending on the resistance cassette used. Selection plates also contained 250 µg/ml cefotaxime, 100 µg/ml streptomycin and 100 µg/ml ampicillin to inhibit further growth of *A. tumefaciens*.

## 2.4 Nucleic acid extraction and manipulation

### 2.4.1 Rapid DNA extraction for PCR

DNA was extracted for cloning and diagnostic PCR following a protocol adapted from that reported by Liu et al. (2000). A small amount of mycelium or yeast-like cells was collected using an inoculation loop and suspended in 500 µl lysis buffer (400 mM Tris-HCl pH 8.0, 60 mM ethylenediaminetetraacetic acid (EDTA;

pH 8.0), 150 mM NaCl, 1% sodium dodecyl sulfate) amended with 50 µg/ml of RNAse A. Cell lysis and RNA degradation was allowed to proceed during incubation for 1 h at 37ºC with 180 rpm shaking. Subsequently, 150 µl of potassium acetate solution (pH 4.8; 3M potassium acetate, 11.5% v/v glacial acetic acid) was added and the tube vortexed, before centrifugation for 3 min at 13,000 x G to pellet the cell debris and precipitated proteins. The supernatant was added to an equal volume of isopropanol, mixed gently and centrifuged at 13,000 x G for 10 min. The supernatant was discarded and the pellet washed with 300 µl of 70% ethanol, before a final centrifugation at 13,000 x G for 3 min and removal of the supernatant. The DNA pellet was dried at 37ºC and resuspended in 20-80 µl TE buffer (10mM Tris, 1mM EDTA [pH 8.0]) depending on the size of the pellet.

### 2.4.2 Extraction of high quality DNA for whole genome resequencing

To extract high quality DNA for Illumina sequencing, 100 mg fresh weight of yeast-like cells was collected from *Z. tritici* culture on YPD agar and snap frozen in liquid nitrogen. The sample was ground into a fine powder in a pestle and mortar. DNA was extracted using the illustra™ Nucleon Phytopure Genomic DNA Extraction Kit (GE Healthcare, UK) following the manufacturers protocol, including the RNAse A digestion step. The resulting DNA pellet was dissolved in HyClone™ water (GE Healthcare, UK). Extracted DNA was then further purified using the DNeasy Plant Mini Kit (Qiagen), before the eluted sample was centrifuged for 2 min at 1000 x G and the supernatant taken forward for DNA quantification using a Qubit™ dsDNA BR Assay Kit (Fisher Scientific, UK).

### 2.4.3 Polymerase chain reaction

PCRs were carried out using Phusion® High-Fidelity DNA Polymerase (New England Biolabs, UK). PCR was carried out following the manufacturer's protocol. The sequences of primers used in PCRs are listed in Table 2.2.

### 2.4.4 Restriction digestion

Restriction digestion of plasmids was implemented using HindIII-HF® and EcoRI-HF® enzymes (New England Biolabs, UK) in 50 µl reactions with CutSmart® Buffer. Double digestion of 1 µg of plasmid DNA was carried out overnight at 37ºC before reactions were terminated by incubation at 80ºC for 2 min. The complete digestion of plasmids was confirmed by gel electrophoresis.

### 2.4.5 Gel electrophoresis

Electrophoresis was carried out using agarose gels made with 1xTris-Acetate-EDTA (TAE) buffer, which was used as the running buffer. DNA electrophoresis was run on 1% agarose gels amended with SYBR$^{TM}$ Safe DNA gel stain (Thermo-Fisher Scientific). Samples were loaded using 6X Gel Loading Dye (New England Biolabs, UK) and fragment sizes assessed using 1 kb DNA Ladder (New England Biolabs, UK). Denaturing RNA electrophoresis samples were prepared by diluting 4 µl of extracted RNA with 12 µl formamide solution (Sigma-Aldrich), 0.5 µl of SYBR$^{TM}$ Safe DNA gel stain and 3.5 µl 6X loading dye. These samples were denatured at 65$^{o}$C for 5 min and immediately transferred to ice for 5 min, before being loaded onto 1.2% agarose gels.

**Table 2.2 Primers used in this study**

| Primer name | Sequence (5'–3') |
|---|---|
| **ZtATG1_LF_F** | CTAGGCCACCATGTTGGGCCCGGCGCGCCAATGGCGAAGAATGTAGCAA |
| **ZtATG1_LF_R** | TCCTTCAATATCAGTTGGGTACCGAGCTCGATGGCGGTAGTGTTGTTGT |
| **ZtATG1_RF_F** | GATCCTCTAGAGTCGACCTGCAGGCATGCGCAAGGATGACTCGCTAGTC |
| **ZtATG1_RF_R** | GTCAGATCTACCATGGTGGACTCCTCTTATCGGCTGGAGATGACAGTAC |
| **ZtATG8_LF_F** | CTAGGCCACCATGTTGGGCCCGGCGCGCCGATGGCTTACTGGGCACAAC |
| **ZtATG8_LF_R** | TCCTTCAATATCAGTTGGGTACCGAGCTCGTTGGCGATGTGTGTTGTGG |
| **ZtATG8_RF_F** | GATCCTCTAGAGTCGACCTGCAGGCATGCACGCCACCTAACATCGACAC |
| **ZtATG8_RF_R** | GTCAGATCTACCATGGTGGACTCCTCTTAGACAGCGAGGTGAAACTTCG |
| **ZtATG1_EXT_F** | GAGTTATTCACTAGGTGCGCGG |
| **ZtATG1_INT_R** | TCGCCACCACTCGACTTCAT |
| **ZtATG8_EXT_F** | ACTCCTCACTCCTCCACTCC |
| **ZtATG8_INT_R** | TCTCGCAAATGACCTTCACG |
| **ZtGFP_F** | ATGGTCTCCAAGGGCGAGGA |
| **ZtGFP_R** | CTTGTAGAGCTCGTCCATGC |
| **ZtATG8_LF_GFP_R** | GTGAAGAGCTCCTCGCCCTTGGAGACCATGTTGGCGATGTGTGTTGTGG |
| **ZtATG8_GFP_F** | GCATGGACGAGCTCTACAAGGCGGCGGCGATGCGCTCCAAGTTCAAGGA |
| **ZtATG8_TERM_R** | TCCTTCAATATCAGTTGGGTACCGAGCTCTGCTGTGGCGCGGTCGTAAA |
| **ZtATG8_RF2_F** | GATCCTCTAGAGTCGACCTGCAGGCATGCGCGTGTCTGACCGCCAACTT |
| **ZtATG8_RF2_R** | GTCAGATCTACCATGGTGGACTCCTCTTAGAGTGCTGCTCGTCTGTCTT |
| **ZtEch1_LF_F** | CTAGGCCACCATGTTGGGCCCGGCGCGCCGAACGAGAGCAGAAAACGTA |
| **ZtEch1_LF_R** | TCCTTCAATATCAGTTGGGTACCGAGCTCTGTGAGTAAGCTGATCACAA |
| **ZtEch1_RF_F** | GATCCTCTAGAGTCGACCTGCAGGCATGCGGGAGAATGTCACAATGAAT |
| **ZtEch1_RF_R** | GTCAGATCTACCATGGTGGACTCCTCTTAGTGGCGCGTAAGTATCTCAA |
| **ZtEch1_INT_R** | GTTCAACTGGGGAGGTGTTA |
| **ZtEch1_EXT_F** | GAGCCGGTATTTGTGATCAG |
| **ZtEch1_F** | ATGTTGGCATCAAGACTCCG |
| **ZtEch1_R** | TCATCTGTGAACCCACTCCG |
| **ZtEch1_LF2_F** | CTAGGCCACCATGTTGGGCCCGGCGCGCCCGCTGAGCACATGCATCACC |

| | |
|---|---|
| **ZtEch1_LF2_R** | TCCTTCAATATCAGTTGGGTACCGAGCTCCCATCGACGGTGCTGCGATC |
| **ZtEch1_PROM_F** | GATCCTCTAGAGTCGACCTGCAGGCATGCGAAGTCGTCGGTCTAGAGAT |
| **ZtMFP1_LF_F** | CTAGGCCACCATGTTGGGCCCGGCGCGCCGAGTTTGAGTTGGGTCGGTT |
| **ZtMFP1_LF_R** | TCCTTCAATATCAGTTGGGTACCGAGCTCGTTTGTGGATGTGAGAGGAA |
| **ZtMFP1_RF_F** | GATCCTCTAGAGTCGACCTGCAGGCATGCTTTCGAAGATGTGTTTGGCG |
| **ZtMFP1_RF_R** | GTCAGATCTACCATGGTGGACTCCTCTTAGATGGGGTTGCCGAGTAGTT |
| **ZtMFP2_LF_F** | CTAGGCCACCATGTTGGGCCCGGCGCGCCATCTACGACCTCCATTCCCC |
| **ZtMFP2_LF_R** | TCCTTCAATATCAGTTGGGTACCGAGCTCTTCGAGAGAGCTCCGAGTAT |
| **ZtMFP2_RF_F** | GATCCTCTAGAGTCGACCTGCAGGCATGCTGGGTGTGAGGAGGGGAAGT |
| **ZtMFP2_RF_R** | GTCAGATCTACCATGGTGGACTCCTCTTAAACATCATCCGGACGTGTCT |
| **ZtMFP1_EXT_F** | CCATTCCTCCTCAGGGACTC |
| **ZtMFP1_INT_R** | GTGGTGTATATCCCTCCTCC |
| **ZtMFP2_INT_F** | GGTATCCGAGTGTGGAGGAT |
| **ZtMFP2_EXT_R** | GCGAACGTTTTGAGATGGAC |
| **ZtBCK1_del_seq_F** | GCGCATACACATACGACCTC |
| **ZtBCK1_del_seq_R** | GCGCGACTGACTTTGTGATT |
| **ZtBCK1_insert_seq_F** | TAGCTTCGCCGCTACGTTTC |
| **ZtBCK1_insert_seq_R** | AGGTATGTAGCCTCCGACGG |
| **ZtBCK1_LF_F** | CTAGGCCACCATGTTGGGCCCGGCGCGCCGCGATGAAGATTGACACGCT |
| **ZtBCK1_LF_R** | TCCTTCAATATCAGTTGGGTACCGAGCTCGTTCGCTGAATCTGCCTTTC |
| **ZtBCK1_RF_F** | GATCCTCTAGAGTCGACCTGCAGGCATGCCGCAGCATAGGAAAGTGTATGG |
| **ZtBCK1_RF_R** | GTCAGATCTACCATGGTGGACTCCTCTTACTCCTTTGATGTCCGGGACT |
| **ZtBCK1_EXT_F** | TGGATTACCCGCAGAGCAAG |
| **ZtBCK1_INT_R** | TCGGAGCAGATTCCTGTCTC |
| **ZtCYR1_SNP_seq_F** | GAACAGCACGATCTTGTGGG |
| **ZtCYR1_SNP_seq_R** | CGTTGGACTTCCTGGATGAA |
| **ZtCYR1_LF_F** | CTAGGCCACCATGTTGGGCCCGGCGCGCCCCGAACAATCTCCCAGCTAC |
| **ZtCYR1_LF_R** | TCCTTCAATATCAGTTGGGTACCGAGCTCCCATCGAGGCTCAGCGGATT |
| **ZtCYR1_RF_F** | GATCCTCTAGAGTCGACCTGCAGGCATGCGCAGTCGTCGGATGCCTGAC |
| **ZtCYR1_RF_R** | GTCAGATCTACCATGGTGGACTCCTCTTACACACATCGCGAACACACAC |
| **ZtCYR1_EXT_F** | GGTGAATAGGCGTGCAGATG |
| **ZtCYR1_INT_R** | CTGAACCATCCTCCTGCGAA |
| **Seq1-F** | TGCGGACGTTTTTAATGTAC |
| **Seq4-R** | GTAATTCACACGTGGTGGTG |
| **Seq2-R** | TTGTTGACCTCCACTAGCTC |
| **HYG-R** | TATTCCTTTGCCCTCGGACGA |
| **HYG-F** | CTCTTCTGGAGGCCGTGGT |
| **HYG-F2** | ATGAAAAAGCCTGAACTCACCG |
| **BAR_END_F** | TTTCTGGCAGCTGGACTTCA |
| **SUR_INT_R** | GCTCGCTCGTGATTCTGACT |
| **SUR_END_F** | GCAAGGATAAGCAACGGAGA |

## 2.5 Bioinformatics analysis

The fully assembled *Z. tritici* genome (Goodwin et al., 2011) was downloaded from Ensembl Fungi (http://fungi.ensembl.org/Zymoseptoria_tritici/Info/Index), with all gene models taken from the latest Rothamsted Research annotation (King et al., 2017). All short read sequence alignments were carried out using genome indices prepared with this annotation. Short read alignments were indexed using the SAMtools *index* function (Li et al., 2009) and visualised using the Integrative Genomics Viewer (IGV) program (version 2.7.0).

Whole genome resequencing was carried out by BGI Tech Solutions Co., Ltd. (Hong Kong) using their BGISEQ-500 platform for paired-end 150 bp reads. Sequencing reads were trimmed with fastp (S. Chen et al., 2018) using the parameters '--cut_tail --cut_tail_mean_quality=20 --detect_adapter_for_pe --length_required=75', and aligned with the IPO323 genome with Bowtie 2 version 2.3.4.1 using --local mode (Langmead & Salzberg, 2012). Single nucleotide polymorphisms (SNPs) and indels were detected in the genome sequences via a Galaxy pipeline (https://usegalaxy.org/), using FreeBayes for variant calling (Garrison & Marth, 2012). The workflow used, including specified parameters, is described in Supplementary Methods. Polymorphisms were validated by inspection using the Integrative Genomics Viewer (IGV; Thorvaldsdóttir et al., 2013). The resulting polymorphisms were filtered to exclude those present in the isogenic IPO323 strain (also resequenced here) and identify those unique to the strains of interest.

The *Z. tritici* genome was mined for gene homologs using BlastP algorithm on the Ensembl BLAST tool (https://fungi.ensembl.org/Zymoseptoria_tritici/Tools/Blast). To analyse sequence identity across the whole protein, pairwise sequence alignments were carried out with the full length predicted protein sequences of resulting hits using the BlastP algorithm. Multiple sequence alignments were carried out using the M-Coffee program (Tommaso et al 2011), with figures generated by the BoxShade server (https://embnet.vital-it.ch/software/BOX_form.html). Phylogenetic trees were generated using multiple sequence alignments generated with Clustal Omega (Madeira et al., 2019). Protein domain searches were done using InterProScan (Madeira et al., 2019).

## 2.6 Virulence assay

*Z. tritici* infection assays were carried out following the protocol based on that described by Motteram et al., (2009). Wheat seedlings (cultivar Riband) were grown in Levington M2 compost with a 3:1 addition of vermiculite, at 18$^{o}$C and 85% relative humidity under a 12:12 h light:dark cycle in a Fitotron SGC120 growth chamber (Weiss Technik, UK). *Z. tritici* blastospores were harvested from YPD agar plates and suspended in SDW containing 0.01% (v/v) Tween 20. Blastospores were filtered through a 100 µm cell strainer, before being diluted to a concentration of 5x10$^{6}$ (unless otherwise stated). The second leaf of 18 day-old seedlings was attached to an aluminium platform using double-sided tape, before blastospore suspensions were inoculated onto the adaxial side using a sterile cotton bud. Plants were placed in large trays containing water and covered with plastic lids to increase humidity for the initial 72 h of infection. Disease symptoms were assessed at 21 days post infection (dpi), at which point the infected section of leaves was harvested and kept in a falcon tube containing 1 ml SDW overnight. Leaves were mounted on laminated white sheets using micropore tape and imaged using an Epson Perfection V850 Pro scanner. For quantitative assessment of virulence, pycnidia counts and infected leaf surface area were calculated using ImageJ in order to quantify pycnidia density. At least 3 leaves were infected in each of three technical replicates of the experiment for each strain analysed. Symptom development by mutant strains was compared to its isogenic background strain and mock leaves inoculated with 0.01% Tween 20.

## 2.7 Germination efficiency assay

*Z. tritici* blastospores were harvested in SDW from YPD agar cultures and filtered through a 100 µm cell strainer, before being washed twice with SDW. Cell suspensions were diluted to 5x10$^{4}$ spores/ml before 500 µl was spread onto 2% water agar plates and allowed to dry. The presence of hyphal growth emanating from 100 spores was assessed microscopically after incubation at 19$^{o}$C for 24 h (unless otherwise stated). The experiment was repeated at least three times.

## 2.8 Radial growth under starvation assay

The growth of *Z. tritici* strains under starvation was assessed on *Aspergillus* minimal medium (Table 2.1), which was adjusted to create a growth medium lacking a carbon source (AMM C-) without glucose or a nitrogen source (AMM N-) without ammonium heptamolybdate and ammonium nitrate. *Z. tritici* blastospores were harvested from YPD agar plates, filtered through a 100 µm cell strainer and washed twice with SDW. Suspensions were diluted to a concentration of $5x10^6$ and 5 µl droplets were plated onto AMM, AMM C- and AMM N- plates. Radial growth was assessed after 14 d (unless otherwise stated) and the experiment repeated 3 times.

## 2.9 Microscopy

All epifluorescence and bright field microscopy was carried out using Zeiss Axiovert 200M microscope, while imaging of *Z. tritici* colonies was done using a Leica M165 FC dissection microscope. Images were taken using a Q-Imaging MicroPublisher 3.3 RTV camera mounted on these microscopes.

The epiphytic growth and stomatal interactions of *Z. tritici* on the wheat leaf surface was assessed through staining with calcofluor white (CFW). Infected leaf sections were harvested and mounted on a slide. Droplets of 35 µg/ml CFW were applied to the leaf surface and a cover slip was secured on top, before *Z. tritici* cells were imaged by epifluorescence microscopy.

# Chapter 3
# Distinct roles for different autophagy-associated genes in virulence of *Z. tritici*

## 3.1 Introduction

Autophagy is the process by which eukaryotic cells sequester cytoplasmic contents for degradation in the vacuole, in order to recycle the constituent macromolecular parts (Klionsky et al., 2011). This includes the breakdown of cytosolic proteins, organelles and intracellular pathogens (Feng et al., 2014; Orvedahl & Levine, 2009). This process plays a crucial role in cellular homeostasis under favourable conditions, through degradation of defective proteins and organelles, and in response to abiotic and biotic stress, most notably during nutrient starvation (Mizushima & Komatsu, 2011). Furthermore, autophagy functions in the extensive remodelling of cellular architecture during differentiation and tissue development (Mizushima & Levine, 2010). As well as these pro-survival and developmental roles, autophagy has been found to play diverse roles in programmed cell death across eukaryotes (Minina et al., 2014; Shimizu et al., 2004).

The term autophagy encompasses two mechanisms for transport of cytoplasmic components to the vacuole; the first by direct invagination of the vacuolar membrane, referred to as microautophagy (Li et al., 2012), and the second through engulfment by a specialised vesicle called an autophagosome, known as macroautophagy (Fig. 3.1A; Reggiori & Klionsky, 2013). Macroautophagy (hereby referred to as autophagy) involves the localisation of autophagy proteins at the pre-autophagosomal structure (PAS) adjacent to the vacuole, which initiate formation of a double membrane structure called a phagophore (Xie & Klionsky, 2007). The phagophore engulfs organelles and other cytosolic contents to form the autophagosome. The autophagosome then fuses with the vacuole, where its cargo is degraded and the resulting macromolecules transported back to the cytoplasm (Fig. 3.1A; Reggiori & Klionsky, 2013). This process can either be utilised for unselective sequestration of bulk cytoplasm, or the selective degradation of cytosolic proteins, via the cytoplasm to vacuole targeting (Cvt) pathway (Lynch-Day & Klionsky, 2010), and organelles, including peroxisomes (pexophagy; Till et al., 2012), mitochondria (mitophagy; Kanki et al., 2009) and lipid droplets (lipophagy; van Zutphen et al., 2014).

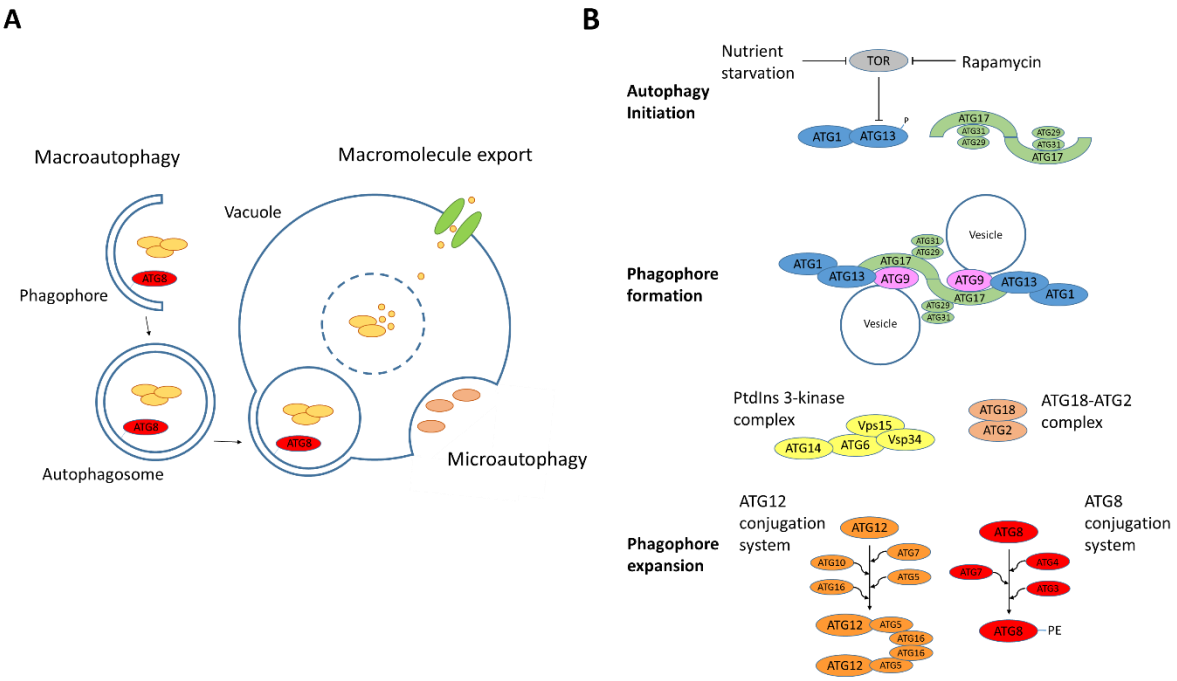


**Figure 3.1 Autophagy in *S. cerevisiae***
(A) Schematic displaying the processes of autophagy and (B) the core molecular autophagy machinery

A suite of 42 *ATG* (AuTophagy-related Genes) genes have been found to be involved in these processes in *Saccharomyces cerevisiae* and other yeast species (Parzych et al., 2018), many of which are conserved in filamentous fungi (Kershaw & Talbot, 2009; Liu et al., 2017; Lv et al., 2017). The core protein machinery involved in autophagy, summarised in Figure 3.1B, can be broken down into 5 complexes (Farré & Subramani, 2016). The ATG1 complex and vesicle-bound ATG9 are involved in protein assembly at the PAS and initiation of phagophore expansion, while the phosphatidylinositol-3- kinase (PI3K) complex, the ATG18-ATG2 complex and the ATG5-ATG12 and ATG8-phosphatidylethanolamine (PE) conjugation systems are required for autophagosome expansion (Fig. 3.1B; Nakatogawa et al., 2009). These core genes are also required for selective forms of autophagy, alongside other pathway specific proteins. This includes the receptors which recruit the targeted cargo to the PAS through interaction with the ATG11 scaffold protein (Zientara-Rytter & Subramani, 2020).

Despite the use of model yeast species in the majority of research into the molecular machinery of fungal autophagy, the role of autophagy in the development of filamentous fungi has been recently investigated (Khan et al.,

2012; Pollack et al., 2009). As in *S. cerevisiae*, autophagy has been shown to be vital for growth under nutrient starvation conditions in many ascomycetes (Josefsen et al., 2012; Nitsche et al., 2013; Richie et al., 2007; Shoji et al., 2010; Voigt & Pöggeler, 2013). In the mycelium of *Aspergillus oryzae*, degradation of organelles by autophagy in basal hyphal compartments is proposed to enable recycling of nutrients to the growing hyphal tips via tubular vacuoles (Shoji et al., 2006, 2010). In this way, autophagy has been proposed as a precursor to autolytic cell death in aging mycelial compartments (Shoji & Craven, 2011), but has also been implicated in programmed cell death in several species (Pinan-Lucarré et al., 2003; Veneault-Fourrey et al., 2006). Furthermore, autophagy has been shown to support developmental transitions between morphological forms during the life cycles of many filamentous ascomycetes (Pollack et al., 2009). To date, autophagy has been shown to play a role in the differentiation of aerial hyphae (Liu et al., 2007; Nguyen et al., 2011; Pinan-Lucarré et al., 2005), spore germination (Liu et al., 2007), conidiation (Liu et al., 2007; Lv et al., 2017) and development of sexual fruiting bodies (Liu et al., 2007; Lv et al., 2017; Pinan-Lucarré et al., 2005).

Autophagy plays a crucial role in the virulence of economically important fungal plant pathogens, often through involvement in cellular differentiation. Disruption of autophagy in *Magnaporthe oryzae* causes loss of pathogenicity, due to the impairment of developmentally-regulated cell death in the conidia and an inability to build sufficient turgor pressure in the appressorium for host penetration (Kershaw & Talbot, 2009; Liu et al., 2007). Similarly, autophagy is required for differentiation of functional appressoria in *Botrytis cinerea* and *Colletotrichum orbiculare* (Asakura et al., 2009; Ren et al., 2017). Furthermore, *Fusarium graminearum* was found to require autophagy to spread between spikelets during infection of wheat (Josefsen et al., 2012). Authors suggested this was caused by the inability of autophagy-deficient mutants to utilise stored carbon to cross the nutrient-limited rachis (Josefsen et al., 2012; Nguyen et al., 2011). Autophagy was also found to support asexual and sexual reproduction in *M. oryzae* and *F. graminearum*, with autophagy mutants in both species displaying reduced conidiation and an inability to generate perithecia (Liu et al., 2007; Lv et al., 2017). These reproductive processes are crucial for completion of the infection cycle and pathogen spread.

Although *Z. tritici* does not form appressoria to penetrate the leaf cuticle, the transition to hyphal growth required for host colonisation involves significant changes in cellular morphology. This morphological switch and subsequent invasive growth is proposed to require recycling of stored lipids in response to the nutrient-limiting conditions on the leaf surface (Rudd et al., 2015). *Z. tritici* spores are densely packed with lipid droplets (LDs), which are less abundant in hyphal filaments (Francisco et al., 2019; Sidhu, 2015), while transcriptome data has identified the upregulation of genes involved in lipid metabolism during early infection (Rudd et al., 2015). Autophagy has a complex relationship with LD dynamics in eukaryotes, with roles in both their formation, through the release of fatty acids (FAs) for synthesis of triacylglycerol (TAG), and their breakdown via lipophagy (Rambold et al., 2015; Singh et al., 2009; van Zutphen et al., 2014). Indeed, disruption of autophagy has been found to not only reduce LD accumulation in fungal spores (Liu et al., 2007; Ren et al., 2017), but also inhibit their breakdown under starvation conditions (Josefsen et al., 2012).

Considering the involvement of autophagy in the growth of other ascomycete fungi under starvation stress (Liu et al., 2007; Shoji et al., 2010), and its widespread importance in virulence, we investigated the role of autophagy in *Z. tritici* development and infection. Autophagy gene homologs were identified in the *Z. tritici* genome, and functional characterisation of the *ZtATG1* and *ZtATG8* was carried out through targeted gene deletion. Autophagy was inhibited by deletion of *ZtATG1*, but this gene was found to be dispensable for hyphal growth under starvation and pathogenicity of *Z. tritici.* However, deletion of *ZtATG8* led to a delay in the necrotrophic switch, indicating an autophagy-independent role of *ZtATG8* during *Z. tritici* infection.

## 3.2 Materials and Methods

### 3.2.1 BlastP searches and alignments

Homologs of previously characterised autophagy proteins from *S. cerevisiae* were identified in the *Z. tritici* genome through BlastP searches on the Ensembl Fungi *Zymoseptoria tritici* genome database (http://fungi.ensembl.org/Zymoseptoria_tritici/Tools/Blast), using default parameters apart from adjustment of the E-value threshold to 1e-3. Additionally, BlastP searches for pexophagy-specific proteins from *Pichia pastoris* (ATG28, ATG30, ATG35, ATG37) and *Pichia angustsa* (ATG25) were carried out. Where

ATG protein sequences from these yeast species yielded no *Z. tritici* homologs, ATG protein sequences from *M. oryzae* were used in BlastP searches, as the closest filamentous ascomycete relative of *Z. tritici* in which autophagy has been extensively characterised. Following identification of *Z. tritici* ATG gene homologs, pairwise protein sequence alignments were carried out with predicted *S. cerevisiae* and *M. oryzae* ATG proteins as query sequences, in order to assess sequence identity across the whole protein.

### 3.2.2 Construction of targeted gene deletion and GFP-fusion vectors

Construction of plasmid vectors for the deletion of *ZtATG1* and *ZtATG8* was carried out by yeast recombinational cloning (see Chapter 2 for details). The plasmid pC-HYG-YR was used as a backbone for these vectors (Sidhu, Chaudhari, et al., 2015). Left flank (LF) and right flank (RF) sequences were PCR amplified using the primer pairs ZtATG1-LF-F/R, ZtATG1-RF-F/R, ZtATG8-LF-F/R and ZtATG8-RF-F/R. LF and RF amplicons were transformed into *S. cerevisiae* alongside the pC-HYG-YR vector, which had been linearised by restriction digestion with the enzymes EcoRI and HindIII (New England Biolabs, UK). This resulted in the plasmids pC-HYG-ATG1KO and pC-HYG-ATG8KO. The fidelity of PCR amplification was confirmed by Sanger sequencing in the completed vectors. These vectors were transformed into *Z. tritici* via *Agrobacterium tumefaciens*-mediated transformation (ATMT; Chapter 2).

The plasmid pC-SUR-GFPATG8 was also generated for expression of a ZtGFP:ZtATG8 fusion protein from the wild type *ZtATG8* locus. This was constructed using the *Z. tritici* codon-optimised GFP (Kilaru, Schuster, et al., 2015). The *ZtATG8* LF sequence, which includes the pZtATG8 native promotor, was amplified with the primers ZtATG8_LF_F and ZtATG8_LF_GFP_R containing 5' primer extensions overlapping the left border sequence and start of *ZtGFP*, respectively. The *ZtATG8* open reading frame and terminator were amplified with primers ZtATG8_GFP_F and ZtATG8_R containing 5' extensions overlapping the end of *ZtGFP* (with the stop codon replaced by a tri-alanine linker) and the start of the $SUR^R$ selection cassette, respectively. A right flank sequence (RF2) starting downstream of the *ZtATG8* terminator was amplified with the primers ZtATG8-RF2-F/R containing 5' extensions overlapping the end of the $SUR^R$ cassette and the right border sequence, respectively. Finally, the

*ZtGFP* coding sequence lacking a stop codon was amplified with the primers ZtGFP_F and ZtGFP_NOSTOP_R. These fragments were transformed into *S. cerevisiae* with the linearised pC-SUR-YR plasmid to form the plasmid pC-SUR-GFPATG8.

### 3.2.3 Soluble protein extraction from *Z. tritici*

The following steps were carried out on ice and at 4$^{o}$C in the centrifuge. Samples from *Z. tritici* liquid cultures were centrifuged in 2 ml micro-centrifuge tubes at 20,000 x G for 10 min and the supernatant removed. Cells were washed with 1 ml ice-cold MilliQ water and the centrifugation repeated. Cell pellets were re-suspended in 500 µl ice-cold breaking buffer (100 mM Tris [pH 7.5], 1 mM DTT, 10% v/v Glycerol, 1 mM EDTA, , 0.01% SDS) containing Pierce Protease Inhibitor Tablets (ThermoFisher Scientific), and pooled into a screw cap tube. Samples were centrifuged for 10 min at 20,000 x G, the supernatant removed and the pellets stored at -20$^{o}$C.

Cells were thawed on ice and re-suspended in a volume of breaking buffer equal to the cell pellet. Glass beads were added to just below the meniscus layer and the cells were lysed using a FastPrep-24™ Classic Instrument (MP Biomedicals), carrying out four runs of 20 sec at 6.5 m/s, interspaced with 1 min intervals of cooling samples on ice. Following cell lysis, the cell debris and glass beads were pelleted by centrifugation at 13,000 x G for 10 min, after which the supernatant was transferred to a new 1.5 ml micro-centrifuge tube and the centrifugation repeated to clarify the protein extract. The total protein concentration of each sample was determined using the Pierce™ Coomassie (Bradford) Protein Assay Kit (ThermoFisher Scientific) following the manufacturer's instructions.

### 3.2.4 Western blotting

Western blots were carried out using 30 µg of each protein sample in 20 µl of breaking buffer, to which 5 µl of NuPAGE™ LDS Sample Buffer (Invitrogen) and 1 µl 0.5 M dithiothreitol (DTT) was added. Samples were denatured at 70$^{o}$C for 10 min before being loaded onto a 10% NuPAGE™ Bis-Tris Gel (Invitrogen) and separated by electrophoresis at 200 V in NuPAGE™ MOPS buffer (Invitrogen). A PVDF membrane was activated by soaking in methanol for 30 seconds, before being equilibrated by soaking in NuPAGE™ Transfer Buffer

(Invitrogen). Proteins were transferred to the activated membrane by electrophoresis at 30 V for 75 min in NuPAGE™ Transfer Buffer. The membrane was then washed in TBS (10 mM Tris-HCl ph8, 137 mM NaCl) before protein transfer was assessed using Ponceau S stain (0.1% Ponceau S, 5% Acetic acid). Ponceau S was washed from the membrane using 100 mM NaOH and rinsed thoroughly with TBS.

The membrane was blocked by incubation in 25 ml TBS-T (TBS amended with 0.1% Tween-20) containing 5% milk powder (TBS-T+M) overnight at 4$^{o}$C. The membrane was then stained in 25 ml TBS-T+M containing 200 ng/ml GFP Polyclonal Antibody (Invitrogen) overnight at 4$^{o}$C. The membrane was washed four times with TBS-T for 5 min and stained with 25 ml TBS-T+M containing 50 ng/ml Goat anti-Rabbit IgG (H+L) Cross-Adsorbed Secondary Antibody, HRP (Invitrogen) for 1 h at room temperature. After washing with TBS-T, SuperSignal™ West Pico Chemiluminescent Substrate (Thermo Scientific) was applied to the membrane according to manufacturer's guidelines.

### 3.2.5 FM4-64 staining

Cells were harvested after growth on YPD agar plates for 5 days and suspended in 1 ml yeast extract glucose (YG) broth containing 16 µM FM4-64 stain (Sigma-Aldrich, UK). Spore suspensions were incubated at 19$^{o}$C for 10 min, before being pelleted for 3 min at 8,000 x G and re-suspended in fresh YG broth for a 15 min chase period at 19$^{o}$C. Spores were imaged under a Zeiss Axiovert 200M microscope with a Q-Imaging MicroPublisher 3.3 RTV camera.

## 3.3 Results

### 3.3.1 Identification of autophagy genes in *Z. tritici*

Analysis of the *Z. tritici* genome identified homologs of 27 *ATG* genes from *S. cerevisiae* and *M. oryzae* (Table 3.1). These results were largely in agreement

## Table 3.1 Autophagy gene homologs identified in the *Z. tritici* genome

| Auophagy process | Function | Yeast Gene | Gene Name | Rothamsted annotation | Ensembl Identifier | Yeast gene ID | Identity (%) | Query coverage (%) | E-value | *M. oryzae* gene | Identity (%) | Query coverage (%) | E-value |
|---|---|---|---|---|---|---|---|---|---|---|---|---|---|
| **Autophagy induction/Phagophore formation** | **ATG1-kinase complex** | ATG1 | ZtATG1 | ZtritIPO323_04g11420 | Mycgr3G73716 | YGL180W | 40.82 | 97 | 7.00E-92 | MGG_06393 | 43.5 | 97 | 0.00E+00 |
| | | ATG13 | ZtATG13[a] | ZtritIPO323_04g09086 | Mycgr3G58223 | YPR185W | 27.98 | 20 | 2.00E-15 | MGG_00454 | 33.07 | 65 | 3.00E-54 |
| | | ATG17 | ZtATG17 | ZtritIPO323_04g08285 | Mycgr3G70424 | YLR423C | 26.72 | 27 | 1.00E-09 | MGG_07667 | 29.61 | 90 | 1.00E-52 |
| | | ATG29 | ZtATG29[a] | ZtritIPO323_04g04445 | Mycgr3G111700 | YPL166W | 27.45 | 78 | 9.00E-11 | MGG_02790 | 42.39 | 19 | 4.00E-25 |
| | | ATG31 | - | - | - | YDR022C | - | - | - | - | - | - | - |
| | **Membrane trafficking to autophagosome** | ATG9 | ZtATG9 | ZtritIPO323_04g10999 | Mycgr3G100550 | YDL149W | 37.72 | 50 | 1.00E-136 | MGG_09559 | 32.19 | 99 | 2.00E-164 |
| | | ATG27 | ZtATG27[a] | ZtritIPO323_04g06412 | Mycgr3G108192 | YJL178C | 32.98 | 33 | 4.00E-09 | MGG_02386 | 41.81 | 95 | 5.00E-84 |
| | | ATG41 | - | - | - | YPL250C | - | - | - | - | - | - | - |
| **Phagophore expansion** | **PtdIns-3K complex** | ATG6/VPS30 | ZtATG6 | ZtritIPO323_04g10366 | Mycgr3G72630 | YPL120W | 30.39 | 68 | 3.00E-49 | MGG_03694 | 46.18 | 97 | 8.00E-146 |
| | | ATG14 | ZtATG14[a] | ZtritIPO323_04g10306 | Mycgr3G109656 | YBR128C | - | - | - | MGG_03698 | 31.84 | 99 | 1.00E-67 |
| | | VPS34 | ZtVPS34 | ZtritIPO323_04g08106 | Mycgr3G70260 | YLR240W | 35.82 | 99 | 9.00E-172 | MGG_03069 | 53.28 | 99 | 0.00E+00 |
| | | VPS15 | ZtVPS15 | ZtritIPO323_04g13304 | Mycgr3G75360 | YBR097W | 32.76 | 85 | 4.00E-162 | MGG_06100 | 42.34 | 99 | 0.00E+00 |
| | | ATG38 | - | - | - | YLR211C | - | - | - | - | - | - | - |
| | **ATG18-ATG2 complex** | ATG2 | ZtATG2 | ZtritIPO323_04g00381 | Mycgr3G83423 | YNL242W | 34.13 | 39 | 6.00E-93 | MGG_05998 | 48.74 | 85 | 4.00E-151 |
| | | ATG18 | ZtATG18 | ZtritIPO323_04g13426 | Mycgr3G75475 | YFR021W | 29.9 | 97 | 2.00E-72 | MGG_03139 | 54.59 | 95 | 6.00E-134 |
| | **ATG12 conjugation complex** | ATG12 | ZtATG12 | ZtritIPO323_04g08764 | Mycgr3G40907 | YBR217W | 42.53 | 45 | 9.00E-24 | MGG_00598 | 51.7 | 80 | 1.00E-43 |
| | | ATG5 | ZtATG5 | ZtritIPO323_04g11307 | Mycgr3G86699 | YPL149W | 22.71 | 84 | 5.00E-15 | MGG_09262 | 37.41 | 73 | 6.00E-52 |
| | | ATG16 | ZtATG16[a] | ZtritIPO323_04g05954 | Mycgr3G90647 | YMR159C | 28.77 | 48 | 5.00E-05 | MGG_05255 | 28.87 | 93 | 8.00E-24 |
| | | ATG10 | ZtATG10[a] | ZtritIPO323_04g11575 | - | YLL042C | - | - | - | MGG_14737 | 36.84 | 53 | 1.00E-26 |
| | **ATG8 conjugation pathway** | ATG8 | ZtATG8 | ZtritIPO323_04g06470[c] | Mycgr3G108219 | YBL078C | 66.19 | 99 | 9.00E-66 | MGG_01062 | 79.29 | 95 | 6.00E-78 |
| | | ATG3 | ZtATG3 | ZtritIPO323_04g08175 | Mycgr3G99699 | YNR007C | 33.15 | 99 | 2.00E-64 | MGG_02959 | 55.07 | 99 | 1.00E-122 |
| | | ATG4 | ZtATG4 | ZtritIPO323_04g03395 | Mycgr3G49421 | YNL223W | 40.06 | 64 | 6.00E-78 | MGG_03580 | 45.53 | 96 | 2.00E-140 |
| | | ATG7 | ZtATG7 | ZtritIPO323_04g10643 | Mycgr3G100434 | YHR171W | 47.17 | 77 | 5.00E-127 | MGG_07297 | 46.91 | 94 | 0.00E+00 |
| **Vaculoar proteins** | **Lysis of autophagic bodies** | ATG15 | ZtATG15 | ZtritIPO323_04g07939 | Mycgr3G108706 | YCR068W | 40.14 | 85 | 3.00E-107 | MGG_12828 | 49.22 | 94 | 0.00E+00 |
| | **Amino acid transport** | ATG22 | ZtATG22 | ZtritIPO323_04g03104 | Mycgr3G76723 | YCL038C | 31.87 | 98 | 1.00E-89 | MGG_09904 | 51.71 | 80 | 1.00E-177 |
| **Selective autophagy** | **Scaffold protein in selective** | ATG11 | ZtATG11 | ZtritIPO323_04g05559 | Mycgr3G54658 | YPR049C | 27.95 | 45 | 1.00E-09 | MGG_04486 | 32.13 | 99 | 0.00E+00 |
| | **Sorting nexins in selective autophagy** | ATG20/Snx42 | ZtSNX41 | ZtritIPO323_04g07437 | Mycgr3G103627 | YDL113C | 24.82 | 74 | 2.00E-42 | MGG_12832 | 58.37 | 99 | 0.00E+00 |
| | | ATG24/Snx4 | ZtATG24 | ZtritIPO323_04g09862 | Mycgr3G100205 | YJL036W | 37.09 | 91 | 1.00E-91 | MGG_03638 | 53.89 | 95 | 8.00E-172 |
| | **Pexophagy** | ATG26 | ZtATG26 | ZtritIPO323_04g10936 | Mycgr3G20064 | YLR189C | 48.09 | 70 | 0.00E+00 | MGG_03459 | 46.1 | 75 | 0.00E+00 |
| | | ATG30 | - | - | - | PAS_chr3_1230[b] | - | - | - | - | - | - | - |
| | | ATG25 | - | - | - | Q6JUT9[b] | - | - | - | - | - | - | - |
| | | ATG35 | - | - | - | PAS_chr1-1_0041[b] | - | - | - | - | - | - | - |
| | | ATG37 | ZtATG37[a] | ZtritIPO323_04g06601 | - | PAS_chr4_0602[b] | 29 | 49.21 | 8.00E-36 | MGG_03156 | 45.65 | 95 | 6.00E-77 |
| | | ATG36 | - | - | - | YJL185C | - | - | - | - | - | - | - |
| | | ATG28 | ZtATG28[a] | ZtritIPO323_04g08930 | Mycgr3G85720 | PAS_chr2-1_0596[b] | - | - | - | MGG_08061 | 29.77 | 58 | 9.00E-40 |
| | **Mitophagy** | ATG32 | - | - | - | YIL146C | - | - | - | - | - | - | - |
| | | ATG33 | ZtATG33[a] | ZtritIPO323_04g07428 | Mycgr3G103620 | YLR356W | 24.41 | 62 | 2.00E-05 | MGG_12948 | 33.17 | 94 | 2.00E-23 |
| | **Reticulophagy and Nucleophagy** | ATG39 | - | - | - | YLR312C | - | - | - | - | - | - | - |
| | | ATG40 | - | - | - | YOR152C | - | - | - | - | - | - | - |
| | **Cvt pathway** | ATG19 | - | - | - | YOL082W | - | - | - | - | - | - | - |
| | | ATG21 | ZtATG18 | ZtritIPO323_04g13426 | Mycgr3G75475 | YPL100W | 30.32 | 68 | 1.00E-29 | - | - | - | - |
| | | ATG23 | - | - | - | YLR431C | - | - | - | - | - | - | - |
| | | ATG34 | - | - | - | YOL083W | - | - | - | - | - | - | - |

[a]Identified from *Magnaporthe oryzae* gene. [b]Ordered locus names of *Pichia pastoris or Pichia angusta* genes.
[c]Correct annotation of exons from MPI annotation Zt09_TU_chr_2_00900

with a recent analysis of *Z. tritici* autophagy genes from a study of 331 fungal species (Wang et al., 2019), with the exception of the identification of *ZtATG10*, *ZtATG14* and *ZtATG37* in the present study. A homolog of the E2-like enzyme ATG10 involved in the ATG12-conjugation complex was absent from the original JGI genome annotation of the *Z. tritici* genome. However, a homolog of *M. oryzae* ATG10 gene was identified in the recent genome annotation from Rothamsted Research (King et al., 2017). Additionally, *ZtATG14* was identified using the sequence of a divergent homolog of *ScATG14* recently identified in *M. oryzae* and conserved in filamentous ascomycetes (Liu et al., 2017). The gene model for *ZtATG37* was absent from the original genome annotation and therefore missed by this previous study (Wang et al., 2019).

The *ZtATG* genes identified include homologs of all autophagy genes involved in the core machinery of autophagosome formation during macroautophagy in *S. cerevisiae*, with the exception of the phosphoprotein ATG31, which forms part of the Atg17-Atg31-Atg29 complex that acts as a scaffold for recruitment of ATG proteins to the PAS (Kabeya et al., 2009). Furthermore, the ATG29 homologs identified in *Z. tritici* (ZtATG29; ZtritIPO323_04g04445; 464 amino acids) and *M. oryzae* (MoATG29; MGG_02790; 443 amino acids) are significantly larger than ScATG29 (YPL166W; 213 amino acids) and show only low homology at the N- and C-terminus, indicating considerable divergence in the Atg17-Atg31-Atg29 complex in filamentous ascomycetes in comparison to yeast.

Homologs of a group of genes (*ZtATG11, ZtATG24, ZtATG26, ZtATG28, ZtATG33, ZtATG37*) required for selective forms of autophagy in yeast were identified in the *Z. tritici* genome (Table 3.1). The predicted *Z. tritici* protein identified with sequence similarity to ScATG20/Snx42, ZtritIPO323_04g0743, displayed higher identity with ScSnx41 and was therefore designated ZtSnx41. This gene likely fulfils the roles of both yeast sorting nexins Snx41 and Snx42/ScATG20 in pexophagy and endosomal retrieval trafficking, as was found for the *M. oryzae* protein MoSnx41 (Deng et al., 2013). However, no evidence was found for the conservation of the yeast Cvt pathway in *Z. tritici*, in the absence of homologs of the Cvt-specific genes ATG19, ATG23 and ATG34, consistent with findings in other filamentous ascomycetes (Wang et al., 2019). Despite this, recent evidence for disrupted maturation of vacuolar

aminopeptidase 1 (Ape1), a well characterised cargo protein of yeast Cvt pathway, in *Δatg1* and *Δatg20* of *A. oryzae* and *F. graminearum*, respectively, has suggested the presence of a distinct Cvt pathway in filamentous fungi (Lv et al., 2020; Yanagisawa et al., 2013). Searches for homologs of ScATG18 and ScATG21 identified the same *Z. tritici* gene, ZtritIPO323_04g13426, although the predicted protein showed higher sequence identity with ScATG18, and was hence designated ZtATG18. This may explain the previous identification of ScATG21 homologs in all fungal classes (Wang et al., 2019), although the role of these genes in the Cvt pathway of these species is yet to be determined.

Considering the essential role of their yeast homologs in both nonselective and selective forms of autophagy, the *Z. tritici* genes *ZtATG1* and *ZtATG8* were selected for further analysis. Based on sequence alignments with MoATG8 and ScATG8, ZtATG8 is incorrectly annotated in the Rothamsted Research (RRes) annotation, with the first intron being truncated in the predicted transcript ZtritIPO323_04t06470 (Figure S3.1A). This was confirmed using the alignments of RNA sequencing reads from *Z. tritici* IPO323 in YPD cultures (Figure S3.1B). Instead, the predicted transcript from the Max Planck Institute (MPI) annotation, Zt09_TU_chr_2_00900, correctly predicts the first intron and was used as the gene model for further analysis. Both ZtATG1 and ZtATG8 show very high sequence identity with their homologs in *S. cerevisiae* and *M. oryzae* (Table 3.1; Figure S3.1A; Figure S3.2), suggesting their conserved function in *Z. tritici* autophagy.

### 3.3.2 Disruption of autophagy by targeted deletion of *ZtATG1* and *ZtATG8*

Targeted deletion of *ZtATG1* and *ZtATG8* was carried out to determine the function of autophagy in *Z. tritici* cellular differentiation and virulence. Wild type *Z. tritici* IPO323 was transformed with the plasmids pC-HYG-ATG1KO and pC-HYG-ATG8KO, resulting in replacement of *ZtATG1* and *ZtATG8* with the $HYG^R$ selective marker through homologous recombination (Fig. 3.2A-B). Correct insertion of the selective marker and absence of the native coding sequences was confirmed by PCR (Fig. 3.2A-B), and three independent *Δztatg1* and *Δztatg8* strains were isolated.

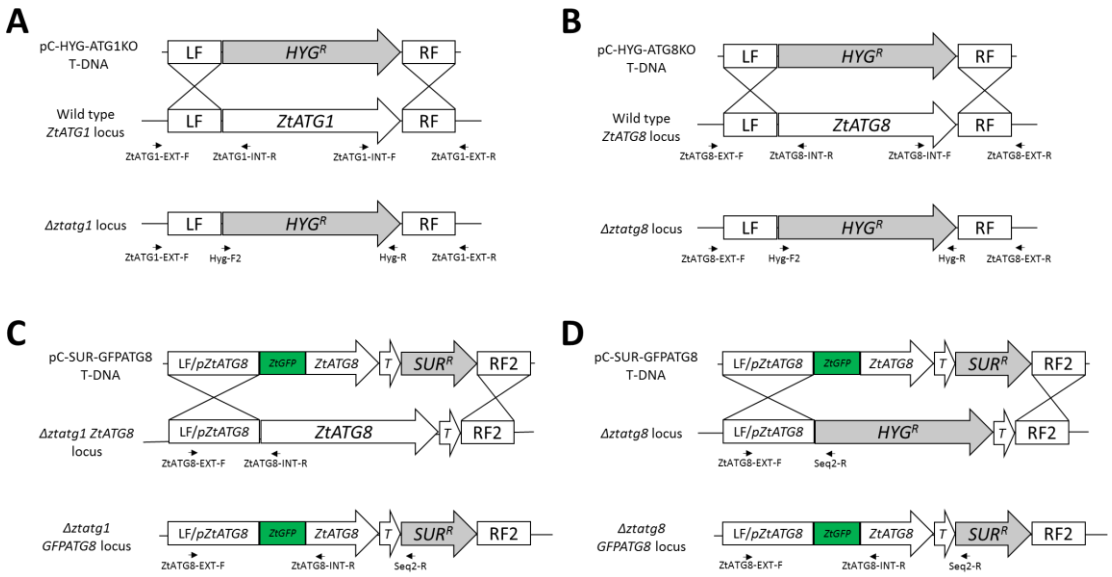


**Figure 3.2 Targeted deletion of *Z. tritici* autophagy genes *ZtATG1* and *ZtATG8* and expression of a ZtGFPZtATG8 fusion**
Schematics displaying homologous recombination between flanking sequences (LF and RF) of T-DNA from the plasmids pC-HYG-ATG1KO (A), pC-HYG-ATG8KO (B) and pC-SUR-GFPATG8 (C and D) and the targeted loci in the *Z. tritici* genome. Below each homologous recombination schematic is the resulting transgenic locus containing the selective markers $HYG^R$ and $SUR^R$ for resistance to hygromycin B and sulfonylurea, respectively. Depicted sequences include the *ZtATG8* promotor (pZtATG8) and terminator (T), as well as the codon-optimised GFP (*ZtGFP*; Kilaru et al 2015). Primers (arrows) used for PCR screening of resulting transformants are shown below their respective target loci.

The activity and progression of autophagy is typically monitored through the fluorophore-tagging of ATG8. This ubiquitin-like protein is associated with the autophagosome from its formation to its breakdown in the vacuole, enabling observation of macroautophagy from initiation to completion (Torggler et al., 2017). Therefore, in order to confirm the inhibition of autophagy in *Δztatg1*, the vector pC_SUR_GFPATG8 was transformed into *Δztatg1* (Fig. 3.2C). This vector contains a cassette for expression of a ZtGFP:ZtATG8 fusion protein, which is under the control of the endogenous *ZtATG8* promotor and targeted to its native locus in the *Z. tritici* genome (Fig. 3.2C). The *Δztatg8* deletion strain was also transformed with pC_SUR_GFP:ATG8, replacing the *hygR* resistant marker with the ZtGFP:ZtATG8 fusion at its native locus (Fig. 3.2D). This was done both as a control for visualisation of autophagy progression in wild type *Z. tritici* and as a complementation assay for any phenotype identified in *Δztatg8* strains.

Localisation of ZtGFP:ZtATG8 was observed in wild type *ZtGFP:ZtATG8* and *Δztatg1 ZtGFP:ZtATG8* cells after 5 days growth on YPD plates (Fig. 3.3). Cells were stained with FM4-64 in order to visualise the vacuolar membrane and assess autophagosome delivery to the lytic compartment. In wild type cells, ZtGFP:ZtATG8 fluorescence was observed at small puncta, indicating the formation of autophagosomes, as well as more dispersed regions of lower intensity fluorescence within the vacuolar membrane, indicating the delivery of ZtGFP:ZtATG8 into the vacuole through autophagy (Fig. 3.3). This suggests that *Z. tritici* is actively undergoing autophagy even during growth by blastosporulation in nutrient-rich conditions. Conversely, ZtGFP:ZtATG8 was localised at bright puncta in *Δztatg1* cells, but was never observed to be dispersed within the vacuolar membrane (Fig. 3.3), indicating that ZtGFP:ZtATG8 is not being transported into the vacuole. This indicates that while ATG proteins are accumulating at the PAS in *Δztatg1* cells, any resulting autophagosomes are not being transported to the vacuole, suggesting that autophagy is blocked in these mutants.

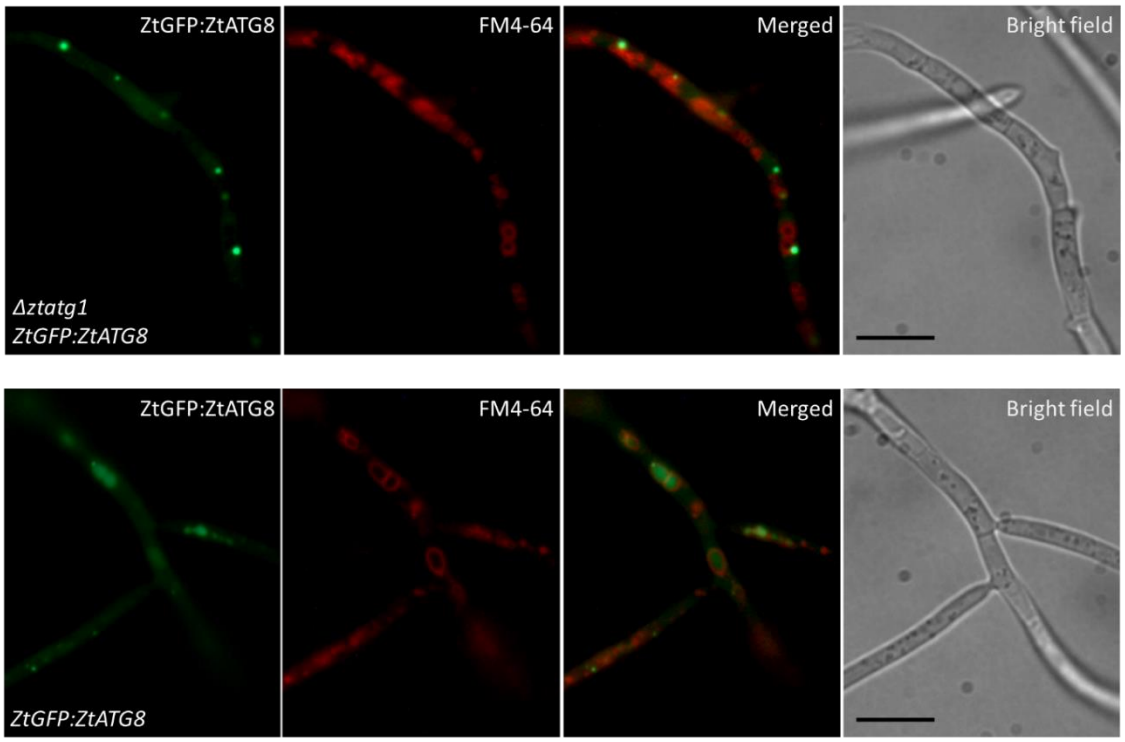


**Figure 3.3 Vacuolar localisation of ZtGFP:ZtATG8 is abolished in *Δztatg1* cells**
Localisation of ZtGFP:ZtATG8 fluorescence within FM4-64 stained vacuoles of *ZtGFP:ZtATG8* cells, which is not observed in *Δztatg1* cells expressing ZtGFP:ZtATG8. Scale bars = 10μm.

To support the observation of inhibited vacuolar delivery of ZtGFP:ZtATG8 in *Δztatg1* from microscopic analysis, western blot assays were carried out to assess the degradation of ZtGFP:ZtATG8 (Fig. 3.4). Upon release of GFP:ATG8 proteins into the vacuole, proteolysis of the ATG8 moiety leads to the release of free-GFP, which is more stable under protease activity (Torggler et al., 2017). This enables assessment of autophagic flux by quantifying the relative abundance of the 41 kDa ZtGFP:ZtATG8 band and the 27 kDa free-GFP band on a western blot using an anti-GFP antibody. *ZtGFP:ZtATG8* and *Δztatg1 ZtGFP:ZtATG8* were grown for 5 d on YPD agar plates before being suspended in YPD broth, PDB and V8 broth at $5x10^6$ spores/ml and incubated at 19$^o$C for 24 h. Total protein was extracted and analysed by western blotting with an anti-GFP antibody. In the wild type background, full length ZtGFP:ZtATG8 protein was detected alongside free-GFP in all conditions tested (Fig. 3.4), indicating that autophagic delivery of ZtGFP:ZtATG8 is occurring during growth in a range of nutrient-rich media. Furthermore, while full length ZtGFP:ZtATG8 was present, no free-GFP was observed in the *Δztatg1* background (Fig. 3.4), corroborating with microscopic evidence of inhibited autophagy in this mutant.

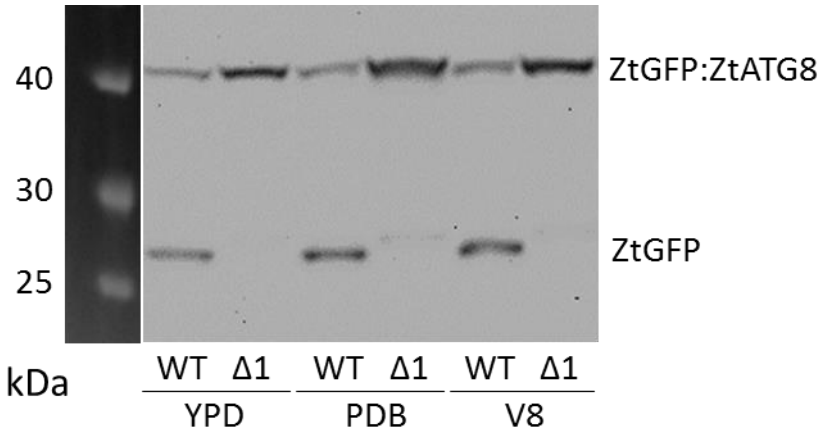


**Figure 3.4 Autophagic breakdown of ZtGFP:ZtATG8 is abolished in *Δztatg1* cells**
Autophagic breakdown of ZtGFP:ZtGFPATG8 protein (41 kDa) releasing free-ZtGFP (27 kDa) protein is observed in wild type (WT) cells during growth on rich media, including yeast extract peptone dextrose broth (YPD), potato dextrose broth (PDB) and V8 juice broth (V8), which is abolished in *Δztatg1* (Δ1) background.

### 3.3.3 Autophagy is not required for germination or growth under starvation in *Z. tritici*

As autophagy has been shown to be important for cellular differentiation and growth under starvation in other fungal species, the involvement of *ZtATG1* and *ZtATG8* in the morphological switch to hyphal growth in response to nutrient deprivation was investigated. The rate of hyphal germination was unchanged in *Δztatg1* and *Δztatg8* compared to IPO323, with all strains displaying a mean germination efficiency over 90% after 48 h on water agar (Fig. 3.5A). This suggests that autophagy is not essential for the hyphal transition in *Z. tritici*. To further investigate whether growth was inhibited in autophagy mutants during nutrient starvation, *Δztatg1* and *Δztatg8* strains were grown on minimal medium deficient in either a nitrogen or carbon source. Hyphal growth was induced under all nutrient regimes, and the radial growth rate of the autophagy mutants was similar to that of the wild type over 14 days in all conditions analysed (Fig 3.5B). However, *Δztatg8* strains showed slightly reduced hyphal density in

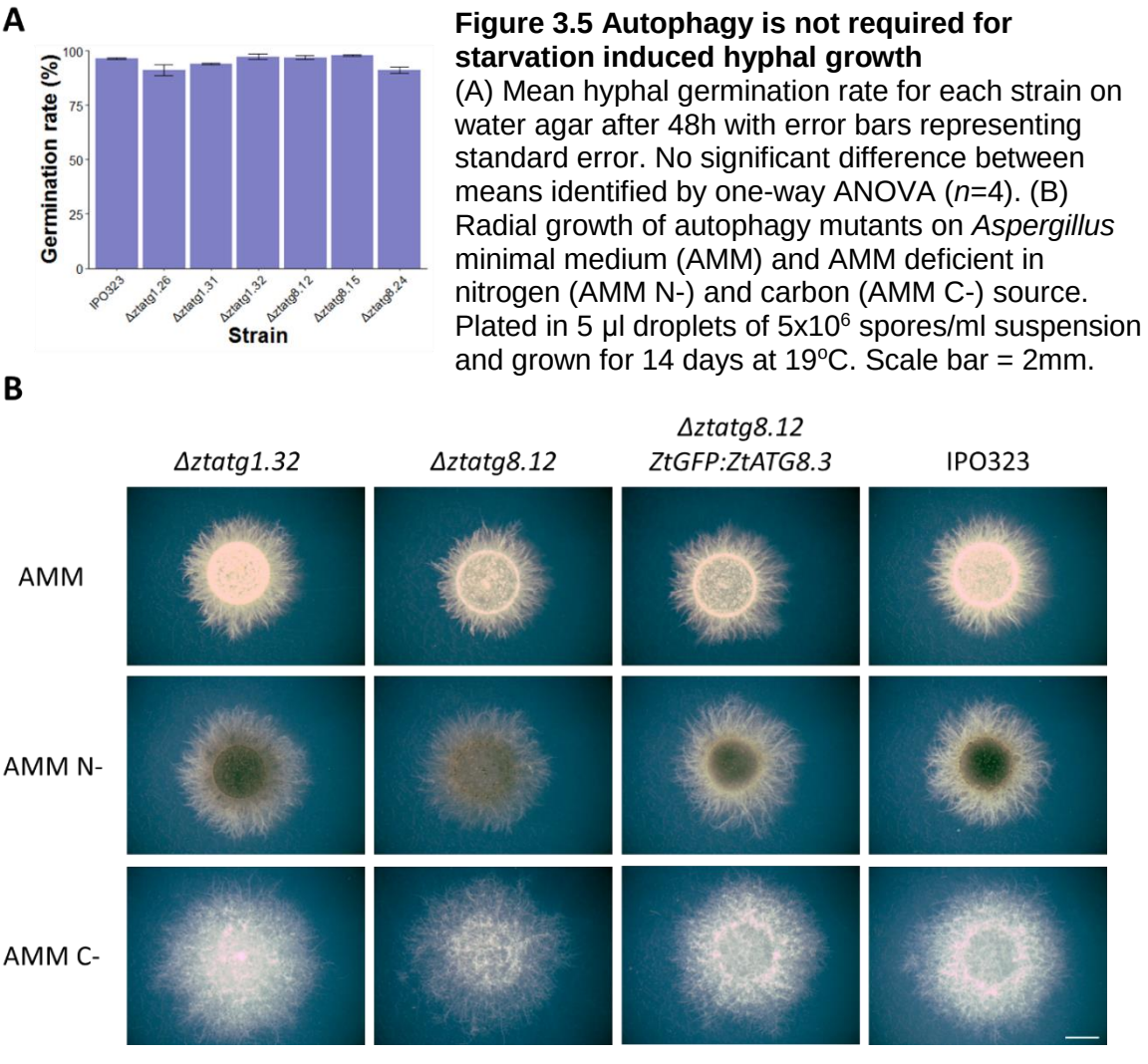


**Figure 3.5 Autophagy is not required for starvation induced hyphal growth**
(A) Mean hyphal germination rate for each strain on water agar after 48h with error bars representing standard error. No significant difference between means identified by one-way ANOVA (*n*=4). (B) Radial growth of autophagy mutants on *Aspergillus* minimal medium (AMM) and AMM deficient in nitrogen (AMM N-) and carbon (AMM C-) source. Plated in 5 µl droplets of $5x10^6$ spores/ml suspension and grown for 14 days at 19°C. Scale bar = 2mm.

radial colonies grown on carbon-depleted medium, and displayed altered pigmentation on nitrogen depleted medium (Fig. 3.5B). Both of these phenotypes were reversed in *Δztatg8 ZtGFP:ZtATG8* complementation strains (Fig. 3.5). This provides evidence that autophagy plays no significant role in starvation induced hyphal growth in *Z. tritici*, while *ZtATG8* deletion has a minor effect on growth morphology under these conditions.

### 3.3.4 Disruption of autophagy causes increased susceptibility to oxidative stress

Growth of *Z. tritici* on YPD was inhibited under oxidative stress induced by hydrogen peroxide at concentrations above 4mM (Fig. 6). While yeast-like growth of *Δztatg1* and *Δztatg8* was equivalent to the wild type on YPD, the inhibitory effect of hydrogen peroxide was enhanced in these mutants (Fig. 6). This phenotype was subtle but reproducible, and increased sensitivity to hydrogen peroxide was not observed in *Δztatg8 ZtGFP:ZtATG8* complementation strains. This suggests that autophagy is involved in maintaining cell viability and growth under oxidative stress in *Z. tritici*.

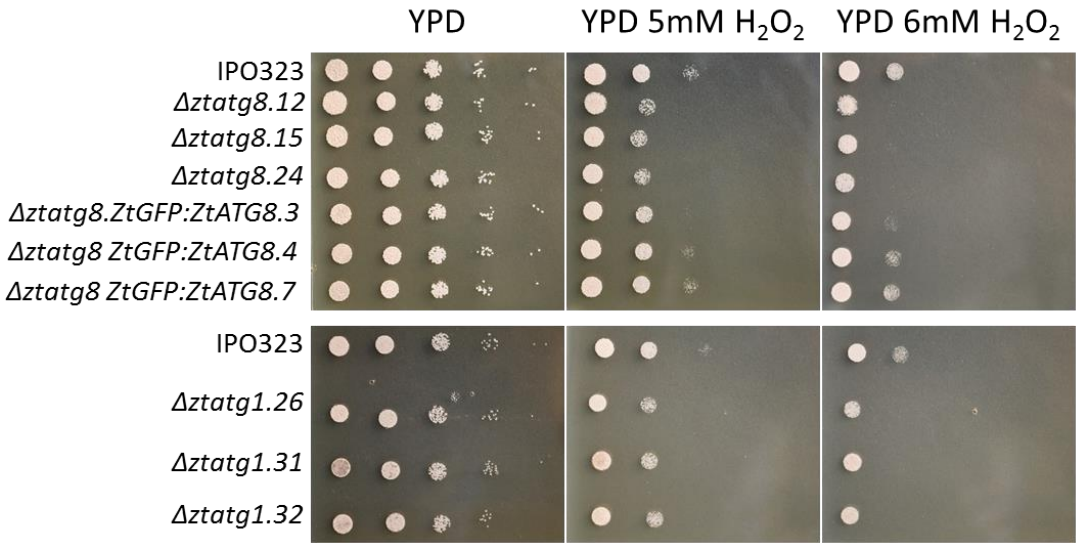


**Figure 3.6 *Δztatg1* and *Δztatg8* strains show increased sensitivity to oxidative stress**
*Z. tritici* strains plated onto YPD containing hydrogen peroxide $H_2O_2$ at increasing concentrations. Spore suspensions prepared in 10-fold dilution series down from $5x10^6$ spores/ml and plated in 5 µl droplets.

### 3.3.5 Autophagy is not required for *Z. tritici* pathogenicity, but *ZtATG8* deletion influences virulence.

Deletion of *ZtATG1* and *ZtATG8* did not inhibit the ability of *Z. tritici* to complete its asexual infection cycle on susceptible wheat leaves. *Δztatg1* and *Δztatg8* strains were able to cause necrosis and form pycnidia in the substomatal cavities of infected leaf tissue 21 days after inoculation (Fig. 3.7A). This provides evidence that autophagy is not required for infection-related development of *Z. tritici.* However, leaves infected with *Δztatg8* strains displayed a significant reduction in pycnidia density compared to IPO323 and *Δztatg8 ZtGFP:ZtATG8* complementation strains at this stage, which was not identified in *Δztatg1* strains (Fig. 3.7B). Despite this, leaves infected with *Δztatg8* strains were covered with pycnidia-bearing necrotic lesions by 28 dpi (Fig. 3.7A). This is consistent with a delay in the onset of the necrotrophic phase in leaves infected with *Δztatg8* strains, which was observed during daily inspection of symptom development. These findings suggest that while autophagy is not required for the pathogenicity of *Z. tritici*, *ZtATG8* has an autophagy-independent role in supporting full virulence of this pathogen.

## 3.4 Discussion

To our knowledge, autophagy has been found to contribute to the virulence of all fungal plant pathogens in which it has been characterised to date (Asakura et al., 2009; Corral-Ramos et al., 2015; Josefsen et al., 2012; Kershaw & Talbot, 2009; Meng et al., 2020; Nadal & Gold, 2010; Ren et al., 2017; L. Shi et al., 2019; Sumita et al., 2017; Zhan et al., 2017). In the present study, the *Z. tritici* genome was found to encode a similar complement of autophagy genes as previously identified in the filamentous pathogens *M. oryzae* and *F. graminearum* (Kershaw & Talbot, 2009; Liu et al., 2017; Lv et al., 2017). Furthermore, deletion of *ZtATG1* was shown to block autophagy in *Z. tritici*, with mutants defective in the transport of autophagosome-bound ZtGFP:ZtATG8 to the vacuole for degradation. The ZtGFP:ZtATG8 puncta observed in *Δztatg1* cells likely represent accumulation of this fusion protein at the PAS, which has also been seen to occur in *Δatg1* strains of *S. cerevisiae* (Cheong et al., 2008; Suzuki et al., 2001) and *F. graminearum* (Lv et al., 2017). However, *Δztatg1* strains remained fully virulent towards wheat leaves,

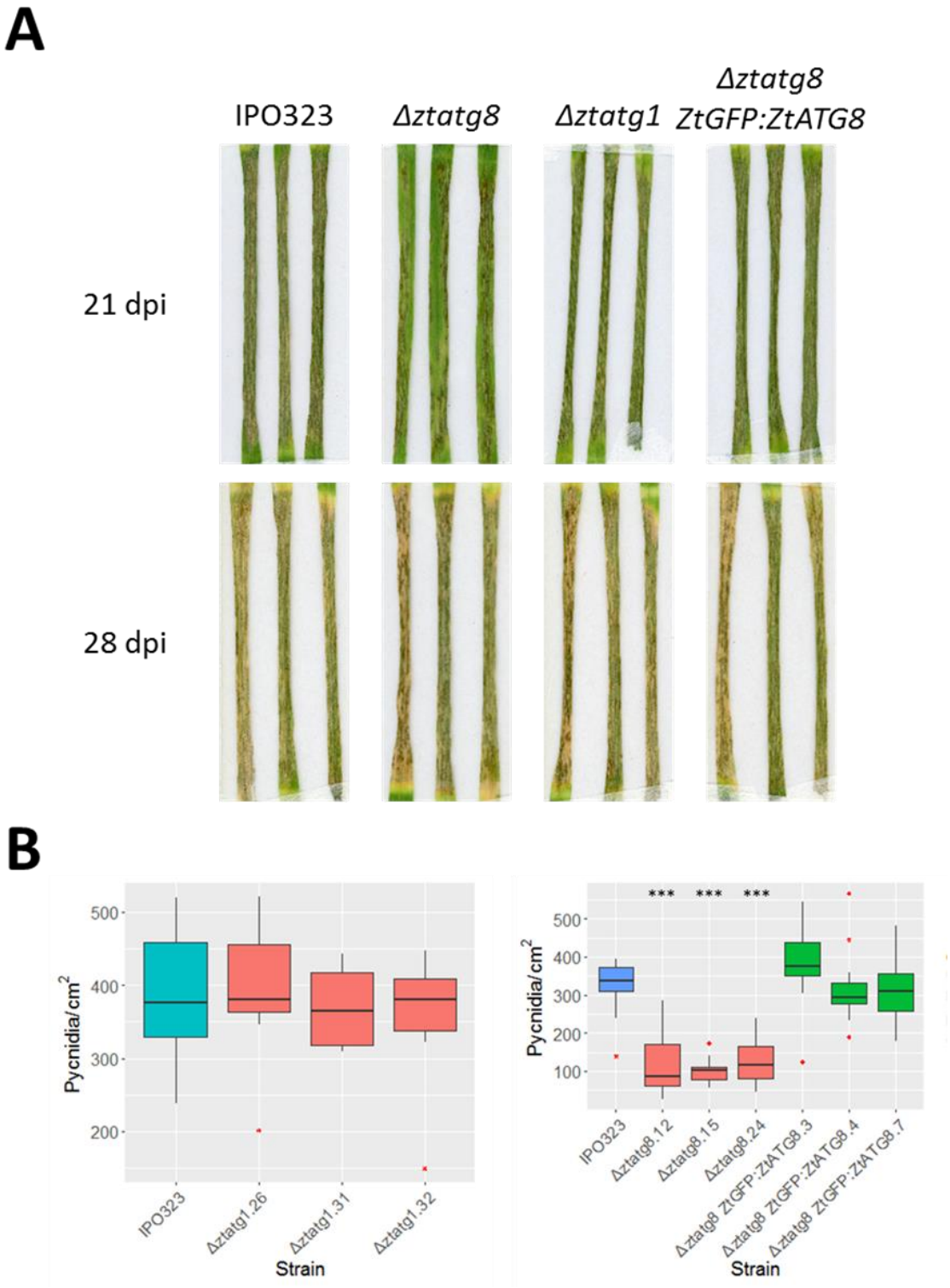


**Figure 3.7 *Δztatg8* is delayed in causing symptoms during infection of wheat leaves**
(A) Scanned wheat leaves infected with *Z. tritici* strains after 21 and 28 days post infection (dpi) with spore suspensions at $5x10^6$ spores/ml. (B) Pycnidia density on infected leaves after 21 dpi. Significant differences between mean pycnidia density on leaves infected with IPO323 and others strain determined by one-way ANOVA and subsequent pairwise comparisons with a Tukey post hoc test, identifying significant reduction (***$p$<0.001) in pycnidia density of *Δztatg8* infected leaves, which was reversed in *Δztatg8 ZtGFP:ZtATG8* strains.

displaying equivalent symptoms and asexual development to the wild type, suggesting that autophagy is dispensable for *Z. tritici* pathogenicity.

Despite some reports of the formation of appressorium-like swellings by *Z. tritici* hyphae (Duncan & Howard, 2000), host invasion is thought not to require the development of complex penetration structures, for which autophagy is required in other plant pathogens (Asakura et al., 2009; Liu et al., 2007; Ren et al., 2017). However, the previously characterised role of autophagy in hyphal germination and growth under starvation conditions in filamentous fungi is relevant to *Z. tritici* infection, as early infection by this fungus is thought to require recycling of stored nutrients for epiphytic growth and initial colonisation of the apoplast (Rudd et al., 2015; Sánchez-Vallet et al., 2015). However, *Δztatg1* strains showed no defect in the morphological switch to filamentous growth under starvation. This suggests that autophagy is not required for this process, and that other mechanisms for mobilising internal energy stores can drive filamentation.

Autophagy is proposed to facilitate the recycling of nutrients from aging hyphae prior to cell death in *A. oryzae* (Shoji & Craven, 2011). Similarly, autophagy is required for developmentally-regulated programmed cell death in the conidia of *M. oryzae*, the contents of which are transported to the developing appressorium (Veneault-Fourrey et al., 2006). However, there is accumulating evidence that epiphytic compartments of *Z. tritici* play important role in infection cycle. Pycnidiospores have been demonstrated to produce blastospores on the leaf surface, which is proposed to provide a source of secondary inoculum without the completion of the invasive infection cycle (Francisco et al., 2019). Experiments using leaf surface-acting fungicides to kill epiphytic hyphae have also demonstrated their contribution to virulence up to 7 days after inoculation (Fones et al., 2017). Furthermore, avirulent *Z. tritici* strains are able to contribute to sexual reproduction despite their inability to colonise the leaf tissue (Kema et al 2018), suggesting that their persistence on the leaf surface may enable them to contribute to sexual reproduction (Suffert et al., 2019). Unselective autophagy of bulk cytoplasm will lead to the degradation of organelles as well as lipid stores (Kiššová et al., 2007; Shoji et al., 2010), which may be detrimental to epiphytic cell survival. Accordingly, there may be a disadvantage to intracellular degradation and autolytic death of epiphytic *Z.*

*tritici* cells after germination and host penetration. This could explain the reduced reliance on autophagy for stored nutrient mobilisation in *Z. tritici* compared to other pathogens such as *M. oryzae*.

*Z. tritici* may therefore preferentially degrade LDs directly in the cytoplasm via the activity of TAG lipases. Crosstalk between lipolysis and autophagy has recently been elucidated in yeast and animal cells (Maeda et al., 2015; Rambold et al., 2015; van Zutphen et al., 2014). Recent evidence suggests that mammalian cells favour mobilisation of FAs from LDs through lipolysis over lipophagy under starvation conditions (Rambold et al., 2015). The authors proposed that lipophagy may lead to toxicity from increases in cytosolic FAs, while lipolysis allows direct flow of FAs from LDs to mitochondria, facilitated by the proximity of these organelles (Rambold et al., 2015). In contrast, yeast cells were found to accumulate lipid droplets in the vacuole under starvation, indicating that autophagy is important for energy mobilisation under these conditions (van Zutphen et al., 2014). Furthermore, TAG lipase activity was found be higher during stationary phase growth after deletion of the vacuolar lipase ATG15, indicating coordinated regulation of lipolysis and lipophagy (Maeda et al., 2015). It is therefore possible that lipolysis is the primary method of LD breakdown in *Z. tritici*, or is at least able to complement the loss of lipophagy in this species.

Investigation of cytosolic lipolysis in *Z. tritici* through functional characterisation of TAG lipases may be hindered by the presence of functional redundancy between these enzymes. Indeed, individual deletion of all putative intracellular TAG lipases in *M. oryzae* led to no alteration in virulence phenotype (Wang et al., 2007). This could result from their redundant function, as suggested by authors (Wang et al., 2007), or from the sole importance of lipophagy for LD degradation in *M. oryzae*. To avoid this, the broad arsenal of selective markers developed for *Z. tritici* could be utilised to generate multiple knockouts in TAG lipase homologs. Alternatively, the potentially overlapping roles of lipophagy and lipolysis in *Z. tritici* could be investigated through deletion of the putative vacuolar lipase *ZtATG15*. ATG15 is responsible for the lysis of autophagic vesicles (Teter et al., 2001), as well as the degradation of neutral lipids during lipophagy (Nguyen et al., 2011; van Zutphen et al., 2014). Deletion of ATG15 in yeast leads to inhibition of both lipophagy and lipolysis, as LDs are sequestered

away from cytosolic lipase activity through autophagy, but remain undigested due to lack of vacuolar lipase activity (van Zutphen et al., 2014).

Autophagy deficient mutants were also found to display increased sensitivity to hydrogen peroxide here, although this effect was not dramatic. Autophagy is known to be involved in the response to oxidative stress through the degradation of organelles and macromolecules damaged by reactive oxygen species (ROS; Filomeni et al., 2015), and increased sensitivity to exogenous ROS is a common phenotype of autophagy deficient filamentous fungi (Meng et al., 2020; Nitsche et al., 2013; Ying et al., 2016). The influence of autophagy disruption on ROS sensitivity may be dampened by the activation of adaptive enzymatic responses to oxidative stress in autophagy mutants, exemplified by the increased superoxide dismutase activity in *S. cerevisiae Δatg* mutants (Zhang et al., 2007). The weak effect of autophagy disruption on ROS sensitivity observed here may reflect the capability of *Z. tritici* to withstand high levels of extracellular ROS during induction of necrotrophy (Keon et al 2007), which is thought to involve the activity of secreted chloroperoxidases and superoxide dismutase enzymes (Palma-Guerrero et al., 2016).

Although *Z. tritici Δztatg1* mutants were fully virulent, deletion of *ZtATG8* led to a delay in symptom development during infection. Distinct phenotypes of ATG8 knockout strains have been observed in multiple fungal pathogen species. Deletion of ATG8 in the entomopathogenic fungus *Metarhizium robertsii* led to severe reductions in appressorium formation, which were not observed in *Δatg1* strains, although reduced virulence was observed in both mutants (Duan et al., 2013). Similarly, defects in *Ustilago maydis* and *Beauveria bassiana* virulence were markedly more severe in *Δatg8* than *Δatg1* (Nadal & Gold, 2010; Ying et al., 2016). However, the cellular mechanisms governing the disparity between the phenotypes of *Δatg1* and *Δatg8* mutants in these species remains to be characterised.

Multiple autophagy-independent functions of ATG8 have been identified in model yeast species, many of which do not involve its conjugation to PE (or lipidation), which is required for its role in autophagosome formation (Liu et al., 2018; Maeda et al., 2017). Deletion of ATG8 was found to impair vacuolar morphology in *Pichia pastoris* during growth on methanol (Tamura et al., 2010)

and in *Schizosaccharomyces pombe* under various stress conditions (Liu et al., 2018; Mikawa et al., 2010), which in both cases was independent of ATG8 lipidation. Similarly, the formation of vacuolar microdomains during the stationary phase in *S. cerevisiae* was impaired in ***Δatg8*** but not in autophagy-deficient strains (Liu et al., 2018). These functions in *S. cerevisiae* and *S. pombe* were governed by the interaction of ATG8 with the vacuolar membrane protein Hfl1, two homologs of which can be identified in the *Z. tritici* genome containing the characteristic TMEM184 domain (IPR005178; ZtritIPO323_04g02580 and ZtritIPO323_04g07778). Crucially, these additional vacuolar functions of yeast ATG8 were dependant on environmental stress or growth phase (Liu et al., 2018; Tamura et al., 2010). *ZtATG8* may therefore influence vacuolar morphology in *Z. tritici* during infection under conditions not characterised *in vitro* in this study.

Furthermore, ATG8 has been shown to bind to LDs in a lipidation-independent manner in *S. cerevisiae* and increase the quantity of LDs in stationary phase cells, which is not observed in TAG lipase-deficient strains (Maeda et al., 2017). LD clustering was observed *in vitro* upon co-incubation with purified ATG8 protein, providing a potential explanation for the ATG8-dependant maintenance of LDs under lipolytic enzyme activity (Maeda et al., 2017). A similar role of *ZtATG8* in LD dynamics may influence invasive growth and therefore virulence of *Z. tritici* in a quantitative manner, which may reflect the minor changes in hyphal growth morphology identified here *in vitro*. These findings provide potential mechanisms by which *ZtATG8* may carry out autophagy-independent functions that impact *Z. tritici* virulence. The localisation of ZtATG8 to vacuolar and LD membranes should be assessed to investigate these possible functions. Additionally, the virulence phenotype of strains deficient in ZtATG8 lipidation, through deletion of *ZtATG4* or *ZtATG7*, should be analysed to assess whether the delayed symptom development of ***Δztatg8*** strains is independent of defects in ZtATG8 conjugation which inhibit autophagy.

## 3.5 Conclusions

In summary, the present study provides evidence that autophagy is not required for the germination and hyphal growth of *Z. tritici* under nutrient deprivation during early invasion of the host, and is therefore dispensable for pathogenicity.

This is contrary to the crucial function of autophagy in infection-related development identified in many other pathogenic fungi. Further study is required to understand how *Z. tritici* mobilises stored fatty acids from LDs to support growth under starvation, focusing on elucidating the role of cytosolic lipolysis and its potential crosstalk with autophagy in this process. Moreover, the potential autophagy- and lipidation-independent functions of ZtATG8 warrant further investigation, considering the quantitative impact deletion of this gene has on *Z. tritici* virulence.

## 3.6 Supplementary information

**Figure S3.1 *ZtATG8* shows high sequence homology with characterised ATG8 proteins**
(A) Gene models for *ZtATG8* from the *Z. tritici* genome annotations by Rothamsted Research (RRes) and the Max Planck Institute (MPI) aligned to ATG8 sequences from *Saccharomyces cerevisiae* (ScATG8; YBL078C) and *Magnaporthe oryzae* (MoATG8; MGG_01062). Coverage of the *ZtATG8* locus with RNA sequencing reads from IPO323 *in vitro* cultures, confirming that the prediction of the first intron is truncated in the RRes annotation, and is consistent instead with the MPI annotation.

**Figure S3.2 *ZtATG1* shows high sequence homology with characterised ATG1 proteins**

Alignment of ATG1 protein sequences, including ZtATG1 from *Z. tritici*, MoATG8 (MGG_06393) from *Magnaporthe oryzae* and ScATG8 (YGL180W) from *Saccharomyces cerevisiae*.

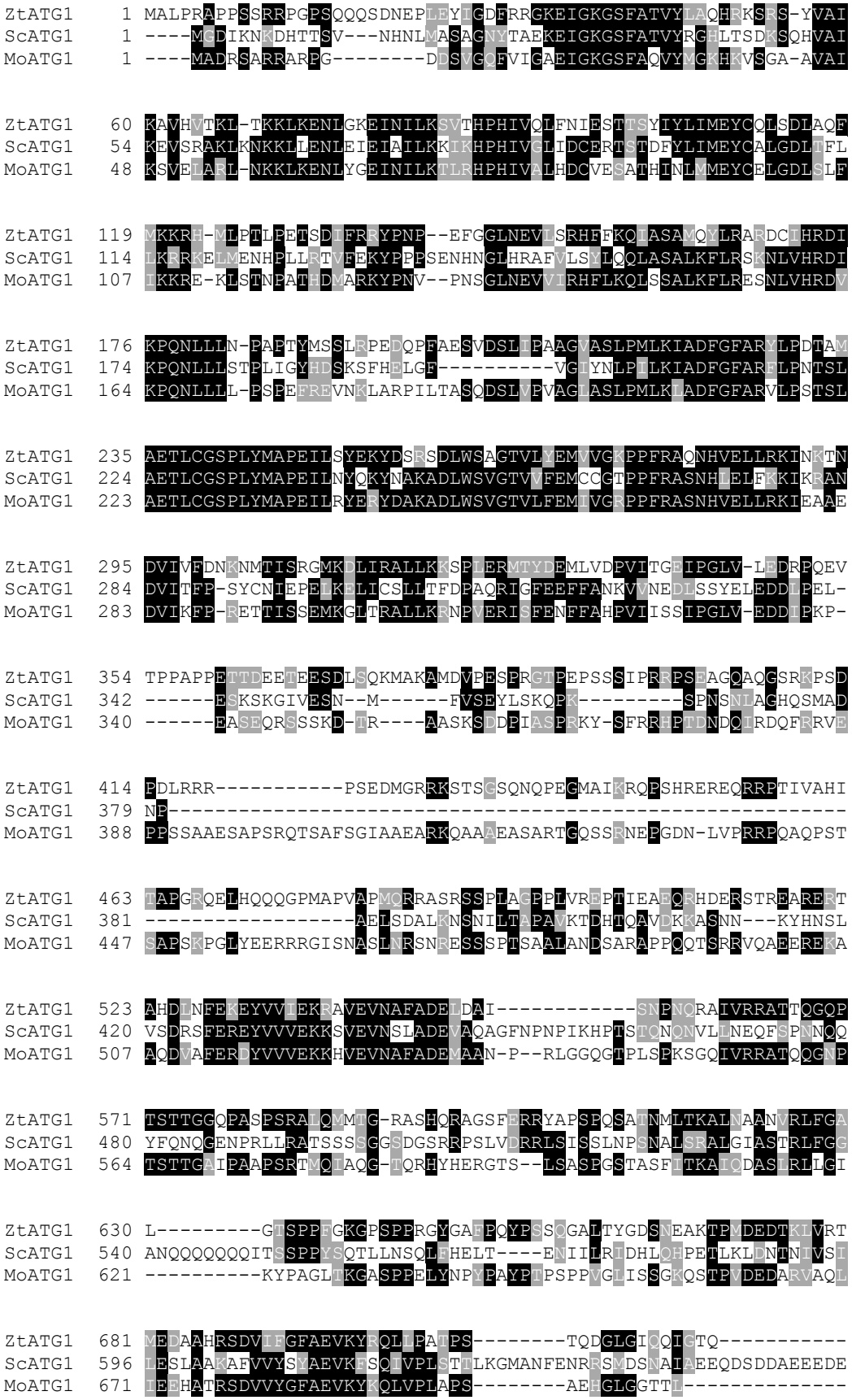

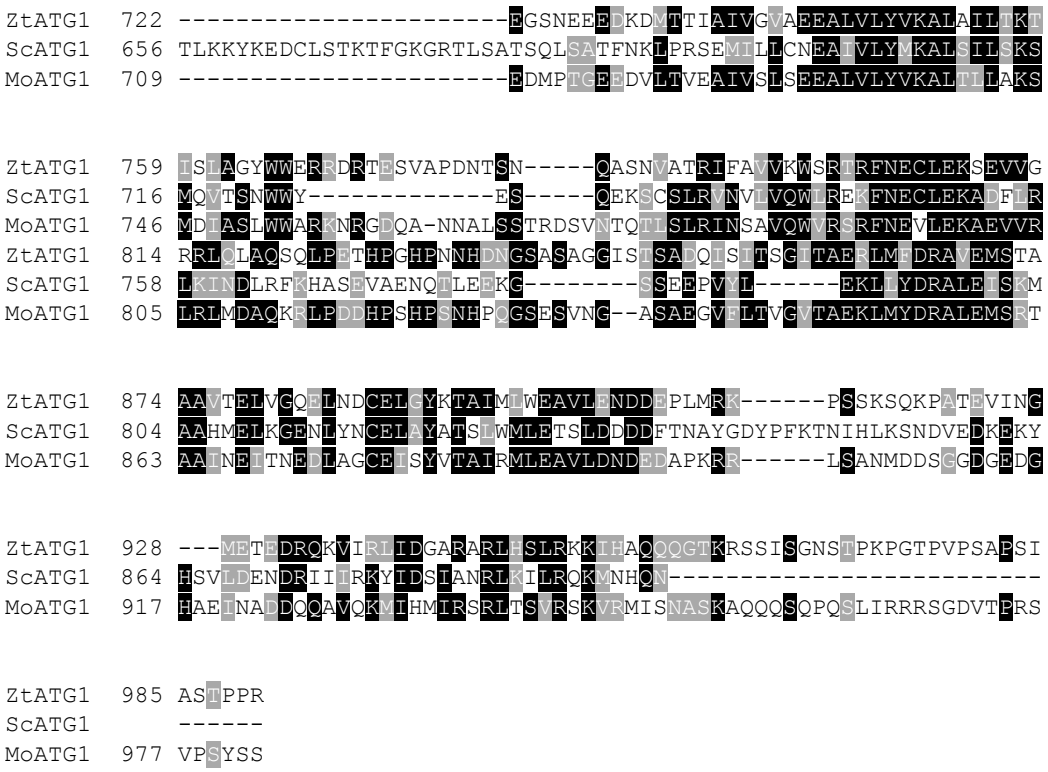
ZtATG1 722 ----------EGSNEEEDKDVTTIAIVGVAEEALVLYVKALAILIKT
ScATG1 656 TLKKYKEDCLSTKTFGKGRTLSATSQLSATFNKLPRSEMILLCNEAIVLYMKALSILSKS
MoATG1 709 ----------EDMPTGEEDVLTVEAIVSLSEEALVLYVKALTLLAKS
ZtATG1 759 ISLAGYWWERRDRTESVAPDNTSN-----QASNVATRIFAVVKWSRTRFNECLEKSEVVG
ScATG1 716 MQVTSNWWY----------ES-----QEKSCSLRVNVLVQWLREKFNECLEKALFLR
MoATG1 746 MDLASLWWARKNRGDQA-NNALSSTRDSVNTQTLSLRINSAVQWVRSRFNEVLEKAEVVR
ZtATG1 814 RRLQLAQSQLPETHPGHPNNHDNGSASAGGISTSADQISTTSGITAERLMFDRAVEMSTA
ScATG1 758 LKINDLRFKHASEVAENQTLEEKG--------SSEEPVYL------EKLLYDRALEISKM
MoATG1 805 LRLMDAQKRLPDDHPSHPSNHPQGSESVNG--ASAEGVFLTVGVTAEKLMYDRALEMSRT
ZtATG1 874 AAVTELVGQELNDCELGYKTAIMLWEAVLENDDEPLMRK------PSSKSQKPATEVING
ScATG1 804 AAHMELKGENLYNCELAYATSLWMLETSLDDDFTNAYGDYPFKTNIHLKSNDVEDKEKY
MoATG1 863 AAINEITNEDLAGCEISYVTAIRMLEAVLDNDEDAPKRR------LSANMDDSGGDGEDG
ZtATG1 928 ---METEDRQKVIRLIDGARARLHSLRKKIHAQQQGTKRSSISGNSTPKPGTPVPSAPSI
ScATG1 864 HSVLDENDRIIIRKYIDSIANRLKILRQKVNHQN--------------------------
MoATG1 917 HAEINADDQQAVQKMIHMIRSRLTSVRSKVRMISNASKAQQQSQPQSLIRRRSGDVTPRS
ZtATG1 985 ASTPPR
ScATG1 ------
MoATG1 977 VPSYSS

# Chapter 4
# **Mitochondrial β-oxidation is required for the pathogenicity of *Z. tritici***

## 4.1 Introduction

The use of neutral lipids for energy storage is ubiquitous amongst eukaryotes and plays a crucial role in survival when external carbon sources are scarce. Lipid metabolism is also crucial for the formation and maintenance of cellular membranes, as well as the generation of signalling molecules. Lipids are stored in the form of triacylglycerols (TAGs) and sterol esters (SEs) in specialised organelles known as lipid droplets (LDs), which are covered in a surfactant phospholipid monolayer to form stable emulsions in the cytoplasm (Tauchi-Sato et al., 2002; Thiam et al., 2013). LD biogenesis occurs at the endoplasmic reticulum, where TAG and SE synthesis occurs. Breakdown of LDs is carried out directly in the cytoplasm by lipolysis, through the activity of TAG lipases and SE hydrolases which localise to the LD membrane (Haemmerle et al., 2006; Köffel et al., 2005; Kurat et al., 2006). Alternatively, LD are digested through autophagic processes, either through bulk autophagy or the selective process of lipophagy (Singh et al., 2009; van Zutphen et al., 2014). The resulting fatty acids (FAs) are utilised for energy production through β-oxidation, or for the production of membrane components and signalling molecules.

FA β-oxidation occurs in both the mitochondria and peroxisomes in mammals. Due to the lack of mitochondrial β-oxidation in *S. cerevisiae*, this pathway was assumed to be absent in fungi until its characterisation in various basidiomycete and ascomycete species (Feron et al., 2005; Maggio-Hall & Keller, 2004; Shen & Burger, 2009). Sequence homology between peroxisomal β-oxidation enzymes and those from α-proteobacteria indicates that eukaryote β-oxidation was originally a mitochondrial process, which has transferred to peroxisomes over time (Camões et al., 2015; Gabaldón, 2014). This may have occurred to reduce the damaging effects of reactive oxygen species (ROS) produced during oxidative phosphorylation associated with β-oxidation in the mitochondria (Speijer, 2011). In plants and *Saccharomycete* yeasts, which lack mitochondrial β-oxidation (Poirier et al., 2006; Shen & Burger, 2009), this process of enzyme transfer is assumed to have been completed. The division of labour in FA β-oxidation between mitochondria and peroxisomes is part of the complex metabolic interaction being elucidated between these two organelles (Schrader

& Yoon, 2007), which have recently been demonstrated to undergo physical tethering in yeast (Mattiazzi Ušaj et al., 2015).

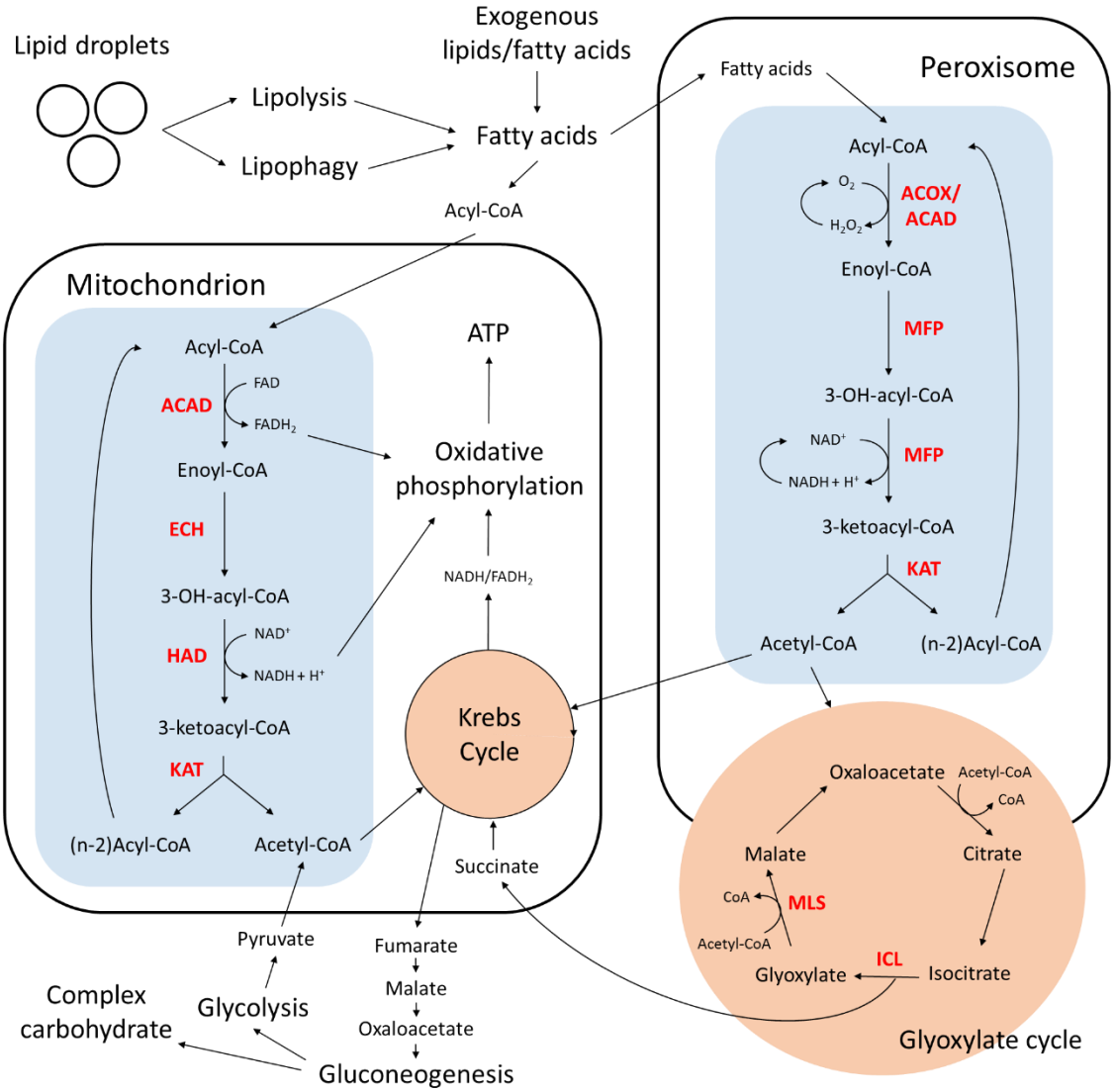


**Figure 4.1 Fatty acid catabolism in fungi**
Metabolic pathways associated with the degradation of stored lipids, including fatty acid β-oxidation in the mitochondria and peroxisome (blue) and utilisation of resulting acetyl-CoA for ATP production and synthesis complex carbohydrates via the glyoxylate and Krebs cycles (orange). The glyoxylate cycle is represented on the edge of the peroxisome due to the flexibility of the partaking enzyme location between this organelle and the cytosol. Enzymes discussed in the text are presented in red; acyl-CoA dehydrogenase (ACAD), acyl-CoA oxidase (ACOX), enoyl-CoA hydratase (ECH), 3-hydroxyacyl-CoA dehydrogenase (HAD), multifunctional protein (MFP), 3-ketoacyl-CoA thiolase (KAT), malate synthase (MLS) and isocitrate lyase (ICL).

The process of β-oxidation is carried out in 4 reactions, which are catalysed by different sets of enzymes in the peroxisomes and mitochondria of fungi (Fig. 4.1). The conversion of acyl-CoA to enoyl-CoA in the first step is catalysed by acyl-CoA dehydrogenase (ACAD) in mitochondria. This first reaction was thought to be carried out exclusively by acyl-CoA oxidases (ACOX) in

peroxisomes, although peroxisomally-localised ACAD enzymes have recently been characterised (Camões et al., 2015). The subsequent two steps are carried out by enoyl-CoA hydratase (ECH) and 3-hydroxyacyl-CoA dehydrogenase (HAD) in mitochondria, while these two enzymatic functions are carried out by multifunctional β-oxidation proteins (MFP; also referred to as FOX2/MFE) in fungal peroxisomes. The final step, which releases acetyl-CoA and the acyl-CoA chain truncated by two carbon atoms, is catalysed by separate 3-ketoacyl-CoA thiolase (KAT) enzymes in both pathways. In mitochondria, electrons and acetyl-CoA generated by β-oxidation can be transferred to the respiratory chain and Krebs cycle, respectively (Fig. 4.1). On the other hand, the acetyl-CoA produced by peroxisomal β-oxidation enters the glyoxylate cycle or is transported into the cytosol (Poirier et al., 2006). The glyoxylate cycle leads to production oxaloacetate, which feeds into glucose production by gluconeogenesis, allowing for carbohydrate synthesis from stored lipids (Fig. 4.1; Dunn et al., 2009).

The metabolism of lipids has been revealed to be crucial for fungal pathogenicity towards plants (Dunn et al., 2009). In particular, plant pathogenic fungi have been shown to utilise stored lipids to overcome the scarcity of nutrients on the host surface during the initial stages of infection (Both et al., 2005; Solomon et al., 2004; Weber et al., 2001). The generation of appressorial turgor pressure for host penetration in *M. oryzae* relies on glycerol generated from the breakdown of LDs transported from the spore (Thines et al., 2000; Weber et al., 2001). Furthermore, the biotrophic barley pathogen *Blumeria graminis f sp hordei* was found to upregulate transcription of lipid metabolism genes in germinating spores. This is followed by a dramatic decrease in expression of these genes coinciding with disappearance of LDs in cells, indicating the importance of mobilizing stored lipids for *in planta* germination (Both et al., 2005). This finding is indicative of an emerging trend that lipid metabolism is involved in supporting spore germination under nutrient limited conditions, with evidence to support this in *Stagonospora nodorum*, *M. oryzae*, *Leptospheria maculans* and *Fusarium graminearum* (Idnurm & Howlett, 2002; Solomon et al., 2004; Tang et al., 2019; Wang et al., 2003).

Initial molecular characterisation of lipid metabolism in plant pathogenic fungi focused on the glyoxylate cycle, following discovery of its importance for the

virulence of bacterial and fungal pathogens of humans (Lorenz & Fink, 2002; McKinney et al., 2000). The key glyoxylate cycle enzymes isocitrate lyase (ICL) and malate synthase (MLS; Fig. 4.1) were found to be crucial for the early stages of leaf infection by multiple species, showing defects in germination and host penetration (Asakura et al., 2006; Idnurm & Howlett, 2002; Solomon et al., 2004; Wang et al., 2003). However, the involvement of glyoxylate cycle as a downstream component of lipid catabolism cannot be assumed. This is exemplified in *Candida albicans*, in which the role of ICL in virulence can be separated from the reliance on FA β-oxidation, indicating the importance of the glyoxylate cycle for metabolism of a different substrate (Piekarska et al., 2006, 2008). Despite this, the mobilisation of LDs from the spores of *M. oryzae* and *S. nodorum* was inhibited by glyoxylate cycle disruption, suggesting that this pathway is required for lipid catabolism and virulence in these species (Solomon et al., 2004; Wang et al., 2003).

Subsequent characterisation of the β-oxidation pathways in peroxisomes and mitochondria of filamentous fungi have revealed a similar division of labour to mammalian lipid metabolism. Characterisation of exogenous FA utilisation in fungal β-oxidation mutants has identified specialisation in the two pathways based on FA chain length and saturation. This specialisation follows a general trend in catabolism of longer, branched and unsaturated FAs by peroxisomal enzymes and short- and medium-chain length FAs by mitochondrial enzymes, although with significant variation between species (Klose & Kronstad, 2006; Kretschmer, Klose, et al., 2012; Kretschmer, Wang, et al., 2012; Maggio-Hall & Keller, 2004; Tang et al., 2019). This is similar to the substrate specificity seen in mammalian β-oxidation (Poirier et al., 2006).

To our knowledge, both β-oxidation pathways have been found to contribute to the virulence of all plant pathogenic fungi in which they have been characterised, including *Ustilago maydis* (Klose & Kronstad, 2006; Kretschmer, Klose, et al., 2012), *M. oryzae* (Patkar et al., 2012; Wang et al., 2007) and *F. graminearum* (Tang et al., 2019). The peroxisomal β-oxidation protein MFP1 was found to be important for *M. oryzae* host penetration through its function in mobilisation and degradation of LDs in the appressorium (Wang et al., 2007). Furthermore, deletion of mitochondrial β-oxidation enzyme MoEch1 caused similar disruption of appressorium formation and host penetration, as well as

reduced conidial germination (Patkar et al., 2012). However, *Δmoech1* also displayed aberrant mitochondrial morphology and increased sensitivity to oxidative stress, which was proposed to inhibit the small number of invasive hyphae formed from entering the host (Patkar et al., 2012). These phenotypes show considerable similarity to *F. graminearum Δech1* strains, which display reduced germination, accumulation of LDs and increased oxidative stress sensitivity, resulting in severely reduced virulence (Tang et al., 2019). These studies indicate the importance of FA β-oxidation for utilising stored lipids during the initiation of infection.

The utilisation of stored lipids has been proposed to support germination and early invasive growth of *Z. tritici* during the symptomless phase of infection (Rudd et al., 2015; Sánchez-Vallet et al., 2015). *Z. tritici* blastospores and chlamydospores have been shown to contain high concentrations of LDs (Francisco et al., 2019; Sidhu, 2015), similar to the spores of other fungal plant pathogens (Solomon et al., 2004; Thines et al., 2000). Transcriptome studies have reported the upregulation of genes putatively involved in lipid metabolism and FA β-oxidation during early infection, suggesting that catabolism of these lipid stores is occurring at this stage (Palma-Guerrero et al., 2016; Rudd et al., 2015). Beyond these gene expression analyses, the only molecular characterisation of *Z. tritici* lipid metabolism investigated the function of the glyoxylate cycle (Sidhu, 2015). Deletion of the MLS1 enzyme was found to severely reduce *Z. tritici* virulence, which correlated with reduced mobilisation of LDs in the spore, similar to other fungi (Solomon et al., 2004; Wang et al., 2003). This loss of virulence could be rescued with application of exogenous glucose, indicating that the contribution of the glyoxylate cycle to gluconeogenesis was supporting growth during infection (Sidhu, 2015).

In the present study, the contribution of FA β-oxidation to *Z. tritici* development and virulence was assessed using a reverse genetic approach. The inventory of genes putatively encoding peroxisomal and mitochondrial β-oxidation enzymes was identified in the *Z. tritici* genome. Homologs of ECH and MFP enzymes were characterised by targeted gene deletion to investigate the contributions of these two pathways to FA metabolism and virulence in the fungus. The results uncover the crucial role of mitochondrial β-oxidation in supporting germination and hyphal growth during host colonisation by *Z. tritici*. Furthermore, MFP

enzymes putatively involved in the peroxisomal β-oxidation pathway were dispensable for growth under starvation and virulence. These results further support the hypothesis that *Z. tritici* uses stored lipids to support growth during the symptomless phase of wheat infection.

## 4.2 Materials and Methods

### 4.2.1 Construction of plasmid vectors

Plasmid vectors for the deletion of *ZtMFP1*, *ZtMFP2* and *ZtEch1* were constructed by yeast recombinational cloning (Chapter 2.2). The plasmids pC-HYG-YR and pC-BAR-YR were used as backbones for these vectors (Sidhu, Chaudhari, et al., 2015), which were linearised by restriction digestion with the enzymes EcoRI and HindIII (New England Biolabs, UK). Left flank (LF) and right flank (RF) sequences were PCR amplified using the primer pairs MFP1-LF-F/R, MFP1-RF-F/R, MFP2-LF-F/R, MFP2-RF-F/R, ECH1-LF-F/R and ECH1-RF-F/R. LF and RF amplicons for *ZtMFP1* and *ZtEch1* were transformed into *S. cerevisiae* with the linearised pC-HYG-YR vector, while the LF and RF amplicons for *ZtMFP2* were transformed alongside pC-BAR-YR, generating the plasmids pC-HYG-MFP1KO, pC-HYG-ECH1KO and pC-BAR-MFP2KO (Fig. 4.2). The fidelity of LF and RF DNA sequence cloning was confirmed by Sanger sequencing in the completed vectors. These vectors were transformed into *Z. tritici* through *Agrobacterium*-mediated transformation (Chapter 2.3). Correct insertion of the selective markers and absence of the native gene was confirmed in the resulting transformant strains by PCR using the primer pairs described in Figure 4.2.

The plasmid vector pC-BAR-ECH1comp was constructed in order to complement the deletion of *ZtEch1* (Fig. 4.2D). A 1000 bp region upstream of the *ZtEch1* promoter (LF2) was amplified using the primer pair ECH1-LF2-F/R, while an amplicon containing a *ZtEch1* promoter region of 600 bp, the *ZtEch1* coding sequence and the RF sequence was amplified with the primer pair ECH1-PROM-F/ECH1-RF-R. These fragments were co-transformation into *S. cerevisiae* along with the linearised pC-BAR-YR backbone to produce pC-BAR-ECH1comp. The sequence of the cloned *ZtEch1* coding region was confirmed by Sanger sequencing before the vector was transformed into the *Δztech1*

strain. Correct insertion of the *BAR*$^R$ selective marker and *ZtEch1* cassette was confirmed by PCR using the primers described in Figure 4.2.

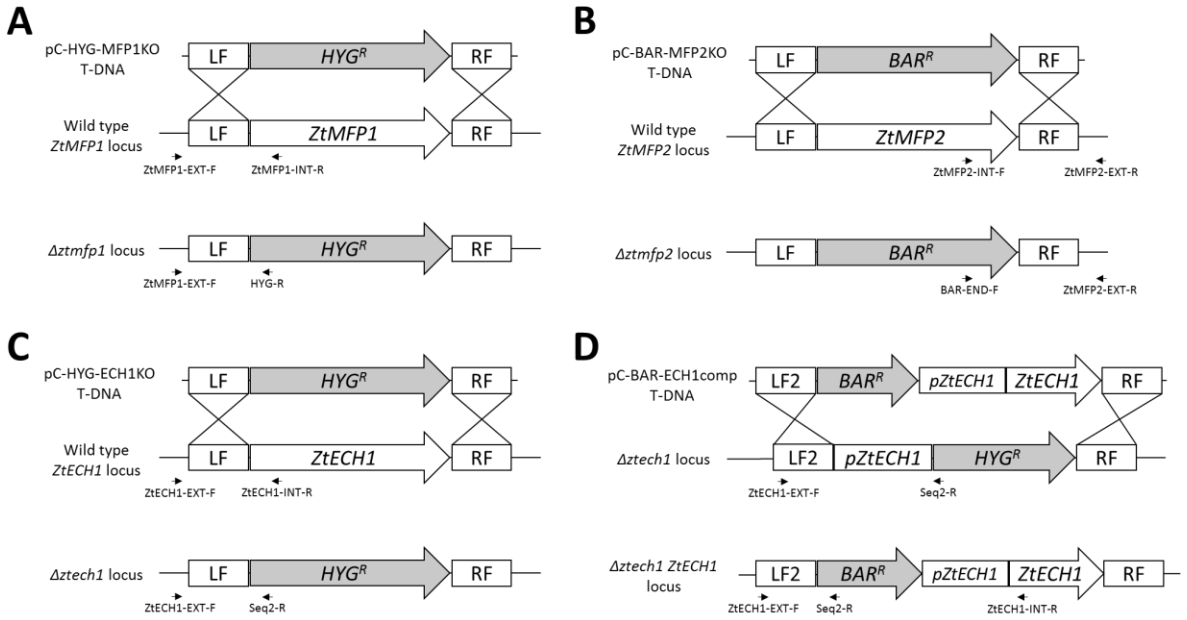


**Figure 4.2 Targeted deletion and complementation of *Z. tritici* β-oxidation genes *ZtMFP1*, *ZtMFP2* and *ZtECH1***
Schematics displaying homologous recombination between flanking sequences (LF and RF) of T-DNA from the plasmids pC-HYG-MFP1KO (A), pC-BAR-MFP2KO (B), pC-HYG-ECH1KO (C) and pC-BAR-ECH1comp (D) and the targeted locus in the *Z. tritici* genome. Below each homologous recombination schematic is the resulting transgenic locus containing the selective markers *HYG*$^R$ and *BAR*$^R$ for resistance to hygromycin B and glufosinate ammonium, respectively. Primers (arrows) used for PCR screening of resulting transformants are shown below their respective target loci.

### 4.2.2 Growth assays on exogenous fatty acids

To assess the ability of *Z. tritici* strains to metabolise FAs, cells were grown on YPD agar for 5 days at 19ºC. Blastospores were harvested, washed three times with AMMC- and diluted to 5x10$^6$ spores/ml in the same medium. A 10-fold dilution series was prepared and 5 µl droplets were plated onto AMMC- agar supplemented with a range of FAs, olive oil (1% v/v), sodium acetate (120mM) or glucose (1% w/v) as the sole carbon source. FAs included butyric acid, valeric acid and octanoic acid at 2.5 mM, and lauric acid, palmitic acid and stearic acid at 5 mM. All FAs were purchased from Sigma-Aldrich (UK). All FAs and olive oil were solubilised with 0.05% Tween 20 (Sigma-Aldrich, UK) apart from butyric acid and valeric acid. Control plates included AMM and AMMC- containing 0.05% Tween 20 to assess toxicity of the surfactant to *Z. tritici* cells.

Plates were incubated at 19ºC for 14 days and growth rate and morphology observed.

### 4.2.3 Rhodamine 123 staining of mitochondria

*Z. tritici* cells were harvested from 5 day old YPD plates, filtered through a cell strainer and suspended in YG broth at a concentration of $1x10^5$ spores/ml. After incubation overnight at 19ºC with 180 rpm shaking, cells were pelleted by centrifugation at 10,000 x G for 3 min and suspended in YG broth amended with 10 µg/ml rhodamine 123 (Sigma-Aldrich, UK). After 30 min incubation in the same conditions, cells were pelleted and washed twice with YG broth, before observation using an epifluorescence microscope.

## 4.3 Results

### 4.3.1 Identification of β-oxidation genes in *Zymoseptoria tritici*

The MFP enzyme was chosen as a target for investigation of the peroxisomal β-oxidation pathway, due to its conserved function in other fungi (Klose & Kronstad, 2006; Maggio-Hall & Keller, 2004; Piekarska et al., 2006; Wang et al., 2007). To identify homologs of MFP enzymes in *Z. tritici*, the sequence of the Fox2 protein from *Neurospora crassa* was used to query the genome using the BlastP algorithm. This identified two genes, ZtritIPO323_04g10198 and ZtritIPO323_04g08334, with predicted protein products displaying high sequence identity to Fox2. Both putative proteins contained a C-terminal tripeptide Alanine–Lysine–Leucine (-AKL) PTS1 targeting sequence (Fig. S4.1) and were predicted to have peroxisomal localisation by DeepLoc (Almagro Armenteros et al., 2017). Multiple sequence alignments revealed that while ZtritIPO323_04g10198 showed sequence homology across the entire length of NcFox2 and MoMFP1 from *M. oryzae*, ZtritIPO323_04g08334 was truncated at the C-terminus by approximately 300 amino acids (Fig. S4.1). Protein domain analysis found that ZtritIPO323_04g10198 displayed typical domain structure of Fox2-like multifunctional β-oxidation enzymes (Fig. 4.3A), containing two short-chain dehydrogenase (SDR) domains (IPR002347) responsible for 3-hydroxyacyl-CoA dehydrogenase activity, and a C-terminal MaoC domain (IPR002539) responsible for ECH activity (Hiltunen et al., 1992). However, ZtritIPO323_04g08334 is missing the MaoC domain corresponding with the

truncation at its C-terminus (Fig. 4.3A). ZtritIPO323_04g10198 and ZtritIPO323_04g08334 were designated *ZtMFP1* and *ZtMFP2* and used for investigation of *Z. tritici* peroxisomal β-oxidation.

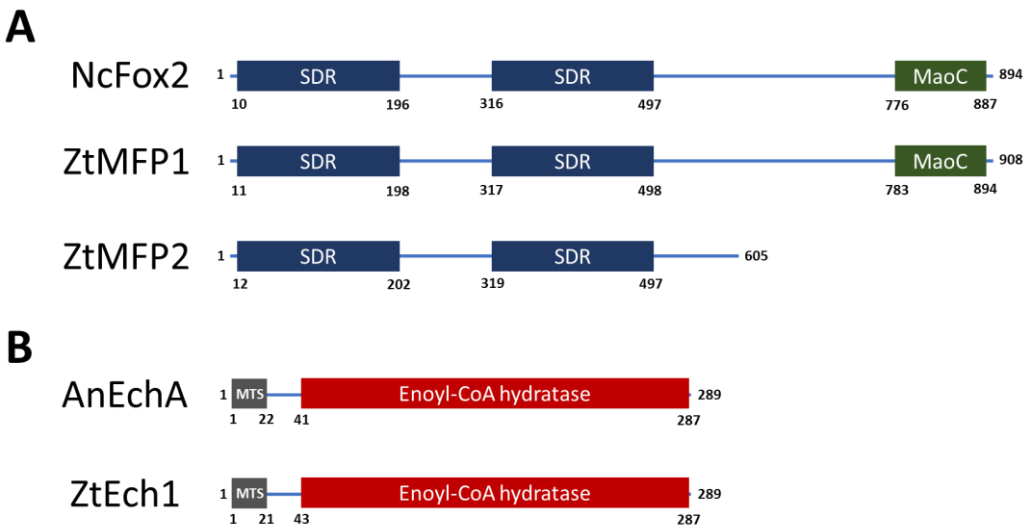


**Figure 4.3. Domain structure of the targeted *Z. tritici* β-oxidation proteins**
(A) Multifunctional protein Fox2 from *Neurospora crassa* (NcFox2) and its *Z. tritici* homologs ZtMFP1 (ZtritIPO323_04g10198) and ZtMFP2 and (ZtritIPO323_04g08334) all contain 2 short-chain dehydrogenase (SDR) domains (IPR002347), while ZtMFP2 lacks the C-terminal MaoC domain (IPR002539). (B) Enoyl-CoA hydratase from *Aspergillus nidulans* (AnEchA) and its *Z. tritici* homolog ZtEch1 (ZtritIPO323_04g07883) both contain an N-terminal mitochondrial targeting sequence (MTS) and a C-terminal Enoyl-CoA hydratase/isomerase domain (IPR001753).

The enzyme ECH was chosen for further investigation of mitochondrial β -oxidation in *Z. tritici*, as it has been the subject of molecular characterisation in *A. nidulans* (Maggio-Hall & Keller, 2004), *M. oryzae* (Patkar et al., 2012) and *F. graminearum* (Tang et al., 2019). Interrogation of the *Z. tritici* genome by BlastP alignment using AnEchA from *A. nidulans* led to identification of 13 hits, all of which contain the crotonase-like domain (IPR029045) typical of ECH enzymes. ZtritIPO323_04g07883 (previously Mycgr3G38857) displayed the strongest sequence identity to previously characterised ECH enzymes, showing between 64-68% identity across 96-98% of the protein sequence with MoEch1, FgEch1 and AnEchA (Fig. 4.4A; Fig. S4.2). ZtritIPO323_04g07883 is one of three crotonase-like domain-containing *Z. tritici* proteins predicted to contain a mitochondrial targeting sequence (MTS) at its N-terminus by MitoFates (Fig. 4.3B; Fukasawa et al., 2015). ZtritIPO323_04g06529 was also predicted to localise to the mitochondria, but had much lower sequence similarity to AnEchA (30% identity across 35% query coverage), and contained 3-hydroxyisobutyryl-

CoA hydrolase-type enoyl-CoA hydratase/isomerase domain (IPR032259) predicted to be involved in valine catabolism (Fig. 4.4A). Similarly, although ZtritIPO323_04g03198 contained a mitochondrial pre-sequence, the predicted protein product showed much lower sequence homology to AnEchA (35% identity across 98% query coverage), and showed significant homology with the human methylglutaconyl-CoA hydratase enzyme AUH which has low ECH activity (Fig. 4.4A; Nakagawa et al., 1995). One additional enoyl-CoA hydratase/isomerase domain protein, ZtritIPO323_04g09620, was predicted to locate to the mitochondria by DeepLoc, although this protein was not predicted to contain an N-terminal MTS (Table 4.1). These results led to selection of ZtritIPO323_04g07883, hereby designated *ZtEch1*, for molecular characterisation of mitochondrial β-oxidation.

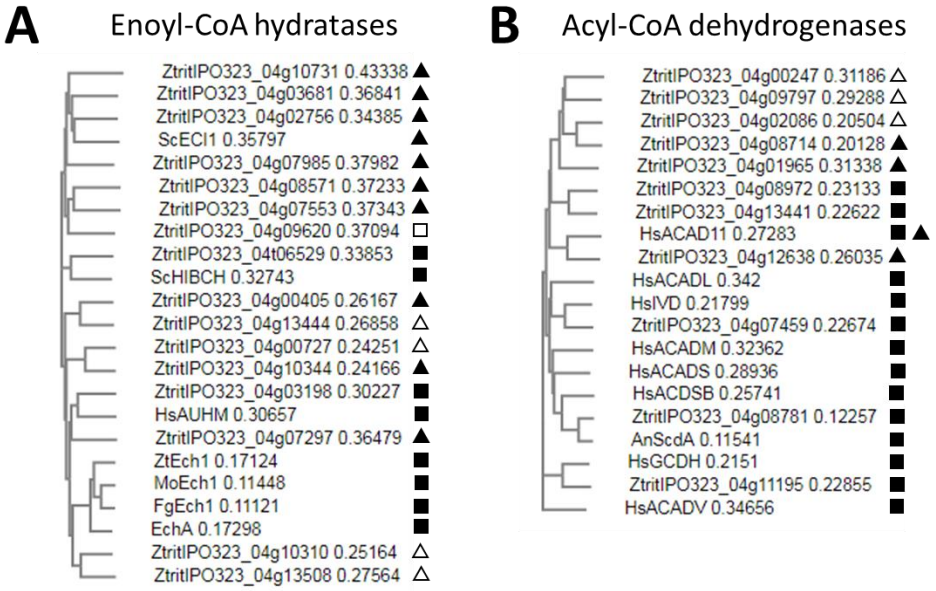


**Figure 4.4 Putative mitochondrial and peroxisomal enoyl-CoA hydratase and acyl-CoA dehydrogenase genes**
Phylogenetic trees of predicted protein sequences of enoyl-coA hydratase genes from *Z. tritici* (putative), *M. oryzae* (MoEch1/MGG_12868), *F. graminearum* (FgEch1/FGSG_13111) and *A. nidulans* (EchA/AN5916), along with *S. cerevisiae* 3,2-trans-enoyl-CoA isomerase (ScECI1/YLR284C) and 3-hydroxyisobutyryl-CoA hydrolase (ScHIBCH/YDR036C) and *Homo sapiens* methylglutaconyl-CoA hydratase (HsAUHM/Q13825), and (B) acyl-CoA dehydrogenases from *Z. tritici* (putative), *A. nidulans* (AnScdA/AN0824) and *H. sapiens* (HsACAD11/Q709F0; HsACADL/P28330; HsIVD/P26440; ACADM/P11310; HsACADS/P16219; HsACADSB/P45954; HsACADV/P49748; HsGCDH/Q92947). Putative subcellular localisation (DeepLoc; Almagro Armenteros et al., 2017) to the mitochondria (square) or peroxisome (triangle), with (black) or without (white) prediction from MitoFates (Fukasawa et al., 2015) or PTS1 predictor (Neuberger et al., 2003), respectively.

Other genes with potential functions in FA β-oxidation in *Z. tritici* were identified through the presence of conserved enzymatic domains and prediction of subcellular localisation to the mitochondria and peroxisomes (Table 4.1). Searches for ACAD enzymes required for the first step of mitochondrial β-oxidation identified 5 proteins, containing the associated InterPro domains (IPR013786; IPR006091; IPR009075) and putative mitochondrial localisation signals (Table 4.1). This includes homologs of mammalian isovaleryl-CoA dehydrogenase and glutaryl-CoA dehydrogenase (Fig. 4.4B), responsible for catabolism of leucine and lysine, respectively. Also identified was a homolog of the *A. nidulans* ACAD *AnScdA* (Fig. 4.4B), which is required for catabolism of short chain FAs and branched-chain amino acids valine, leucine and isoleucine (Maggio-Hall et al., 2008). The remaining two ADADS are likely to display activity towards other FA chain lengths (Table 4.1; Fig. 4.4B). Individual 3-hydroxyacyl-CoA dehydrogenase domain (IPR022694) and thiolase domain (IPR002155) proteins were predicted to have mitochondrial localisation, which are assumed to carry out the third and fourth steps of mitochondrial β-oxidation in *Z. tritici* (Table 4.1).

Searches for peroxisomal β-oxidation enzymes identified two ACOX domain (IPR012258) proteins predicted to be localised to the peroxisome (Table 4.1). Furthermore, seven putative ACAD enzymes were also predicted to localise to the peroxisome, which is consistent with the characterisation of a 'hybrid' peroxisomal pathway including this enzyme activity in several fungal lineages (Shen & Burger, 2009). This included a homolog of ACAD11 (ZtritIPO323_04g12638), which was experimentally verified to have peroxisomal localisation in *U. maydis* (Camões et al., 2015). Two of these putative ACAD proteins (ZtritIPO323_04g00247 and ZtritIPO323_04g09797) contained an additional Cytochrome b5-like heme/steroid binding domain (IPR001199) at the N-terminal end of the sequence, which may act as an electron acceptor domain (Camões et al., 2015). Additionally, four proteins with thiolase domains were predicted to localise to the peroxisome, although none contained a canonical PTS1 sequence (Table 4.1). These findings indicate that *Z. tritici* peroxisomes may be equipped to metabolise a broad range of FA chain lengths, as seen in the chain length-specificity of mammalian mitochondrial ACAD enzymes (Bartlett & Eaton, 2004).

**Table 4.1 Putative fatty acid β-oxidation genes from *Z. tritici***

| Pathway | Step | Enzyme | Gene ID | DeepLoc prediction[a] (Likelihood) | PTS1[b] | MTS[c] |
|---|---|---|---|---|---|---|
| Peroxisomal β-oxidation | 1 | Acyl-CoA oxidase (ACOX) | ZtritIPO323_04g08552 | Peroxisome (0.9294) | Targeted | No |
| | | | ZtritIPO323_04g03879 | Peroxisome (0.9234) | Not targeted | No |
| | 1 | Acyl-CoA dehydrogenase (ACAD) | ZtritIPO323_04g00247 | Peroxisome (0.4118) | Twilight zone | No |
| | | | ZtritIPO323_04g01965 | Peroxisome (0.4807) | Targeted | No |
| | | | ZtritIPO323_04g02086 | Peroxisome (0.7335) | Twilight zone | No |
| | | | ZtritIPO323_04g08714 | Peroxisome (0.6874) | Targeted | No |
| | | | ZtritIPO323_04g09797 | Peroxisome (0.418) | Not targeted | No |
| | | | ZtritIPO323_04g11779 | Peroxisome (0.8578) | Targeted | No |
| | | | ZtritIPO323_04g12638 | Peroxisome (0.4552) | Targeted | No |
| | 2+3 | Mulifunctional protein (MFP) | ZtritIPO323_04g10198 | Peroxisome (0.8722) | Targeted | No |
| | | | ZtritIPO323_04g08334 | Peroxisome (0.9359) | Targeted | No |
| | 2 | Enoyl-CoA hydratase (ECH) | ZtritIPO323_04t10310 | Peroxisome (0.8603) | Twilight zone | No |
| | | | ZtritIPO323_04g00405 | Peroxisome (0.9848) | Targeted | No |
| | | | ZtritIPO323_04g00727 | Peroxisome (0.9865) | Not targeted | No |
| | | | ZtritIPO323_04g07297 | Peroxisome (0.9722) | Targeted | No |
| | | | ZtritIPO323_04g08571 | Peroxisome (0.9849) | Targeted | No |
| | | | ZtritIPO323_04g10344 | Peroxisome (0.9854) | Targeted | No |
| | | | ZtritIPO323_04g13444 | Peroxisome (0.9872) | Not targeted | No |
| | | | ZtritIPO323_04g13508 | Peroxisome (0.9716) | Twilight zone | No |
| | | | ZtritIPO323_04g07985 | Peroxisome (0.9787) | Targeted | No |
| | | | ZtritIPO323_04g07553 | Peroxisome (0.6218) | Targeted | No |
| | 3 | 3-Hydroxyacyl-CoA dehydrogenase (HAD) | ZtritIPO323_04g00887 | Peroxisome (0.5087) | Not targeted | No |
| | | | ZtritIPO323_04g10778 | Peroxisome (0.6854) | Not targeted | No |
| | 4 | 3-Ketoacyl-CoA thiolase (KAT) | ZtritIPO323_04g07699 | Peroxisome (0.6707) | Not targeted | No |
| | | | ZtritIPO323_04g07910 | Peroxisome (0.7597) | Not targeted | No |
| | | | ZtritIPO323_04g02591 | Peroxisome (0.6163) | Not targeted | No |
| | | | ZtritIPO323_04g09880 | Peroxisome (0.6098) | Not targeted | No |
| | Accessory | 3,2-Trans-enoyl-CoA isomerase | ZtritIPO323_04g02756 | Peroxisome (0.9444) | Twilight zone | No |
| | | | ZtritIPO323_04g03681 | Peroxisome (0.9721) | Targeted | No |
| Mitochondrial β-oxidation | 1 | Acyl-CoA dehydrogenase (ACAD) | ZtritIPO323_04g08781 | Mitochondrial (0.9997) | Not targeted | Yes |
| | | | ZtritIPO323_04g08972 | Mitochondrial (0.995) | Not targeted | Yes |
| | | | ZtritIPO323_04g13441 | Mitochondrial (0.994) | Not targeted | Yes |
| | | | ZtritIPO323_04g07459 | Mitochondrial (0.9999) | Not targeted | Yes |
| | | | ZtritIPO323_04g11195 | Mitochondrial (0.9993) | Not targeted | Yes |
| | 2 | Enoyl-CoA hydratase (ECH) | ZtritIPO323_04t07883 | Mitochondrial (0.9987) | Not targeted | Yes |
| | | | ZtritIPO323_04g09620 | Mitochondrial (0.9407) | Not targeted | No |
| | 3 | 3-Hydroxyacyl-CoA dehydrogenase (HAD) | ZtritIPO323_04g05493 | Mitochondrial (0.9994) | Not targeted | Yes |
| | 4 | 3-Ketoacyl-CoA thiolase (KAT) | ZtritIPO323_04g00471 | Mitochondrial (0.9979) | Not targeted | No |

[a]Predicted by DeepLoc (Almagro Almenteros et al 2017)
[b]Predicted by PTS1 predictor – positive scores give reliable PTS1 prediction ('Targeted'), scores between -10 and 0 are considered 'Twilight zone' hits with some divergence in binding motifs and potential inaccessibility to Pex5 protein, and scores below -10 are considered 'Not targeted' (Neuberger et al 2003)
[c]Predicted by MitoFates (Fukasawa et al 2015)

Despite the function of MFP enzymes in the second and third steps of the canonical peroxisomal β-oxidation pathway, 13 proteins containing enoyl-CoA hydratase/isomerase domains (IPR001753) were predicted to localise to the peroxisome (Table 4.1; Fig. 4.4A). Two of these proteins (ZtritIPO323_04g02756 and ZtritIPO323_04g03681) showed homology with peroxisomal δ3,δ2-enoyl-CoA isomerase from *S. cerevisiae* involved in β-oxidation of unsaturated FAs (Table 4.1; Fig 4.4A; Geisbrecht et al., 1998). Furthermore, two proteins containing HAD domains were predicted to localise to the peroxisome, although neither of these contained a canonical C-terminal PTS1 sequence (Table 4.1). These findings raise the possibility that there may be other peroxisomal proteins which could perform the enzymatic functions of MFP proteins.

### 4.3.2 MFP-dependant peroxisomal β-oxidation is not required for growth under starvation or virulence

Targeted deletion of *ZtMFP1* and *ZtMFP2* was carried out by gene replacement using *Agrobacterium*-mediated transformation. The *Δku70* strain, deficient in the non-homologous end joining pathway (Bowler et al., 2010), was used as the background for these gene deletions due to difficulty targeting T-DNA inserts to the *ZtMFP2* locus in wild type IPO323. *ZtMFP1* was replaced with the $HYG^R$ selective marker using the plasmid pC-HYG-MFP1KO, while *ZtMFP2* was replaced with the $BAR^R$ resistance marker using the plasmid pC-BAR-MFP2KO (Fig. 4.2). Antibiotic resistant transformants were screened by PCR for correct integration of T-DNA at the target locus and absence of the coding sequence (Fig. 4.2), and three independent mutants were isolated per gene. *Δmfp1.1* was further transformed with pC-BAR-Δmfp2 to generate three independent *Δmfp1Δmfp2* double knockout strains.

Deletion of *ZtMFP1* and *ZtMFP2* was found to cause no defect in the morphological switch or hyphal growth under nutrient-limited conditions (Fig. 4.5). The radial growth rate of all *Δmfp1*, *Δmfp2* and *Δmfp1Δmfp2* strains was indistinguishable from *Δku70* on AMM deficient in a nitrogen and/or carbon source (Fig. 4.5A). Furthermore, the rate of hyphal germination of these strains on 2% water agar (WA) was not significantly different to the progenitor *Δku70* strain, with all strains displaying over 90% germination efficiency after 24h (Fig. 4.5B). These results suggest that MFP-dependant peroxisomal β-oxidation is not required for the breakdown of stored lipids in the spore to support starvation-induced hyphal growth.

To assess the impact of disrupting peroxisomal β-oxidation on *Z. tritici* virulence, *Δmfp1*, *Δmfp2* and *Δmfp1Δmfp2* strains were inoculated onto susceptible wheat leaves. All strains displayed typical development of symptoms, with signs of chlorosis appearing around 9-10 dpi and developing into necrotic lesions which covered the leaf by the termination of the experiment at 21 dpi (Fig. 4.5C). This was accompanied by the appearance of pycnidia within disease lesions, which exuded abundant pycnidiospores upon exposure to high humidity. This indicates that peroxisomal β-oxidation via the putative

multifunctional enzymes *ZtMFP1* and *ZtMFP2* is not required for the pathogenicity of *Z. tritici*.

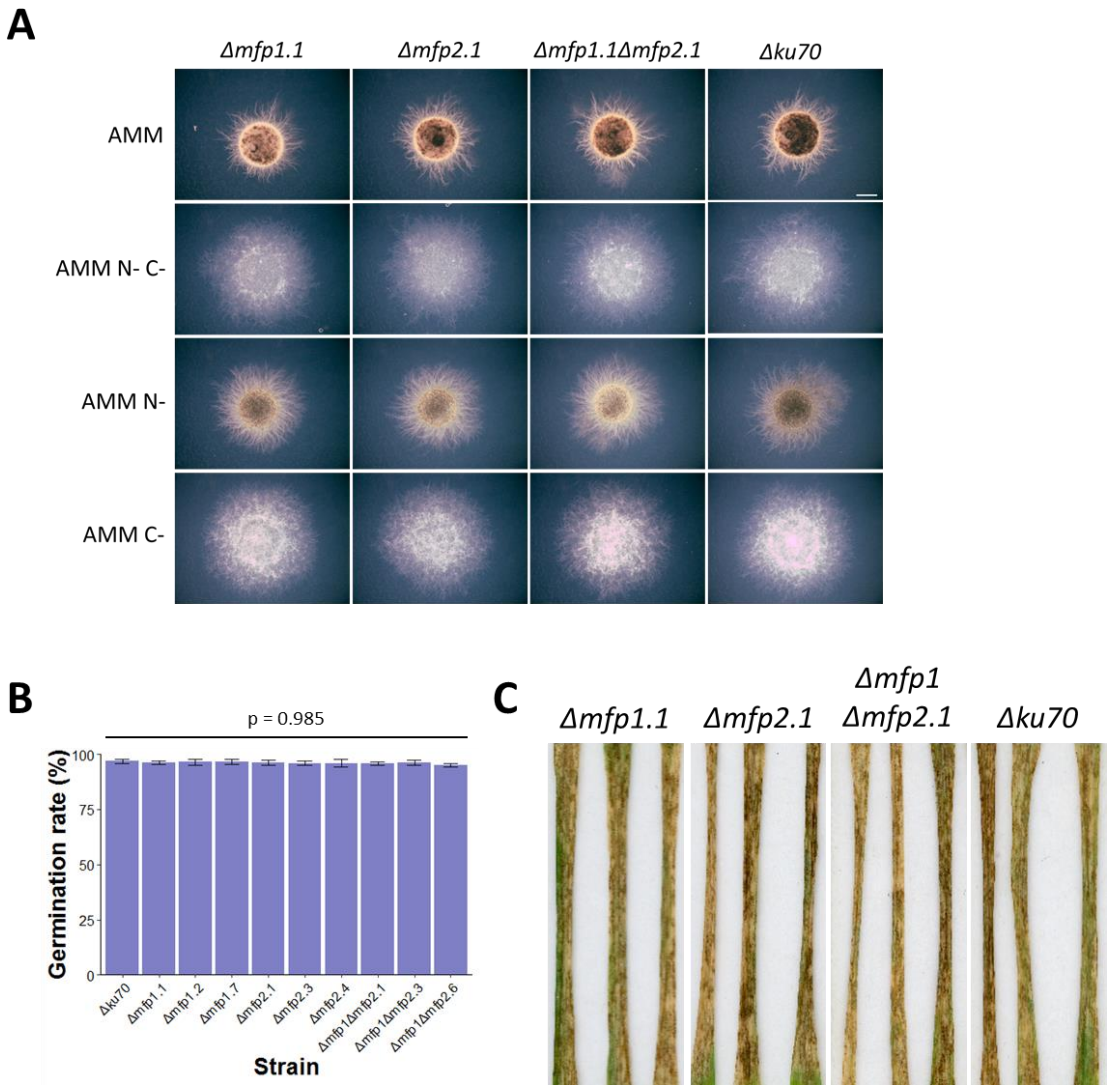


**Figure 4.5 ZtMFP1 and ZtMFP2 are not required for growth under starvation or virulence**
(A) Radial growth after 14 days at 19ºC on *Aspergillus* minimal medium (AMM) and AMM deficient in carbon source (AMMC-), nitrogen source (AMMN-) or both (AMMN-C-). Spores were inoculated in 5 µl droplets at $5x10^6$ spores/ml. Scale bar = 2mm. (B) Percentage germination rate of blastospores on 2% water agar after 24 h shows no significant difference between strains. Mean ± SEM of 4 independent experiments is shown, with p-value representing result of one-way ANOVA (C) Infection symptoms on wheat (cultivar Riband) at 21 days post infection with *Z. tritici* strains at $5x10^6$ spores/ml.

### 4.3.3 *ZtEch1* deletion impacts blastospore growth rate but undergoes spontaneous phenotypic rescue

Mitochondrial β-oxidation was disrupted by targeted deletion of *ZtEch1* in the wild type IPO323 background using the plasmid vector pC-HYG-Δech1.

Insertion of the *HYG*$^{R}$ cassette in place of the native *ZtEch1* allele was confirmed in isolated transformants by PCR (Fig. 4.2). Three independent *Δztech1* strains were isolated and used for further analysis. The growth rate of purified *Δztech1* blastospores on YPD agar plates was observed to be slower than the wild type (Fig. 4.6A). Interestingly, *Δztech1* strains developed faster replicating colonies within the slower growing lawn of yeast-like cells (Fig. 4.6A). Upon subculturing, these rapidly replicating colonies continued to grow at a similar rate to the wild type. Selection of faster growing single colonies from these strains was used to purify cells displaying this reverting phenotype, which were designated *Δztech1 Rev* strains.

To rule out contamination with untransformed cells, correct insertion of the *HYG*$^{R}$ cassette and absence of *ZtEch1* gene was confirmed in these strains through diagnostic PCR (Fig. 4.2). Moreover, patches subcultured from the lawn of slower growing *Δztech1* cells continued to display retarded replication, but also the development of further faster replicating colonies. To confirm that phenotypes observed in *Δztech1* mutants were caused by the targeted gene deletion, the full length coding sequence of *ZtEch1* was replaced at its native locus using the plasmid pC-BAR-Ech1comp. Transformants were screened by PCR to confirm successful complementation of *ZtEch1* (Fig. 4.2), and designated *Δztech1 ZtEch1* strains.

### 4.3.4 Mitochondrial β-oxidation supports the starvation-induced morphological switch

To assess whether mitochondrial β-oxidation is involved in the breakdown of stored lipids during starvation-induced hyphal growth, the germination rate of blastospores taken from the slow replicating lawn of *Δztech1* cells was assessed on 2% WA. Hyphal germination was almost completely abolished in *Δztech1* strains (Fig. 4.6B). This phenotype was rescued in *Δztech1 ZtEch1* complementation strains, while *Δztech1 Rev* strains displayed an intermediate germination rate (Fig. 4.6B). This defect in hyphal germination of *Δztech1* strains was investigated further through analysis of growth on AMM deficient in a carbon and/or nitrogen source (Fig. 4.6C). While radial growth of hyphae of *Δztech1* was slower than IPO323 and *Δztech1 ZtEch1* strains on regular and nitrogen-deficient AMM, germination of *Δztech1* hyphae was almost completely

abolished on carbon-deficient AMM (Fig. 4.6C). The ability of *Δztech1* blastospores to germinate hyphae on regular AMM provides evidence that the abolishment of germination on 2% WA is not caused by a defect in the basic cellular machinery involved in the morphological switch to hyphal growth. This is supported by the ability of *Δztech1* to form aerial hyphae in response to incubation at 25ºC on rich media (Fig. 4.6C). Furthermore, the abolished germination in *Δztech1* is associated specifically with the lack of external carbon-source and not nitrogen-deficient conditions, suggesting that this mutant lacks the ability to utilise stored lipids as a carbon source.

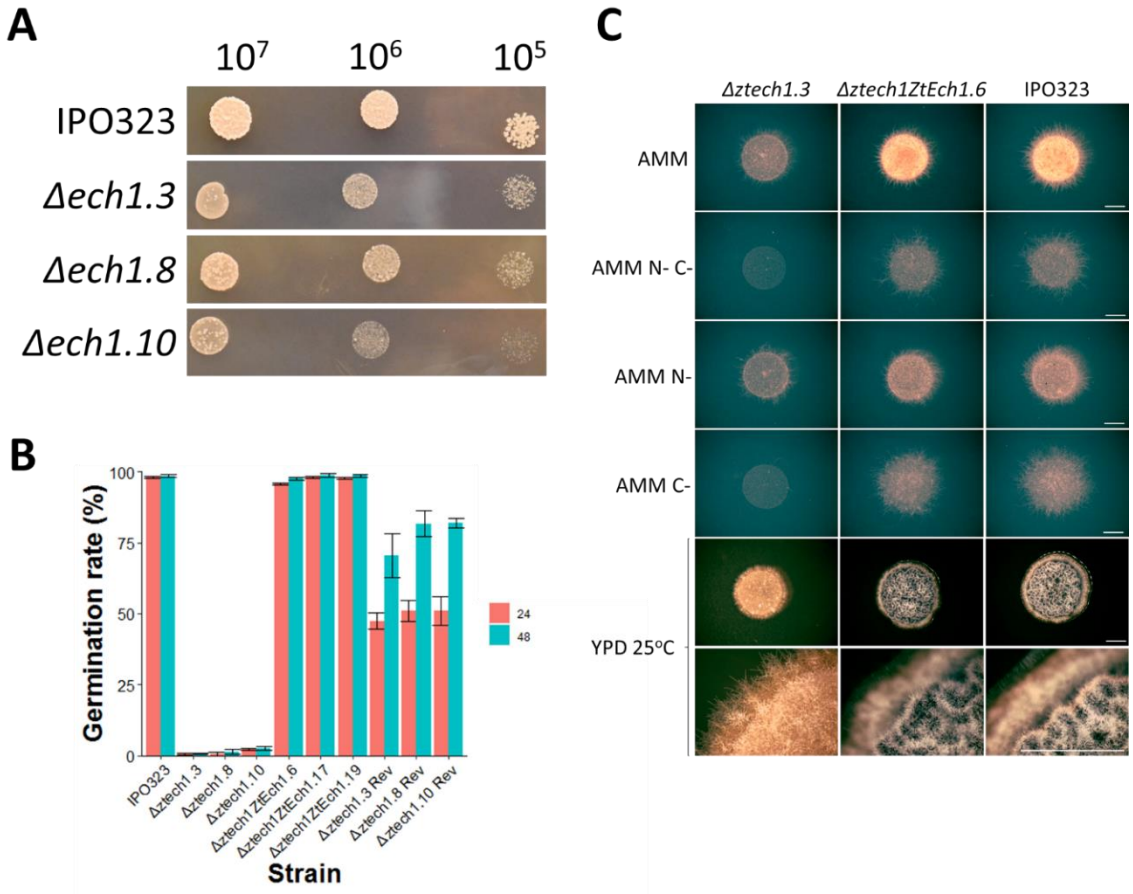


**Figure 4.6 *ZtEch1* deletion reduces growth rate on rich media and inhibits germination under carbon starvation**
*In vitro* phenotypes of three independent deletion (*Δztech1.3*/*8*/*10*), complementation (*Δztech1ZtEch1.6*/*17*/*19*) and reverting phenotype (*Δztech1.3*/*8*/*10 Rev*) strains. (A) Growth of blastospores on YPD at 19ºC for 6 days after inoculation in 5 µl droplets at concentrations provided in spores/ml. (B) Percentage germination rate of blastospores on 2% water agar after 24 and 48 h. (C) Radial growth after 7 days at 19ºC on *Aspergillus* minimal medium (AMM) and AMM deficient in carbon source (AMMC-), nitrogen source (AMMN-) or both (AMMN-C-). Growth of *Z. tritici* strains on YPD for 7 days at 25ºC is also shown. Spores were inoculated in 5 µl droplets at $5x10^6$ spores/ml. Scale bars = 2mm.

### 4.3.5 Mitochondrial β-oxidation enables utilisation of external fatty acids

To assess the impact of disrupting β-oxidation on utilisation of external FAs, *Δztech1* and *Δztmfp1Δztmfp2* strains were grown on AMMC- containing olive oil and a range of FAs as the sole carbon source. Interestingly, the presence of butyric acid (4:0), valeric acid (5:0), octanoic acid (8:0) and lauric acid (12:0) in the media completely inhibited growth of wild type IPO323, which developed extensive hyphal filaments on AMMC- without an additional carbon source (data not shown). This indicates that these short- and medium-chain FAs are toxic to *Z. tritici.* Furthermore, growth of the wild type on palmitic acid (16:0) and stearic acid (18:0) was similar to the control containing only the surfactant Tween-20 used to dissolve FAs (Fig. 4.7), suggesting *Z. tritici* cannot utilise these exogenous FAs. The inability of *Δztech1* strains to grow in these conditions is therefore consistent with their lack of germination without an available exogenous carbon source (Fig. 4.6; Fig. 4.7).

However, IPO323 displayed enhanced yeast-like growth in the presence olive oil compared to the AMMC- control (Fig. 4.7). This indicates that *Z. tritici* is able to utilise the FAs in olive oil (primarily oleic acid (18:1) and linoleic acid (18:2)) as a carbon source. Conversely, *Δztech1* strains were unable to grow on media containing olive oil. The lack of growth of *Δztech1* strains on olive oil could be caused by the accumulation of toxic FAs or β-oxidation intermediates. To investigate this, FA growth media was supplemented with glucose. Growth of *Δztech1* strains was rescued when glucose was added alongside these FAs (Fig. 4.7). This suggests that toxic compounds do not accumulate in *Δztech1* under these conditions, and that lack of growth on FAs is caused by the inability of this mutant to utilise both external and internal FAs. However, as FA uptake and catabolism may be suppressed by the presence of exogenous glucose, this does not completely eliminate the possibility of toxic intermediates causing growth inhibition in *Δztech1* strains when exogenous FAs are supplied as the sole carbon source. All growth phenotypes of *Δztech1* mutants were rescued in *Δztech1 ZtEch1* and partially reversed in purified *Δztech1 Rev* strains. Furthermore, *Δztmfp1Δztmfp2* strains displayed similar growth rate to the isogenic *Δku70* strain under all conditions tested (Fig. 4.7). These findings

indicate that mitochondrial β-oxidation, and not MFP-dependant peroxisomal β-oxidation, is required for metabolism of exogenous unsaturated long chain FAs.

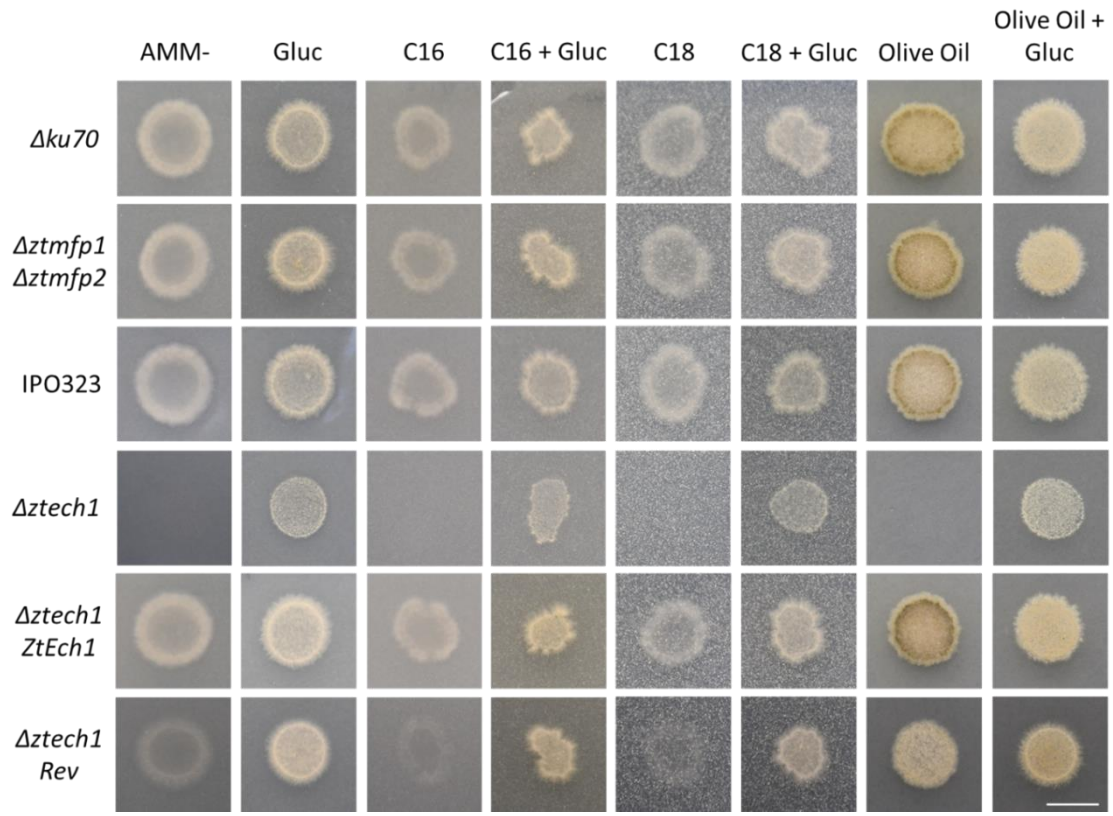


**Figure 4.7 Growth of *Z. tritici* β-oxidation mutants on exogenous fatty acids**
Control media consists of *Aspergillus* minimal media without glucose amended with 0.05% Tween 20 (AMM-) to dissolve fatty acids. This medium was supplemented with 1% glucose (Gluc), 2.5 mM palmitic acid (C16), 2.5 mM stearic acid (C18), 1% olive oil or combinations of the above. Scale bar = 1cm.

### 4.3.6 Mitochondrial β-oxidation influences mitochondrial morphology

Considering the retarded growth of *Δztech1* on rich media, and previous reports of altered mitochondrial morphology in equivalent strains of *M. oryzae* (Patkar et al., 2012), the effect of *ZtEch1* deletion on mitochondrial fusion was investigated. Blastospores were grown in rich media and mitochondria were stained with rhodamine 123. Preliminary evidence suggested that, while the mitochondria of IPO323 blastospores appeared tubular, *Δztech1* cells contained largely punctate mitochondria (Fig. 4.8). This suggests that mitochondria in wild type *Z. tritici* blastospores form a highly fused network, and that mitochondrial fusion is disrupted by the deletion of *ZtEch1*. Further characterisation of mitochondrial morphology in these strains, using confocal microscopy followed

by quantification of circularity and aspect ratio (Chacko & Ananthanarayanan, 2019; Jugé et al., 2016), is required to confirm these observations.

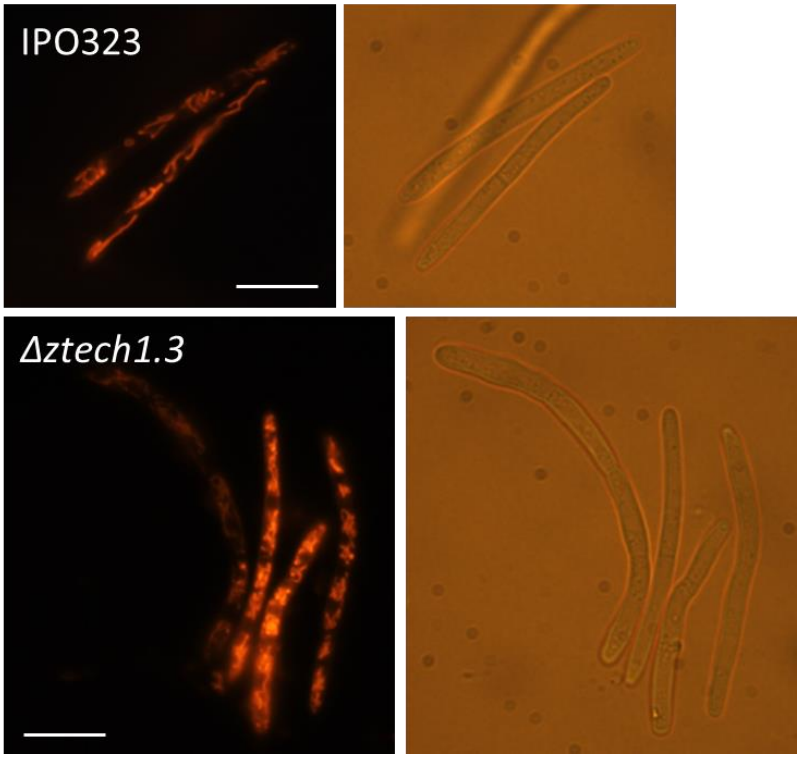


**Figure 4.8 Abnormal mitochondrial morphology of *Z. tritici Δztech1* blastospores**
Cells stained with rhodamine 123 in YG broth. Scale bar = 10 µm.

### 4.3.7 *ZtEch1* deletion severely reduces pathogenicity

The impact of disrupting mitochondrial β-oxidation on the pathogenicity of *Z. tritici* was assessed through infection of susceptible wheat leaves with *Δztech1* strains. While IPO323 and *Δztech1 ZtEch1* strains caused necrotic lesions across the entire leaf surface after 21 dpi, *Δztech1* strains only caused small localised necrotic lesions (Fig. 4.9A). Localised disease lesions caused by *Δztech1* still harboured pycnidia. The prevalence of these localised lesions was found to correlate with the spore concentration used for inoculation (Fig. S4.3). Furthermore, purified *Δztech1 Rev* strains were able to cause significant levels of necrosis on the leaf, although lesions were not as widespread as those caused by infection with IPO323 and *Δztech1 ZtEch1* (Fig. 4.9A). These findings suggest that the localised lesions caused during *Δztech1* infection are likely to be the result of cells within the inoculum expressing the recovered phenotype observed in *Δztech1 Rev* strains.

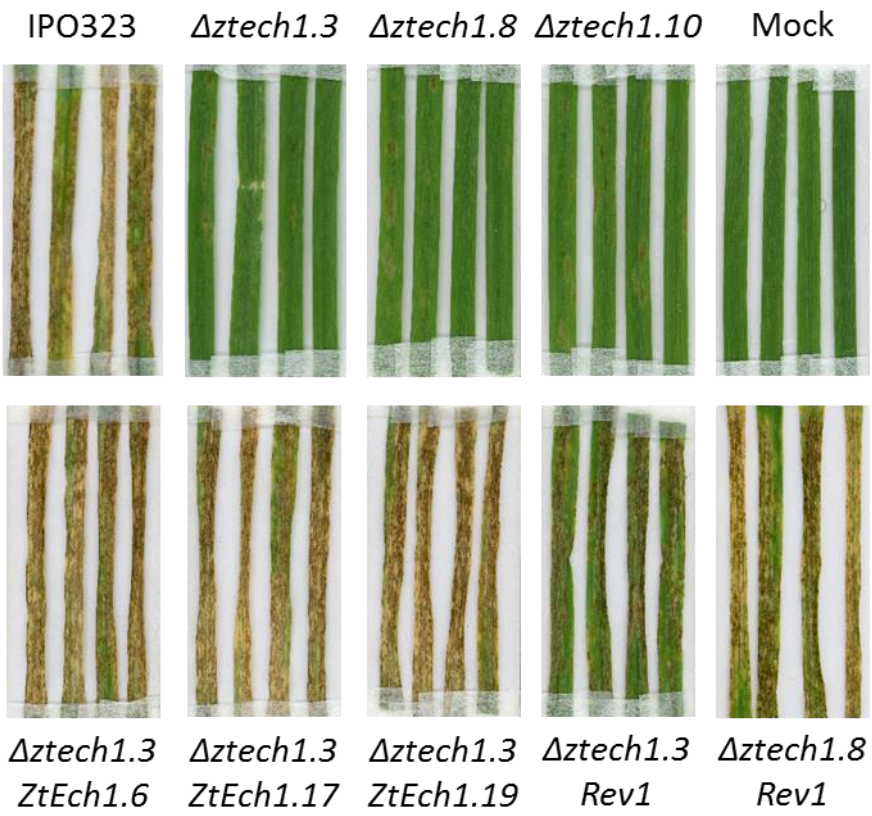


**Figure 4.9 *ZtEch1* is required for *Z. tritici* pathogenicity**
*Z. tritici* infection symptoms on wheat (cultivar Riband) at 21 days post-inoculation with wild type IPO323, *Δztech1, Δztech1 ZtEch1* complementation and *Δztech1 Rev* spontaneous recovery strains at $5x10^6$ spores/ml.

In order to assess whether the severely reduced pathogenicity of *Δztech1* is caused by a germination defect similar to that observed in carbon-deficient cultures *in vitro*, the morphological switch to hyphal growth on the leaf surface was investigated by microscopic analysis. Calcofluor white stain was used to stain chitin in the cell walls of *Z. tritici* on the leaf surface at 24h intervals for the first three days of infection. IPO323 and *Δztech1 ZtEch1* were observed to germinate before 24h, extending hyphae across the leaf surface which were seen to interact with stomatal apertures with increasing frequency over the three days of observation (Fig. 4.9B). Conversely, *Δztech1* blastospores were unable to germinate hyphae on the leaf surface even after three days, and interaction of hyphae with host stomata was not observed (Fig. 4.9B). These results suggest that breakdown of stored lipids, specifically via mitochondrial β-oxidation, is required for *in planta* germination of *Z. tritici* spores.

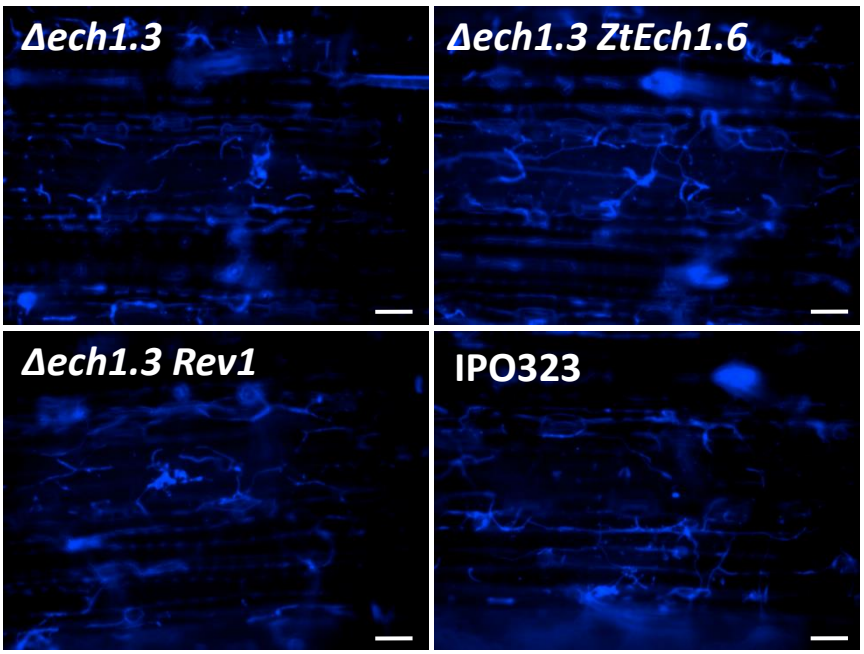


**Figure 4.10 *ZtEch1* deletion inhibits germination of *Z. tritici* on the leaf surface**
Calcofluor white stained *Z. tritici* cells on the wheat leaf surface 48h post-inoculation with $5x10^6$ spores/ml. Scale bars = 50 µm.

## 4.4 Discussion

Lipid metabolism has recently emerged as a crucial prerequisite for fungal pathogenicity on plants. Gene expression studies have provided evidence for the importance of lipid metabolism during early host colonisation by *Z. tritici* (Palma-Guerrero et al., 2016; Rudd et al., 2015). Here, the function of FA β-oxidation in starvation-induced hyphal growth and virulence of *Z. tritici* was investigated. The contribution of parallel β-oxidation pathways was assessed through targeted deletion of mitochondrial ZtEch1 and peroxisomal ZtMFP enzymes. While the peroxisomal β-oxidation enzymes were found to be dispensable for virulence, ZtEch1 was found to be crucial for germination of spores on the leaf surface, and therefore pathogenicity of *Z. tritici*.

Many fungi are able to utilise exogenous FAs as a carbon source, which has been used to investigate the molecular machinery involved in FA metabolism in filamentous fungi. While *A. nidulans*, *F. graminearum* and *U. maydis* are able to use short- and medium- chain FAs as a sole carbon source (Maggio-Hall & Keller, 2004; Tang et al., 2019), these were found to be toxic to *Z. tritici* in the present study. This finding is consistent with observations of toxicity of C5 to C12 FAs to *M. oryzae* (Patkar et al., 2012) and C4 to C6 FAs in *Cryptococcus*

*neoformans* (Kretschmer, Wang, et al., 2012). Despite the general trend for the importance of peroxisomal β-oxidation in metabolising long chain FAs, some overlapping function with the mitochondrial pathway has been identified regarding these chain lengths (Maggio-Hall & Keller, 2004; Patkar et al., 2012; Tang et al., 2019). Here, results suggest that the mitochondrial pathway is required for metabolism of unsaturated long chain FAs, with *Δztech1* mutants showing a severe defect in growth on olive oil, which supports extensive yeast-like growth in the wild type. In comparison, *Δztmfp1Δztmfp2* strains showed unaltered growth on all exogenous FAs tested, suggesting that conventional MFP-dependant peroxisomal β-oxidation is not involved in metabolism of these substrates.

Genes involved in FA metabolism have been shown to have dynamic expression profiles in response to both exogenous FA supply (Maggio-Hall & Keller, 2004; Patkar et al., 2012) and infection cycle progression (Both et al., 2005; Wang et al., 2007). However, *ZtEch1* and other putative mitochondrial β-oxidation genes show consistent expression between *in vitro* yeast-like and *in planta* growth (Rudd et al., 2015). Interestingly, in this study, *Δztech1* strains displayed a reduced growth rate compared to the wild type on rich media containing glucose. Moreover, preliminary evidence suggested that *Δztech1* strains develop a defect in mitochondrial morphology, displaying punctate rather than highly fused tubular networks of mitochondria as seen in wild type blastospores. Mitochondrial fusion occurs in starved mammalian cells, and has been shown to be crucial for the efficiency of FA metabolism (Rambold et al., 2015).

Combined, these findings suggest that FA metabolism is required for efficient yeast-like growth in *Z. tritici*, and therefore that turnover of intracellular lipids may be occurring during blastosporulation despite the availability of exogenous glucose. The reduced growth rate could be caused by the build-up of toxic intermediates, which was proposed to explain defects in growth rate in *C. neoformans* MFP mutants when grown on rich media (Kretschmer, Wang, et al., 2012). This may also be explained by altered cellular FA content leading to perturbation of membrane phospholipid and sterol composition, as has been suggested for causing the sensitivity of *S. cerevisiae* peroxisome mutants to oleic acid (Lockshon et al., 2007). Alternatively, disruption of mitochondrial β-

oxidation may have pleiotropic impacts on mitochondrial processes such as oxidative phosphorylation, considering enzymes in these pathways have been demonstrated to have a physical connection in mammals (Wang et al., 2010). Indeed, mitochondrial fragmentation, as seen in *Δztech1* cells, is known to be caused by inhibition of oxidative phosphorylation (Toyama et al., 2016), as well as oxidative stress induced by disruption of mitochondrial β-oxidation in mammalian cells (Schmidt et al., 2010).

Starvation induces the morphological switch to filamentous growth in *Z. tritici*, after which hyphae are able to grow extensively without an external carbon source (Francisco et al., 2019; Mehrabi, Zwiers, et al., 2006). The abolishment of hyphal germination in *Δztech1* when starved of a carbon source suggests that mitochondrial β-oxidation is required for the morphological switch to hyphal growth when external nutrients are scarce. Furthermore, the ability of *Δztech1* strains to form hyphae under nitrogen-starvation and high incubation temperatures, which also induce germination in *Z. tritici* (Francisco et al., 2019), suggests that this is due to inability to mobilise stored carbon sources, as opposed to a more serious defect in the mechanism of germination. In contrast, hyphal growth under carbon starvation was found to be unaltered upon deletion of both MFP proteins, indicating that MFP-dependant FA β-oxidation in peroxisomes is not required for this process. Similarly, germination on glass coverslips was reduced in *M. oryzae Δech1* mutants, while it remained unchanged in *Δfox2* (*Δmfp1*) strains (Patkar et al., 2012). However, the germination rate of *M. oryzae Δech1* remained above 50%, which highlights the extreme reliance of *Z. tritici* on mitochondrial β-oxidation for carbon acquisition under starvation identified here.

The *Δztech1* mutants were also unable to germinate on the leaf surface, which in turn led to the loss of virulence in these strains. This suggests that mitochondrial β-oxidation is required for *Z. tritici* pathogenicity, and provides further evidence to support the hypothesis that *in planta* germination and invasive growth in *Z. tritici* is enabled by utilisation of stored lipids within the spore (Rudd et al., 2015). This is consistent with findings of the importance stored lipid metabolism for development in response to the nutrient-deficient host surface in other plant pathogens (Solomon et al., 2004; Thines et al., 2000; Wang et al., 2007). Along with other recent studies, this supports growing

evidence that Ech1 is an important virulence factor in plant pathogenic fungi (Patkar et al., 2012; Tang et al., 2019). However, these findings do not confirm that *Z. tritici* continues to utilise the metabolism of stored FA following germination for subsequent invasive growth during symptomless colonisation. The ability to conditionally inactivate the ZtEch1 enzyme would allow functional characterisation at different stages during *in vitro* development and infection. This would enable assessment of the continued requirement of mitochondrial β-oxidation for catabolism of lipid stores throughout the symptomless phase. A similar approach was recently used to characterise the function of PMK1 kinase during *M. oryzae* infection beyond its essential role in cuticle penetration (Sakulkoo et al., 2018). This could be achieved through conditional repression of *ZtEch1* using the suite of promotors characterised in *Z. tritici* (Kilaru, Ma, et al., 2015), or through implementation of a conditional protein degradation system such as the auxin-inducible degron method (Yesbolatova et al., 2020).

The reason for spontaneous recovery of germination and virulence in *Δztech1* mutants also requires further investigation. This may have been caused by the appearance of suppressor mutations, or through epigenetic changes leading to alterations in gene expression. Loss of ZtEch1 activity may have been complemented by other enoyl-CoA hydratase/isomerase domain proteins predicted to localise to the peroxisomes, with enhanced transport of intermediates between the two organelles. Alternatively, products of peroxisomal β-oxidation, including acetyl-CoA and glucose (via the glyoxylate cycle and gluconeogenesis), could complement the loss of mitochondrial energy generation through β-oxidation, with enhanced transport of these metabolites to the mitochondria in recovering cells. This metabolic recovery may represent another fascinating insight into the interaction between peroxisomes and mitochondria, which are increasingly being found to cooperate in metabolic processes (Schrader et al., 2015; Wanders et al., 2016).

While disruption of mitochondrial β-oxidation led to defects in germination and virulence *in planta*, we found no evidence for the role of the peroxisomal pathway during *Z. tritici* infection. This is surprising considering the upregulated expression of both MFP genes in during early infection (Rudd et al., 2015). To our knowledge, this is the first time MFP homologs have been found to be dispensable for virulence in a fungal plant pathogen (Kretschmer, Klose, et al.,

2012; Wang et al., 2007). One possible explanation is that the ZtMFP enzymes are not required for peroxisomal β-oxidation in *Z. tritici*. A recent study found evidence for a putative Fox2-independent peroxisomal β-oxidation pathway in *Candida lusitaniae*, with the level of *in vitro* FA consumption by peroxisomal fractions of *Δfox2* cells showing no reduction compared to the wild type (Gabriel et al., 2014). Furthermore, it has been proposed that genes encoding putative ECH and HAD enzymes with predicted PTS1 sequences could carry out the function of MFP enzymes in *U. maydis* peroxisomes (Camões et al., 2015). Similarly, putative peroxisomal ECH and HAD enzymes were identified in the *Z. tritici* genome here. However, confirmation of peroxisomal localisation and functional characterisation is certainly required to substantiate these speculations. Peroxisomal β-oxidation has been demonstrated as a well conserved process in eukaryotes, from mammals to fungi (Shen & Burger, 2009). Moreover, deletion of MFP homologs has caused significant defects in lipid and FA utilisation in all other fungi in which they have been investigated, including *U. maydis* (Hiltunen et al., 1992; Kretschmer, Klose, et al., 2012; Kretschmer, Wang, et al., 2012; Maggio-Hall & Keller, 2004; Wang et al., 2007).

Previously, the glyoxylate cycle was found to be required for full virulence of *Z. tritici,* which was presumed to utilise acetyl-CoA produced by FA metabolism in the peroxisome (Sidhu, 2015). If peroxisomal β-oxidation is indeed inhibited in *Δmfp1Δmfp2* mutants without impacting fungal virulence, the question remains what the source of substrates is for the glyoxylate cycle in these strains. Apart from FA β-oxidation, other sources of acetyl-CoA include ethanol and acetate (Dunn et al., 2009), which are unlikely to be abundant in the *Z. tritici* spore, or breakdown of ketogenic amino acids. This raises the possibility that acetyl-CoA from mitochondrial β-oxidation may be fuelling the glyoxylate cycle, which could complement the loss of peroxisomal β-oxidation in *Δmfp1Δmfp2* mutants. Peroxisomal localisation of the glyoxylate cycle enzymes is not required for their function, evidenced by the maintenance of a functional glyoxylate cycle in peroxisome-deficient mutants of several yeast species (Erdmann et al., 1989; Piekarska et al., 2008). Indeed, localisation of the enzymes, metabolic intermediates and products of the glyoxylate cycle is understood to be flexible depending on the available substrates and required downstream metabolic pathways (Kunze et al., 2006). For example, *S. cerevisiae* MLS1 was found to

locate to the cytosol or peroxisomes in cells grown on ethanol and oleic acid, respectively, corresponding to the location of the acetyl-CoA generated by the substrates (Kunze et al., 2002). Therefore, although MLS1 in *Z. tritici* possesses the C-terminal -SKL motif for peroxisomal targeting (Kunze et al., 2002; Sidhu, 2015), the localisation of this enzyme in wild type and *Δmfp1Δmfp2 Z. tritici* cells should be investigated.

## 4.5 Conclusions

In this study, mitochondrial β-oxidation was shown to support germination of *Z. tritici* spores on the wheat leaf surface, and therefore the pathogenicity of the fungus. This supports the hypothesis that mobilisation of stored lipids provides a crucial carbon source for *Z. tritici* when faced with the nutrient-limited environment of the leaf surface, which is reflected in previous work on other fungal plant pathogens. Intriguingly, the two homologs of the conserved peroxisomal β-oxidation multifunctional enzyme MFP were dispensable for virulence. Further investigation is required to determine whether these enzymes are functionally redundant with other putative peroxisomal proteins, or if peroxisomal β-oxidation is indeed dispensable for *Z. tritici* pathogenicity.

## 4.6 Supplementary information

**Figure S4.1 Alignment of peroxisomal β-oxidation multifunctional protein sequences**

Sequences include ZtMFP1 (ZtritIPO323_04g10198) and ZtMFP2 (ZtritIPO323_04g08334) from *Z. tritici*, MoMFP1 (MGG_06148) from *Magnaporthe oryzae*, NcFox2 (Q01373) from *Neurospora crassa*, ScFox2 (YKR009C) from *Saccharomyces cerevisiae*, UmMfe2 (um10038) from *Usitlago maydis*, AnFoxA (AN7111.2) from *Aspergillus nidulans* and CaFox2 (A0A1D8PJ13) from *Candida albicans*.

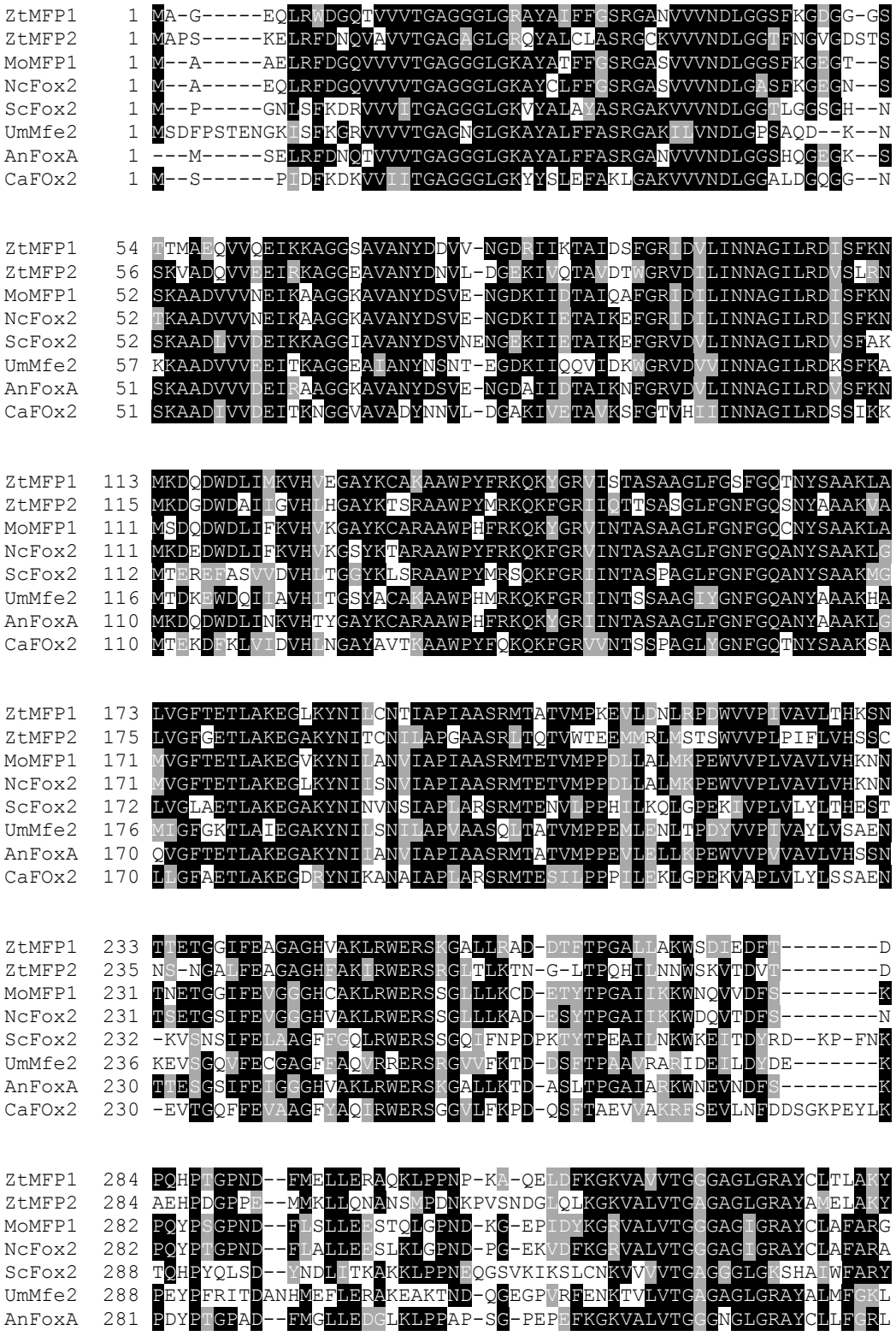

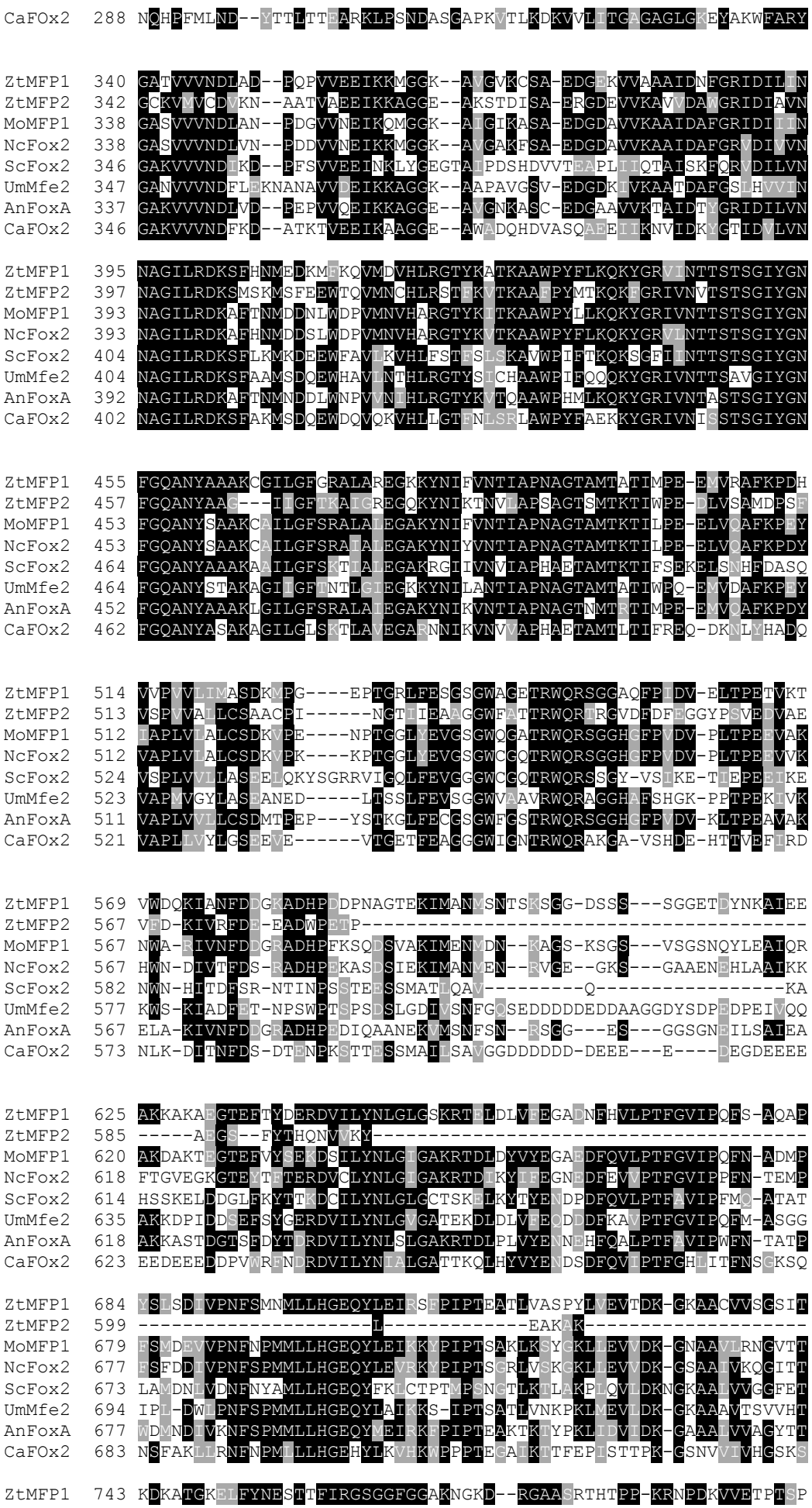

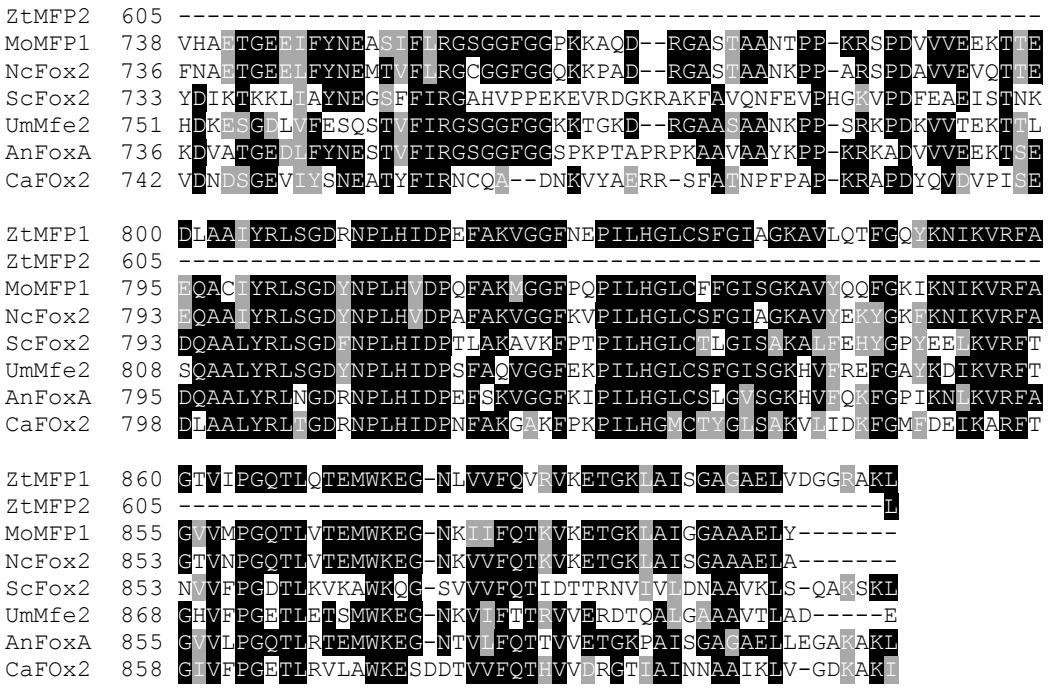
ZtMFP2 605
MoMFP1 738
NcFox2 736
ScFox2 733
UmMfe2 751
AnFoxA 736
CaFOx2 742
ZtMFP1 800
ZtMFP2 605
MoMFP1 795
NcFox2 793
ScFox2 793
UmMfe2 808
AnFoxA 795
CaFOx2 798
ZtMFP1 860
ZtMFP2 605
MoMFP1 855
NcFox2 853
ScFox2 853
UmMfe2 868
AnFoxA 855
CaFOx2 858

**Figure S4.2 Alignment of mitochondrial enoyl-CoA hydratases**

Sequences from *Z. tritici* (ZtEch1; ZtritIPO323_04g07883), *Magnaporthe oryzae* (MoEch1; MGG_12868), *Fusarium graminearum* (FgEch1; FGSG_13111) and *Aspergillus nidulans* (AnEchA; AN5916.2).

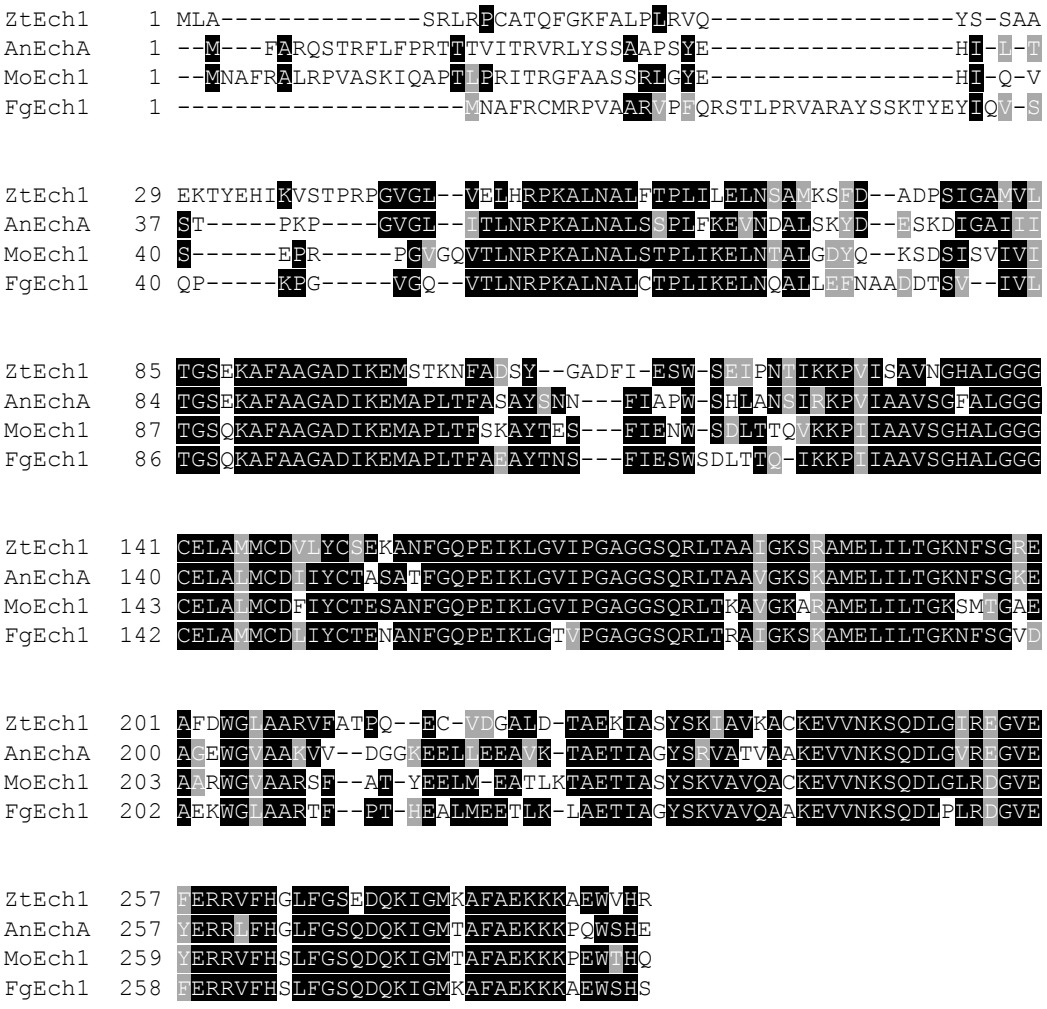

**Figure S4.3 Necrotic lesions caused by *Δztech1* are proportional to the inoculum spore concentration**

*Z. tritici* infection symptoms on wheat (cultivar Riband) at 21 days post-inoculation with wild type IPO323, *Δztech1* and *Δztech1 Rev* spontaneous recovery strains at a range of spore concentrations. Necrotic lesions caused by *Δztech1* decrease with lower inoculum concentration.

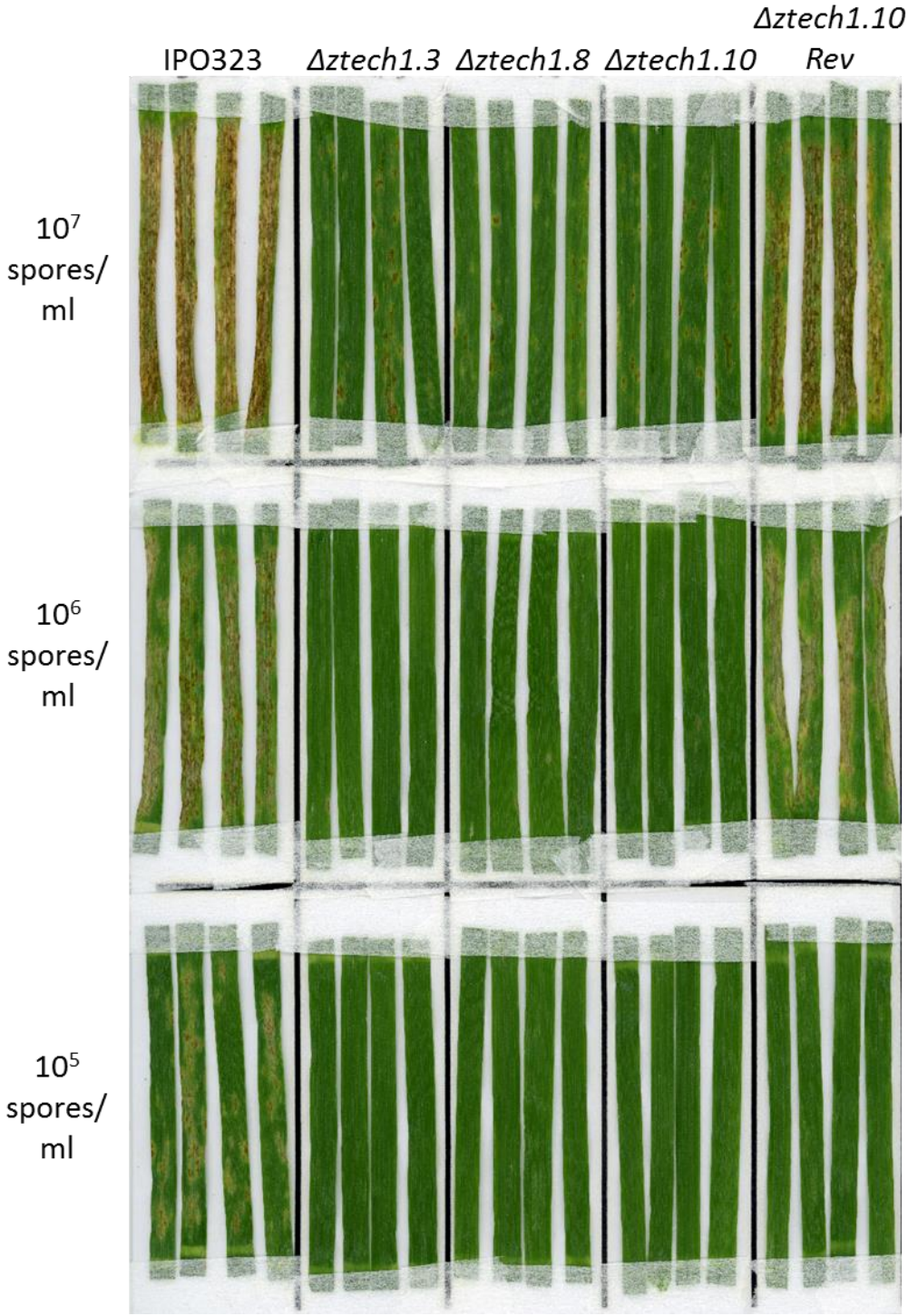

# Chapter 5
# The cell wall integrity and cAMP signalling pathways are essential for *Z. tritici* invasive growth

## 5.1 Introduction

Signalling cascades are integral for the ability of cells to adapt to their environment, enabling them to couple the recognition of external cues at the surface with appropriate intracellular processes, such as regulation of gene expression and protein activity. For fungal pathogens of plants, this involves regulating crucial changes in morphology and expression of virulence factors in response to the host environment. This is essential for controlling developmental transitions during infection, involving host surface recognition and penetration, invasive growth, and differentiation of reproductive structures. It is also important for responding to the stresses imposed by the host environment, such as nutrient deprivation and the plant immune response.

The signalling pathways involved in regulating fungal pathogenicity often function by transduction through a cascade of protein kinases, culminating in the phosphorylation of a mitogen-activated protein kinases (MAPKs). One of the conserved fungal MAPKs is Slt2, which forms part of the cell wall integrity (CWI) pathway required for regulating remodelling of the cell wall (Fig. 5.1; Levin, 2011). Through this pathway, cell wall perturbations are recognised by mechanosensors at the cell surface, which transmit the signal through the GTPase Rho1 to protein kinase C (PKC). PKC then initiates consecutive phosphorylation of the MAPK cascade, culminating in activation of Slt2, which is transported to the nucleus to activate transcription factors involved in regulation of cell wall homeostasis genes (Fig. 5.1).

Modulation of cell wall composition is required for fungal growth and morphological transitions, as these processes require localised digestion and re-building of the cell wall to allow cellular expansion (Cabib & Arroyo, 2013; Riquelme et al., 2018). Remodelling of the cell wall is crucial for responses to various stresses, including those encountered in the host environment (Geoghegan et al., 2017; Hopke et al., 2018). Furthermore, the fungal cell wall components chitin and β-1,3-glucan are recognised as pathogen-associated molecular patterns (PAMPs) by host immune systems, to which pathogens respond by adapting wall composition to mask cells from elicitation of defence responses (Ballou et al., 2016; El Gueddari et al., 2002; Fujikawa et al., 2012).

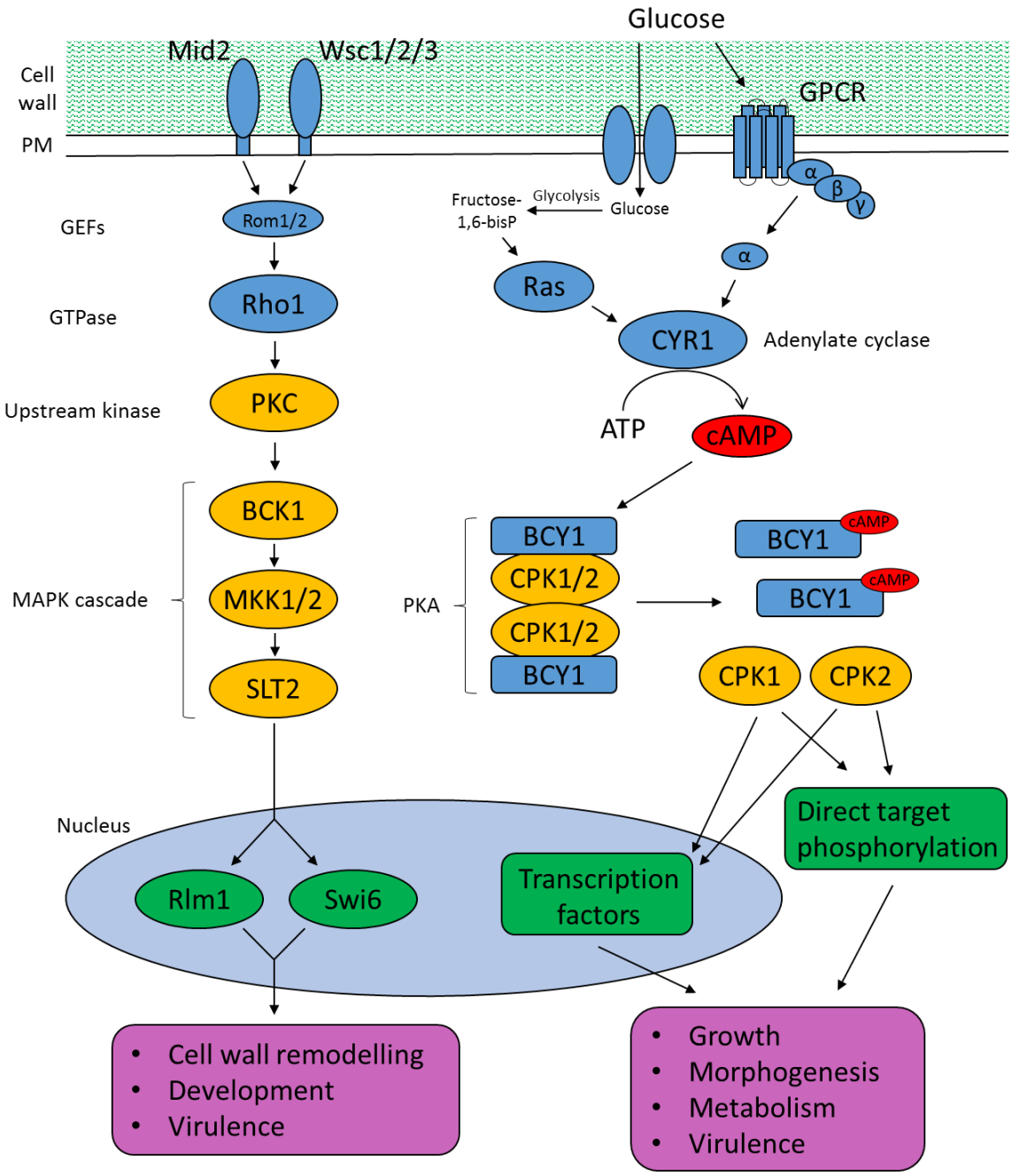


**Figure 5.1 The fungal cAMP-PKA and CWI pathways**
The CWI pathway is initiated by membrane-bound mechanosensors (Wcs1/2/3 and Mid2) with extracellular regions embedded in the cells wall, which transmit the signal via Rho GTPase to protein kinase C (PKC1). PKC activates the MAPK cascade, and the phosphorylated MAPK Slt2 activates transcription factors, including Rlm1 and Swi6 to regulate downstream processes. The cAMP-PKA pathway is activated by glucose in *S. cerevisiae*, which leads to activation of adenylate cyclase (CYR1) via Ras and G-protein coupled receptors. CYR1 catalyses synthesis of cAMP, which acts as a signalling molecule to activate protein kinase A (PKA) by binding to the regulatory PKA subunit (BCY1), releasing the catalytic PKA subunits (CPK1/2), of which there are two homologs in many filamentous fungi. PKA catalytic subunits then control downstream processes by regulation of transcription factors and direct phosphorylation of target proteins. Colours represent pathway regulators (blue), kinases (yellow), transcription factors (green) and regulated processes (purple).

It is therefore unsurprising that the CWI pathway has been found to play a crucial role in the virulence of both animal and plant fungal pathogens (Dichtl et al., 2016; Turrà et al., 2014). Initially, Slt2 homologs were found to be essential for functional appressorium formation in *M. oryzae* (Xu et al., 1998), and this function in host penetration was confirmed in other plant pathogens (Kojima et al., 2002; Rui & Hahn, 2007). However, subsequent studies identified a further function of the CWI pathway in invasive growth following plant penetration (Joubert et al., 2011; Mehrabi et al., 2008; Mey et al., 2002; Rui & Hahn, 2007). These studies proposed that the CWI pathway was required to withstand host defences, as Slt2 deletion was shown to increase sensitivity to hydrolytic enzymes (Mey et al., 2002; Rui & Hahn, 2007; Xu et al., 1998), as well as plant-derived antimicrobial compounds (Joubert et al., 2011; Ramamoorthy et al., 2007). Clear evidence to support this hypothesis was presented for *Alternaria alternata*, in which avirulence of *Δslt2* mutants was rescued during infection of *A. thaliana* plants deficient in the production of the antifungal compound camalexin (Joubert et al., 2011).

Another signalling cascade which has emerged as crucial for the virulence of fungal plant pathogens is the cyclic adenosine monophosphate (cAMP)-dependant protein kinase A (PKA) pathway (Turrà et al., 2014). In *S. cerevisiae*, the PKA complex is formed from a tetrameric protein containing two regulatory subunits, encoded by *BCY1,* which inhibit the activity of two catalytic subunits, encoded by three homologous genes (*TPK1-3*) with partially overlapping functions. cAMP generated by the adenylate cyclase enzyme binds to the regulatory subunits, allowing the catalytic subunits to dissociate and phosphorylate downstream targets (Fig. 5.1). This pathway functions in nutrient sensing in yeast, responding to both intra- and extra-cellular glucose concentration through Ras proteins and G-protein coupled receptors, respectively, to regulate carbohydrate metabolism, the cell cycle, growth and development (Zaman et al., 2008). However, the cAMP-PKA pathway is known to regulate an extremely diverse range of fungal processes, including morphological transitions (D'Souza & Heitman, 2001), sexual reproduction (Hu et al., 2014), secondary metabolism (Studt et al., 2013) and responses to diverse nutritional signals (Caza & Kronstad, 2019). One unifying trait of the cAMP-PKA pathway is its widespread function in the virulence of fungal

pathogens, although the underlying causes of this outcome include many of the aforementioned diverse cellular processes to which it contributes.

Similarly to the CWI pathway, cAMP-PKA signalling has been found to be required for development of host penetration structures in many plant pathogenic fungi, including *M. oryzae* (Choi & Dean, 1997; Xu et al., 1997) and *F. graminearum* (Bormann et al., 2014). However, an additional role of this pathway during post-penetration invasive growth was identified recently in *M. oryzae*, as strains lacking both PKA catalytic subunits were unable to cause disease symptoms after inoculation by injection (Li et al., 2017). Similar roles of cAMP-signalling have been identified in the appressorium-forming pathogen *Colletotrichum lagenarium*, with adenylate cyclase and PKA mutants unable to cause disease on wounded hosts (Yamauchi et al., 2004). However, unlike the easily characterised defects in infection-related development, the contribution of cAMP-PKA signalling to virulence once these pathogens enter the host is harder to decipher due to the pleiotropic influences it has on fungal biology.

Colonisation of wheat by *Z. tritici* requires complex regulation of morphological development and the molecular interaction with the host, which is exemplified by the dramatic shifts in gene expression across different infection stages (Rudd et al., 2015). Early molecular studies of *Z. tritici* MAPK genes found that the developmental switch to hyphal growth was regulated by the HOG1 pathway (Mehrabi, Zwiers, et al., 2006), while stomatal penetration required the control of FUS3 (Cousin et al., 2006). Furthermore, the CWI pathway was proposed to control *Z. tritici* resistance to apoplastic wheat defence compounds, as *Δmgslt2* mutants were unable to colonise the mesophyll tissue following stomatal penetration, leading to abolishment of virulence, and showed increased sensitivity to cell wall degrading enzymes (Mehrabi, Van Der Lee, et al., 2006). Furthermore, while deletion of the PKA catalytic subunit *MgTpk2* in *Z. tritici* did not impair host penetration or invasive growth in the mesophyll, *Δmgtpk2* mutants showed reduced symptom development and abolished pycnidia formation (Mehrabi & Kema, 2006).

Despite these investigations, the regulatory pathways that control genes involved in host manipulation by *Z. tritici* remain elusive. The expression of predicted small secreted effector proteins, which are crucial for host

colonisation by plant pathogens (Lo Presti et al., 2015), is tightly regulated at specific stages of *Z. tritici* infection (Rudd et al., 2015). *Z. tritici* effectors expressed during asymptomatic infection are thought to be required for the suppression and evasion of wheat defence (Rudd et al., 2015). This includes transcriptional activation of the LysM effectors, which suppress host recognition of the fungal PAMP chitin and are required for *Z. tritici* virulence (Marshall et al., 2011; Tian et al., 2021). Transcriptional reprogramming at the transition to necrotrophic growth includes upregulation of a distinct set of effectors, which are proposed to induce host programmed cell death, alongside expression of secreted proteins required for nutrient acquisition from dying host tissue (Rudd et al., 2015). Recent studies have revealed that transcriptional repression of some effector genes *in vitro* is influenced by the heterochromatin-rich genomic regions in which they reside, and that de-repression of these genes *in planta* is regulated by histone modifications (Meile et al., 2020; Soyer et al., 2019). However, the external or internal cues and signal transduction pathways that trigger these transcriptional changes during host colonisation remain to be elucidated.

*Agrobacterium tumefaciens*-mediated transformation (*At*MT) has been widely implemented in reverse genetic characterisation of fungal genes, as demonstrated in the previous chapters, but can also be used for random T-DNA insertional mutagenesis in forward genetics studies (Idnurm et al., 2017). This mutagenesis technique has been implemented successfully in the discovery of *Z. tritici* virulence genes by forward genetic screens (King et al., 2017; Motteram et al., 2011; Yemelin et al., 2017). However, random T-DNA insertion occurs at a high rate (65-95%) during transformations of wild type *Z. tritici* that intend to introduce targeted insertions by homologous recombination (Sidhu, Cairns, et al., 2015; Zwiers & De Waard, 2001), making this a viable technique for virulence gene identification alongside reverse genetic screens.

In this study, a forward genetic approach was used to identify the genetic causes of avirulence in strains that were isolated from T-DNA insertion transformations. Whole genome resequencing identified disruptions to *Z. tritici* genes encoding adenylate cyclase and the CWI MAPK cascade enzyme BCK1, before targeted gene deletion was used to confirm that loss of these gene functions led to abolishment of pathogenicity. Despite showing defects during *in*

*vitro* vegetative growth, deletion strains were able to penetrate host stomata, supporting previous evidence for the role of the CWI and cAMP-PKA pathways during infection post-penetration. Finally, RNA sequencing was used to characterise transcription in both *Z. tritici* and wheat during infection by these strains, in order to investigate the enigmatic *in planta* functions of these pathways. This provided evidence for the role of the CWI pathway in adaptation to the host environment, through transcriptional regulation of secreted proteins required to supress the host immune response. Furthermore, cAMP signalling was implicated in controlling the expression of genes putatively involved in the transition to necrotrophic growth.

## 5.2 Materials and methods

### 5.2.1 Whole genome resequencing

In order to identify ectopic T-DNA insertions and mutations in transformant strains, whole genome resequencing and variant calling was carried out as described previously (Chapter 2.5). The genomic location of T-DNA sequences was identified using discordant alignment of paired-end sequencing mates to chromosomal loci and T-DNA sequences. To achieve this, the relevant selective cassette was included in the reference genome as a separate chromosome. Alignments were carried out using the Bowtie 2 parameters --local, allowing reads to be soft clipped to achieve optimum alignment score, and -k 2, allowing up to 2 distinct alignments for each read. These parameters allow reads which arise from the junction between T-DNA sequences and their insertion sites to align to both of these regions. T-DNA insertion sites were determined using the mate location of reads aligned to the ends of heterologous T-DNA sequences and flanking regions used in the transformation vector.

### 5.2.2 Construction of plasmid vectors

The plasmids pC-HYG-CYR1KO and pC-HYG-BCK1KO were constructed by homologous recombination in yeast (see Chapter 2 for details). The plasmid pC-HYG-YR was used as a backbone for these vectors (Sidhu, Chaudhari, et al., 2015). PCR amplification of left flank (LF) and right flank (RF) regions from either side of the *ZtBCK1* and *ZtCYR1* coding sequences was carried out using the primer pairs ZtCYR1-LF-F/R, ZtCYR1-RF-F/R, ZtBCK1-LF-F/R and

ZtBCK1-RF-F/R. LF and RF amplicons were transformed into *S. cerevisiae* alongside the pC-HYG-YR vector, which had been linearised by restriction digestion with the enzymes EcoRI and HindIII (New England Biolabs, UK). The sequences of flanking regions were confirmed to be correct in the completed vectors by Sanger sequencing. These vectors were transformed into *Z. tritici* via *At*MT (Chapter 2.3).

### 5.2.3 Enzymatic spore lysis assays

The ability of *Z. tritici* strains to withstand disruption of cell wall integrity was assessed using an enzymatic spore lysis assay based on that described by Yemelin et al., (2017). Spores were harvested from YPD agar cultures grown for 5 days at 19$^{o}$C, suspended in isotonic buffer solution (IBS; 1.4 M KCl, 0.15 M$Na_2HPO_4$, 0.08 M citric acid; pH 5.8) and passed through a 100 µm cell strainer (Fisher Scientific). The spores were washed twice with IBS, centrifuging cell suspensions for 3 mins at 8,000 x G after each wash. Cells were then suspended in 1ml IBS containing 30 mg/ml lysing enzymes from *Trichoderma harzianum* (Sigma-Aldrich, UK) at a concentration of 5x10$^6$ spores/ml and incubated for 2 h at 30$^{o}$C with 70 rpm shaking. The extent of spore lysis upon termination of the experiment was assessed microscopically using a Zeiss Axiovert 200M inverted microscope, and the experiment was repeated three times.

A second enzymatic assay to assess cell wall stress sensitivity was carried out using Lyticase from *Arthrobacter luteus* (Sigma-Aldrich, UK). Cells were harvested from YPD agar cultures and suspended at a concentration of 5x10$^6$ spores/ml in sterile water containing a range of concentrations of lyticase enzyme, following a two-fold dilution from 40 U/ml to 0.625 U/ml. Suspensions were incubated at 25$^{o}$C for 2 h with 120 rpm shaking, before cell suspensions were diluted 1:40 and 100 µl plated onto YPD agar plates. Viability of *Z. tritici* after lyticase treatment was assessed by observing growth after 5 days at 19$^{o}$C. The experiment was repeated 3 times to ensure reproducibility.

### 5.2.4 RNA sequencing

Wheat leaves (cultivar Riband) were infected with *Z. tritici* strains IPO323, *Δztcyr1.4* and *Δztbck1.4* at a concentration of 5x10$^6$. Leaf samples were

harvested at 6 and 9 days post infection (dpi), with each sample comprised of 6x6cm leaf sections infected with the same *Z. tritici* strain, and frozen immediately in liquid nitrogen before storage at -80ºC. Three technical replicates of this experiment were carried out. RNA was extracted from *Z. tritici*-infected wheat leaf tissue using TRIzol™ reagent (Fisher Scientific, UK). Samples were ground in liquid nitrogen using a pestle and mortar and transferred immediately to 3 ml TRIzol™ reagent in a 50 ml falcon tube and vortexed to homogenise. All subsequent centrifugation steps were carried out at 12, 000 x G and 4ºC. 1.5 ml of the sample was then transferred to a 2 ml Eppendorf tube and centrifuged for 10 min. The supernatant was then added to 150 µl of 1-Bromo-3-chloropropane and vortexed. After phase separation by centrifugation for 10 min, the aqueous phase was added to 750 µl of isopropanol and vortexed. RNA was allowed to precipitate for 10 min at room temperature before centrifuging for 10 min to pellet the RNA. The pellet was washed twice with 70% ethanol before being allowed to dry for 7 min. The RNA was suspended in 100 µl RNase-free water and purified using the RNeasy Plant Mini Kit (Qiagen), following the "RNA Cleanup" protocol including an on-column DNA digestion step using the RNase-Free DNase Set (Qiagen).

The concentration of extracted RNA and absence of contaminating DNA was determined using a Qubit™ 3.0 Fluorometer with the Qubit™ RNA BR Assay Kit and Qubit™ dsDNA BR Assay Kit (Fisher Scientific, UK), respectively. RNA purity was assessed using a NanoDrop 1000 (Fisher Scientific, UK) and RNA quality was determined using an Agilent 2200 TapeStation system (Agilent Technologies). Library preparation and RNA sequencing steps were carried out by the Exeter Sequencing Service. The mRNA libraries were prepared using the TruSeq HT stranded mRNA preparation kit following the manufacturer's protocol, and sequenced as paired-ends using an Illumina Novaseq 6000 on an S4 flow cell at 2x150bp. The resulting raw reads will be available in the NCBI Short Read Archive repository upon publication.

### 5.2.5 *Z. tritici* alignments and differential expression analysis

The *Z. tritici* IPO323 reference genome was indexed with genes annotated using the recent annotation from Rothamsted Research (King et al., 2017); https://figshare.com/articles/dataset/Zym_tritici_RRes_v4_0_RK_public_gff/475

3708/1). Reads were trimmed to remove sequencing adapters and low quality bases using fastp (Chen et al., 2018), using the parameters '--cut_tail --cut_tail_mean_quality=20 --detect_adapter_for_pe --length_required=75'. Trimmed reads were aligned to the genome and gene counts calculated with STAR (Dobin et al., 2013), using the default parameters and set to quant mode --quantMode GeneCounts. Normalisation of gene counts and differential expression analysis was carried out using DESeq2 (Love et al., 2014). Sample clustering was assessed by principal component analysis using the *plotPCA* function on count data transformed with the *rlog* function, which accounts for sequencing depth and differences in variance between genes due to expression level (Love et al., 2014). Sets of genes which were differentially expressed (DE) between each mutant strain and the wild type at each time point were identified using the *results* function. Furthermore, sets of genes which were DE between 6 and 9 dpi for each strain were also identified. Pre-filtering of lowly expressed genes is not required when running DESeq2 differential expression analysis, as this program carries out independent filtering of genes below a mean normalised count threshold to maximise the number of DE genes for a given *p*-value threshold (Love et al., 2014). Wald test *p*-values were adjusted for multiple testing using the Benjamin–Hochberg (BH) correction method, and genes were deemed as DE when *padj*<0.01.

Plots displaying expression of individual genes across samples represent the mean of normalised gene counts from DESeq2, with normalised counts extracted using the *plotCounts* function from DESeq2 and summary statistics calculated using *summarySE* function from the Rmisc package. Heat maps representing the expression levels of different gene sets were generated with the *pheatmap* function. Heat maps represent log2 fold-changes compared to the mean of normalised counts calculated by the *rlog* function.

### 5.2.6 Wheat alignments and differential expression analysis

The *Triticum aestivum* (cv. Chinese Spring) wheat genome assembly and annotation from the International Wheat Genome Sequencing Consortium (IWGSC; Appels et al., 2018) was downloaded from Ensembl Plants (http://plants.ensembl.org/Triticum_aestivum). RSEM was chosen for wheat transcript quantification as it factors in the high number of multi-mapped reads,

which result from the polyploidy of the wheat genome, using an expectation maximization (EM) algorithm (Deschamps-Francoeur et al., 2020; Li & Dewey, 2011). The reference genome was indexed with the RSEM *rsem-prepare-reference*, using the parameters --star and --star-sjdboverhang 149 to build indices for alignment with STAR (Dobin et al., 2013). Trimmed reads were then aligned to this reference and expected counts calculated using *rsem-calculate-expression*, specifying the parameters --star and --paired-end. Expected gene-level counts were filtered using the *filterByExpr* function before normalisation factors were calculated using the trimmed mean of M-values (TMM) method in EdgeR (Robinson et al., 2010; Robinson & Oshlack, 2010). The data was then transformed using the *voom* function, linear models were fitted to each gene using the *lmfit* function and empirical Bayes moderation of the standard errors was carried out using the *eBayes* function, all within the limma package (Ritchie et al., 2015). Genes were identified as DE between treatments using the moderated *t*-test within the *topTable* function, testing whether the log2-fold-change values for a particular contrast differ from 0 at a BH-corrected *padj*-threshold of 0.01.

Visualisation of expression of individual genes between samples was done by extracting the counts per million (CPM) values and plotting the mean CPM across each treatment. Heat maps were generated for gene sets using log-CPM values calculated using the *cpm* function in EdgeR.

## 5.3 Results

### 5.3.1 Investigation of avirulent T-DNA insertion strains

Two transformants with abolished virulence were identified during *in planta* phenotyping of targeted deletion mutants in the genes ZtritIPO323_04g10737 (Mycgr3G43288), encoding a secreted lipase (*ZtL2*), and ZtritIPO323_04g13543 (Mycgr3G18212), encoding a secreted cutinase (*ZtCUT5*). These strains were designated L2 and C5, respectively. Leaves infected with L2 and C5 did not display necrotic lesions or the appearance of pycnidia, although patches of mild chlorosis were observed after 21 dpi (Fig. 5.2A). The avirulent phenotypes of these strains were contrary to two other independent transformants harbouring deletions in each of these target genes

(Fig. 5.2A), all of which displayed equivalent virulence to the wild type. This suggested that avirulence was caused by ectopic T-DNA insertion and/or random mutations in these strains.

To identify the genetic cause of avirulence in C5 and L2, whole genome resequencing was carried out on these strains along with the isogenic IPO323 wild type background strain. Reads were aligned to the reference IPO323 genome, with the T-DNA sequence from the plasmid pC-BAR-YR included as a separate chromosome. C5 and L2 were found to contain the glufosinate ammonium resistance cassette (*BAR*$^{R}$) at the expected loci determined by the flanking sequences in the transformed T-DNA (Fig. S5.1), with no evidence of ectopic insertion. This suggests that avirulence in these strains is caused by random mutation(s) in their genomes and not secondary T-DNA insertion. Variant calling for single nucleotide polymorphisms (SNPs) and small indels

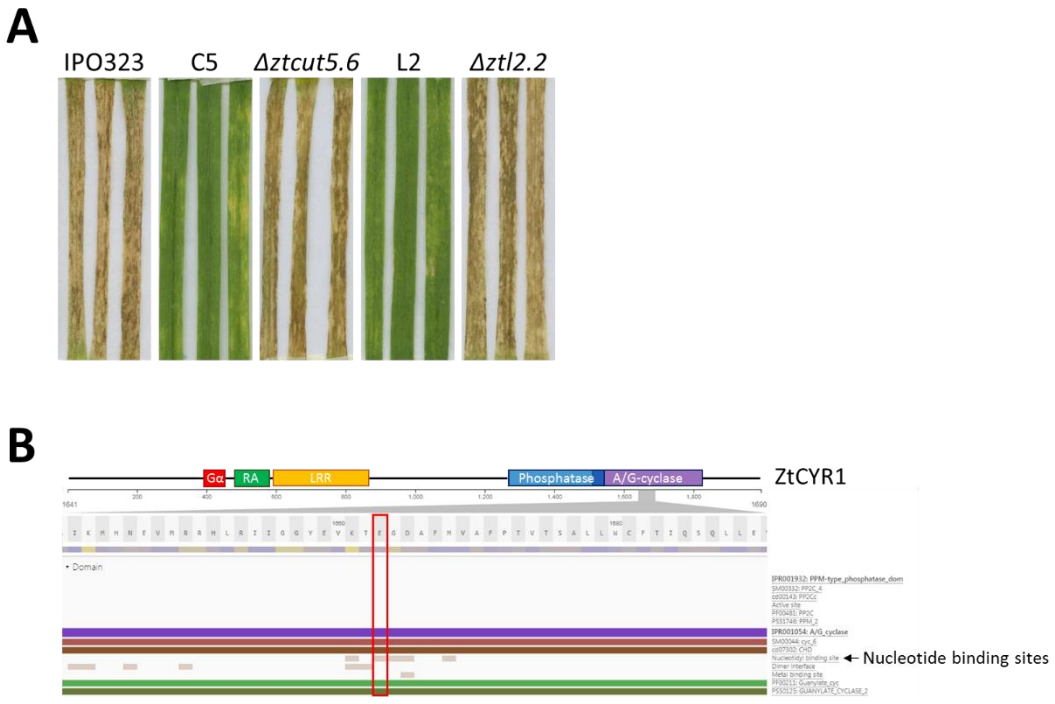


**Figure 5.2 Identification of a nonsynonymous point mutation in the *ZtCYR1* coding sequence of the avirulent *Z. tritici* strains C5 and L2**
(A) Disease symptoms on wheat leaves after 21 days infection by C5 and L2 compared to wild type IPO323 and representative independent *Δztcut5* and *Δztl2* deletion strains. (B) Site of the point mutation (red box) in the A/G-cyclase domain of *ZtCYR1* identified in both C5 and L2, with the *ZtCYR1* domain structure (above) and the domains and features identified by InterProScan in the region of the mutation, including the putative nucleotide binding site at the mutation position.

identified three and four unique polymorphisms in strains C5 and L2, respectively, all of which were located in intergenic regions (Table 5.1).

**Table 5.1 Polymorphisms identified in avirulent strains**

| Strain | Position[a] | Polymorphism[b] | Reference sequence | Mutated sequence | Location |
|---|---|---|---|---|---|
| L2 and C5 | 1:3263621 | SNP | G | A | Intergenic region |
| | 2:400119 | SNP | C | T | Intergenic region |
| | 2:1459200 | SNP | T | C | Intergenic region |
| | 3:2633702 | Deletion | AGGCG | AG | *ZtAGO1* (ZtritIPO323_04g08085) |
| | 4:999781 | SNP | G | C | Intergenic region |
| | 6:1362751 | Insertion | GCTCTCTCTCTCTCTCTCTCTCTCTCTCTCTCTCTCTT | GCTCTCTCTCTCTCTCTCTCTCTCTCTCTCTCTCTCTT | Intergenic region |
| | 6:2444773 | SNP | G | A | *ZtCYR1* (ZtritIPO323_04g11209) |
| | 9:2142308 | Deletion | TTCATTGTACTTGTTTATAT | TT | Intergenic region |
| | 9:2142331 | SNP | C | G | Intergenic region |
| | 9:2142337 | SNP | C | G | Intergenic region |
| | 10:1321821 | SNP | A | C | Intergenic region |
| | 11:1063938 | SNP | A | C | Intergenic region |
| | 12:99 | SNP | CC | CTA | Intergenic region |
| | 12:605733 | Deletion | GCTCC | GC | Intergenic region |
| | 20:174432 | Deletion | TGAAGAAGAGGAAGAAGAGG | TGAAGAAGAGG | Intergenic region |
| L2 | 10:262311 | Deletion | GAGGCTTG | GG | Intergenic region |
| | 13:26841 | SNP | C | T | Intergenic region |
| | 15:611895 | SNP | C | T | Intergenic region |
| C5 | 13:24680 | SNP | C | A | Intergenic region |
| | 15:638738 | SNP | A | G | Intergenic region |
| | 15:638748 | SNP | T | C | Intergenic region |
| | 8:2443477 | SNP | G | T | Intergenic region |
| T21 | 3:3451357 | SNP | T | C | Intergenic region |
| | 3:3451365 | SNP | G | A | Intergenic region |
| | 5:929375 | SNP | A | G | Intergenic region |
| | 6:2255788 | SNP | A | C | ZtritIPO323_04g11145 |
| | 8:10911 | SNP | T | C | Intergenic region |
| | 11:240720 | Deletion | ACGGCTACCGTCGC | AC | *ZtBCK1* (ZtritIPO323_04g03043) |
| | 11:970076 | SNP | T | C | Intergenic region |
| | 14:772867 | SNP | T | C | Intergenic region |
| | 15:14224 | SNP | G | C | Intergenic region |
| | 18:422745 | SNP | TATAA | TGTTAT | Intergenic region |
| C5 and T2 | 21:37878 | SNP | C | T | Intergenic region |

[a]Position on chromosome (chr:bp)
[b]Type of polymorphism; deletion, insertion or single nucleotide polymorphism (SNP)

Interestingly, these strains were found to share 15 polymorphisms which were not identified in the other sequenced strains (Table 5.1), suggesting that they originate from the same variant within the population of background IPO323 genotypes.

These 15 polymorphisms included two within the coding regions of genes. A three base pair deletion was identified in the first exon of *ZtAGO1*

(ZtritIPO323_04g08085/Mycgr3G38035), which causes a frame shift in the predicted coding sequence (Table 5.1). However, as this gene has been shown previously to be dispensable for virulence in *Z. tritici* (Kettles et al., 2019), this deletion was deemed unlikely to have caused the avirulence of C5 and L2. The second exonic polymorphism shared by these strains was a nonsynonymous SNP in the second exon of the *Z. tritici* homolog of adenylate cyclase enzyme *MgCYR1* (ZtritIPO323_04g11209/Mycgr3G86659), which will hereafter be referred to as *ZtCYR1*. PCR amplification of the region and subsequent Sanger sequencing was carried out to confirm the presence of this SNP in both C5 and L2. This substitution causes a missense mutation of E1663K, a residue which is predicted to be a nucleotidyl binding site in the cyclase domain (IPR001054) of the enzyme (Fig. 5.2B). Previous studies have identified the contribution of both G-protein and protein kinase A (PKA) subunits to the virulence of *Z. tritici* (Mehrabi et al., 2009; Mehrabi & Kema, 2006), which act upstream and downstream of adenylate cyclase in the PKA signalling pathway in yeast, respectively (Tamaki, 2007; Toda et al., 1987). Considering this, disruption of *ZtCYR1* was hypothesised to cause the loss of virulence in the strains C5 and L2, prompting further functional characterisation of this gene.

A third avirulent T-DNA insertion mutant, referred to as T21, was identified during screening of transformants generated for targeted deletion of ZtritIPO323_04g07737 (Mycgr3G108617), encoding a triacylglycerol lipase (*ZtTGL1*). This strain was identified as having a defect in melanisation during subculturing after transformation, which was not identified in other transformants, warranting further investigation. PCR screening failed to identify insertion of the T-DNA into the target *ZtTGL1* locus, indicating the failure of homologous recombination to delete this gene. However, T21 displayed equivalent hygromycin resistance to other transformants and was confirmed to contain the *HygR* gene by PCR, suggesting that this strain contained an ectopic T-DNA insertion. Subsequent virulence phenotyping assays found this strain to be incapable of causing symptoms on susceptible wheat leaves, while three

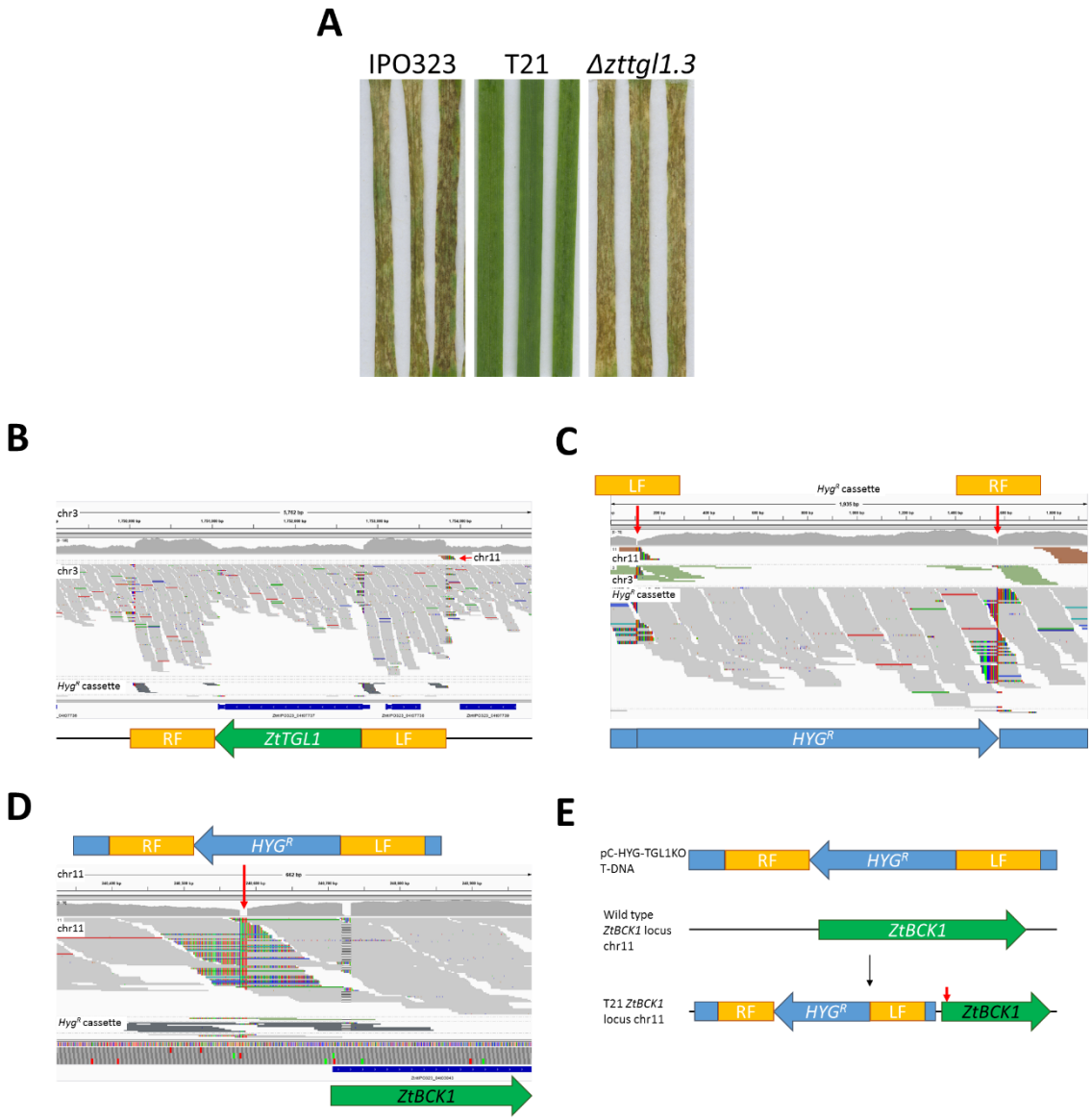


**Figure 5.3 Identification of disruptive frame-shift deletion upstream of *ZtBCK1* in the avirulent *Z. tritici* strain T21**

(A) Disease symptoms on wheat leaves caused by T21 compared to IPO323 and a confirmed *Δzttgl1* deletion strain at 21 days post inoculation. (B-D) Integrative Genomics Viewer (IGV) screenshot showing alignment of T21 whole genome resequencing reads, clustered vertically by the chromosome to which their pair is aligned. (B) T21 reads aligned to *ZtTGL1* locus showing presence of wild type allele and increased coverage over each flanking region (LF and RF), indicating the presence of these sequences elsewhere in the genome. Reads aligning to either end of the flanking sequences have pairs aligning to the *HYG*$^R$ cassette. (C) Reads aligned to the T-DNA sequence transformed into this strain, showing reads aligning to the 5' and 3' ends of the sequence whose pairs align to chromosome 11. Red arrows represent locations of LF and RF sequences in inserted T-DNA, which are surrounded by aligned reads whose pairs are mapped to the loci of LF and RF in chromosome 3. (D) Reads aligned to the *ZtBCK1* locus on chromosome 11. Red arrow represents site of T-DNA insertion, showing reads aligned either side of this site whose pairs are mapped to the T-DNA sequence. A deletion was identified at the start of the *ZtBCK1* coding sequence (E) Diagram displaying insertion of T-DNA upstream of *ZtBCK1* in strain T21 and the deletion site (red arrow) in the *ZtBCK1* coding sequence.

other independent transformants with confirmed deletion of *ZtTGL1* displayed wild type virulence levels (Fig. 5.3A). Hence, the aberrant phenotype in this case could potentially have arisen from random integration of the T-DNA into another locus.

To identify the location of the ectopic T-DNA insertion in T21, whole genome resequencing was carried out and the resulting reads aligned to the reference IPO323 genome, including the T-DNA sequence from the plasmid pC-HYG-YR as a separate chromosome. Investigation of the *ZtTGL1* locus on chromosome 3 confirmed the absence of targeted T-DNA insertion (Fig. 5.3B). Furthermore, increased coverage was observed at genomic regions cloned to flank the selective marker in the inserted T-DNA, suggesting the duplication of these sequences at an ectopic locus (Fig. 5.3B). A subset of reads aligning to the end of the genomic left flank sequence have pairs mapping to a locus on chromosome 11. Additionally, a subset of reads aligning with the end of the genomic right flank sequence have pairs mapping to the T-DNA sequence. The T-DNA region that these reads align to is beyond the right flank sequence, which would not normally be inserted into the genome during targeted integration by homologous recombination. Inspection of the reads aligned to this region of the pC-HYG-YR T-DNA sequence identified those with pairs mapped to the same locus of chromosome 11 (Fig. 5.3C). This suggests that the full T-DNA sequence, including regions beyond the flanking sequences, has been inserted ectopically into chromosome 11.

Inspection of T21 sequencing reads aligned to this region of chromosome 11 confirms presence of this insertion (Fig. 5.3D). Soft clipped sequences of reads aligning either side of the insertion site are identical to the ends of the T-DNA sequence, confirming that the complete T-DNA sequence from left border to right border repeat has been inserted (Fig. 5.3D). The ectopic insertion site lies 133 bp upstream of the start codon of the gene ZtritIPO323_04g03043, encoding the *Z. tritici* homolog of the MAP kinase kinase kinase BCK1, hereafter referred to as *ZtBCK1* (Fig. 5.3D; Fig. 5.3E). The T-DNA insertion at this locus could therefore have disrupted the promotor of *ZtBCK1*, potentially leading to changes in the expression of this gene. Furthermore, variant calling and examination of this region identified a 12bp deletion (chr11:240,721-240,732; Fig. 5.3D) in the coding sequence of *ZtBCK1* (Table 5.1; Fig. 5.3D),

which is presumed to have occurred during the T-DNA insertion event. The presence of this deletion was confirmed through Sanger sequencing. This deletion causes the loss of residues 6-9 ('GYRR') in the predicted amino acid sequence, which are outside any predicted conserved domains. Any disruption of *ZtBCK1* gene function by ectopic T-DNA insertion at this locus is therefore likely to have been caused by interference in the *ZtBCK1* promoter and altered transcriptional regulation.

Apart from the deletion within *ZtBCK1*, variant calling only identified one other unique polymorphism within the coding sequence of a gene in the T21 genome (Table 5.1). This SNP occurs in the second exon of ZtritIPO323_04t11145 (Mycgr3G60318), encoding a putative major facilitator superfamily (MFS) transporter, causing a V560G substitution in the predicted protein. Furthermore, the left flank sequence in the T-DNA from the plasmid pC-HYG-TGL1KO contains the complete sequence of the gene ZtritIPO323_04g07738 (Mycgr3G103740; Fig. 5.3B), which encodes a homolog of the yeast cytochrome C oxidase assembly protein PET191 (McEwen et al., 1993). As a consequence, the ectopic T-DNA insertion into the T21 genome will cause a full copy of this gene to be inserted, potentially altering the expression of this protein compared to the wild type. However, considering the previous evidence for the virulence-related function of the CWI pathway in *Z. tritici* (Mehrabi, Van Der Lee, et al., 2006), the disruption of *ZtBCK1* was chosen for further investigation into the cause of avirulence in T21.

### 5.3.2 Targeted deletion of *ZtBCK1* and *ZtCYR1* abolishes virulence in *Z. tritici*

To support the hypothesis that the avirulence of strains C5/L2 and T21 is caused by the disruption of *ZtBCK1* and *ZtCYR1*, respectively, these genes were targeted for deletion. Functional complementation of these strains, through introduction of the wild type *ZtBCK1* (including the promotor region) and *ZtCYR1* alleles, is required to confirm the role of the identified mutations in causing attenuated virulence. However, due to time constraints and the desire to investigate the impact of complete loss of *ZtBCK1* and *ZtCYR1* gene function, a targeted gene deletion approach was taken. The plasmid vectors pC-HYG-CYR1KO and pC-HYG-BCK1KO were transformed into *Z. tritici*

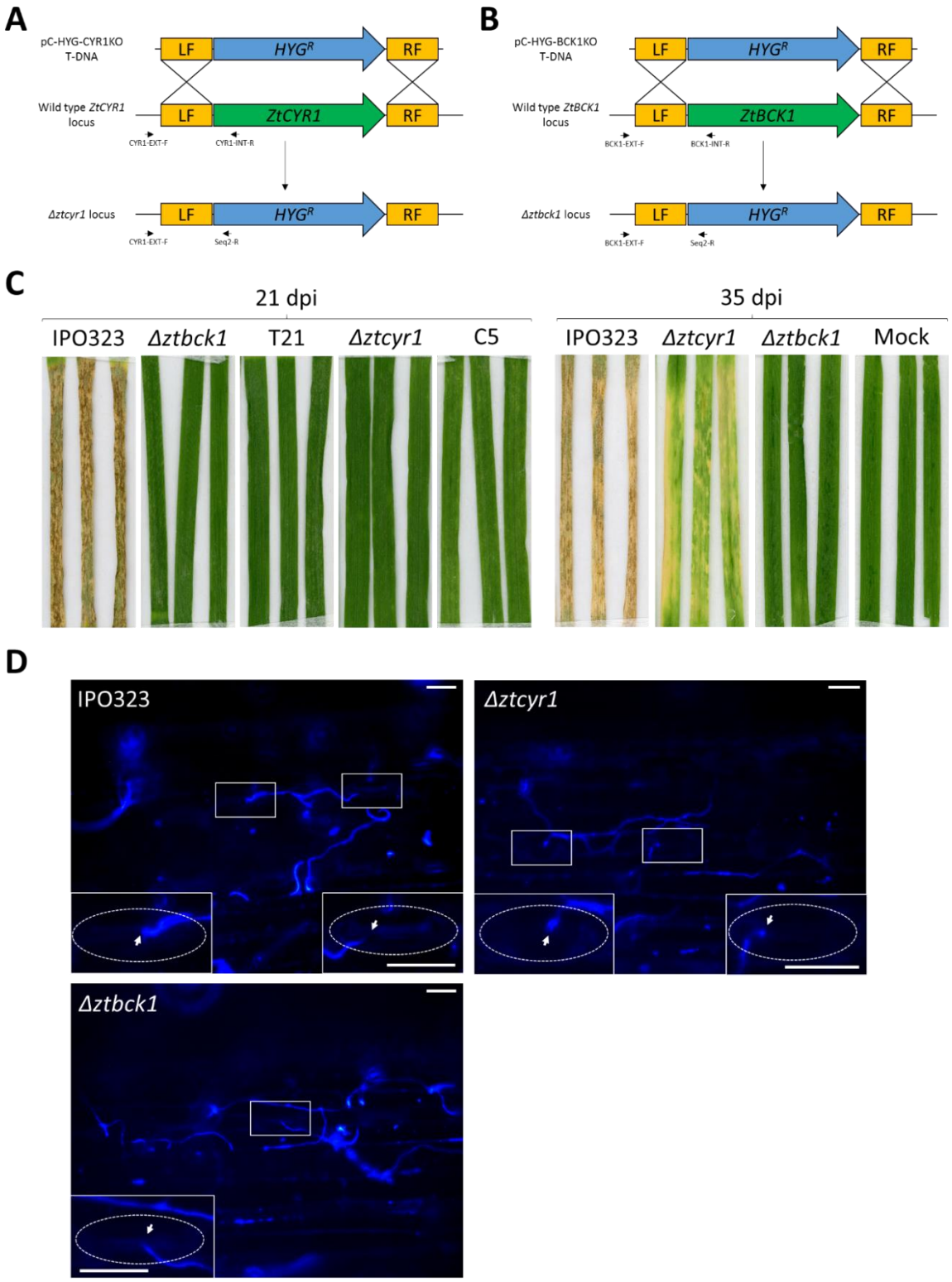


**Figure 5.4 Targeted deletion of *ZtBCK1* and *ZtCYR1* leads to abolishment of *Z. tritici* virulence**

Diagrams showing strategy for deletion of (A) *ZtCYR1 and* (B) *ZtBCK1* using the plasmids pC-HYG-CYR1KO and pC-HYG-BCK1KO, respectively, with primers used to screen transformants under their respective target loci. (C) Disease symptoms on wheat leaves after 21 and 35 days post infection by *Δztcyr1* and *Δztbck1* strains compared to wild type IPO323, C5 and T21. (D) Epiphytic *Z. tritici* hyphae stained with calcofluor white on the leaf surface 3 days post inoculation. Magnified images detailing stomatal penetration events (arrows), with guard cells indicated by dotted oval. Scale bars = 40μm.

IPO323. The resulting hygromycin resistant transformants were screened for insertion of the *HYG*$^{R}$ cassette in place of the wild type coding sequences of *ZtCYR1* and *ZtBCK1* by PCR (Fig. 5.4A; Fig. 5.4B). Three independent deletion mutants were purified for each gene, and designated *Δztcyr1* and *Δztbck1* strains.

Infection assays on susceptible wheat leaves found that these *Δztcyr1* and *Δztbck1* strains showed equivalent attenuation of virulence to that displayed by strains L2/C5 and T21, with all deletion strains unable to induce the necrotic lesions and pycnidia seen on leaves infected with the wild type after 21 dpi (Fig. 5.4C). Although the mild chlorosis caused by L2 and C5 was not observed on *Δztcyr1* infected leaves at 21 dpi, continuation of infection to 35 dpi led to the appearance of chlorosis on these leaves (Fig. 5.4C). Chlorosis was not observed on mock inoculated or *Δztbck1* infected leaves, confirming that this was not the result of environmental conditions or senescence (Fig. 5.4C). These findings provide supporting evidence that the avirulence of L2/C5 and T21 is caused by disruption of *ZtCYR1* and *ZtBCK1,* respectively.

Microscopic observations confirmed that both *Δztcyr1* and *Δztbck1* strains were able to penetrate the leaf through stomata (Fig. 5.4D). Spores of both mutants germinated on the leaf surface to produce epiphytic hyphae, and numerous stomatal interactions were observed for all strains after 3 dpi (Fig. 5.4D). These findings establish that avirulence in these strains is not caused by disruption of the morphological switch to hyphal growth, sensory perception of the host surface or recognition of stomatal apertures. Instead, this suggests that signalling via ZtCYR1 and ZtBCK1 is required during infection stages after host penetration, during symptomless invasive growth of the mesophyll and/or the switch to necrotrophy.

### 5.3.3 Deletion of *ZtBCK1* impacts vegetative growth and the cell wall stress response

Considering previous reports of the CWI pathway influencing both yeast-like and hyphal growth of *Z. tritici* (Mehrabi, Van Der Lee, et al., 2006), the vegetative growth characteristics of *Δztbck1* strains were investigated. While the growth rate by blastosporulation on YPD agar was consistent between

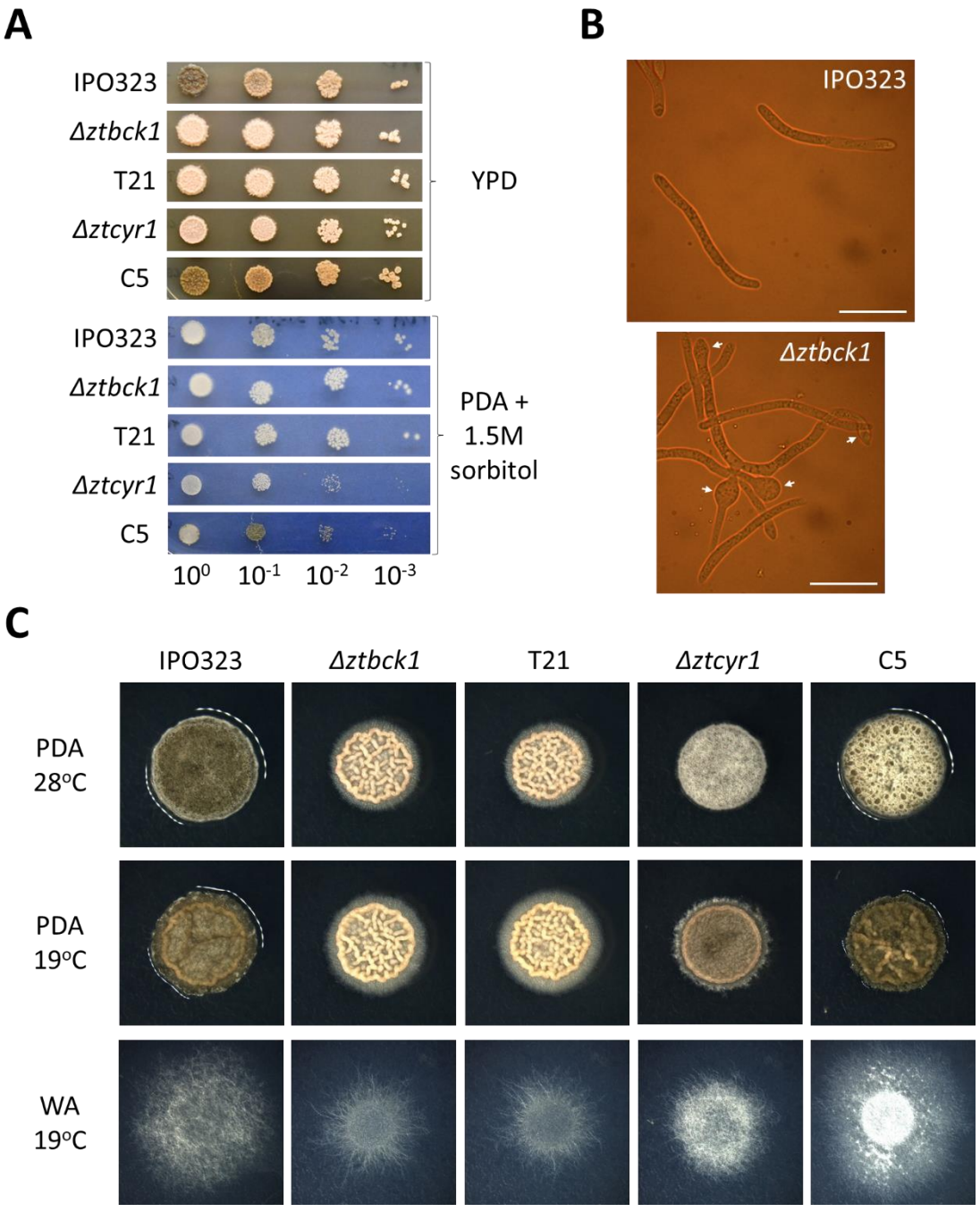


**Figure 5.5 Vegetative growth phenotypes of *ZtBCK1* and *ZtCYR1* deletion strains**
(A) *Z. tritici* grown for 10 days on PDA containing sorbitol and YPD at 19°C, 5 µl droplets of a 10-fold serial dilution starting at a concentration of $5x10^6$ spores/ml. (B) Blastospores grown on YPD for 6 days, with appearance of swollen cells (arrows) in *Δztbck1.* Scale bar = 20 µm. (C) Growth on potato dextrose agar (PDA) at 28°C and 19°C for 7 days and radial hyphal growth on water agar (WA) at 19°C for 14 days.

*Δztbck1* strains and IPO323, a defect in melanisation was seen in *Δztbck1* mutants after a prolonged growth period (Fig. 5.5A). Furthermore, swollen cells were observed regularly in the blastospores of *Δztbck1* strains after 6 days of growth on YPD, which were absent in IPO323 cells under the same conditions (Fig. 5.5B). Defects in hyphal growth were also identified in *ZtBCK1* deficient strains. Initially, the germination efficiency and early colony formation on water agar (WA) was similar between *Δztbck1* strains and the wild type. However, the growth rate of *Δztbck1* strains reduced as radial growth continued, resulting in colonies with significantly smaller diameter than the wild type after 14 days (Fig. 5.5C). Furthermore, compared to the wild type which produced abundant aerial hyphae when grown at 28$^{o}$C on PDA, *Δztbck1* strains continued to grow by blastosporulation, with no visible difference in colony formation between 19$^{o}$C and 28$^{o}$C in these strains (Fig. 5.5C). These findings suggest that the *Z. tritici* CWI pathway is involved in regulating the morphological switch to hyphal growth in response to heat stress, as well as in prolonged hyphal growth under starvation. Furthermore, the *in vitro* phenotypes of *Δztbck1* were consistent with those of T21, providing further evidence for *ZtBCK1* disruption being the sole genetic cause of the phenotypes of this strain.

The sensitivity of wild type and *Δztbck1* strains to cell wall stress was assessed by exposure to various enzyme mixtures possessing β-1,3-glucanase activity. Exposure of IPO323 spores to lysing enzymes from *Trichoderma harzianum* led to some cell wall degradation and cell lysis, although many cells remained intact (Fig. 5.6A). Cell wall degradation of *Δztbck1* blastospores was dramatically enhanced compared to the wild type, with almost all cells either forming spheroplasts or undergoing lysis (Fig. 5.6A). To support this, the viability of wild type and *Δztbck1* cells following treatment with lyticase enzymes from *Arthrobacter luteus* was assessed. The wild type was able to maintain viability after exposure to a higher concentration of lyticase than *Δztbck1*, providing further evidence that deletion of *ZtBCK1* leads to enhanced sensitivity to cell wall stress (Fig. 5.6B). To investigate whether this effect was specific to disruption of β-1,3-glucan, the sensitivity of *Δztbck1* to calcofluor white, which disrupts chitin synthesis, and caspofungin, which inhibits β-1,3-glucan synthesis, was assessed. While *Δztbck1* strains displayed no change in sensitivity to calcofluor white, they were found to have elevated sensitivity to

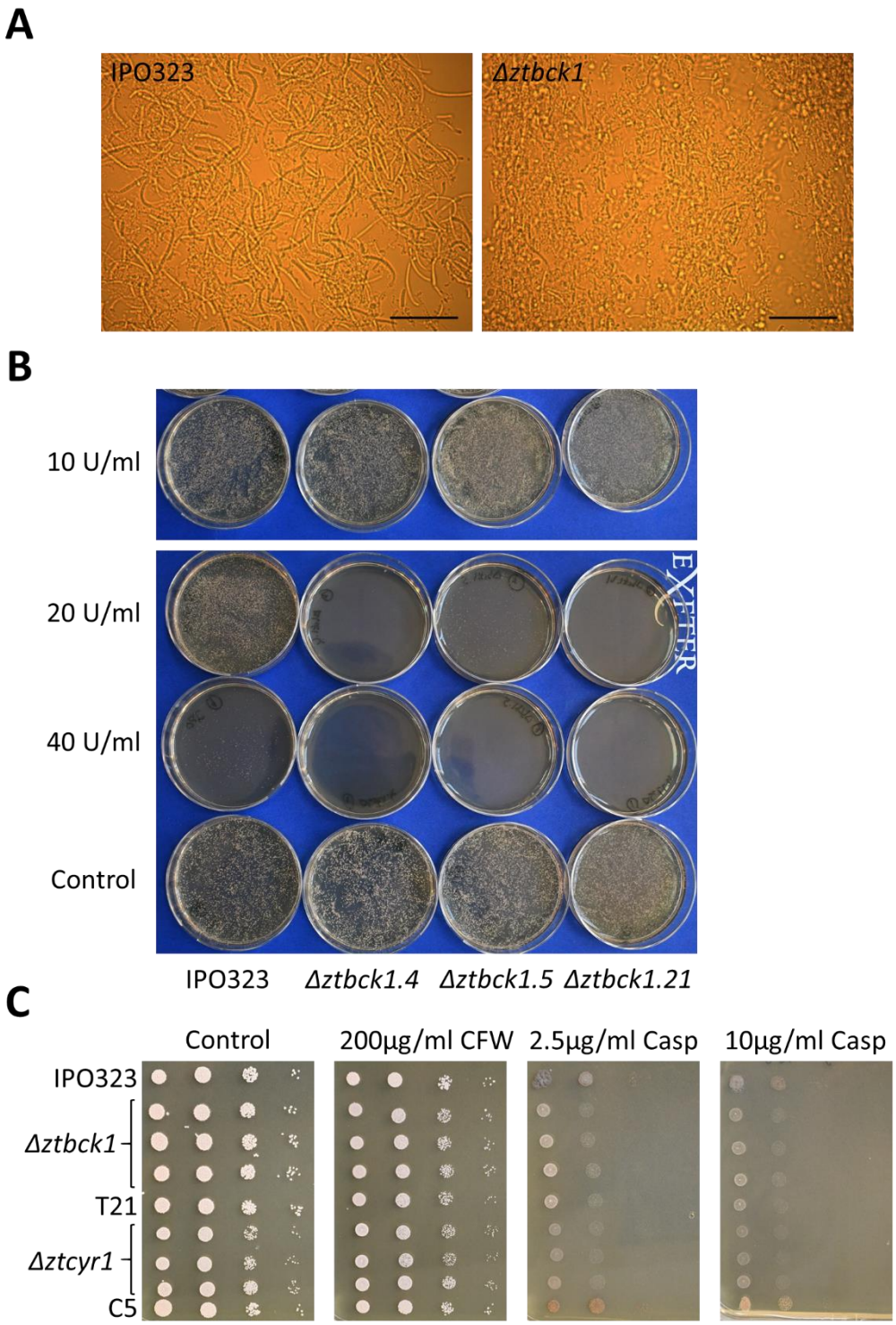


**Figure 5.6 Deletion of ZtBCK1 leads to increased sensitivity to cell wall degrading enzymes**
(A) *Z. tritici* cells incubated with 30 mg/ml lysing enzymes from *Trichoderma harzianum* for 2 h. Scale bars = 50 µm (B) *Z. tritici* cell suspensions exposed to various concentrations of Lyticase enzyme from *Arthrobacter luteus* for 2 h 25°C before being cultured on YPD agar for 5 days at 19°C, showing loss of viability of *Δztbck1* strains at lower enzyme concentrations than the wild type. (C) Sensitivity assays of *Z. tritici* strains grown on YPD supplemented with calcofluor white (CFW) and caspofungin (Casp). 5 µl droplets of a 10-fold serial dilution starting at a concentration of $5x10^6$ spores/ml.

caspofungin (Fig. 5.6C). Together, these results suggest that the *ZtBCK1* is specifically involved in regulation of the *Z. tritici* response to perturbation of β-1,3-glucan integrity. Furthermore, *Δztcyr1* strains, but not strain C5, also displayed increased sensitivity to caspofungin (Fig. 5.6C), suggesting that cAMP signalling may also plays a role in this response.

### 5.3.4 Deletion of *ZtCYR1* impairs melanisation and increases osmosensitivity

Vegetative growth phenotypes of *Δztcyr1* strains were also investigated for comparison with previous characterisation of other components of the PKA signalling pathway (Mehrabi et al., 2009; Mehrabi & Kema, 2006). The growth rate by blastosporulation on YPD was indistinguishable from the wild type (Fig. 5.5A). However, melanisation was impaired in *Δztcyr1* when grown on YPD and PDA at 19$^{o}$C in the dark (Fig. 5.5A; Fig. 5.5C). Similarly, melanisation of aerial hyphae was not observed in *Δztcyr1* strains when grown on PDA at 28$^{o}$C. Furthermore, while the germination efficiency of *Δztcyr1* strains on water agar was unchanged from the wild type, subsequent hyphal growth proceeded at a much slower rate in these mutants (Fig. 5.5C). Interestingly, this disruption of melanisation and hyphal growth rate was not observed in the C5 strain. Finally, sensitivity to high osmolarity of the growth media was increased in the C5 and *Δztcyr1* strains, which displayed a reduced growth rate compared to the wild type on PDA amended with 1.5M sorbitol (Fig. 5.5A). These findings suggest that *ZtCYR1* is involved in the regulation of melanisation, hyphal growth and the osmotic stress responses, but that the phenotype caused by the point mutation in *ZtCYR1* in the C5 strain is distinct from that resulting from deletion of the whole coding sequence.

### 5.3.5 Transcriptome profiling of *Δztcyr1* and *Δztbck1* strains during infection

Considering the observation of successful epiphytic growth and stomatal interactions during infection by *Δztcyr1* and *Δztbck1* strains, it was hypothesised that avirulence in these strains was caused by defective regulation of intercellular colonisation in the leaf tissue. This could include impaired adaptation to the host environment, abnormal fungal development during

invasive growth or an inability to effectively manipulate the host defence response, all of which have been shown to be crucial for successful *Z. tritici* infection of wheat (Francisco et al., 2020; Marshall et al., 2011; Rudd et al., 2015). To investigate such possible explanations, whole genome transcriptome profiling of both *Z. tritici* and wheat during infection by the wild type IPO323, *Δztcyr1* and *Δztbck1* was carried out by RNA sequencing. Infected leaf samples were taken at 6 dpi to assess differences in gene expression during the late symptomless phase of wild type infection, when stomatal penetration by most epiphytic hyphae has occurred and invasive growth is being established in the mesophyll. Samples were also taken at 9 dpi at the start of the transition to necrotrophic growth by the wild type IPO323, which has been shown previously to coincide with dramatic transcriptional changes in both the pathogen and host (Rudd et al 2015). It must be noted that leaf samples infected by all *Z. tritici* strains remained asymptomatic at 9 dpi, before the wild type began to induce chlorosis between 10 and 12 dpi.

The progress of leaf colonisation by each strain between the sampled time points was assessed quantitatively through the relative abundance of *Z. tritici* transcripts. The proportion of RNA reads uniquely mapping to the *Z. tritici* genome was calculated to indicate the level of fungal biomass in each sample. No significant difference in the proportion of *Z. tritici* transcripts was identified between the strains at 6dpi, suggesting that fungal growth rate up to this point of infection was largely equivalent (Fig. 5.7A). IPO323 displayed significant increases in the proportion of reads mapped to the *Z. tritici* genome at 9dpi (Fig. 5.7A). This is consistent with previous reports of measurable increases in fungal biomass as *Z. tritici* transitions to necrotrophy, changes in which are difficult to detect during early symptomless growth (Keon et al., 2007; Palma-Guerrero et al., 2016; Rudd et al., 2015). This provides evidence that the sampled infection time points effectively encompass this transition in infection stage.

Conversely, no significant increase in the percentage of reads mapped to the *Z. tritici* genome was identified between 6dpi and 9dpi in *Δztbck1* samples, indicating that there was no significant increase in the relative biomass of this strain in infected leaf tissue (Fig 5.7A). This suggests that colonisation of the wheat leaf by *Δztbck1* is inhibited during the symptomless phase of infection. Furthermore, while *Δztcyr1* samples did display an increase in *Z. tritici* mapped

reads between 6dpi and 9dpi (Fig. 5.7A), the magnitude of this increase was significantly greater in IPO323 than in *Δztcyr1* infected leaves (Fig. 5.7B). This suggests that the increase in fungal biomass between these time points was less pronounced in *Δztcyr1*.

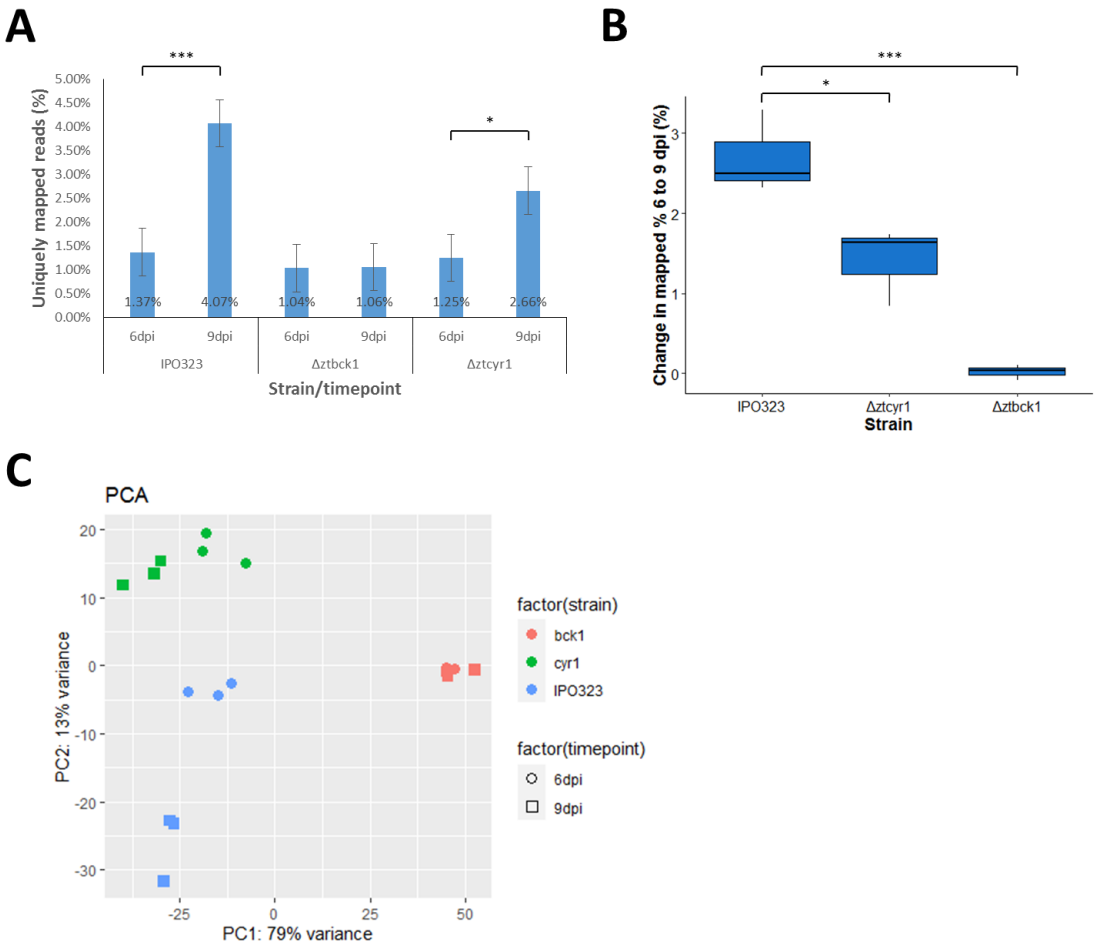


**Figure 5.7 *In planta* growth and global gene transcription are impacted by deletion of *ZtBCK1* and *ZtCYR1***
(A) Percentage of RNA sequencing reads uniquely mapped to the *Z. tritici* genome across infection time points in each strain, as an indication of *in planta* fungal biomass. Mean values across each repeated sample are plotted along with the standard error. Statistically significant differences between mean percentages across time points in each strain from one-way ANOVA are indicated (***p<0.001, *p<0.05). (B) Change in the percentage of uniquely mapped reads between 6 and 9 dpi in each experimental repeat grouped by strain, as an indication of growth between these time points. Statistically significant differences from one-way ANOVA are indicated (***p<0.001, *p<0.05). (C) Principal component analysis of global normalised gene expression data.

Principle component analysis (PCA) using global normalised gene expression data revealed that the *Z. tritici* transcriptome of each sample could be most easily distinguished by the strain used for infection (Fig. 5.7C). The first principle component (PC1) encompasses most of the variation in gene

expression between *Δztbck1* and both *Δztcyr1* and IPO323, explaining 76% of the variation in the dataset (Fig. 5.7C). Meanwhile the second principal component (PC2), which explains 16% of the variation in gene expression, appears to comprise the majority of variation between *Δztcyr1* and IPO323, which is accentuated by the progression of infection to 9 dpi (Fig. 5.7C). Although global gene expression in *Δztcyr1* does appear to change between the time points, with clear grouping of *Δztcyr1* 6 dpi and 9 dpi samples, this change is not as dramatic as the wild type (Fig. 5.7C). These results suggest that divergence in global gene expression between IPO323 and *Δztcyr1* increases as the wild type transitions to necrotrophic growth. This led to the hypothesis that disruption of cAMP signalling impairs the ability of *Z. tritici* to undergo this necrotrophic switch. Furthermore, the variation along PC2 between 6 and 9 dpi in the wild type further differentiates the difference in global gene expression with *Δztbck1*, which shows no variation between the sampled time points along either axis (Fig. 5.7C). Along with the stasis in *Δztbck1* biomass between 6 and 9 dpi, this supports the hypothesis that colonisation by *Δztbck1* does not progress beyond the initial invasion of the wheat leaf.

### 5.3.6 *ZtBCK1* regulates *in planta* expression of fungal genes encoding putative secreted proteins and candidate effectors

Differential expression analysis led to the identification of 682 DE genes in *Δztbck1* at 6 dpi, which increased to 1652 DE genes at 9 dpi compared to the expression profile in IPO323 (Fig. 5.8A; Table S5.1). Furthermore, only three genes were found to be DE between the sampling time points in *Δztbck1*, compared to 198 DE genes identified between 6 and 9 dpi in IPO323 (Fig. 5.8B; Table S5.1). This is consistent with the results of PCA in finding that global transcription in *Δztbck1* diverges further from that of IPO323 between 6 and 9 dpi during infection, and that this largely results from changes in gene expression in the wild type across infection. These results suggest that not only is gene expression in the *Δztbck1* mutant significantly different to the wild type during early infection, but that it also displays none of the transcriptional changes associated with the transition to necrotrophy.

Given the importance of secreted proteins in the molecular interaction between *Z. tritici* and wheat, the differential expression of genes within the recently

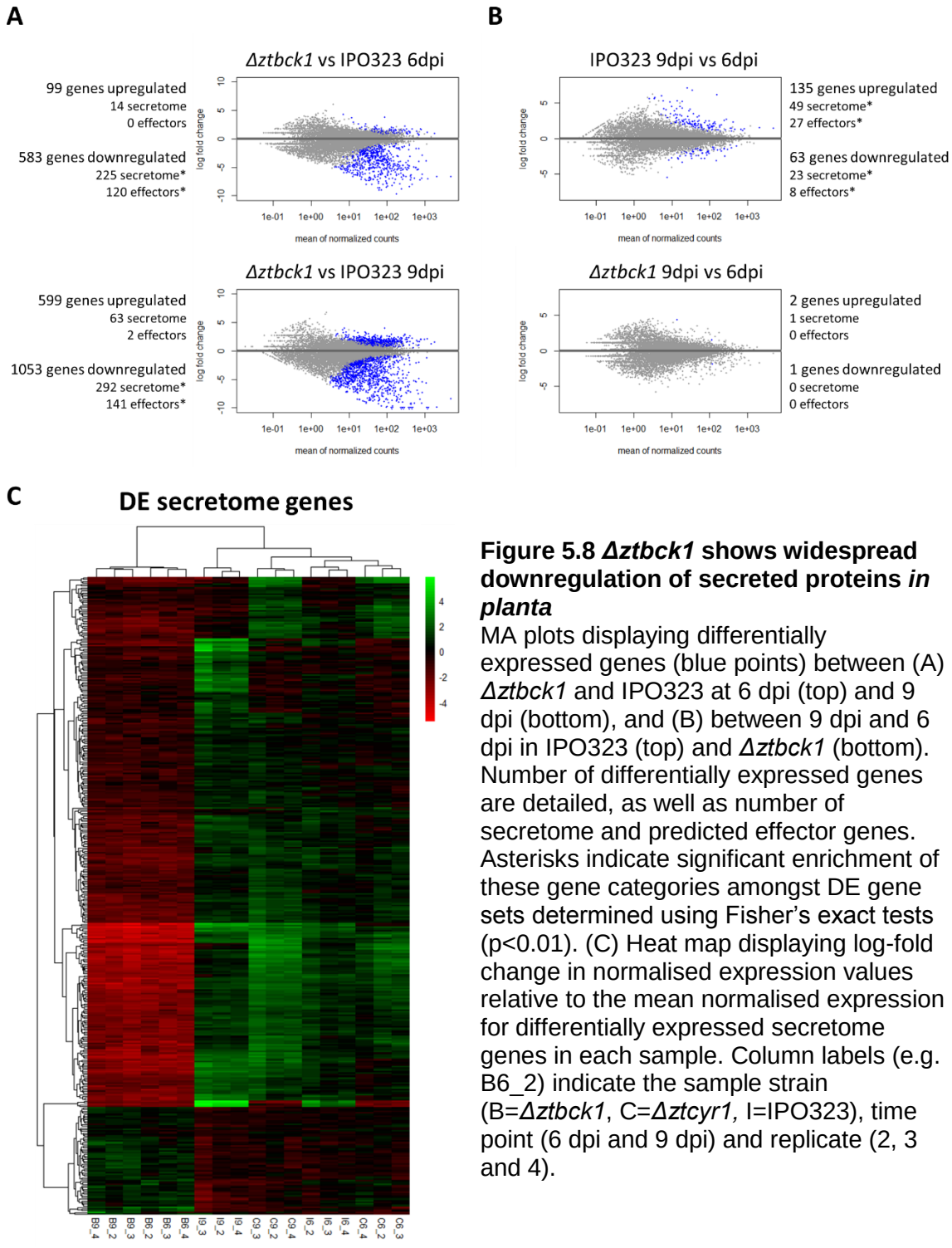


**Figure 5.8 *Δztbck1* shows widespread downregulation of secreted proteins *in planta***
MA plots displaying differentially expressed genes (blue points) between (A) *Δztbck1* and IPO323 at 6 dpi (top) and 9 dpi (bottom), and (B) between 9 dpi and 6 dpi in IPO323 (top) and *Δztbck1* (bottom). Number of differentially expressed genes are detailed, as well as number of secretome and predicted effector genes. Asterisks indicate significant enrichment of these gene categories amongst DE gene sets determined using Fisher's exact tests ($p<0.01$). (C) Heat map displaying log-fold change in normalised expression values relative to the mean normalised expression for differentially expressed secretome genes in each sample. Column labels (e.g. B6_2) indicate the sample strain (B=*Δztbck1*, C=*Δztcyr1,* I=IPO323), time point (6 dpi and 9 dpi) and replicate (2, 3 and 4).

updated *Z. tritici* secretome was investigated (Rudd et al., unpublished). The secretome was defined as those genes within the Rothamsted genome annotation that contain a predicted signal peptide and do not contain a predicted transmembrane domain (Rudd et al., unpublished). *Δztbck1* displayed widespread downregulation of genes within the secretome compared to IPO323 during infection (Fig. 5.8C; Table S5.1). Secretome genes were significantly enriched in the downregulated genes identified in *Δztbck1* at both 6 and 9 dpi,

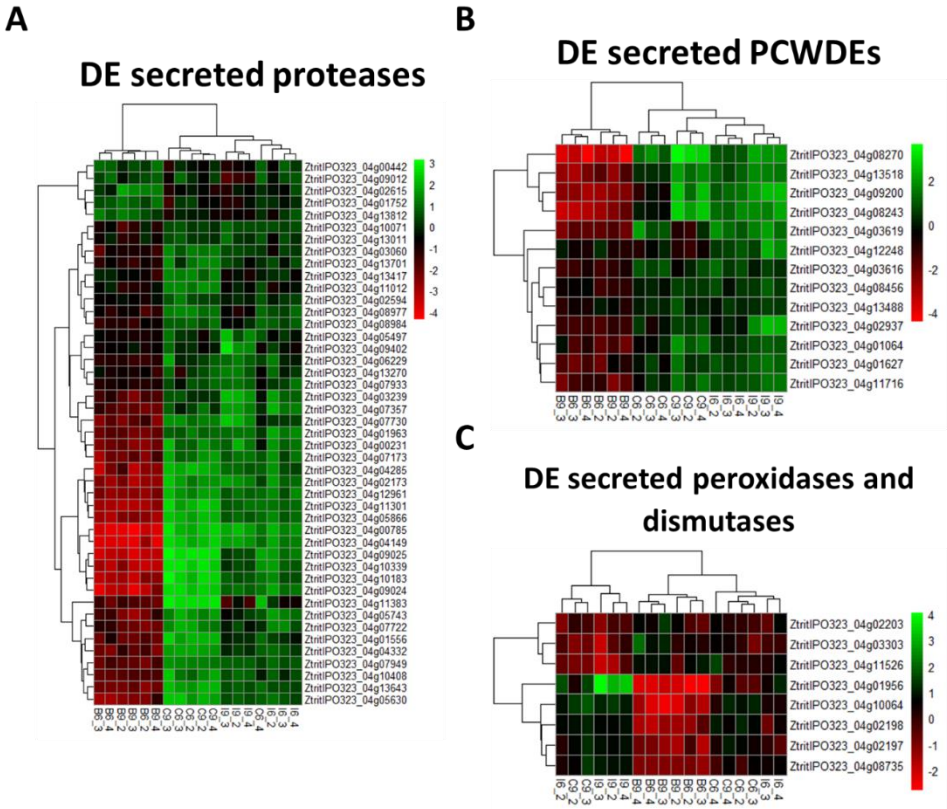


**Figure 5.9 Genes encoding putative infection-related secreted proteins show differential regulation in *Δztbck1* and *Δztcyr1***
Heat maps displaying log-fold change in normalised expression values relative to the mean normalised expression for differentially expressed secreted (A) proteases, (B) plant cell wall degrading enzymes (PCWDEs) and (C) peroxidase/superoxide dismutase genes in each sample. Column labels (e.g. B6_2) indicate the sample strain (B=*Δztbck1*, C=*Δztcyr1,* I=IPO323), time point (6 dpi and 9 dpi) and replicate (2, 3 and 4).

making up 38.6% and 27.7% in these sets, respectively (Fig. 5.8A). Functional annotation based on InterPro domains revealed that these downregulated secreted proteins include many with enzymatic activities that have been shown to be induced during wild type *Z. tritici* infection (Table S5.1; Palma-Guerrero et al., 2016; Rudd et al., 2015). This includes a host of secreted proteases, plant cell wall degrading enzymes, peroxidases and superoxide dismutases (Fig. 5.9). There were some exceptions to this, including 5 secreted proteases and 3 chloroperoxidases which were upregulated at 9 dpi in *Δztbck1* (Fig. 5.9A; Fig. 5.9C). However, in these cases there was clear evidence for peak expression during early infection in the wild type, both here (Table S5.1) and in previous studies (Palma-Guerrero et al., 2016; Rudd et al., 2015). This indicates that a minority of the secreted proteins associated with the symptomless phase displayed continued expression in *Δztbck1* at 9dpi. Overall, these results

suggests that *Δztbck1* is unable to induce the transcription of a broad range of infection-related secreted proteins in response to colonisation of the host environment.

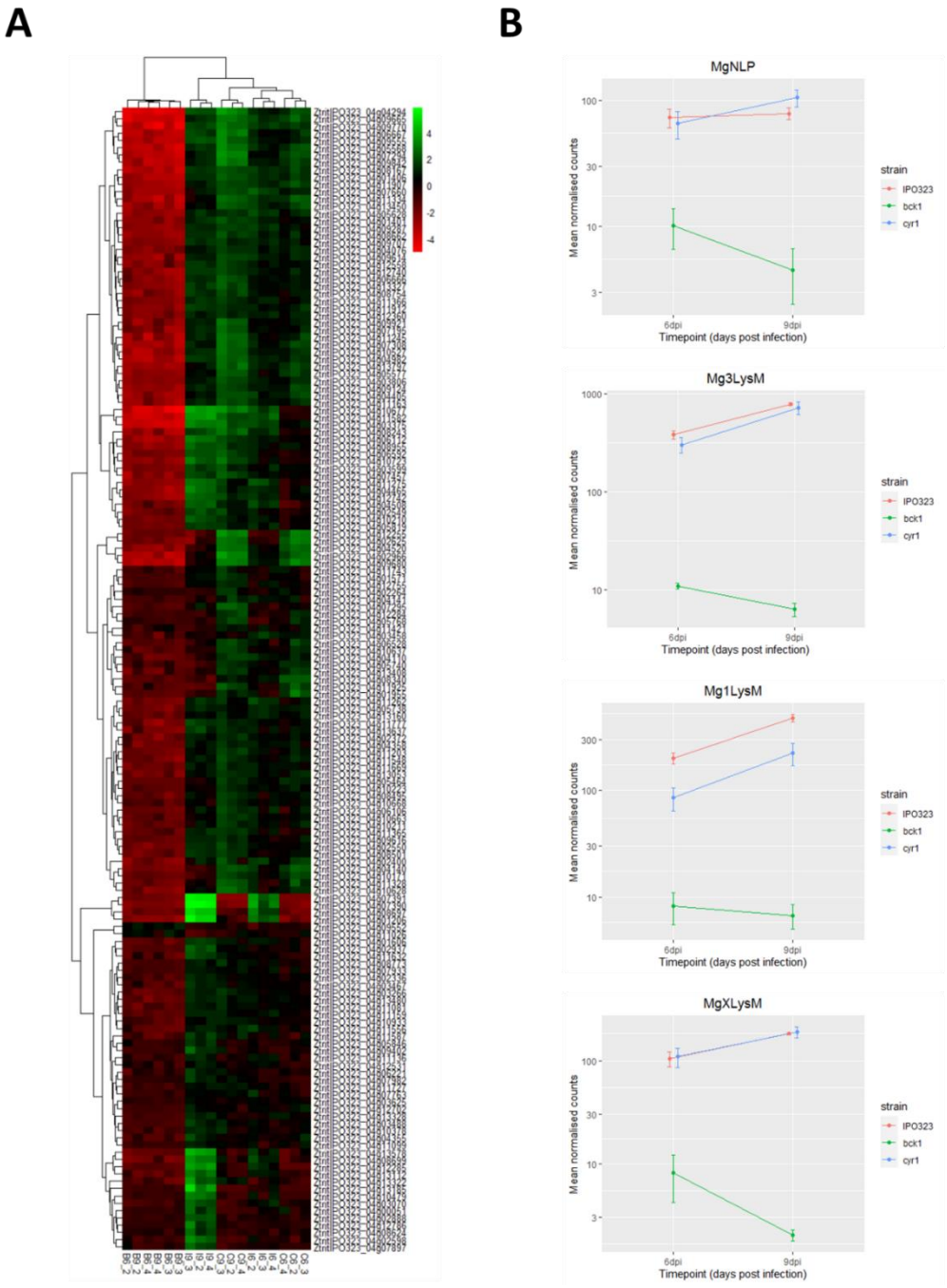


**Figure 5.10 Putative effector genes show differential regulation in *Δztbck1* and *Δztcyr1***
(A) Heat maps displaying log-fold change in normalised expression values relative to the mean normalised expression for differentially expressed secreted effector genes in each sample. Column labels (e.g. B6_2) indicate the sample strain (B=*Δztbck1*, C=*Δztcyr1,* I=IPO323), time point (6 dpi and 9 dpi) and replicate (2, 3 and 4). (B) Mean of the normalised count values for MgNLP (ZtritIPO323_04g04358), Mg3LysM (ZtritIPO323_04g03143), Mg1LysM (ZtritIPO323_04g12742) and MgXLysM (ZtritIPO323_04g12740) in each strain at 6 dpi and 9 dpi. Error bars represent standard error.

Considering their crucial function in the molecular interactions of plant pathogens and their hosts (Lo Presti et al., 2015), and the lack of knowledge surrounding their regulation, analysis was also carried out for genes encoding predicted effectors. Putative effectors were predicted from the putative protein sequences of genes within the secretome using EffectorP v2.0 (Sperschneider et al., 2018). The sets of genes downregulated in *Δztbck1* at both time points were significantly enriched for predicted effectors (Fig. 5.8A; Fig. 5.10A), supporting the hypothesis that *Δztbck1* is defective in infection-specific protein secretion. This includes the necrosis- and ethylene-inducing protein 1 (Nep1)-like protein MgNLP, which is known to be highly upregulated during the late symptomless phase but is dispensable for virulence (Motteram et al., 2009). Crucially, all three LysM-domain containing effectors, which are known to be *Z. tritici* virulence factors (Tian et al., 2021), are strongly downregulated in *Δztbck1* at both 6 and 9 dpi (Fig. 5.10B). This finding suggests that host colonisation by *Δztbck1* is inhibited by the inability of this strain to supress and withstand the host defence response.

Furthermore, genes involved in cell wall biosynthesis were also found to be differentially regulated in *Δztbck1* during infection (Fig. 5.11). A *Z. tritici* homolog of the *A. fumigatus* β-1-3 glucanosyltransferase *ZtGel2*, involved in the formation of β-1,3-glucan branches, and an α-1,3 glucan synthase were both downregulated in *Δztbck1* compared to IPO323 at both time points (Fig. 5.11A). Along with the sensitivity of *Δztbck1* to caspofungin and glucanase enzymes, this suggests that the *Z. tritici* CWI pathway is responsible for responding to β-1,3-glucan perturbation. Conversely, four chitin synthase genes were found to show significantly higher expression in *Δztbck1* during infection (Fig. 5.11B). Enhanced expression of chitin synthases in *Δztbck1* could indicate the absence of an adaptive repression of chitin biosynthesis during infection by the wild type to avoid host recognition, although there is no evidence for such a response from previous transcriptome data (Rudd et al., 2015). Alternatively, an enhanced host defence response to *Δztbck1* due to lack of immune suppression by secreted effectors, including LysM proteins (Marshall et al., 2011), could lead to elevated chitin synthase expression in response to cell wall damage, regulated by signalling mechanisms other than the CWI pathway.

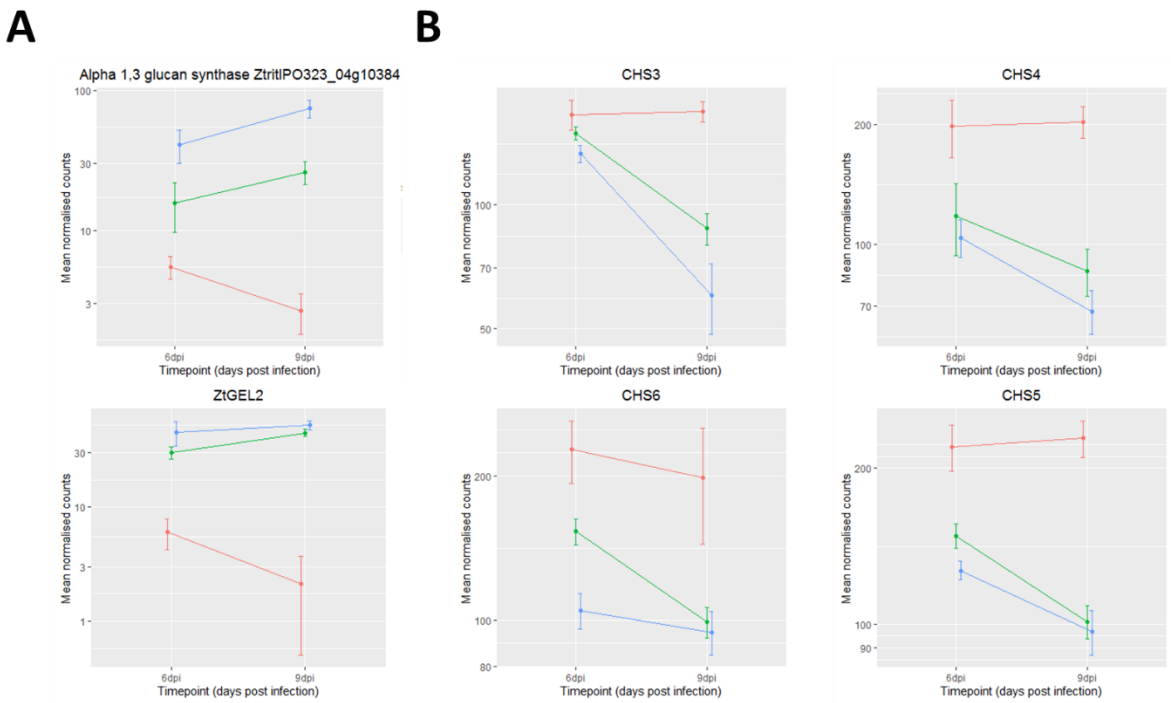


**Figure 5.11 Cell wall biosynthesis enzymes are differentially expressed in *Δztbck1***
Mean of the normalised count values in each strain at 6 dpi and 9 dpi for (A) alpha-1,3-glucan synthase (ZtritIPO323_04g10384) and *ZtGEL2* (ZtritIPO323_04g13416) and (B) differentially expressed chitin synthase genes (*CHS3*/ZtritIPO323_04g00292, *CHS4*/ZtritIPO323_04g09937, *CHS5*/ZtritIPO323_04g06329 and *CHS6*/ZtritIPO323_04g06328. Error bars represent standard error.

## 5.3.7 Infection-associated gene expression in *Δztcyr1* diverges from IPO323 as infection progresses

Differential expression analysis found there to be 84 DE genes between *Δztcyr1* and IPO323 at 6 dpi, which increased to 346 DE genes at 9 dpi (Fig. 5.12A; Table S5.1). Furthermore, a set of 182 genes was found to be DE between 6 and 9 dpi in *Δztcyr1* (Fig. 5.12B; Table S5.1). Although this set showed some similarity to the genes found to be DE between the time points in IPO323, the majority (66%) were distinct (Fig. 5.12C). These results support those from PCA analysis in suggesting that while global transcription is similar between *Δztcyr1* and IPO323 at 6 dpi, the progression of infection to 9 dpi leads to divergence in gene expression between these strains.

The sets of up- and downregulated genes in *Δztcyr1* compared to IPO323 from both time points were significantly enriched with secretome genes (Fig. 5.12A). The majority of these putative secreted proteins were functionally

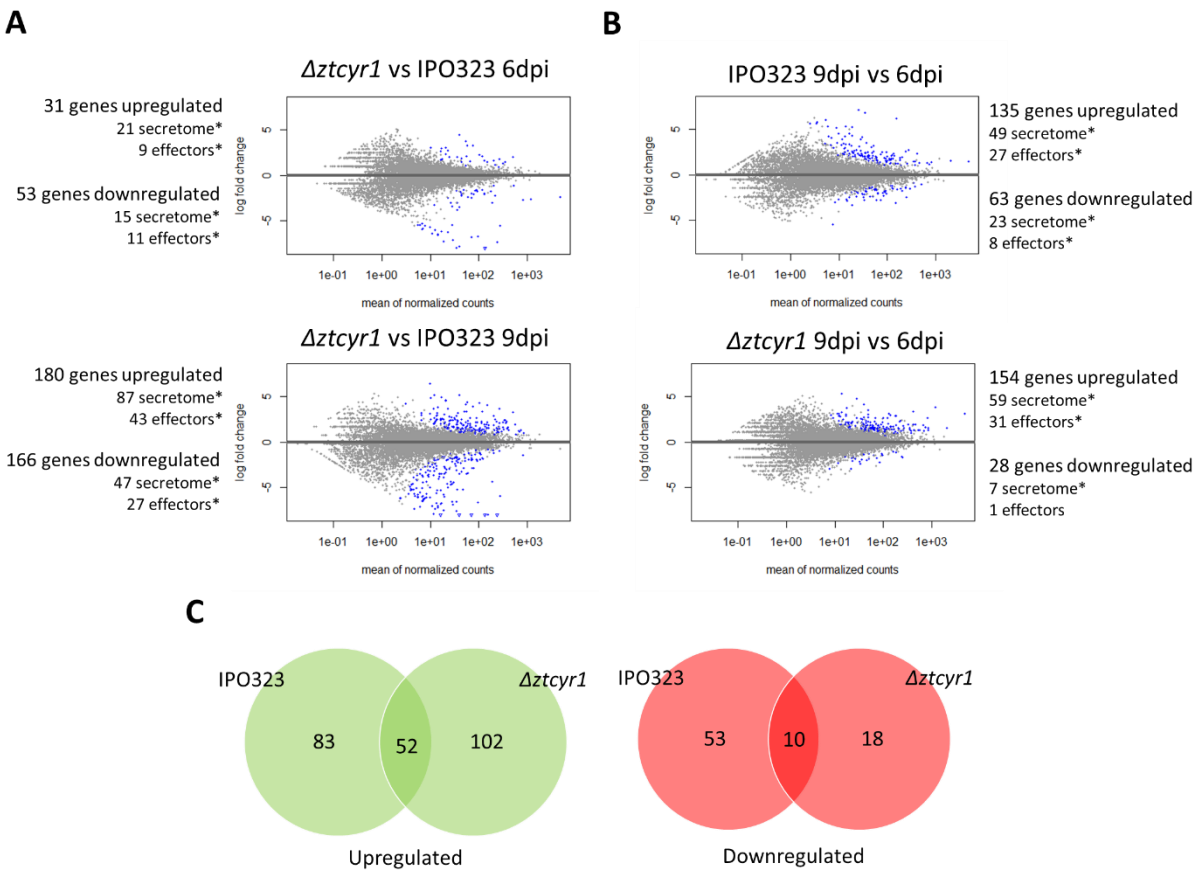


**Figure 5.12 *Δztcyr1* gene expression diverges from IPO323 as infection progresses**
MA plots displaying differentially expressed genes (blue points) between (A) *Δztcyr1* and IPO323 at 6 dpi (top) and 9 dpi (bottom), and (B) between 9 dpi and 6 dpi in IPO323 (top) and *Δztcyr1* (bottom). Number of differentially expressed genes are detailed, as well as number of secretome and predicted effector genes. Asterisks indicate significant enrichment of these gene categories amongst DE gene sets determined using Fisher's exact tests ($p<0.01$). (C) Comparison of genes found to be differentially expressed between 6 and 9 dpi in IPO323 and *Δztcyr1*.

uncharacterised, and all sets of *Δztcyr1* DE genes were significantly enriched for predicted effectors (Fig. 5.12A). Nine putative effectors were upregulated in *Δztcyr1* at 6 dpi, which increased to 43 at 9 dpi (Fig. 5.12A; Fig 5.13A). Similarly, the number of putative effectors downregulated in *Δztcyr1* increased from 11 to 27 between 6 and 9 dpi (Figure 5.12A; Fig. 5.13B). Nineteen of the 27 effectors downregulated in *Δztcyr1* at 9dpi were upregulated between 6 and 9 dpi in IPO323 (Figure 5.13B; Table S5.1), suggesting that they function in the onset of necrotrophy. To support this, it was found that all of the effectors in this set of 27 (that were included in the old genome annotation) displayed peak expression at the transition to, or during, the necrotrophic phase in a previous study (Rudd et al., 2015). As well as protein effectors, two polyketide synthase (PKS) genes and the hybrid PKS ribosomal peptide synthase *HSP1* (Rudd et al

2015), which could function in biosynthesis of secondary metabolite effectors, were downregulated in *Δztcyr1* at 9 dpi (Fig. 5.13C). These results indicate that the expression of effectors is diverging between *Δztcyr1* and the wild type as infection moves towards the necrotrophic phase.

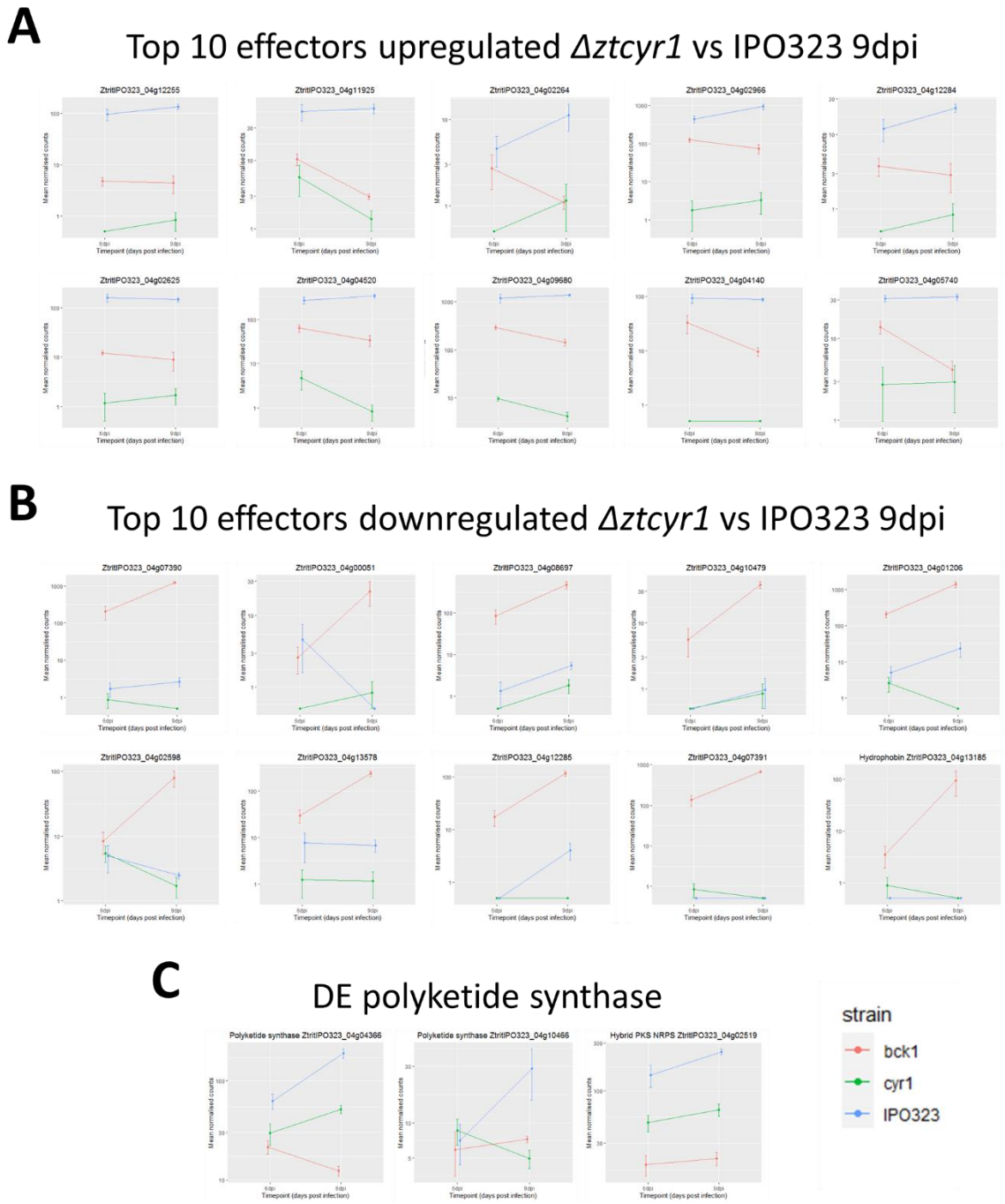


**Figure 5.13 Top 10 putative effectors up- and downregulated in *Δztcyr1***
Expression profiles of putative effectors that were upregulated (A) and downregulated (B) by the largest fold-change, as well as differentially expressed polyketide synthase genes, in *Δztcyr1* at 9 dpi compared to IPO323. Mean of the normalised count values in each strain at 6 dpi and 9 dpi are plotted, with error bars representing standard error.
.

Another striking difference in expression between *Δztcyr1* and IPO323 during infection was the upregulation of secreted proteases in the mutant (Fig. 5.9A). The number of significantly upregulated secreted proteases in *Δztcyr1* compared the wild type increased from 5 to 16 between 6 and 9 dpi (Table S5.1). All of these secreted proteases were found previously to show peak expression at the transition to necrotrophy during IPO323 infection, which was proposed to represent a switch to the use of host proteins as a carbon source (Rudd et al., 2015). Also heavily represented in the DE genes in *Δztcyr1* were the major facilitator superfamily (MFS) transporters, 18 of which were downregulated at 9dpi in this strain (Table S5.1). Of these, 10 were annotated as sugar transporters (Fig. 5.14). Also downregulated at 9dpi were three predicted amino acid transporters (Table S5.1). Furthermore, 6 MFS proteins were upregulated in *Δztcyr1* at 9 dpi (Table S5.1), three of which were putative sugar transporters (Fig. 5.14). Together, these results suggest that genes potentially involved in acquisition of nutrients from the host are differentially regulated in *Δztcyr1* as infection progresses.

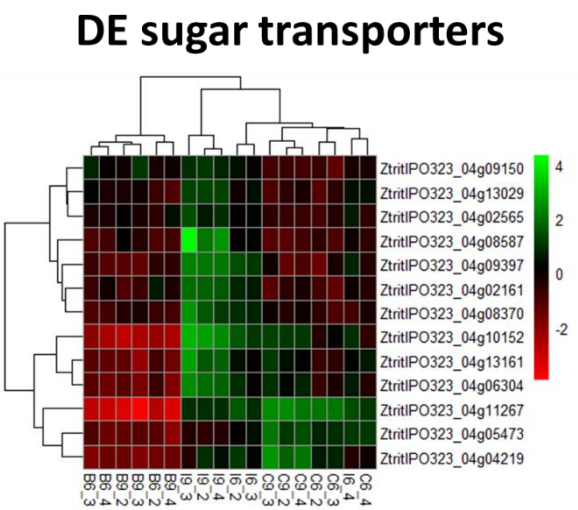


**Figure 5.14 Sugar transporters differentially expressed in *Δztcyr1* and *Δztbck1***
Heat maps displaying log-fold change in normalised expression values relative to the mean normalised expression for major facilitator superfamily (MFS) sugar transporters that were differentially expressed between *Δztcyr1* and IPO323 at 9 dpi. Column labels (e.g. B6_2) indicate the sample strain (B=*Δztbck1*, C=*Δztcyr1,* I=IPO323), time point (6 dpi and 9 dpi) and replicate (2, 3 and 4).
.

### 5.3.8 Transcriptome profiling of wheat reveals different defence response to infection by *Δztcyr1* and *Δztbck1*

Analysis of RNA sequencing reads aligned to the wheat genome was used to investigate whether the host response to *Δztcyr1* and *Δztbck1* infection was altered compared to colonisation by the wild type. Clustering of samples based on global wheat gene expression data was investigated by multi-dimensional scaling (MDS) analysis (Fig. 5.15). This revealed that 40% of the variance

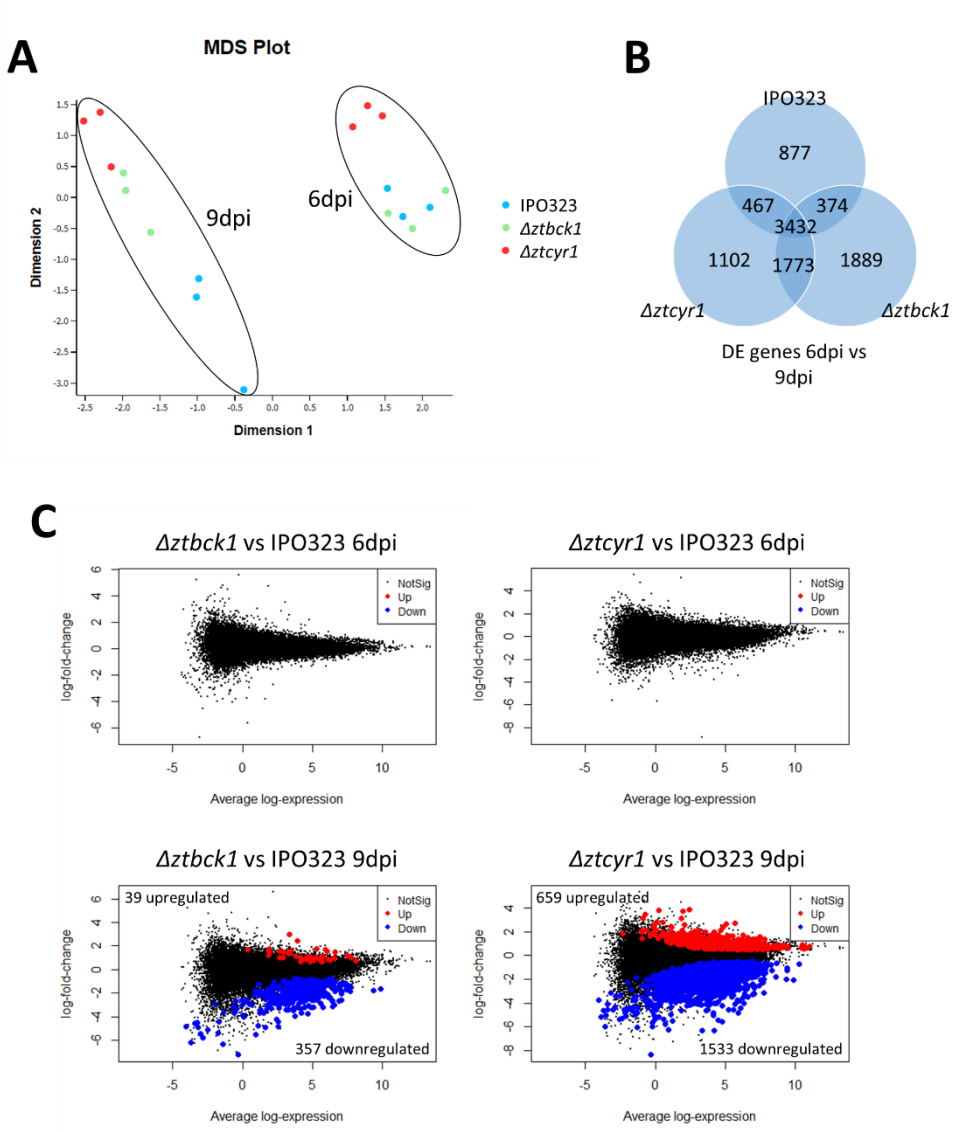


**Figure 5.15. Global wheat gene expression analysis during infection**
(A) Multidimensional scaling (MDS) plot on global wheat gene expression data. (B) Comparison of genes differentially expressed between 6 dpi and 9 dpi in leaves infected with IPO323, *Δztbck1* and *Δztcyr1.* (C) MA plots displaying differentially expressed genes between leaves infected with *Δztbck1* at 6 dpi (top left) and 9 dpi (bottom left) and *Δztcyr1* at 6 dpi (top right) and 9 dpi (bottom right), using leaves infected with IPO323 each time point as a reference. Number of differentially expressed genes are detailed.

between the samples can be summarised by the first dimension, which broadly segregates the samples by time point during infection at which they were taken (Fig. 5.15A). To investigate this further, the sets of genes that were DE between 6 and 9 dpi for each strain were compared, which identified 3,432 genes that were differentially regulated in the same direction in all strains (Fig. 5.15B). This suggests that gene expression in leaves infected by all strains showed highly similar responses to the sampling time point. However, samples did cluster depending on the inoculated strain, and this variation could be largely explained

by dimension two (Fig. 5.15A). More specifically, leaf samples infected with IPO323 and *Δztbck1* clustered separately from *Δztcyr1* at 6 dpi, before samples infected by IPO323 diverged further from *Δztcyr1* and *Δztbck1* at 9dpi (Fig. 5.15A).

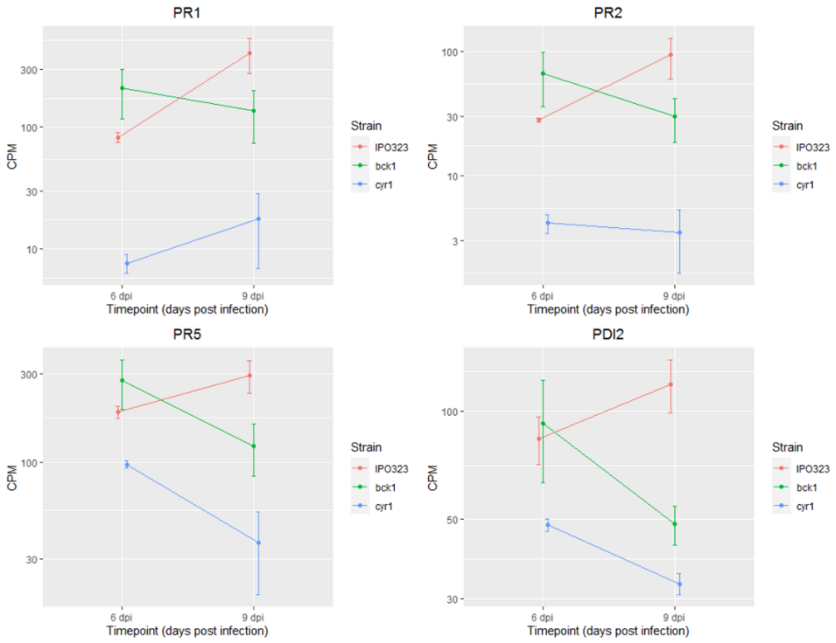


**Figure 5.16 Expression profiles of wheat defence genes**
The mean counts per million (CPM) of each gene across samples infected with each strain at 6 dpi and 9dpi is plotted, with error bars representing the standard error.

To investigate which genes were causing this variation in the wheat transcriptome profile depending on the inoculated strain, gene level differential expression analysis was implemented. Despite the apparent difference in global transcription between samples infected by *Δztcyr1* and IPO323 at 6 dpi from MDS analysis, no statistically significant DE genes were identified between any strains at this time point (Fig. 5.15C). However, a set of 396 DE genes were identified between *Δztbck1* and IPO323 infected samples at 9 dpi (Fig. 5.15C; Supplementary Table S2). Furthermore, 2192 DE genes were identified between *Δztcyr1* and IPO323 infected samples at 9dpi (Fig. 5.15C; Table S5.2).

Further analysis of these DE gene sets focused on wheat genes with predicted functions in defence responses against pathogens. The expression profiles of genes which have been characterised as responding to *Z. tritici* infection in a previous study (Ray et al., 2003) were investigated (Fig. 5.16). This included the pathogenesis-related (PR) proteins the PR1 protein *PR-1-4*

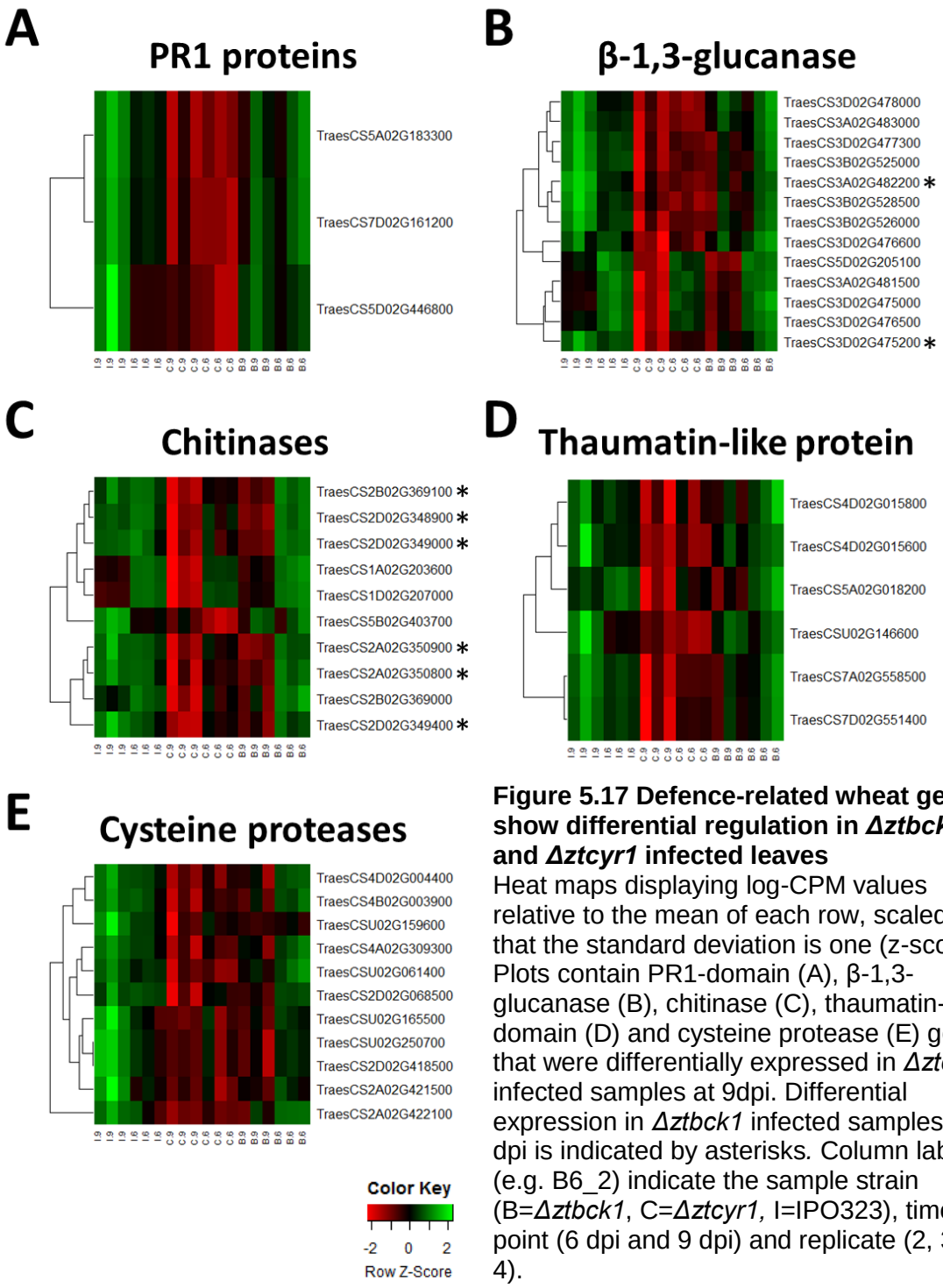


**Figure 5.17 Defence-related wheat genes show differential regulation in *Δztbck1* and *Δztcyr1* infected leaves**
Heat maps displaying log-CPM values relative to the mean of each row, scaled so that the standard deviation is one (z-score). Plots contain PR1-domain (A), β-1,3-glucanase (B), chitinase (C), thaumatin-like domain (D) and cysteine protease (E) genes that were differentially expressed in *Δztcyr1* infected samples at 9dpi. Differential expression in *Δztbck1* infected samples at 9 dpi is indicated by asterisks. Column labels (e.g. B6_2) indicate the sample strain (B=*Δztbck1*, C=*Δztcyr1,* I=IPO323), time point (6 dpi and 9 dpi) and replicate (2, 3 and 4).

(TraesCS7D02G161200), the beta-1,3-glucanase *PR2* (TraesCS7D02G551400) and the thaumatin-like protein PR5 (TraesCS7D02G551400), as well as the protein disulphide isomerase *PDI2* (TraesCS4B02G101800). All four of these genes were significantly downregulated in *Δztcyr1* at 9dpi. Although no further statistically significant differences were identified, these genes displayed similar expression profiles. The lowest expression value for these genes was consistently in *Δztcyr1* at both

time points. The highest expression of these genes at 6 dpi was in *Δztbck1*, which decreased by 9 dpi, at which point their expression had increased in IPO323 infected samples (Fig. 5.16). In addition to these genes, 2 other PR1 proteins, 12 other beta-1,3-glucanases (PR2), 10 chitinases (PR3) and 5 other thaumatin-like proteins (PR5) were found to be downregulated in *Δztcyr1* infected samples at 9 dpi (Fig. 5.17). A subset of these was also downregulated in *Δztbck1* infected samples at 9dpi (Fig. 5.17).

Other protein annotations that were highly represented in the downregulated genes in *Δztcyr1* were proteases, including Cys- (Fig. 5.17E), metallo- and subtilisin-like families, ubiquitination proteins and drug resistance ABC transporters (Table S5.2), all of which were also associated with the switch to necrotrophy in the wild type (Rudd et al 2015). Also highly represented in the DE genes within *Δztbck1* and *Δztcyr1* infected leaves at 9dpi were receptor-like kinases (RLKs), including many from the wall-associated, leucine-rich repeat, cysteine-rich and lectin kinase families (Table S5.2). These families have previously been found to be upregulated in wild type infected wheat leaves around the transition to necrotrophy (Rudd et al., 2015). A total of 223 RLK genes were downregulated in *Δztcyr1* at 9dpi, while 53 were downregulated in *Δztbck1* (Fig. 5.18A; Table S5.2). Furthermore, three LysM domain GPI-anchored proteins of the chitin elicitor binding protein (CEBiP), which have been characterised in chitin-induced defence responses to *Z. tritici* (W. S. Lee et al., 2014), were also downregulated at 9 dpi in *Δztcyr1* (Table S5.2). These findings strongly suggest that *Δztcyr1* is unable to induce the wheat defence response seen during wild type infection, despite continuing to grow in the host environment.

Another gene previously identified as specifically associated with the host defence response during the transition to necrotrophy is the MAP kinase *TaMPK3* (Rudd et al., 2008). *TaMPK3* was significantly downregulated between 6 and 9 dpi in leaves infected with all the strains (Fig. 5.18B). As this gene is known to be involved in responses to various abiotic stresses in wheat (Goyal et al., 2018; Zhan et al., 2017), this might suggest that all plants were under environmental stress at 6 dpi. This could have been the cause of the large proportion of shared variation in global gene expression observed between the time points in infections by all of the *Z. tritici* strains (Fig. 5.15B; Table S5.2).

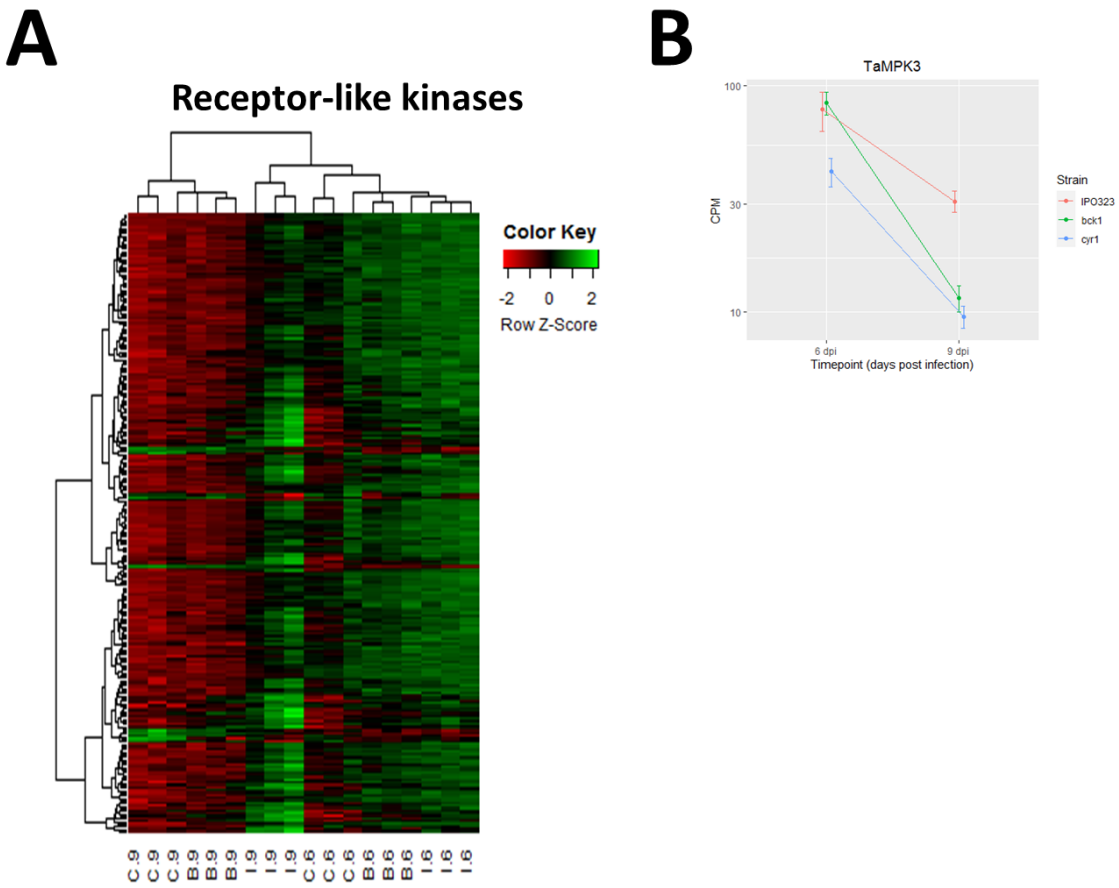


**Figure 5.18 Receptor-like kinase and *TaMPK3* gene expression is downregulated in *Δztbck1* and *Δztcyr1* at 9dpi**
(A) Expression profiles of receptor-like kinases that were differentially expressed in *Δztbck1* and *Δztcyr1* infected leaves at 9dpi. Heat map displaying log-CPM values relative to the mean of each row, scaled so that the standard deviation is one (z-score). Column labels (e.g. B6_2) indicate the sample strain (B=*Δztbck1*, C=*Δztcyr1,* I=IPO323), time point (6 dpi and 9 dpi) and replicate (2, 3 and 4). (B) Expression profile of *TaMPK3* (TraesCS4A02G106400) across samples, displaying mean counts per million across repeated samples from same treatment and error bars displaying standard error.

Moreover, downregulation of *TaMPK3* was not as dramatic in IPO323 infected samples (Fig. 5.18B), meaning it was identified as significantly downregulated in *Δztcyr1* infected leaves at 9 dpi. This is consistent with its involvement in the wild type *Z. tritici*-induced defence response at this stage (Rudd et al., 2008). A similar expression pattern, consisting of significant downregulation between 6 and 9 dpi in mutant infected leaves and either less dramatic downregulation, unchanged expression or even upregulation in IPO323 infected leaves, is seen for many of the previously mentioned RLK genes (Fig. 5.18A; Table S5.2). As expression of RLKs is known to respond to diverse abiotic stresses (Lehti-Shiu et al., 2009; Shumayla, Sharma, Kumar, et al., 2016; Shumayla, Sharma,

Pandey, et al., 2016), this supports the hypothesis that all wheat plants were under some environmental stress at 6 dpi.

With regard to the host transcriptional response to *Δztbck1*, many of the aforementioned defence-related genes were found amongst those downregulated between 6 and 9 dpi specifically in *Δztbck1* samples, and not in IPO323 or *Δztcyr1* infected leaves (Table S5.2). This suggests that the host defence response was induced in *Δztbck1* infected leaves at 6 dpi, and subsequently declined at 9 dpi. This is supported by the fact that many of these defence-related genes then become significantly downregulated in *Δztbck1* infected leaves compared to IPO323 infected samples at 9 dpi (Fig. 5.17; Table S5.2), as the wild type progresses towards the necrotrophic phase and induction of the hypersensitive host response. Along with the finding that *Δztbck1* fungal biomass does not increase between the time points, this suggests that *Δztbck1* colonisation is inhibited early on by the host defence response. This is likely enabled by the lack of secretion of effectors in *Δztbck1*, including LysM-domain proteins, which function to suppress the host defence response during early infection by the wild type. This defence response then starts to subside as less fungal penetration events occur.

## 5.4 Discussion

The cAMP-PKA and CWI pathways are emerging as crucial signalling cascades regulating the invasion of plants by fungal pathogens (Turrà et al., 2014). The present study identified elements of both of these pathways that were essential for *Z. tritici* pathogenicity on wheat using a forward genetic approach. Whole genome resequencing of avirulent T-DNA transformants identified disruptive mutations in *ZtBCK1*, a homolog of the yeast MAPKKK regulating Slt2 in the CWI pathway (Lee et al., 1992), and the adenylate cyclase gene *ZtCYR1*. Targeted deletion of these genes abolished pathogenicity of the fungus and led to similar *in vitro* phenotypes to those associated with disruption of putative downstream kinases (Mehrabi, Van Der Lee, et al., 2006; Mehrabi & Kema, 2006). RNA-sequencing was used to investigate the effect of *ZtBCK1* and *ZtCYR1* deletion on gene expression in both *Z. tritici* and wheat during infection, providing insight into the contribution of these genes to the regulation of host colonisation.

The hyphal growth rate of *Δztbck1* was found to be reduced during prolonged growth on water agar, similar to the previously characterised *Δmgslt2* mutant (Mehrabi et al 2006). This indicates that disruption of the CWI pathway may have a negative impact on *Z. tritici* polarised growth, through de-regulation of proteins involved in cell wall biosynthesis at the hyphal apex. However, despite causing defects in vegetative growth *in vitro*, deletion of *ZtBCK1* did not influence the ability of *Z. tritici* spores to germinate on the leaf surface or penetrate through stomata. Furthermore, no evidence was found for the growth of *Δztbck1* mutants beyond the symptomless phase, with no increase in fungal biomass detected after 6 dpi. These findings are consistent with the phenotypes identified in *Δmgslt2* mutants, which were unable to colonise the mesophyll to the same extent as the wild type after entering the substomatal cavities (Mehrabi, Van Der Lee, et al., 2006). These findings point towards the role of the CWI pathway in regulating adaptation to the host environment.

Transcriptome profiling revealed that *Δztbck1* was severely inhibited in the expression of predicted secreted proteins during infection. This included the LysM effectors Mg3LysM, Mg1LysM and MgXLysM, which are known to have partially redundant functions in the evasion and tolerance of the chitin-induced wheat defence response, and together are essential for *Z. tritici* virulence (Marshall et al., 2011; Tian et al., 2021). Furthermore, wheat expression analysis revealed the high expression of numerous defence-related genes in response to infection by *Δztbck1*, including many *bona fide* PR proteins. Analysis of *Δztbck1* gene expression at an earlier time point during infection is required to confirm that downregulation of the infection-related secretome is caused by an inability to respond to the host environment, rather than suppression under the stress of the host defence response. Together, these findings suggest that the CWI pathway is involved in regulation of virulence-associated secreted proteins in response to the host apoplast, and that this is required for suppression of the host immune response to enable mesophyll colonisation.

In *S. cerevisiae*, the CWI pathway is required for controlling cell wall homeostasis in response to stress caused by hydrolytic enzymes and cell wall perturbing agents, as well as heat, osmotic and pH stress (Garcia et al., 2009; Kamada et al., 1995; Reinoso-Martín et al., 2003). Here, *Δztbck1* mutants were

found to have increased sensitivity to beta-1,3-glucanase enzymes and the beta-1,3-glucan synthesis-inhibiting echinocandin fungicide caspofungin, but not to chitin disruption by calcofluor white. This corroborates previous findings that deletion of *MgSLT2* increases sensitivity to glucanase by not chitinase enzymes (Mehrabi, Van Der Lee, et al., 2006). Furthermore, genes involved in biosynthesis of beta-1,3-glucan and alpha-1,3-glucan were found to be downregulated in *Δztbck1* during infection, while chitin synthases were upregulated in this strain. These findings suggest that the *Z. tritici* CWI signalling specifically regulates responses to glucan perturbation, while responses to chitin disruption are regulated by a separate pathway. Increased chitin synthase expression in *Δztbck1* could occur in response to the cell wall perturbation caused by the enhanced host defence response to this strain, exacerbated in the absence of the protective influence of LysM effectors against host chitinases (Marshall et al., 2011). Both the HOG1 MAPK and calcineurin pathways have been shown to contribute to chitin synthase regulation and the cell wall stress response in *C. albicans* and *A. fumigatus* (Bruder Nascimento et al., 2016; Fortwendel et al., 2010; Munro et al., 2007), while their contribution to these processes requires further investigation in *Z. tritici*.

The secretion system is known to be crucial for fungal cell wall homeostasis, through delivery of cell wall biosynthesis and remodelling enzymes to the cell surface, and the virulence of plant and human fungal pathogens, through secretion of effectors and hydrolytic enzymes (Heimel et al., 2013; Malavazi et al., 2014). This is exemplified in the importance of the unfolded protein response (UPR), which regulates endoplasmic reticulum (ER) homeostasis, in the response to cell wall stress and virulence in *A. fumigatus* (Richie et al., 2009). Furthermore, the CWI pathway regulates components of the UPR in *S. cerevisiae* (Scrimale et al., 2009), as well as in *A. fumigatus* under cell wall stress (Rocha et al., 2015). If there is similar regulation of the UPR by the CWI pathway in *Z. tritici*, this could lead to increased ER stress and disrupted protein secretion in *Δztbck1* mutants. However, this may not explain the reduced expression of secreted proteins in this strain. In fact, induction of the UPR is known to reduce expression of secreted proteins in *A. niger* and *T. reesei* (Guillemette et al., 2007; Pakula et al., 2003), suggesting UPR disruption in *Δztbck1* would increase secretome gene transcription.

Instead, the CWI pathway in *Z. tritici* could have adapted to co-regulate secreted proteins involved in cell wall remodelling and virulence-related functions, explaining the downregulation of these genes in *Δztbck1* during infection. These findings raise the possibility that *ZtBCK1* regulates secreted protein expression during infection following cell wall perturbation by host beta-1,3-glucanases in the apoplast. Alternatively, this could occur upon recognition of other environmental stimuli in the apoplast, such as the acidic pH, response to which is known to be controlled by the CWI pathway in yeast (Claret et al., 2005). The transcriptional response of wild type and *Δztbck1* cells to low concentrations of beta-1,3-glucanase, as well as other abiotic stresses, should be investigated. Comparison of these transcriptional responses with those during the early host colonisation would test the hypothesis that these stimuli induce secretome gene expression *in planta*, and that the cell wall stress response and virulence-factor secretion are co-regulated.

Recently, it was found that expression of a set of virulence-related genes was co-regulated with the morphological switch to hyphal growth under carbon deprivation in *Z. tritici* (Francisco et al., 2019). Extending the RNA sequencing experiment in the present study to include a comparison with starvation–induced hyphal growth would determine whether the downregulation of secreted protein expression in *Δztbck1* is specific to the host environment, and if CWI-dependant virulence gene expression is independent of that co-regulated with the starvation response. Preliminary comparison of the “mycelial growth” genes identified by Francisco *et al* (2019) with those DE in *Δztbck1* at 6dpi found that 27 of the 225 secreted proteins downregulated in this mutant were common between the gene sets. This did not include many virulence-associated genes repressed in *Δztbck1*, including proteases, PCWDEs and LysM effectors. This suggests that, while there is overlap with hyphal growth-associated genes, there are many more secreted proteins putatively regulated by the CWI pathway in *Z. tritici*.

Furthermore, other elements of the CWI pathway in *Z. tritici* require investigation, such as the sensors involved in recognition of cell wall perturbation at the cell surface. CWI monitoring in *S. cerevisiae* requires the action of five well characterised surface mechanosensors, Wsc1-3, Mid2 and Mtl1 (Levin, 2011). Filamentous fungal homologs of Wsc and Mid2 have been

characterised in the *Aspergilli*, and demonstrated to function in response to cell wall and acidic pH stress (Dichtl et al., 2012; Futagami et al., 2011; Futagami & Goto, 2012). Preliminary investigation found that one homolog with similar domain structure to Wsc CWI sensors in *Aspergilli* was present in the *Z. tritici* genome (ZtritIPO323_04g03354/Mycgr3G106153), while no homolog of MidA or Mid2-like proteins from *A. fumigatus* and *A. nidulans*, respectively, was identified. Investigation is required into whether this putative Wsc mechanosensor is involved in *Z. tritici* CWI signalling in response to stresses faced in the host environment.

Similar to disruption of *ZtBCK1, ZtCYR1* deletion did not inhibit epiphytic growth and stomatal penetration by *Z. tritici*. However, unlike *Δztbck1* mutants, whose invasive growth appeared to be suppressed by the host during the early symptomless phase, *Δztcyr1* strains continued to grow late into the symptomless phase. This was evident from the continued accumulation of fungal biomass by *Δztcyr1* at this stage, albeit slower than the wild type. These findings are consistent with phenotypes identified upon deletion of catalytic and regulatory subunits of PKA, which were able to extensively colonise the mesophyll tissue (Mehrabi & Kema, 2006). This suggests that the function of *ZtCYR1* in *Z. tritici* infection is distinct from the role of cAMP-PKA signalling in host penetration by appressorium-forming *M. oryzae* and *Colletotrichum sp.*(Choi & Dean, 1997; Yamauchi et al., 2004), and even fungal phytopathogens which don't develop true appressoria such as *F. graminearum* (Bormann et al., 2014).

While the *Δztcyr1* mutants have completely abolished virulence, previously characterised deletion strains in the *Z. tritici* PKA subunit *MgTPK2* are still able to cause delayed necrosis, but do not develop pycnidia (Mehrabi & Kema, 2006). The discrepancy in phenotypes of these mutants could be explained by the presence of multiple PKA catalytic subunits in *Z. tritici*, as has been identified in other filamentous ascomycetes, including *M. oryzae, F. graminearum* and *Aspergillus fumigatus* (Fuller et al., 2011; Hu et al., 2014; Li et al., 2017). In these species, the PKA catalytic subunits have both redundant and divergent functions in development and virulence. *CPKA* in *M. oryzae* is required for appressorial turgor generation and virulence (Xu et al., 1997), while *CPK2* was dispensable to virulence (Li et al., 2017). However, the *cpkacpk1*

double mutant displayed an enhanced phenotype of inability to form appressoria (Li et al., 2017). Similarly, *CPK1* deletion in *F. graminearum* led to reduced virulence, while the *cpk1cpk2* double mutant and adenylate cyclase deletion strain were non-pathogenic (Hu et al., 2014). The *Z. tritici* genome contains two PKA catalytic genes; the previously characterised ZtritIPO323_04g08276 (TPK2; Mehrabi & Kema, 2006) and ZtritIPO323_04g08063 (previously *MgTPK1*), which are proposed here to be renamed *ZtCPK1* and *ZtCPK2* in line with their homologs in *F. graminearum* and *M. oryzae* (Fig. 5.19). The remaining ability of *Z. tritici* to cause necrosis following deletion of *MgTPK2*/*ZtCPK1* is therefore likely to be enabled by the overlapping function of *ZtCPK2*. This hypothesis should be tested through generation of a *Δztcpk1Δztcpk2* double mutant.

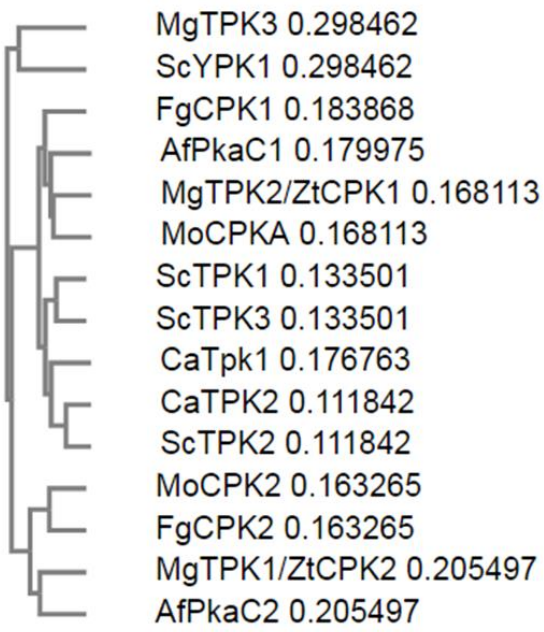


**Figure 5.19 Phylogenetic tree of protein kinase A catalytic subunit gene sequences**
This includes *Z. tritici* genes MgTPK1/ZtCPK2 (ZtritIPO323_04g08063), MgTPK2/ZtCPK1 (ZtritIPO323_04g08276) and MgTPK3 (ZtritIPO323_04g10427), *S. cerevisiae* genes ScTPK1 (YJL164C), ScTPK2 (YPL203W) and ScTPK3 (YKL166C), *M. oryzae* genes *MoCPKA* (MGG_06368) and *MoCPK2* (MGG_02832), *C. albicans* genes *CaTPK1* (C2_07210C_A) and *CaTPK2* (C1_10220C_A), *A. fumigatus* genes *AfPKAC1* (Afu2g12200) and *AfPKAC2* (Afu5g08570), *F. graminearum* genes *FgCPK1 (*FG07251) and *FgCPK2* (FG08729). Previously annotated as a PKA catalytic subunit homolog, MgTPK3 shows closer homology to *S. cerevisiae* gene *ScYPK1* (YKL126W).

Slow hyphal growth of *Δztcyr1* suggested that cAMP signalling regulates vegetative growth rate in *Z. tritici*, which has been identified as a common phenotype in adenylate cyclase mutants of filamentous fungi (Bormann et al., 2014; Choi & Dean, 1997). Interestingly, other *in vitro* phenotypes observed in *Δztcyr1* strains, such as sensitivity to high osmolarity and defective melanisation, were more similar to those previously observed in *Z. tritici* mutants lacking the PKA regulatory subunit (MgBCY1), than the catalytic subunit MgTPK2 (Mehrabi & Kema, 2006). This is unexpected, as BCY1 inhibits

the activity of PKA catalytic subunits, while CYR1 activates this pathway. However, BCY1 is known to control the nuclear localisation of PKA in *S. cerevisiae* and *C. albicans* (Cassola et al., 2004; Griffioen et al., 2001). Moreover, deletion of the *BCY1* homolog in *M. oryzae* led to similar defects in appressorium formation to PKA catalytic subunit and adenylate cyclase mutants (Selvaraj, Tham, et al., 2017). Combined, these results suggest that *MgBCY1* has additional roles in regulating the PKA pathway beyond its inhibitory effect, which are required for proper PKA function.

The *Δztcyr1* strains were also found to display increased sensitivity to caspofungin. This is contrary to findings in *S. cerevisiae*, in which PKA signalling is inhibited during cell wall stress, and even negatively regulates some aspects of the cell wall stress response (García et al., 2017, 2019). However, positive regulation of the cell wall stress response through crosstalk between the CWI and PKA pathways was identified in *Cryptococcus neoformans* (Donlin et al., 2014). Furthermore, PKA has been shown to facilitate the response to cell wall stress in *A. fumigatus*, through its involvement in carbohydrate mobilisation in conjunction with the high osmolarity glycerol (HOG) pathway (de Assis et al., 2018; Shwab et al., 2017). This interaction with HOG MAPKs was also found to be involved in cell wall remodelling in response to osmotic stress (de Assis et al., 2018). This provides a potential mechanism by which PKA signalling may contribute to the response to cell wall and osmotic stress in *Z. tritici*.

Interestingly, the C5 strain did not show consistent *in vitro* phenotypes to *Δztcyr1*, and also retained the ability to cause some chlorosis by 21 dpi, which was not observed until much later in the deletion strain. This suggests that the SNP at a putative nucleotide binding site has not abolished the function of *ZtCYR1*, but has potentially led to a reduction in its activity. This may cause a dramatic reduction in cytoplasmic cAMP that could inhibit PKA activity in a similar manner to deletion of individual catalytic PKA subunits, which is known to cause an intermediate phenotype in filamentous fungi (Hu et al., 2014; Li et al., 2017). Analysis of the cAMP content of C5 and *Δztcyr1* strains compared to the wild type should be carried out to investigate this. Furthermore, complementation of C5 with the wild type *ZtCYR1* allele is required to confirm that the identified SNP is the cause of avirulence in this strain.

Along with the previously characterised role of PKA in *Z. tritici* asexual development (Mehrabi & Kema, 2006), results presented here suggest that cAMP signalling is required for the induction of necrosis during infection. Transcriptome analysis found that gene expression in *Δztcyr1* was similar to IPO323 during the symptomless phase at 6 dpi, but diverged as infection moved towards the transition to necrotrophy. This divergence in expression was particularly noticeable in predicted effector genes, including many which display peak expression around the necrotrophic switch (Rudd et al., 2015). Furthermore, analysis of wheat gene expression revealed that *Δztcyr1* infected leaves show widespread downregulation of defence-related genes compared to wild type infected leaves at 9 dpi. This strongly suggests that *Δztcyr1* is unable to induce the immune response required for the onset of necrosis. Those effector genes which are strongly downregulated in *Δztcyr1* at 9 dpi may therefore be involved in inducing the host hypersensitive response, and warrant further functional characterisation.

Similar functions of the cAMP-PKA pathway in controlling invasive growth have been identified in *M. oryzae* (Li et al., 2017). Authors demonstrated that *ΔcpkaΔcpk1* double mutants were unable to cause necrosis even when injected into the rice leaf, bypassing the defect in appressorium formation. However, the mechanisms by which PKA regulates invasive growth in *M. oryzae* and *Z. tritici* remain elusive. One possible mechanism is through interaction between the PKA and Fus3 pathways (aka Kss1/Pmk1), which has been previously demonstrated in *U. maydis* and *S. cerevisiae* (Kaffarnik et al., 2003; Mösch et al., 1999). Pmk1 is known to be required for invasive growth in *M. oryzae*, by regulating expression of effectors which suppress the host defence response and controlling cell-to-cell movement (Xu and Harmer 1996; Sakulkoo et al 2018). Furthermore, a suppressor mutant in the *Δrpka* (PKA regulatory subunit) background displayed recovery of appressorium penetration, but remained defective in invasive growth beyond the first cell. This suppressor strain was found to induce ROS and PR protein defence responses after penetration (Selvaraj, Tham, et al., 2017). This provides evidence that PKA is involved in suppressing host immune responses as well as Pmk1 (Sakulkoo et al., 2018), and points to their potential interaction in this function.

However, current understanding of the interaction between PKA and Pmk1 in *M. oryzae* is unclear, with conflicting evidence of activation (Li et al., 2017) and repression (Selvaraj, Shen, et al., 2017) of Pmk1 during vegetative growth in *ΔcpkaΔcpk1* mutants from two separate studies. Furthermore, although MgFus3 is known to be required for stomatal penetration in *Z. tritici* (Cousin et al., 2006), its potential roll in invasive growth and the transition to necrotrophy has not been investigated. This could be assessed by the infection of *Δmgfus3* strains onto wounded wheat leaves, similar to early experiments on *M. oryzae Δpmk1* mutants (Xu & Hamer, 1996). Moreover, the phosphorylation status of MgFUS3 in wild type and *Δztcyr1* should be investigated. Equally, the cAMP-PKA pathway may control invasive growth in these pathogens through regulation of distinct transcription factors yet to be described.

Expansion of the RNA sequencing experiment presented here is required to investigate the differential regulation of virulence-associated gene expression in *Δztcyr1* further. Analysis of *Δztcyr1* expression during the early symptomless and late necrotrophic phases would test the hypothesis that gene expression in *Δztcyr1* diverges from the wild type across the course of infection. It would also be interesting to investigate whether growth of *Δztcyr1* continues during later infection despite not causing necrosis. Rapid growth in the wild type at this stage is assumed to be enabled by nutrients released from necrotic host tissues (Keon et al., 2007). It is known that avirulent *Z. tritici* strains are able to survive and contribute to sexual reproduction, even when a successful host defence response is induced (Kema et al., 2018). In this study, we observed low expression of many wheat defence-related genes at both time points during infection by *Δztcyr1,* suggesting that suppression of host immunity by this mutant is effective. Furthermore, the upregulated expression of secreted proteases compared to the wild type at 9 dpi suggests that *Δztcyr1* may be diverging in its nutrient acquisition strategy. The appearance of chlorosis on *Δztcyr1* infected leaves more than four weeks after inoculation also suggests that this strain continues to grow in the mesophyll for a prolonged period without inducing necrosis, and potentially causes nutrient stress to the host. This raises the possibility that *Δztcyr1* is colonising the leaf somewhat like an endophyte.

## 5.5 Conclusions

The findings presented here further our understanding of how CWI and cAMP signalling contribute to *Z. tritici* pathogenicity. The CWI pathway appears to regulate the transcriptional response to the host environment, which goes beyond genes involved in cell wall remodelling to activate expression of effector proteins. This includes virulence factors known to be required for suppression of the chitin-triggered host immune response. This points towards the possible co-regulation of the cell wall stress response with virulence-related genes, which could occur in response to host environmental factors such as hydrolytic enzymes or acidic pH. Furthermore, this study implicates the PKA pathway in controlling the switch to necrotrophic growth in addition to its previously characterised function in asexual development, and suggests that this requires the combined activity of MgTPK2 and an as yet uncharacterised catalytic PKA subunit. The absence of *ZtCYR1* influences the expression of putative effectors and genes involved in accessing nutrients around the transition to necrotrophy, which may disrupt the induction of host necrosis. Further study is required into the signals which activate both pathways during infection, as well as the regulatory components that detect these signals. Investigation of their downstream targets should also be carried out using phosphoproteomics, in order to further understand their contribution to *Z. tritici* infection.

## 5.6 Supplementary information

**Figure S5.1. Strains C5 and L2 contain T-DNA insertions at targeted loci**
Integrative Genomics Viewer screenshots of strains (A) C5 and (B) L2 whole genome resequencing reads aligned at the *ZtCUT5* and *ZtL2* loci, respectively, in the *Z. tritici* IPO323 genome. Absence of reads aligned to coding sequences of genes and reads at the 3' end of the left flank (LF) and 5' end of the right flank (RF) aligning to the *BAR*$^{R}$ cassette. Reads are clustered vertically by the chromosome to which their pair is aligned.

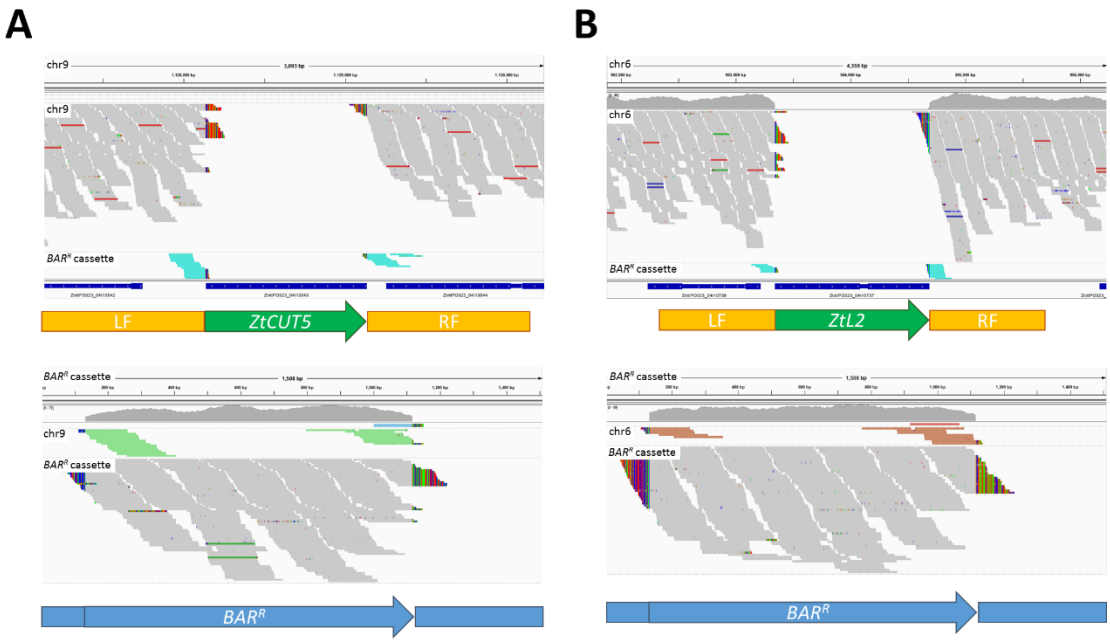

# Chapter 6
# Omics-based investigations into a spontaneous mutant of *Z. tritici* with a reduced virulence phenotype

## 6.1 Introduction

The ability to culture pathogenic microorganisms in the laboratory has revolutionised our ability to understand their biology, allowing detailed microscopic investigation of their development during infection, controlled assessment of virulence and genetic manipulation to analyse the host-pathogen interaction at the molecular level. However, removing microorganisms from their adapted life cycle inevitably exposes them to different conditions than they would experience in their natural environment. This often includes constant access to easily metabolised nutrients, different temperature and light regimes and the lack of biotic interactions. This has the potential to have impacts at the physiological, metabolic, epigenetic and genetic levels, which may influence our ability to make inferences about their biology. Crucially with pathogens, *in vitro* culturing removes the necessity to complete an infection cycle to reproduce. This in turn removes the selection pressure on traits which influence pathogenicity and virulence, such as infection related developmental transitions, adaptation to the host environment and interaction with the host immune response.

*In vitro* subculture can therefore lead to a reduction in virulence over time in the laboratory, which has been observed in many pathogenic fungi and bacteria (Almagro Armenteros et al., 2017; Fux et al., 2005; Loesch et al., 2010; Songe et al., 2014), and has even been utilised to create attenuated strains for immunization (Behr, 2002). This phenomenon is especially well studied in bacterial pathogens, which have been demonstrated to lose phenotypes associated with virulence alongside increases in growth rate across *in vitro* generations (Fux et al., 2005). This has often been associated with the loss of flagella and biofilm production, both of which are costly to growth rate *in vitro* (Cooper et al., 2003; Head & Yu, 2004). Laboratory and clinical strains of *Candida sp.* were also found to show variation in biofilm formation, which is known to be an important virulence trait in these fungal pathogens (Alnuaimi et al., 2013). Differences between *in vitro* and *in vivo* growth phenotypes of pathogens lead to difficulties using laboratory strains and conditions to study morphologies that are crucial to the host-pathogen interaction, which often show co-regulation with other virulence determinants (Gallego-Hernandez et al., 2020; Strateva & Mitov, 2011). For example, laboratory characterisation of the

virulence-enhancing titan cell phenotype of the human fungal pathogen *Cryptococcus neoformans* was limited until recent development of protocols for robust induction of this morphology *in vitro* (Zhou & Ballou, 2018).

Investigations into cases of reduced pathogen virulence resulting from *in vitro* subculturing have revealed multiple mechanisms by which this can occur. Accumulation of mutations across many generations in isolation from host-induced selection pressures can have a negative influence on virulence (Klockgether et al., 2010). Genetic variations causing *in vitro* deterioration of virulence in bacterial pathogens often involve loss of genetic elements that commonly undergo horizontal gene transfer, such as the pathogenicity islands of *Pseudomonas aeruginosa,* which have been lost in the laboratory reference strain PAO1 (Head & Yu, 2004). Similarly, many fungal plant pathogens contain conditionally dispensable chromosomes, which harbour genes involved in virulence and host specificity (Hatta et al., 2002; Ma et al., 2010). These can be lost during meiosis, but also during vegetative propagation *in vitro* (Plaumann et al., 2018; Vlaardingerbroek et al., 2016). These mechanisms of virulence degeneration are potentially exacerbated by the absence of a sexual cycle or horizontal transfer between strains through anastomosis in laboratory conditions (Ma et al., 2010), which may help to compensate for accumulation of deleterious mutations and chromosome losses. Furthermore, abiotic conditions *in vitro* can also induce epigenetic changes which can be maintained and influence gene expression when the pathogen next encounters a host. This was demonstrated during long term sub-culturing of *Botrytis cinerea*, in which DNA methylation markers were shown to correlate with loss of virulence over generations, before subsequent recovery after completion of an infection cycle (Breen et al., 2016).

Furthermore, the presence of mycoviruses in laboratory strains of fungi is being rapidly elucidated through mining of the abundant sequence data being generated. A recent study surveying unmapped reads from fungal transcriptome datasets identified many novel viral species (Gilbert et al., 2019), while *de novo* assembly of RNA sequencing data from collections of five plant pathogens identified 66 new mycoviruses (Marzano et al., 2016). Some mycoviruses from plant pathogenic fungi have been found to attenuate the virulence of their hosts (Castro et al., 2003; Chu et al., 2002; Hao et al., 2018; Zhong et al., 2016),

leading to their proposed use as a novel biocontrol agent (Ghabrial et al., 2015). The potential for clinical use of mycoviruses to combat human pathogenic fungi has also been discussed (Van De Sande & Vonk, 2019). However, many mycovirus infections remain symptomless, while some have been characterised as having a beneficial impact on host fitness by increasing virulence and producing antifungal compounds to kill competing microorganisms (Allen et al., 2013; Muñoz-Adalia et al., 2016). Although infection by many mycoviruses is cryptic, their impact on host phenotype may change conditionally with alteration of viral and host genotype, as well as under different growth conditions and stresses (Pearson et al., 2009).

*Z. tritici* has an extremely dynamic and unstable genome (Möller et al., 2018). Of the 21 chromosomes identified in the reference isolate IPO323, eight are known to show presence/absence variation in field strains (Badet et al., 2020). Frequent loss and rearrangement of these accessory chromosomes (ACs) is well characterised during meiosis (Fouché et al., 2018; Habig et al., 2018). Although ACs are dispensable for *Z. tritici* growth and survival (Goodwin et al., 2011), they were recently shown to make small contributions to quantitative virulence in a manner dependant on host cultivar and background *Z. tritici* strain (Fouché et al., 2018; Habig et al., 2017; Möller et al., 2018). In some cases, AC losses were associated with virulence increases, suggesting that they harbour genes encoding avirulence factors that influence host specificity (Möller et al., 2018).

Chromosomal polymorphisms were also reported recently during mitotic reproduction of *Z. tritici* in laboratory strains (Möller et al., 2018). *Z. tritici* reproduces asexually in culture on rich media through the production of elongated multicellular spores, termed blastospores (Francisco et al., 2019), generally consisting of 2-8 cells fused end-to-end (Steinberg, 2015). AC losses will inevitably accumulate during routine asexual propagation without sexual reproduction. Furthermore, chromosomal rearrangements were found to increase under heat stress, and involved core chromosomes as well as ACs (Möller et al., 2018). These findings suggest that *Z. tritici* genome instability could cause significant complications during research in the laboratory.

Additionally, one mycovirus has been identified in laboratory strains of *Z. tritici* (Gilbert et al., 2019; Kema et al., 2008). An early *Z. tritici* gene expression study by Kema et al. (2008) identified RNA sequences with high similarity to *Fusarium graminearum* virus 1 (FgV1), which is known to reduce the virulence and mycelial growth rate of its host (Chu et al., 2002). This mycovirus displayed variation in abundance depending on *Z. tritici in vitro* growth conditions, which was particularly high during hyphal growth under nitrogen starvation, and was predicted to show high abundance during infection (Kema et al., 2008). The same virus was subsequently identified within RNA sequencing data from two different laboratories (Kellner et al., 2014; Rudd et al., 2015), being designated *Zymoseptoria tritici* fusarivirus 1 (ZtFV1) and classified as part of the newly proposed *Fusariviridae* family (Gilbert et al., 2019). However, the influence of ZtFV1 on *Z. tritici* morphology and virulence is yet to be determined.

A variant of the *Z. tritici* reference strain IPO323, which is characterised by reduced virulence and a tendency to produce shorter blastospores when cultured on rich media, has been identified in laboratory stocks at the University of Exeter. Observations of similar phenotypes arising in IPO323 strains have been reported by multiple other laboratories (Fraaije pers. comm.; Kanyuka pers. comm.), prompting the present investigation into the underlying causes of this phenotype. Detailed *in vitro* analysis was carried out to characterise the development and infection phenotype of this strain, identifying defects in filamentous growth and response to oxidative stress. Whole genome resequencing was utilised to uncover two large deletions in the core chromosomes, while RNA sequencing revealed dramatic changes in gene expression and mycovirus abundance. The findings provide clues as to the underlying causes of the phenotype and novel insights into the regulation of *Z. tritici* development and virulence.

## 6.2 Materials and Methods

### 6.2.1 Cell measurements

*Z. tritici* blastospores were harvested after 5 days growth on YPD and stained with 10 µg/ml calcofluor white stain (Sigma-Aldrich, UK) to visualise the cell walls and septa within the spores. Images were taken using a Zeiss Axiovert

200M with a Q-Imaging MicroPublisher 3.3 RTV camera mounted. The length of each internal cell was measured using ImageJ, before the total spore length, the mean of the cell lengths within each spore and the number of cells in each spore were calculated.

### 6.2.2 Infection passage

Wheat leaves (cultivar Riband) were inoculated with *Z. tritici* blastospores at a concentration of $10^7$ spores/ml and infected leaves collected at 21 days post infection (dpi). Infected leaves were stored in a humidity chamber overnight to induce pycnidia to exude pycnidiospores, which were harvested by vortexing the leaves in 2 ml of sterile water and filtering through a 100 µm cell strainer. Pycnidiospore suspensions, along with blastospore suspensions from YPD agar cultures, were diluted to a concentration of $10^6$ spores/ml and inoculated onto wheat leaves. Infection symptoms were evaluated at 21 dpi, with leaves scanned in order to make measurements of pycnidia density. The germination efficiency of these blastospore and pycnidiospore suspensions was also determined on water agar (Chapter 2.7). Pycnidiospores were also inoculated onto YPD agar plates and grown for 5 days, resulting in subcultured pycnidiospores. Cell measurements of blastospores, pycnidiospores and subcultured pycnidiospore were taken as described above. The experiment was repeated three times, with 100 of each spore type measured for each repeat. All YPD cultures were grown for 5 days at 19$^o$C under darkness.

### 6.2.3 RNA sequencing

Total RNA was extracted from *Z. tritici in vitro* cultures using the RNeasy Plant Mini Kit (Qiagen), following the supplier's instructions for "Purification of Total RNA from Yeast". *Z. tritici* blastospores were harvested from YPD agar plates after 5 days growth and suspended in 600 µl of Buffer RLT containing 1% 14.3M β-Mercaptoethanol in a 1.5 ml screw-capped tube, before 600 µl of glass beads were added. Cell lysis was carried out using a FastPrep-24™ Classic Instrument (MP Biomedicals). Samples were agitated for four runs of 20 sec at 6.5 m/s, with samples placed on ice to cool for 1 min between each run. After the glass beads and cell debris were allowed to settle, 350 µl of lysate was pipetted into a new 1.5 Eppendorf and centrifuged at 20,000 x G for 2 min. The

supernatant was transferred to a new microcentrifuge tube and an equal volume of 70% ethanol was added and mixed with clarified lysate by pipetting. The sample was then transferred to an RNeasy spin column for purification. After identification of DNA contamination using a Qubit™ 3.0 Fluorometer (Thermo Fisher Scientific) with the Qubit™ dsDNA BR Assay Kit (Thermo Fisher Scientific), the RNA samples were subjected to DNA digestion in solution using an RNase-Free DNase Set (Qiagen) before purification with the RNeasy columns following the "RNA Cleanup" protocol. The concentration of extracted RNA was determined using a Qubit™ 3.0 Fluorometer with the Qubit™ RNA BR Assay Kit (Fisher Scientific, UK). RNA purity was assessed using a NanoDrop 1000 (Fisher Scientific, UK) and RNA quality was determined by denaturing gel electrophoresis (Chapter 2.4.5).

Four replicates of this experiment were carried out. Library preparation and RNA sequencing was carried out by GENEWIZ (Takeley, UK). The mRNA libraries were prepared using the NEBNext Ultra RNA Library Preparation Kit following the manufacturer's protocol, and sequenced as paired-ends using an Illumina HiSeq platform at 2x150bp. The resulting raw reads will be available in the NCBI Short Read Archive repository upon publication of these results.

### 6.2.4 RNA sequencing alignments and differential expression analysis

The *Z. tritici* IPO323 reference genome was indexed using the recent annotation from Rothamsted Research to identify gene models (King et al., 2017). Reads were trimmed to remove sequencing adapters and low quality bases using fastp (Chen et al., 2018), using the parameters '--cut_tail --cut_tail_mean_quality=20 --detect_adapter_for_pe --length_required=75'. Resulting reads were aligned to the genome and gene counts calculated with STAR (Dobin et al., 2013), using the default parameters and set to quant mode ('--quantMode GeneCounts'). Gene counts were normalised and differential expression analysis was carried out using DESeq2 (Love et al., 2014). Clustering of samples based on global expression data was assessed by principal component analysis using the *plotPCA* function. This was done using count data transformed with the *rlog* function, which accounts for sequencing depth and differences in variance between genes due to expression level (Love

et al., 2014). Sets of differentially expressed (DE) genes between strains were determined using the *results* function. Wald test *p*-values were adjusted for multiple testing using the Benjamin–Hochberg (BH) correction method. DE genes were determined as having $p_{adj} < 0.01$ and displaying a $\log_2$ fold change > 0.58 (equivalent to 1.5-fold change threshold) between the strains, following recommendations for experiments with low replicate number (Schurch et al., 2016).

Plots displaying expression of individual genes across samples were generated using normalised counts extracted using the *plotCounts* function in DESeq2. Kyoto Encyclopedia of Genes and Genomes (KEGG) K number gene annotations were identified using BlastKOALA (Kanehisa et al., 2016) on protein sequences predicted by the Rothamsted Research genome annotation. The resulting annotation was used to generate *Z. tritici* KEGG pathway maps, integrating data from DE gene sets using KEGG Mapper (Kanehisa & Sato, 2020). Gene Ontology (GO) terms were identified for all predicted genes using the OmicsBox (v.1.2.4) program, using Blastx searches against all fungal sequences in the non-redundant protein sequences (nr_v5) and protein domain prediction using InterProScan, using the default parameters. Functional enrichment analysis was carried out using topGo (version 2.42.0) in R using the Fisher's exact test (FDR<0.01 following correction of p-values with the BH method).

## 6.3 Results

### 6.3.1 Spontaneous IPO323 variant displays reduced virulence and short blastospores

Aliquots were identified in frozen stocks of *Z. tritici* IPO323 which showed reduced virulence on wheat plants (Fig. 6.1A). Initial microscopic observation of these stocks found the blastospores to be much shorter compared to aliquots of IPO323 displaying a wild type level of virulence (Fig. 6.1B), leading to the designation of this strain as IPO323_SSV (Small Spore Variant). Similar to the wild type, IPO323_SSV was able to cause necrotic lesions and develop mature pycnidia in host stomata, which produced pycnidiospores after exposure to high humidity (Fig. 6.1A). However, IPO323_SSV displayed reduced symptom

development compared to the wild type after 21 days of infection, with reductions in the area of the leaf displaying necrosis and the number of pycnidia observed (Fig. 6.1A). IPO323_SSV was therefore thought to be a naturally occurring mutant which may have arisen during subculturing of IPO323.

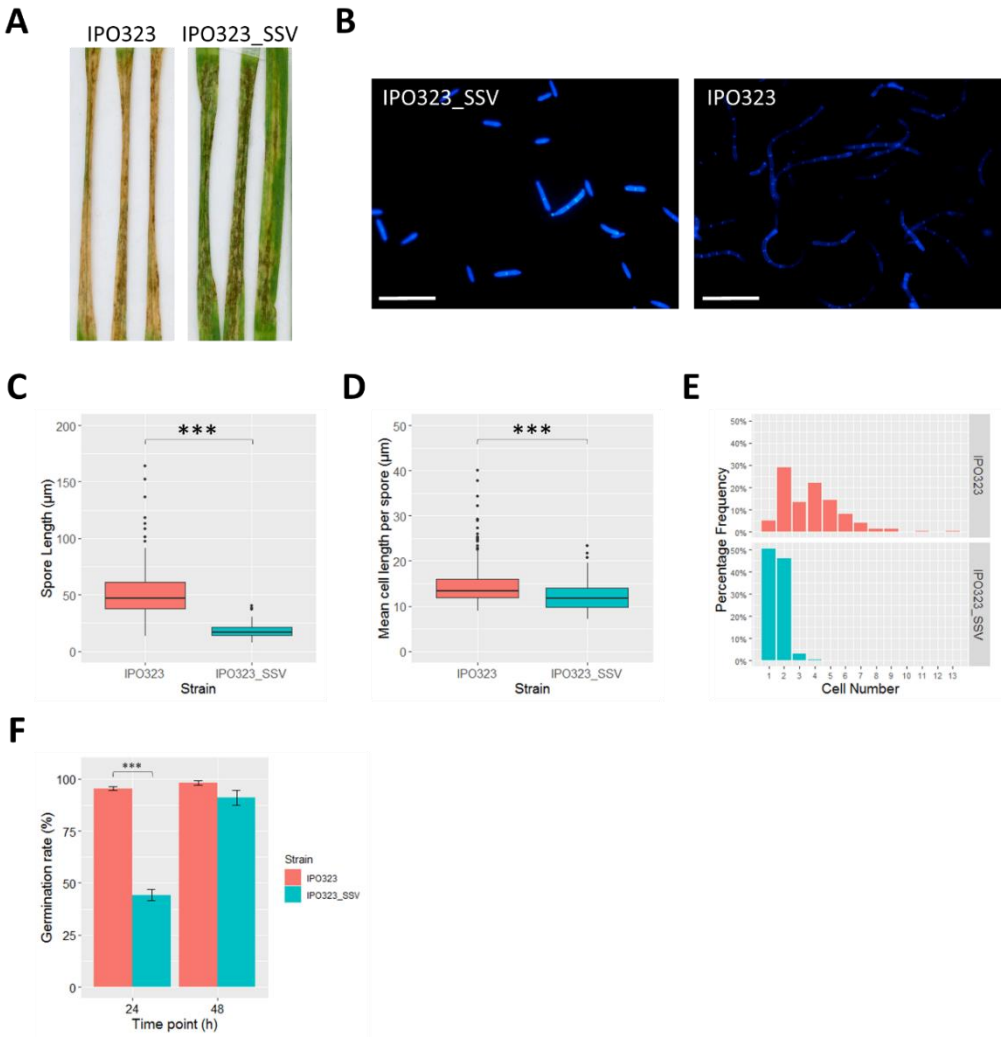


**Figure 6.1 Identification of IPO323_SSV strain with small spores, reduced germination rate and attenuated virulence**
(A) Infection symptoms on wheat 21 days after inoculation at a concentration of $10^7$ spores/ml. (B) Blastospores of IPO323 and IPO323_SSV after 5 days growth on YPD agar stained with calcofluor white. Scale bar = 50µm. (C) Boxplot showing lengths of IPO323 and IPO323_SSV blastospores. Statistically significant difference determined using Wilcoxon signed-rank test (W = 39073, $n_1$=$n_2$=200, p-value < 2.2e-16). (D) Boxplot showing mean length of cells within IPO323 and IPO323_SSV blastospores. Statistically significant difference determined using Wilcoxon signed-rank test (W = 27506, $n_1$=$n_2$=200, p-value = 8.479e-11). (E) Relative frequencies of the number of cells within blastospores of IPO323 and IPO323_SSV. (F) Mean germination rate of blastospores on water agar, found to be significantly lower in IPO323_SSV after 24h (Welch Two Sample t-test, *n*=6, ****p*<0.0001). Error bars represent standard error.

In order to characterise the morphology of IPO323_SSV blastospores grown *in vitro*, the length of spores and their component cells was analysed. Spores of IPO323_SSV were significantly shorter than the wild type (Fig. 6.1C), with a mean length of 17.7 µm (sd = 5.5) compared to 51.7 µm (sd = 22.6) in wild type IPO323. The mean length of cells within each spore was calculated, and this was found to be significantly shorter in IPO323_SSV blastospores (Fig. 6.1D). However, this difference in average cell length per spore was small, with a mean of 15 µm (sd = 5.2) in IPO323 and 12.2 µm (sd = 3.1) in IPO323_SSV. Crucially, the spores of IPO323_SSV were found to contain less cells than the wild type, with 96.5% of IPO323_SSV spores containing only one or two cells (Fig. 6.1E). This is compared to IPO323 spores which contained between 1-13 cells, with the majority (91%) having 2-7 cells. This suggests that the reduced size of blastospores observed in IPO323_SSV is attributed mainly to a reduction in component cell number, with only a slight reduction in the length of the individual cells.

Considering the importance of the morphological switch to hyphal growth in colonisation of the leaf, the hyphal germination of IPO323_SSV was analysed *in vitro* on nutrient deficient water agar medium. The germination efficiency of IPO323_SSV was severely reduced compared to the wild type after 24 h, although the number of colonies displaying evidence of hyphal growth was not significantly different from the wild type at 48 h (Fig. 6.1F). However, the growth rate and morphology of IPO323_SSV colony development was dramatically different to IPO323 (Fig. 6.2). The majority of wild type IPO323 spores had germinated hyphae from the spore apex after 16 h, and many produced hyphae laterally from the spore after 24 h. More branching of wild type hyphae was found to occur after 48 h, and significant blastosporulation was observed along these hyphae by 120 h after inoculation. Conversely, IPO323_SSV spores that germinated hyphae showed a reduced rate of filamentous growth at all observed time-points, and started to produce many blastospores after 48 h (Fig. 6.2). Those which didn't germinate hyphae displayed blastosporulation as early as 16h after inoculation, and continued to do so to form colonies of blastospores with no visible hyphae after 120 h (Fig. 6.2). The blastospores produced by IPO323_SSV on water agar were shorter than those in IPO323 (Fig. 6.2), consistent with the observations of blastospores grown on YPD. The reduced

germination efficiency, slower hyphal growth and increased investment in blastosporulation seen in IPO323_SSV could indicate the cause of the reduced virulence observed in this strain.

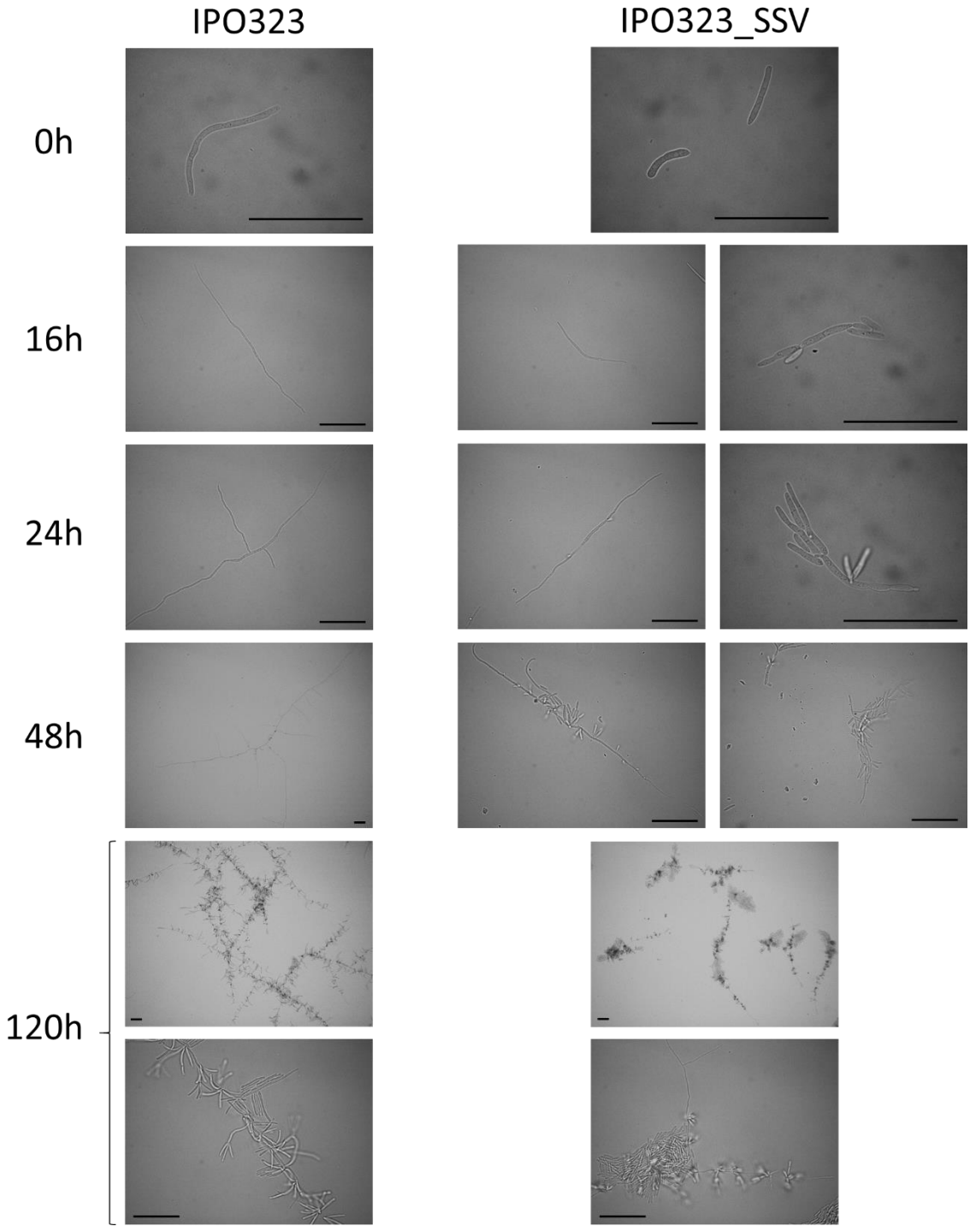


**Figure 6.2 Hyphal growth is impaired and blastosporulation increased in IPO323_SSV under starvation**
Germination of IPO323 and IPO323_SSV blastospores on 2% water agar. Scale bars = 50 µm.

### 6.3.2 IPO323_SSV shows defects in the response to nutrient starvation and oxidative stress

The hyphal growth rate and morphology of IPO323_SSV under nutrient stress was examined by assessing growth on medium deficient in a nitrogen or carbon source. Although hyphae were observed to grow at the periphery of droplet IPO323_SSV colonies, they displayed a severely reduced radial growth rate under both nitrogen and carbon starvation compared to the wild type (Fig. 6.3A). This confirms the observations of reduced hyphal growth rate from single spore germination analysis.

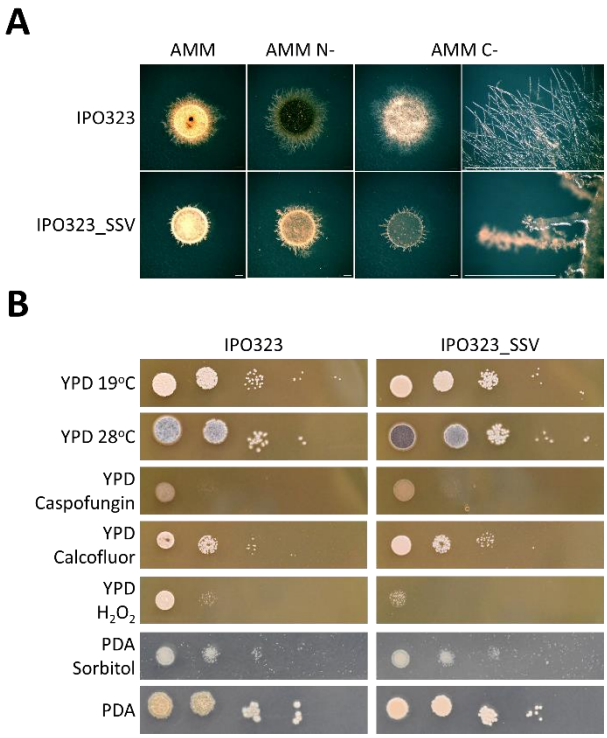


**Figure 6.3 IPO323_SSV is defective in the response to nutrient starvation and oxidative stress**
(A) Radial growth after 14 days on *Aspergillus* minimal medium (AMM) and AMM deficient in a nitrogen (AMM N-) or carbon (AMM C-) source. Plated in 5 µl droplets of $5x10^6$ spores/ml suspension. Scale bars = 1mm (B) Growth after 6 days on YPD at 19°C, 28°C and 19°C amended with 10 µg/ml caspofungin, 200 µg/ml calcofluor white, 5 µM hydrogen peroxide, as well as 19°C on PDA with and without 1.5M sorbitol. Plated in 5 µl droplets of a 10-fold dilution series (left to right) starting at $5x10^6$ spores/ml.

To investigate whether IPO323_SSV is altered in its response to stress other than nutrient deprivation, the sensitivity of this strain to various abiotic stressors was compared with wild type IPO323. IPO323_SSV showed no change in sensitivity to osmotic stress or the cell wall perturbing agents caspofungin and calcofluor white, but was more sensitive to the presence of hydrogen peroxide in the growth medium (Fig. 6.3B). Furthermore, IPO323_SSV was able to germinate aerial hyphae in response to heat stress, although to a lesser extent than IPO323, and displayed similar levels of melanisation to the wild type under these conditions (Fig. 6.3B). These results suggest that, along with aberrant germination response to nutrient deprivation, IPO323_SSV shows increased

sensitivity to oxidative stress and reduced hyphal growth in response to heat stress.

### 6.3.3 IPO323_SSV develops normal pycnidiospores on plants but reverts to the short blastospore phenotype upon subculturing onto rich media

To assess if the phenotype of this variant is maintained across infection, the spore morphology, germination rate and virulence of IPO323_SSV was assessed before and after passage through an infection cycle. Interestingly, pycnidiospores isolated from IPO323_SSV infected leaves were found to be significantly larger than the IPO323_SSV blastospores used to inoculate the plant, displaying similar lengths to wild type IPO323 pycnidiospores (Fig. 6.4A). Furthermore, pycnidiospores of IPO323 and IPO323_SSV were found to have similar numbers of cells (Fig. 6.4B), with the vast majority of pycnidiospores from both strains containing 1-4 cells. These findings suggest that the *in planta* asexual development of IPO323_SSV through pycnidiospore production is similar to the wild type.

Furthermore, while IPO323_SSV blastospores were found to be significantly less virulent than blastospores of IPO323, IPO323_SSV pycnidiospores displayed similar virulence to wild type pycnidiospores, as determined by the density of pycnidia on infected leaves (Fig. 6.4C-D). This was attributed to the significantly increased germination rate of IPO323_SSV pycnidiospores compared to the blastospores of this strain (Fig. 6.4E). However, when subcultured onto YPD, all single colonies arising from IPO323_SSV pycnidiospores were found to once again consist of short blastospores rarely formed of more than two cells (Fig. 6.4A-B). This suggests that the IPO323_SSV phenotype has not recovered stably after passage through the host infection cycle, reverting once again to the short blastospore phenotype when subsequently cultured on rich media.

### 6.3.4 Whole genome resequencing of IPO323_SSV

To investigate the genetic causes of the morphological and virulence phenotypes observed in IPO323_SSV, the genome of IPO323_SSV and the fully virulent IPO323 strain were resequenced by paired-end 150 bp Illumina

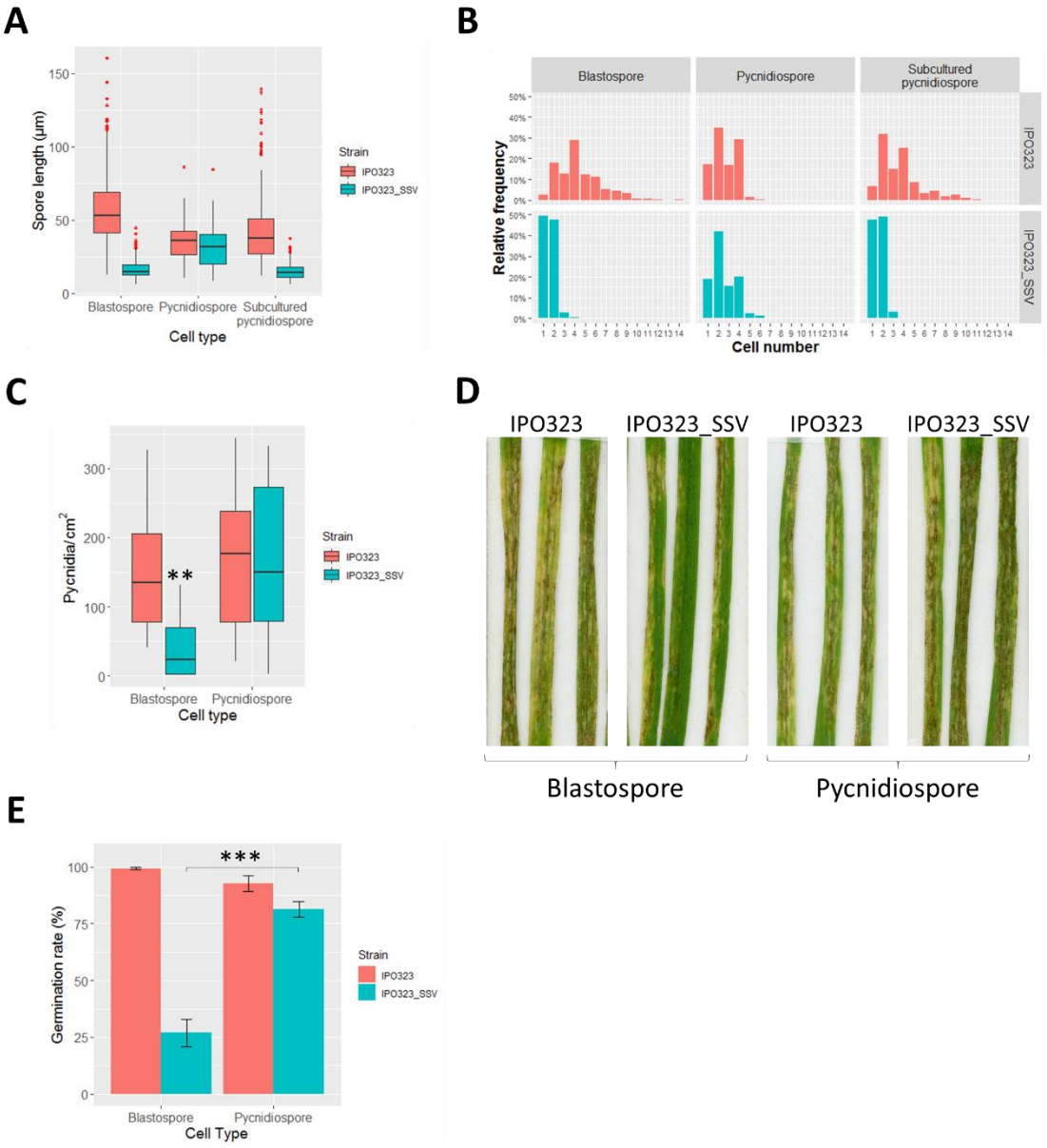


**Figure 6.4 Pycnidiospores of IPO323_SSV show recovered germination and virulence, but revert to small spore morphology upon subculture**
Spore lengths (A) and number of cells within each spore (B) for blastospores, pycnidiospores (isolated from infected leaves) and subcultured pycnidiospores (following growth on YPD agar) of IPO323 and IPO323_SSV. Statistically significant differences (Wilcoxon rank-sum test with Benjamini-Hochberg correction, $p \leq 0.01$, $n=300$) identified between spore lengths of all groups. (C) Virulence of IPO323 and IPO323_SSV blastospores and pycnidiospores quantified by the number of pycnidia per $cm^2$ on infected leaves 21 days after inoculation, with statistically significant difference (Wilcoxon rank-sum test with Benjamini-Hochberg correction, $^{**}p \leq 0.01$, $n=12$) between IPO323_SSV blastospores and all other groups. (D) Reduced leaf area covered by necrotic lesions in leaves infected by IPO323_SSV blastospores, which is recovered in IPO233_SSV pycnidiospores. (E) Pycnidiospores of IPO323_SSV show a significant increase in germination rate compared to IPO323_SSV blastospores (Welch Two Sample t-test, $n=3$, $^{***}p=0.0006$), while no significant difference was found between IPO323 blastospores and pycnidiospores.

sequencing and aligned to the reference IPO323 genome. Analysis of the read coverage across the whole IPO323 genome revealed the loss of accessory chromosome 18 in this strain (Fig. S6.1), an event which has been frequently observed in other laboratory *Z. tritici* strains (Habig et al., 2017; Kellner et al., 2014) and field isolates (Badet et al., 2020), and has not been reported to result in altered blastospore morphology. Additionally, a large deletion was identified at the 3' end of chromosome 5, covering a 34 kb region at the end of the contig (Fig. 6.5A; Fig. S6.1). This region contains multiple transposable elements but no predicted protein encoding genes.

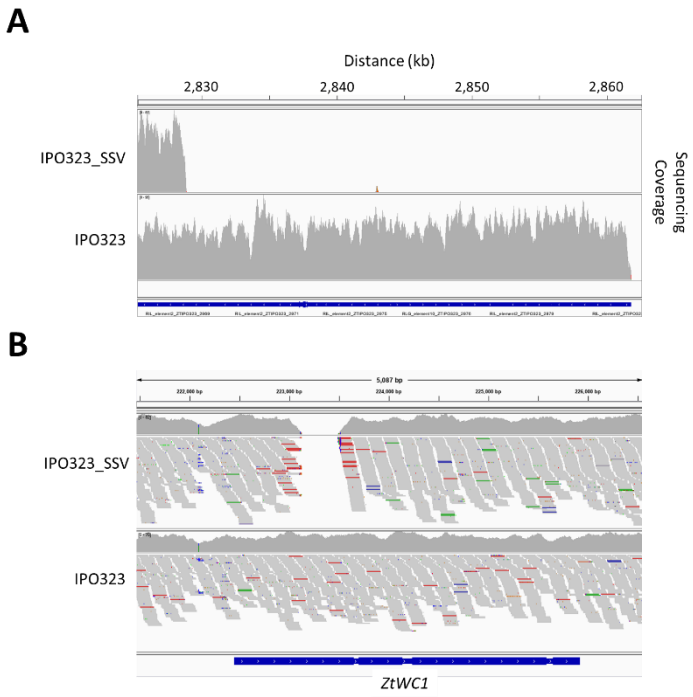


**Figure 6.5 Large deletions identified in the genome of IPO323_SSV**
Reads from whole genome resequencing of IPO323_SSV and IPO323 aligned to the (A) 3' end of chromosome 5 and (B) *ZtWC1* locus (ZtritIPO323_04g03036).

Variant analysis was carried out on the IPO323_SSV alignment, and the resulting single nucleotide polymorphisms (SNPs) and short indels were compared to those from the wild type IPO323 and the other sequenced strains from Chapter 5. This was used to compile a list of the mutations unique to IPO323_SSV (Table S6.1). No unique mutations were identified within the coding regions of annotated genes, with all the observed polymorphisms lying in intergenic regions or the predicted regulatory regions upstream and downstream of predicted genes (Table S6.1). Many of the genes in the vicinity of these mutations encoded hypothetical proteins with no functional annotation.

During the present study, whole genome resequencing analysis of IPO323 strains displaying reduced virulence at Rothamsted Research and the Max

Planck Institute identified the same large deletion in the gene ZtritIPO323_04g03036 (*ZtWC1*; Habig et al 2020; Rudd pers. comm.). This gene encodes the *Z. tritici* homolog of the light-responsive *Neurospora crassa* transcription factor white collar 1 (WC1; Ballario et al 1996). Inspection of IPO323_SSV reads aligned to this locus identified the same deletion of 404bp in the first intron of *ZtWC1* (Figure 6.5B), suggesting that these strains originate from vertical transmission of the same mutant arising in IPO323. The deletion lies upstream of all conserved domains in the putative ZtWC1 protein and is predicted to cause a frame shift leading to a premature stop codon in the translated sequence. This mutation is therefore likely to abolish ZtWC1 function and represents a strong candidate for the genotype causing the reduced virulence phenotype observed in IPO323_SSV.

### 6.3.5 Transcriptome analysis of IPO323_SSV *in vitro*

To investigate transcriptional changes associated with the generation of the small blastospores in IPO323_SSV, RNA sequencing analysis was carried out on IPO323_SSV and wild type IPO323 spores grown on rich media. Visualisation of global gene expression revealed dramatic variation in transcription between the strains (Fig. 6.6). PCA analysis reduced 96% of the observed variation to a single principle component which separated the samples by strain (Fig. 6.6A). Consistent with the loss of chromosome 18 indicated by genome sequencing results, annotated genes on chromosome 18 showed minimal coverage by IPO323_SSV RNA sequencing reads. Genes on

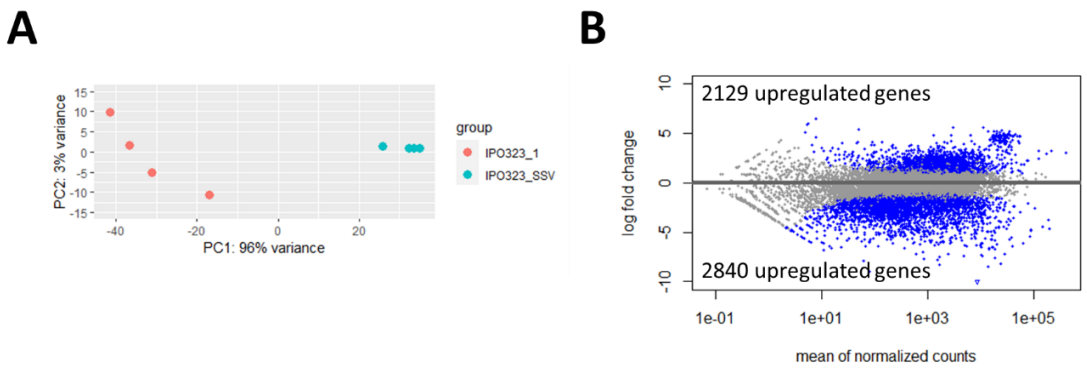


**Figure 6.6 Dramatic transcriptional differences in IPO323_SSV during growth on YPD**
(A) Principal component analysis of global normalised gene expression data. (B) MA plot displaying log2-fold change (LFC) of each gene plotted against the mean of normalised counts across all samples, with differentially expressed genes ($p$<0.01, LFC>0.58) in blue.

chromosome 18 were subsequently omitted from differential expression analysis. A total of 4,969 DE ($p_{adj} < 0.01$) genes were identified, including 2,129 upregulated and 2,840 downregulated genes (Fig. 6.6B).

To investigate cellular processes displaying differential regulation in IPO323_SSV, the sets of DE genes were analysed for significant enrichment of Biological Process Gene Ontology terms (Table 6.1). To support this, genes that were identified as part of relevant KEGG pathways were assessed for differential expression. Transcriptionally upregulated genes were enriched with GO terms related to gene expression, including mRNA and tRNA processing, ribosome biogenesis and translation machinery (Table 6.1; Fig. 6.7; Fig. S6.2). In concordance with this, nucleotide biosynthesis genes were also upregulated (Table 6.1; Figure S6.3), along with components of the pentose phosphate pathway involved in the synthesis of the nucleotide precursors (Table 6.1; Figure S6.4). This suggests that IPO323_SSV is displaying an increased rate of protein synthesis which could indicate an increase in growth rate. To support this, many components of the mitochondrial ATP synthase complex were upregulated (Table S6.2), suggesting an increase in the requirement for energy in IPO323_SSV.

Enrichment analysis also identified the term ‘attachment of spindle microtubules to kinetochore’, ‘DNA replication’ and ‘chromosome organisation’ as upregulated in IPO323_SSV (Table 6.1), indicating the upregulation of genes involved in mitosis in this strain. This is supported by the finding that many elements of the KEGG DNA replication pathway are upregulated in IPO323_SSV (Fig. S6.5). Many components of the *Z. tritici* cell cycle KEGG pathway were significantly upregulated in IPO323_SSV (Table 6.1; Fig. 6.8A), including the transcription cofactor *ZtSWI6* (ZtritIPO323_04g02603; Fig. 6.8B), which controls cell cycle progression to S-phase in *S. cerevisiae* (Koch et al., 1993; Lowndes et al., 1992). Furthermore, *ZtMBP1* (ZtritIPO323_04g00971), the homolog of which forms the MBF complex with SWI6 in yeast, also showed higher expression in IPO323_SSV samples (Fig. 6.8B), although this difference was not statistically significant. The GO term ‘Arp2/3 complex-mediated actin nucleation’ was also enriched in the upregulated genes (Table 6.1), which may correspond with the upregulation of mitotic machinery, considering the roles of actin in organelle transport and cleavage during cytokinesis. Overall, this

**Table 6.1 Significantly enriched Biological Process GO terms in IPO323_SSV differentially expressed genes**

| Gene Set | GO.ID | GO Term | Total[a] | DE[b] | Expected[c] | p-value |
|---|---|---|---|---|---|---|
| **Upregulated** | GO:0006412 | translation | 225 | 158 | 49.29 | < 1e-30 |
| | GO:0042254 | ribosome biogenesis | 66 | 51 | 14.46 | 7.10E-09 |
| | GO:0006364 | rRNA processing | 36 | 25 | 7.89 | 3.80E-06 |
| | GO:0006886 | intracellular protein transport | 113 | 54 | 24.75 | 2.80E-05 |
| | GO:0006414 | translational elongation | 20 | 13 | 4.38 | 3.70E-05 |
| | GO:0006396 | RNA processing | 205 | 104 | 44.91 | 4.70E-05 |
| | GO:0006260 | DNA replication | 55 | 31 | 12.05 | 8.20E-05 |
| | GO:0006413 | translational initiation | 24 | 15 | 5.26 | 8.40E-05 |
| | GO:0006457 | protein folding | 38 | 20 | 8.32 | 0.0004 |
| | GO:0006401 | RNA catabolic process | 26 | 12 | 5.7 | 0.00049 |
| | GO:0006098 | pentose-phosphate shunt | 6 | 6 | 1.31 | 0.0005 |
| | GO:0006189 | 'de novo' IMP biosynthetic process | 5 | 5 | 1.1 | 0.0005 |
| | GO:0008608 | attachment of spindle microtubules to kinetochore | 9 | 7 | 1.97 | 0.00062 |
| | GO:0000413 | protein peptidyl-prolyl isomerization | 14 | 9 | 3.07 | 0.00077 |
| | GO:0006164 | purine nucleotide biosynthetic process | 45 | 24 | 9.86 | 0.0022 |
| | GO:0042273 | ribosomal large subunit biogenesis | 11 | 10 | 2.41 | 0.00225 |
| | GO:0000398 | mRNA splicing, via spliceosome | 46 | 24 | 10.08 | 0.00303 |
| | GO:0001522 | pseudouridine synthesis | 10 | 7 | 2.19 | 0.00493 |
| | GO:0034314 | Arp2/3 complex-mediated actin nucleation | 7 | 5 | 1.53 | 0.00705 |
| | GO:0008033 | tRNA processing | 57 | 27 | 12.49 | 0.00741 |
| | GO:0051276 | chromosome organization | 120 | 44 | 26.29 | 0.00894 |
| | GO:0000027 | ribosomal large subunit assembly | 5 | 4 | 1.1 | 0.00946 |
| | GO:0045292 | mRNA cis splicing, via spliceosome | 5 | 4 | 1.1 | 0.00946 |
| | GO:0009165 | nucleotide biosynthetic process | 74 | 38 | 16.21 | 0.0099 |
| **Downregulated** | GO:0055085 | transmembrane transport | 634 | 212 | 108.53 | < 1e-30 |
| | GO:0055114 | oxidation-reduction process | 805 | 197 | 137.81 | 3.50E-10 |
| | GO:0005975 | carbohydrate metabolic process | 235 | 60 | 40.23 | 3.90E-06 |
| | GO:0043386 | mycotoxin biosynthetic process | 45 | 19 | 7.7 | 6.20E-05 |
| | GO:0009308 | amine metabolic process | 27 | 10 | 4.62 | 0.0049 |

Total number genes annotated with GO term in [a]genome, [b]differentially expressed gene set (DE) and [c]expected in DE gene set.

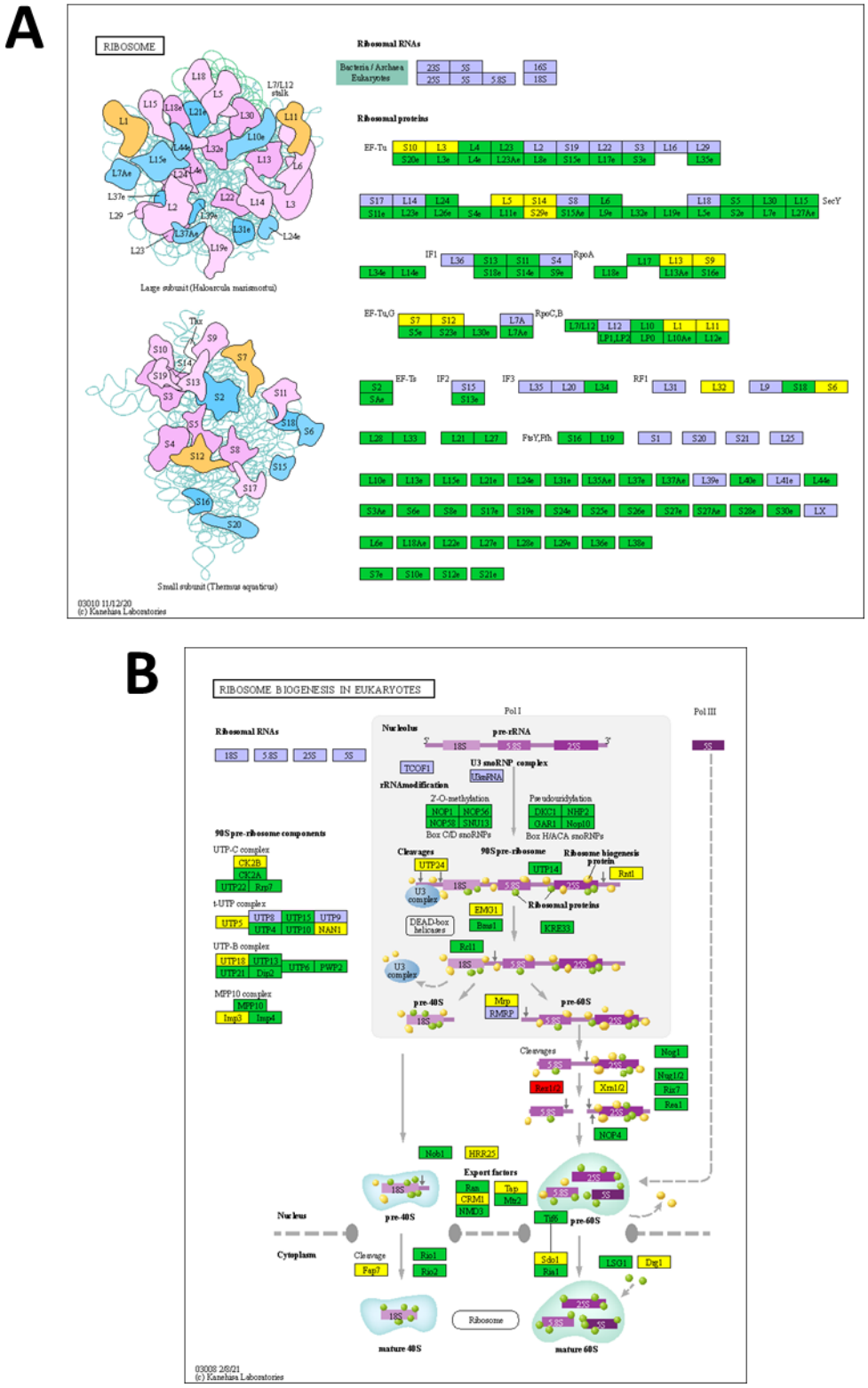


**Figure 6.7 Ribosome biogenesis is upregulated in IPO323_SSV**
*Z. tritici* KEGG pathways for (A) the ribosome (ko03010) and (B) ribosome biogenesis (ko03008), with genes upregulated (green), downregulated (red) or not differentially expressed (yellow) in IPO323_SSV compared to IPO233. Pathway components with no annotated genes are displayed in blue.

provides evidence for accelerated cell cycle progression in IPO323_SSV during growth on rich media.

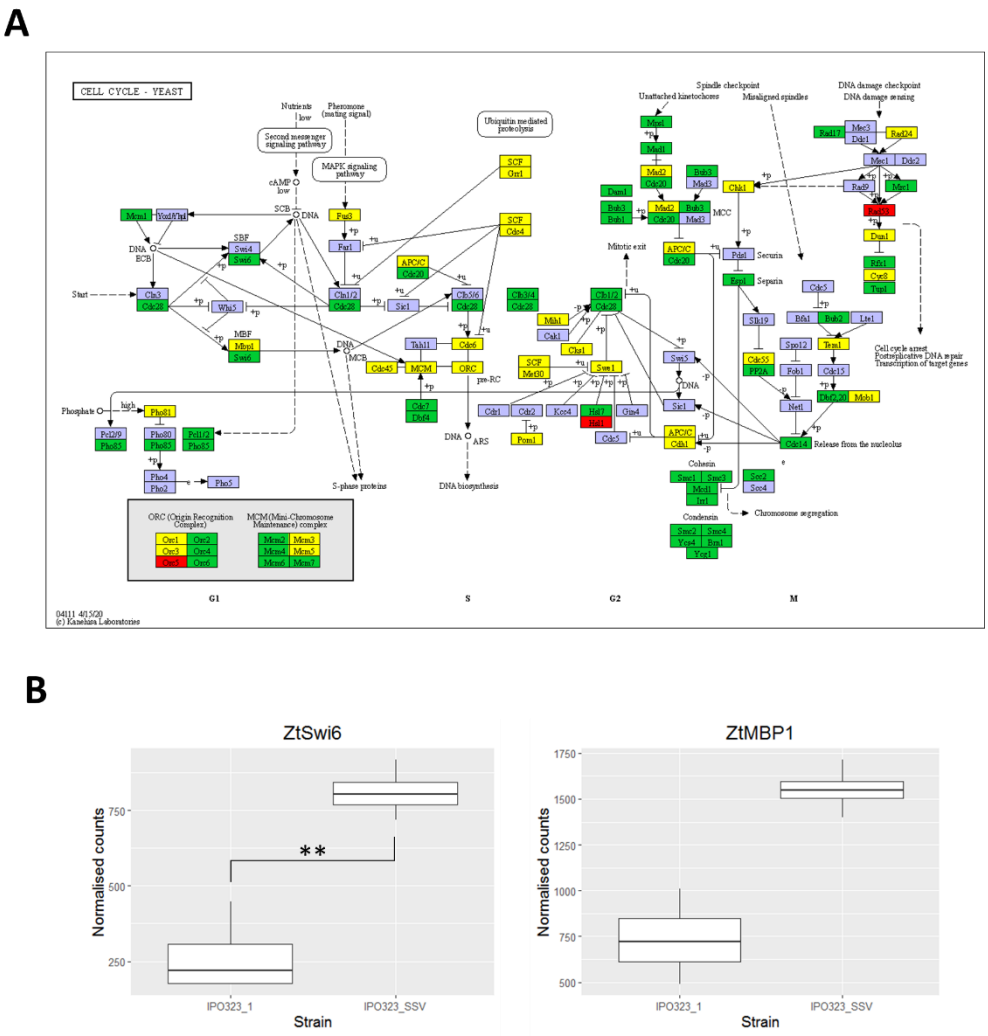


**Figure 6.8 Cell cycle genes are upregulated in IPO323_SSV**
*Z. tritici* KEGG pathway for the cell cycle (ko04111), with genes upregulated (green), downregulated (red) or not differentially expressed (yellow) in IPO323_SSV compared to IPO233. Pathway components with no annotated genes are displayed in blue. Boxplots showing normalised expression values of cell cycle genes ZtSWI6 (ZtritIPO323_04g02603; *padj*=0.004387) and ZtMPB1 (ZtritIPO323_04g00971; *padj*=0.086565).

Assessing the functional annotation of the top 50 genes with the highest positive fold-change, it is clear that most dramatically upregulated genes encode ribosomal proteins (Table S6.2). Additionally, a putative sugar transporter and a 3-dehydroquinate synthase enzyme, involved in aromatic amino acid biosynthesis, were strongly upregulated, consistent with the proposed increase in protein synthesis and energy metabolism in IPO323_SSV. Furthermore, a secreted phosphatidylethanolamine-binding protein (PEBP; ZtritIPO323_04g10011) was also highly expressed in IPO323_SSV, a homolog

of which is known to be involved in regulating cell signalling and metabolism in yeast (Beaufour et al., 2012). Also strongly upregulated is the *Z. tritici* homolog of *S. cerevisiae Asc1* (ZtritIPO323_04g08681), which has multiple functions as a ribosomal protein and a G-protein β-subunit, through which it regulates a broad range of cellular processes from protein synthesis to signal transduction (Schmitt et al., 2017). These proteins therefore represent potential signalling components which may control the phenotypes observed in IPO323_SSV.

On the other hand, the downregulated gene set was enriched with the GO terms 'transmembrane transport' (Table 6.1). More detailed investigation of the functional annotation of downregulated genes revealed an enrichment of genes with predicted secretory signals and transmembrane domains, suggesting that the expression of many extracellular and cell surface proteins is repressed in IPO323_SSV. Many of the transmembrane proteins were annotated as transporters from the major facilitator superfamily, with 167 representatives of this family in the downregulated gene set (Table S6.2). There were 388 genes from the predicted *Z. tritici* secretome downregulated in IPO323_SSV, including many which have potential functions during infection such as plant cell wall degrading enzymes (PCWDEs), proteases, lipases and putative effector proteins (Table S6.2). Furthermore, the downregulated gene set was also enriched for the GO term 'mycotoxin biosynthetic process' (Table 6.1), suggesting that secondary metabolism is repressed in IPO323_SSV. Closer inspection confirmed that many genes predicted to encode polyketide synthases and non-ribosomal peptide synthases were downregulated (Table S6.2). Combined, these findings suggest that IPO323_SSV displays reduced expression of genes involved in adaptation to the complex environment of the wheat host, both in terms of nutrient acquisition and biotic interactions.

The downregulated gene set is also enriched for 'carbohydrate metabolic process' genes (Table 6.1), including many with predicted glycoside hydrolase and glycosyltransferase activity (Table S6.2). As well as the aforementioned PCWDEs, six putative chitinases were downregulated, along with many other genes with predicted functions in cell wall biosynthesis and modification. This includes two α-1,3-glucan synthases (ZtritIPO323_04g10384 and ZtritIPO323_04g01966), a homolog of *S. cerevisiae* SKN1 involved in β-1,6-glucan synthesis (ZtritIPO323_04g02687), and four homologs of *A. fumigatus*

GEL proteins (ZtritIPO323_04g00352, ZtritIPO323_04g04422, ZtritIPO323_04g01445 and ZtritIPO323_04g07582) involved in β-1,3-glucan biosynthesis. Furthermore, two homologs of CRH (Congo red hypersensitivity) transglycosylase proteins were downregulated (ZtritIPO323_04g01145 and ZtritIPO323_04g00257), which are known to be involved in crosslinking of cell wall polymers in *A. fumigatus* (Fang et al 2019). Also downregulated are homologs of mannan endo-1,6-alpha-mannosidase DCW1 (ZtritIPO323_04g08092) and DFG5 (ZtritIPO323_04g00508) involved in cell wall biogenesis (Kitagaki et al., 2002), the latter of which is known to be involved in hyphal growth in *S. cerevisiae* and *C. albicans* (Mösch & Fink, 1997; Spreghini et al., 2003). Finally, a homolog of *A. fumigatus* 1,2-α -mannosidase MsdS (ZtritIPO323_04g05652), involved in N-glycosylation and required for normal polarised growth and cell wall biogenesis (Yanjie Li et al., 2008), is also downregulated. IPO232_SSV therefore displays repression of many factors involved in cell wall remodelling, which may contribute to its altered morphology and suppressed hyphal germination.

Inspection of the top 50 downregulated genes by fold-change identified the dramatic repression of the $Zn(II)_2Cys_6$ zinc cluster DNA binding protein ZtritIPO323_04g11374 (Table S6.2), homolog of the transcription factor PRO1 from *Sodaria macrospora* (Steffens et al., 2016). This transcription factor is well characterised as a regulator of sexual development in ascomycetes (Vienken & Fischer, 2006), as well as in other developmental processes and virulence (Y. Cho et al., 2009; Steffens et al., 2016). A conserved function of this gene, designated *ZtPRO1*, in *Z. tritici* is suggested by the concurrent downregulation of other putative regulators of sexual development. This includes homologs of EsdC (ZtritIPO323_04g00320), which is known to be regulated by Pro1 (Steffens et al., 2016; Tanaka et al., 2013), and LsdA (ZtritIPO323_04g13246; Table S6.2). Additionally, the *Z. tritici* homolog of the *A. nidulans* NsdD, a GATA-type transcriptional activator of sexual development (Han et al., 2001), was downregulated in IPO323_SSV (ZtritIPO323_04g01931; Table S6.2). This gene is also a homolog of light-responsive *N. crassa* gene *SUB1*, expression of which is directly regulated by WC1 during light exposure (Chen et al., 2009), providing some corroborative evidence that the IPO323_SSV phenotype is caused by the deletion in *ZtWC1*.

Also amongst the most strongly downregulated genes in IPO323_SSV were two RTA1-like genes (Table S6.2), while eight of the 11 RTA domain genes in *Z. tritici* were downregulated in total (Table S6.2). These transmembrane proteins are known to be expressed in response to various stress conditions, including during the multidrug resistance response, and function in tolerance against various drugs and toxins in yeast (Manente & Ghislain, 2009). Furthermore, IPO323_SSV also shows downregulation of glutathione s-transferases and ABC transporters (Table S6.2), which are involved in resistance to xenobiotic compounds. Additionally, many of the *Z. tritici* core autophagy genes are downregulated in the IPO323_SSV, including *ZtATG1*, *ZtATG2*, *ZtATG4*, *ZtATG9*, *ZtATG13*, *ZtATG14*, *ZtATG16* and *ZtATG22* (Table S6.2). This suggests that IPO323 shows downregulation of various stress response genes.

Genes in the vicinity of unique SNPs in IPO323_SSV were assessed for changes in expression in this strain. One gene encoding a major facilitator superfamily (MFS) transporter was significantly downregulated in IPO323_SSV, while four genes were upregulated, two of which were functionally uncharacterised (Table 6.1). One upregulated gene encoded a 1-acyl-sn-glycerol-3-phosphate acyltransferase, involved in biosynthesis of the membrane phosphoglycerides and storage lipids (Benghezal et al., 2007). The final DE gene adjacent to an SNP was annotated as a putative folylpolyglutamate synthetase (IPR001645). These enzymes catalyse the conversion of folates to polyglutamate derivatives, enhancing the cellular retention these important cofactors in the biosynthesis of nucleotides and amino acids. Although the identified polymorphisms could have an influence on the expression of these genes, their functional annotations are consistent with the other observed transcriptomic trends in IPO323_SSV, suggesting that they are unlikely to have caused the phenotype of this strain.

### 6.3.6 The mycovirus ZtFV1 is less abundant in IPO323_SSV

Considering previous reports of mycoviruses causing altered morphological development and virulence of fungal pathogens, the presence of the mycovirus ZtFV1 within *in vitro* samples of IPO323_SSV was compared with the wild type. RNA sequencing reads were aligned to the *Z. tritici* genome containing the full ZtFV1 genome sequence as an additional chromosome (Gilbert et al., 2019;

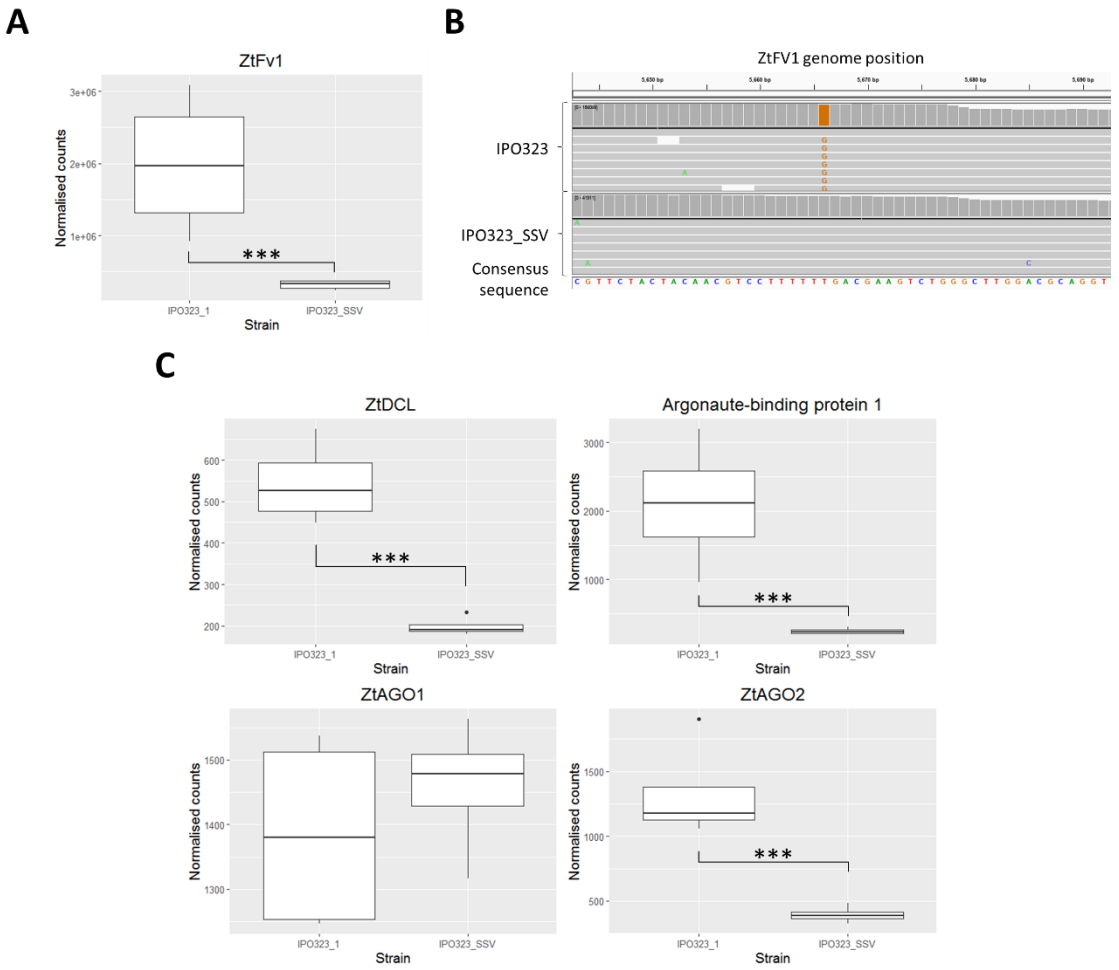


**Figure 6.9 The mycovirus ZtFV1 is less abundant in IPO323_SSV, coinciding with downregulation of RNA silencing machinery**
(A) Abundance of RNA-sequencing reads aligned to ZtFV1 genome, normalised alongside gene expression counts, which is significantly lower in IPO323_SSV (****padj*=3.35E-07). (B) IGV screenshot of RNA sequencing reads aligned to the ZtFV1 genome, displaying the point mutation at position 5,666 in wild type IPO323 samples. (C) Boxplots displaying the normalised count values for the Dicer-like gene *ZtDCL* (ZtritIPO323_04g13718; ****padj*=2.76E-05), the argonaute-binding protein gene (ZtritIPO323_04g13344; ****padj*=2.33E-11) and the argonaute genes *ZtAGO1* (ZtritIPO323_04g08085) and *ZtAGO2* (ZtritIPO323_04g03320; ****padj*=7.25E-06).

GenBank Accession MK279506). An incredible 3-7% of the reads uniquely mapped to this amended reference genome aligned with the viral genome in wild type IPO323 samples. Surprisingly, IPO323_SSV samples were found to contain significantly less abundant viral sequences through differential expression analysis (Fig 6.9A), making up between 0.7-1% of the uniquely mapped reads. Furthermore, inspection of RNA reads aligned to the ZtFV1 genome identified a nonsynonymous point mutation (T>G) in wild type IPO323 samples, at position 5,666 within the coding sequence of the hypothetical protein ‘ZtFV1_gp2’, causing a F413L substitution (Fig. 6.9B). An additional

synonymous mutation (G>A) was identified at position 1,908, within the predicted RNA-dependent RNA polymerase encoding sequence, in over half of the viral sequences from IPO323 (data not shown).

Due to the importance of RNA silencing in cellular defences against RNA viruses, the expression of previously characterised *Z. tritici* Argonaute and Dicer-like genes was investigated (Kettles et al., 2019). Surprisingly, *ZtDCL*, *ZtAGO2* and an Argonaute-binding protein (ZtritIPO323_04g13344; IPR018606) displayed significant downregulation in IPO323_SSV samples, while *ZtAGO1* expression was unchanged (Fig. 6.9C). This suggests that the high viral load in wild type IPO323 could be causing strong induction of RNA silencing machinery, while the reduced abundance of ZtFV1 in IPO323_SSV is caused by an alternative mechanism to interference by host RNA silencing.

## 6.4 Discussion

In this study, a spontaneously arising variant of the *Z. tritici* reference isolate IPO323, designated IPO323_SSV, was characterised. This strain produces blastospores consisting of one or two cells during growth on rich media, which display reduced virulence compared to the multicellular blastospores of the wild type. This is likely to be caused by a defect in host penetration, considering the reduced germination efficiency and hyphal growth rate of IPO323_SSV blastospores when induced by nutrient starvation. Analysis of gene transcription during growth on rich media provided evidence to suggest that IPO323_SSV is undergoing an accelerated cell cycle under these conditions, supported by an increase in the cells capacity for gene transcription and translation, as well as nucleotide biosynthesis and DNA replication. This is consistent with the proliferation of unicellular and bicellular spores by this strain, which could be explained by an increased propensity to undergo cytokinesis rather than continue to invest in growth of multicellular blastospores. Reduced germination and filamentous growth rate of IPO323_SSV could reflect a trade-off between a high replication rate in rich culture medium and investment of resources in lipid storage required for growth under nutrient limitation during early infection.

The recovery of germination efficiency and virulence in IPO323_SSV pycnidiospores collected from infected leaves suggests that the aberrant

phenotype of this strain is largely restricted to *in vitro* conditions. However, when these IPO323_SSV pycnidiospores were subcultured onto rich media, they reverted to the morphological phenotype observed in IPO323_SSV before infection. This suggests that the IPO323_SSV phenotype is caused by stable genetic variation in this strain, rather than epigenetic signatures built up during *in vitro* subculturing, as was previously identified alongside deterioration of virulence in laboratory strains of *B. cinerea* (Breen et al., 2016). Whole genome resequencing of IPO323_SSV identified the lack chromosome 18, loss of which has previously been shown to cause no significant decrease in IPO323 virulence towards the cultivar Riband used here (Habig et al., 2017). However, a large deletion was identified at the 3' end of chromosome 5 in IPO323_SSV, including loss of the telomere, which may have contributed to the observed phenotype, despite this region not containing any predicted genes.

Similar subtelomeric deletions were identified in *smooth* mutants of the ascomycete yeast *Yarrowia lipolytica*, which were also defective in the transition to hyphal growth (Pomraning et al., 2018). Moreover, transcriptional analysis of these mutants revealed striking parallels with the present study, identifying upregulation of genes involved in the cell cycle, gene transcription and DNA replication, alongside downregulation of those related to stress responses and cell wall remodelling. In particular, *smooth* mutants and IPO323_SSV displayed enhanced expression of the cell cycle regulator *SWI6*, deletion of which led to partial recovery of hyphal growth in *Y. lipolytica* (Pomraning et al., 2018). Furthermore, *smooth* mutants showed downregulated expression of *YlMSN2*, a stress responsive transcription factor which was shown to be essential for hyphal germination. Although the *Z. tritici* homolog of MSN2 (ZtritIPO323_04g11517) was not found to be differentially expressed in IPO323_SSV, this strain did display defects in its response to nutrient starvation and oxidative stress, stimuli which are known to induce hyphal morphogenesis in *Z. tritici* (Francisco et al., 2019). Additionally, IPO323_SSV showed downregulated expression of cell wall remodelling genes that are known to be involved in polarised growth and morphogenesis in other ascomycetes (Li et al., 2008; Mouyna et al., 2005; Spreghini et al., 2003; Yamazaki et al., 2008). Together, these results point towards the occurrence of similar processes in mutants of distantly related fungal species, with defects in the hyphal transition

associated with activated cell cycle progression and repressed stress responses. Further characterisation of gene expression in IPO323_SSV under hyphal growth-inducing conditions will help elucidate the causes of defective germination in this strain.

IPO323_SSV was also found to harbour a large deletion in the *Z. tritici* homolog of WC1, a photoreceptor which forms the White Collar complex (WCC) transcription factor with white collar 2 (WC-2) to regulate the expression of blue light responsive genes in *N. crassa* (He et al., 2002). This deletion has also been reported in association with reduced virulence of IPO323 strains in other laboratories (Habig et al., 2020; Rudd pers. comm.). Subsequent communication with these groups has confirmed that the chromosome 5 deletion identified here is also present in these strains, providing strong evidence that both mutations arose in IPO323 prior to dissemination. Screening for this *ZtWC1* deletion in IPO323 stocks from other laboratories is required to understand its prevalence, and inform the interpretation of results from previous studies using this strain.

Light is a crucial environmental cue controlling the development and metabolism of fungi through the regulation of widespread transcriptional changes (Wu et al., 2014). Furthermore, the molecular machinery involved in recognition of light has been found to be involved in the virulence of multiple plant pathogens (Canessa et al., 2013; Kim et al., 2011). Several developmental processes in *Z. tritici* are known to be responsive to light, including the induction of aerial hypha formation (Choi & Goodwin, 2011), and the regulation of asexual development and vegetative growth (Tiley et al., 2018, 2019). Furthermore, different light regimes were recently found to cause dramatic changes in *Z. tritici* gene expression (McCorison & Goodwin, 2020).

Evidence for defective light signalling in IPO323_SSV was identified by transcriptomic analysis, supporting the hypothesis that the phenotype of this strain is caused by *ZtWC1* disruption. Upregulation of the light-regulated transcription factor SUB1 is one of the earliest responses to light controlled by WC1 in *N. crassa* (Chen et al., 2009). The *Z. tritici* homolog of *SUB1* was found to be repressed in IPO323_SSV, supporting the conserved regulatory function of *ZtWC1*. Exposure to light was also found to cause transcriptional activation of

the oxidative stress response and repression of genes involved in ribosome biogenesis in *N. crassa* (Wu et al 2014), which authors associated with the repression of protein synthesis caused by other environmental stresses (Spriggs et al 2010). This suggests that widespread upregulation of ribosomal proteins observed here in IPO323_SSV could be caused by repression of light-responsive pathways through *ZtWC1* disruption. Furthermore, exposure of *Z. tritici* to light was reported to induce repression of genes involved in the cell cycle and growth and upregulation of genes related to secondary metabolism (McCorison & Goodwin, 2020). Genes involved in these processes were differentially expressed in the opposite directions in IPO323_SSV, suggesting that *ZtWC1* may underpin some of the transcriptional changes identified by McCorison and Goodwin (2020).

Complementation of the *ZtWC1* deletion with the full length coding sequence will elucidate the role of this polymorphism in the IPO323_SSV phenotype, and is currently underway in the laboratory. Targeted deletion of the complete *ZtWC1* coding sequence and comparison of the resulting phenotype with IPO323_SSV will also confirm whether the mutation in *ZtWC1* identified here results in complete inhibition of its function. Furthermore, while the present study assessed the IPO323_SSV phenotype under darkness, the effect of *ZtWC1*-disruption on growth morphology and gene transcription during exposure to light requires investigation to fully characterise elements of the *Z. tritici* light response controlled by *ZtWC1*. The present findings, along with these subsequent investigations, will help elucidate the role of ZtWC1 signalling in *Z. tritici* virulence.

Transcriptional analysis in this study also identified two putative signalling proteins which were strongly upregulated in IPO323_SSV. The *Z. tritici* homolog of *S. cerevisiae* ASC1, a ribosomal protein which also acts as a G protein β-subunit in the regulation of many proteins involved in translation and cellular signalling (Schmitt et al., 2017). This includes the inhibition of both the cAMP-PKA and KSS1 MAPK pathways (Zeller et al., 2007). Deletion of ASC1 in yeast leads to reduced dimorphism, probably through over-activation of glucose signalling pathways causing inhibition of the developmental response to glucose limitation (Zeller et al., 2007). Additionally, a PEBP-encoding gene was also among the most strongly induced in IPO323_SSV. The closest homolog of this

gene in *S. cerevisiae* is TFS1, which is upregulated during stress and proposed to form a negative feedback loop on the stress response through activation of PKA-cAMP signalling and regulation of metabolism (Beaufour et al., 2012). However, unlike TFS1, the *Z. tritici* PEBP is predicted to be secreted, suggesting that this protein may have divergent functions in *Z. tritici*. The contribution of these possible signalling components to *Z. tritici* development should be investigated further.

Furthermore, the *Z. tritici* homolog of the transcription factor PRO1, involved in sexual development of *Sodaria macrospora* (Masloff et al., 1999), *N. crassa* (*ADV-1*; Colot et al., 2006) and *A. nidulans* (Vienken & Fischer, 2006), was strongly downregulated in IPO323_SSV. In *N. crassa*, *ADV-1* transcription is induced by light under the direct control of the WCC, and controls genes involved in sexual development and hyphal growth (Colot et al., 2006; Dekhang et al., 2017; Smith et al., 2010). The *Z. tritici* homologs of several genes involved in sexual development in these species were also downregulated in IPO323_SSV, indicating some conservation in the function of *ZtPRO1*. Although sexual development was not assessed here, this provides further evidence implicating disruption of *ZtWC1* as the cause of the IPO323_SSV phenotype, and suggests that light signalling may be involved in *Z. tritici* sexual development. Furthermore, deletion of PRO1 homologs causes an increase in the vegetative growth rate of various ascomycetes (Soukup et al., 2012), including the grass endophyte *Epichloë festucae*, which leads to breakdown of the symbiotic relationship and stunted growth of the host (Tanaka et al., 2013). Similar regulation of vegetative growth by *ZtPRO1* could be implicated in causing the *in vitro* and virulence phenotypes of IPO323_SSV. The role of *ZtPRO1* in regulating the IPO323_SSV phenotype and *Z. tritici* development therefore requires further enquiry through targeted deletion and overexpression.

In addition to identifying its conserved role in sexual development, deletion of PRO1 in *Cryphonectria parasitica* also led to reduced asexual sporulation, a phenotype similar to the symptoms caused by the mycovirus CHV1 (Sun et al., 2009). Furthermore, CHV1 infection was previously found to repress PRO1 expression in this fungus (Allen & Nuss, 2004), suggesting that this transcriptional response may be the cause of the defect in asexual development (Sun et al., 2009). Intriguingly, *Δpro1* mutants were also able to escape CHV1

infection in rapidly-growing mycelial segments, indicating that PRO1 is required for the maintenance of CHV1 infection. The authors state: “The observation that a virus downregulates a host transcription factor gene that is also required for virus maintenance presents an intriguing paradox” (Sun et al., 2009). However, it seems more likely that the *CpPRO1* downregulation represents a successful host defence response which restricts viral propagation.

In this study, the *Z. tritici* mycovirus, ZtFV1, was found to be significantly less abundant in the blastospores of IPO323_SSV, coinciding with the strong repression of *ZtPRO1* expression. This raises the possible function of PRO1 in viral infection of these two fungal species. Whether ZtPRO1 downregulation in IPO323_SSV, and the accompanying phenotypes, is indicative of a defence response to ZtFV1 infection requires further investigation. To understand whether this viral suppression in IPO323_SSV is specific to *in vitro* conditions, *ZtPRO1* expression and ZtFV1 abundance should be analysed during IPO323_SSV infection after the development of pycnidiospores, which display similar morphology and virulence to the wild type. If *ZtPRO1* downregulation does represent a defence response against ZtFV1, this is likely to only be adaptive *in vitro*, as the associated reductions in germination and virulence are unlikely to be advantageous during natural infection cycles. Alternatively, viral suppression in IPO323_SSV may be a pleiotropic effect of the genotype of this strain, and may not contribute to its fitness.

Results presented here also show multiple inconsistencies with studies of *F. graminearum* infection by FgV1, a mycovirus which causes reduced virulence in its host (Chu et al., 2002). Expression of genes involved in transcription and protein synthesis was found to increase in *F. graminearum* in response to FgV1, which is proposed to facilitate enhanced viral replication (Cho et al., 2012). Conversely, these processes displayed higher activity in IPO323_SSV, which contained a reduced abundance of ZtFV1. Secondly, FgV1 was recently found to combat RNA interference (RNAi)-based antiviral defence by suppressing the expression of *FgDICER2* and *FgAGO1*, enabled by the binding of a viral protein upstream of these genes (Yu et al., 2020). Here, wild type IPO323 showed higher expression of RNAi machinery despite the increased viral load of this strain compared to IPO323_SSV. This supports the hypothesis that the repression of ZtFV1 in IPO323_SSV is not the result of a conventional antiviral

defence, but a pleiotropic consequence of its developmental phenotype. Furthermore, upregulation of RNAi machinery in wild type IPO323 may represent a transcriptional defence response against ZtFV1, but suggests that this response is ineffective at suppressing the virus. Due to the importance of RNAi in antiviral defence, many viruses have coevolved to produce viral suppressors of RNA silencing (VSRs). VSRs are known to inhibit host RNAi via a wide variety of mechanisms other than transcriptional repression (Csorba et al., 2015). Although VSRs have been abundantly characterised in plant viruses, only one VSR has been identified in a mycovirus (Segers et al., 2006). The lack of ZtFV1 suppression in IPO323 despite the expression of RNAi machinery indicates that this virus might encode a VSR.

Mycoviruses are known to influence plant pathogen fitness through their influence on growth, development and virulence factor production (Castro et al., 2003; Chu et al., 2002; Hao et al., 2018). The impact of ZtFV1 on host fitness should be explored by inoculation of uninfected *Z. tritici* strains with *in vitro* transcribed viral RNA, as has been previously demonstrated in *Sclerotinium sclerotiorum* (Marzano et al., 2015). It is likely that all maintained laboratory IPO323 strains contain ZtFV1, as mycoviruses are mainly transmitted intracellularly through asexual reproduction and hyphal anastomosis (Pearson et al., 2009). Furthermore, ZtFV1 was identified in multiple RNA-seq studies of IPO323 from different laboratories (Gilbert et al., 2019). Therefore, a naïve host needs to be identified by screening for ZtFV1 in the transcriptome datasets from other *Z. tritici* strains (Haueisen et al., 2019; Palma-Guerrero et al., 2017), which will also help elucidate the global prevalence of this mycovirus in *Z. tritici* populations. Given the abundance of ZtFV1 in wild type IPO323, which displays normal morphology and symptom development on susceptible hosts, it is implausible that this virus causes major repression of host virulence as reported in other species (Chu et al., 2002; Hao et al., 2018). However, the possibility of enhanced *Z. tritici* virulence caused by ZtFV1 warrants additional study.

Moreover, further study is required to uncover any impact on viral infection caused by the SNP identified here in the ZtFV1 genome. The sequences of ZtFV1 in IPO323 strains from other laboratories have so far been identical (Gilbert et al., 2019), suggesting remarkable stability of the viral genome through *in vitro* subculture. Whether the ZtFV1 variant identified in the wild type

IPO323 strain from our laboratory is associated with the high abundance of viral RNA in this strain, and whether this has an impact on *Z. tritici* phenotype, should be investigated.

## 6.5 Conclusions

This study elucidates the genetic and transcriptomic causes of abnormal morphological development, defective hyphal germination and reduced virulence in IPO323_SSV, a spontaneous variant of the *Z. tritici* reference isolate which has been identified in multiple laboratories. Genome resequencing identified a large deletion at the end of chromosome 5, as well as a disruptive deletion in the putative light-regulated transcription factor *ZtWC1*. Transcriptome analysis identified activation of cell cycle and protein biosynthesis machinery and downregulation of stress response and cell wall remodelling genes, revealing the cellular processes underlying the IPO323_SSV phenotype. Homologs of light-responsive genes from other ascomycetes were repressed in IPO322_SSV, strongly supporting the hypothesis that *ZtWC1* disruption is the principal cause of the phenotype of this strain, and implicating this transcription factor in regulating *Z. tritici* development and virulence. Finally, the *Z. tritici* mycovirus ZtFV1 was shown to display reduced abundance in IPO323_SSV, providing insights into this hitherto uncharacterised interaction.

## 6.6 Supplementary information

**Figure S6.1 IPO323_SSV has lost chromosome 18 and the 3' end of chromosome 5**
Coverage of *Z. tritici* chromosomes by reads from whole genome resequencing of IPO323 and IPO323_SSV. Generated using Qualimap v.2.2.1 *bamqc* function on BAM alignment files

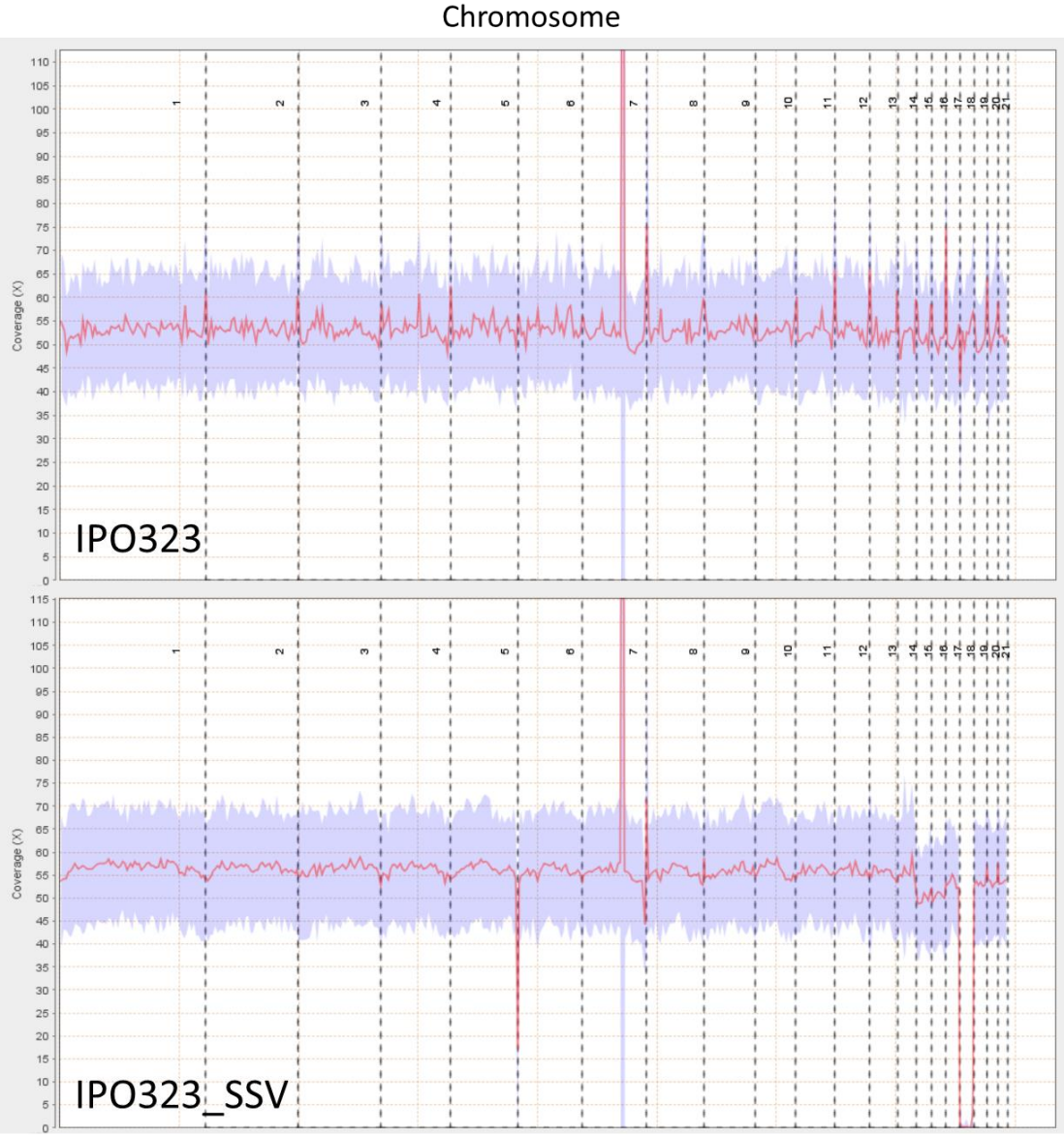

## Table S6.1 Unique polymorphisms in IPO323_SSV genome sequence

| Position | Reference | IPO323_SSV | Type | Sequence Name | Gene Location | Sequence Description | InterPro Name | Differentially expressed |
|---|---|---|---|---|---|---|---|---|
| 3:2780000 | A | T | upstream_gene_variant | ZtritIPO323_04g08144 | 3:2775363-2776256 | 3-oxoacyl-reductase like | Short-chain dehydrogenase/reductase SDR;NAD(P)-binding domain | No |
| | | | upstream_gene_variant | ZtritIPO323_04g08145 | 3:2776737-2777822 | 1-acyl-sn-glycerol-3-phosphate acyltransferase beta like | Phospholipid/glycerol acyltransferase;1-acyl-sn-glycerol-3-phosphate acyltransferase | Upregulated |
| | | | upstream_gene_variant | ZtritIPO323_04g08146 | 3:2777963-2779282 | hypothetical protein TI39_contig5832g00011 | Ribosomal protein S35, mitochondrial | No |
| | | | upstream_gene_variant | ZtritIPO323_04g08147 | 3:2780807-2782753 | synaptic vesicle transporter svop | Major facilitator superfamily | Downregulated |
| | | | downstream_gene_variant | ZtritIPO323_04g08143 | 3:2773312-2775238 | MFS transporter | Major facilitator superfamily | No |
| | | | downstream_gene_variant | ZtritIPO323_04g08148 | 3:2782932-2790467 | beige BEACH domain-containing | BEACH domain;WD40/YVTN repeat-like-containing domain;PH-BEACH domain;Concanavalin A-like lectin/glucanase domain | No |
| 4:138 | A | G | intergenic_region | ZtritIPO323_04g08435 | 4:5701-6531 | NA | NA | No |
| 4:2879854 | GTT | GT | intergenic_region | ZtritIPO323_04g09442 | 4:2861265-2862581 | P450 monooxygenase | Cytochrome P450 | No |
| 5:2842982 | A | G | intergenic_region | ZtritIPO323_04g10445 | 5:2837214-2837805 | NA | Reverse transcriptase domain | No |
| 8:9437 | T | C | intergenic_region | ZtritIPO323_04g12284 | 8:25014-25374 | NA | NA | No |
| 8:9463 | C | T | intergenic_region | ZtritIPO323_04g12284 | 8:25014-25374 | NA | NA | No |
| 9:245952 | A | G | intergenic_region | ZtritIPO323_04g13213 | 9:229502-230026 | hypothetical protein MYCGRDRAFT_95526 | NA | Upregulated |
| | | | | ZtritIPO323_04g13214 | 9:253716-255161 | hypothetical protein MYCGRDRAFT_95527 | NA | No |
| 11:1480176 | T | G | upstream_gene_variant | ZtritIPO323_04g03529 | 11:1482755-1488544 | 20S cyclosome subunit (APC1 ) like | Anaphase-promoting complex subunit 1 | No |
| | | | downstream_gene_variant | ZtritIPO323_04g03526 | 11:1476457-1478013 | oxalate decarboxylase oxdC | Cupin 1;Bicupin, oxalate decarboxylase/oxidase;RmlC-like jelly roll fold;RmlC-like cupin domain | No |
| | | | downstream_gene_variant | ZtritIPO323_04g03527 | 11:1478295-1479368 | hypothetical protein TI39_contig516g00002 | NA | No |
| | | | downstream_gene_variant | ZtritIPO323_04g03528 | 11:1480387-1482195 | hypothetical protein MYCGRDRAFT_111361 | WD40/YVTN repeat-like-containing domain;WD40-repeat-containing domain | No |
| 12:935185 | TGA | TA | upstream_gene_variant | ZtritIPO323_04g03894 | 12:937745-938650 | hypothetical protein MYCGRDRAFT_97103 | NA | Upregulated |
| | | | downstream_gene_variant | ZtritIPO323_04g03892 | 12:931436-934838 | ddenn domain-containing | DENN domain;dDENN domain;uDENN domainProtein kinase C-like, phorbol ester/diacylglycerol-binding domain | No |
| | | | downstream_gene_variant | ZtritIPO323_04g03893 | 12:935684-937528 | bifunctional partial | Mur ligase, central;Mur ligase, C-terminal; Folylpolyglutamate synthetase | Upregulated |
| | | | downstream_gene_variant | ZtritIPO323_04g03895 | 12:938892-939957 | pex19 family | null;Pex19 protein;Pex19 protein | No |
| 14:535214 | G | A | downstream_gene_variant | ZtritIPO323_04g04660 | 14:529029-530824 | Phosphonoacetaldehyde hydrolase | null;null;null | No |

**Figure S6.2 Transcription machinery is upregulated in IPO323_SSV**
*Z. tritici* KEGG pathways for RNA polymerase (ko03020) and splicosome (ko03040), with genes upregulated (green), downregulated (red) or not differentially expressed (yellow) in IPO323_SSV compared to IPO233. Pathway components with no annotated genes are displayed in blue

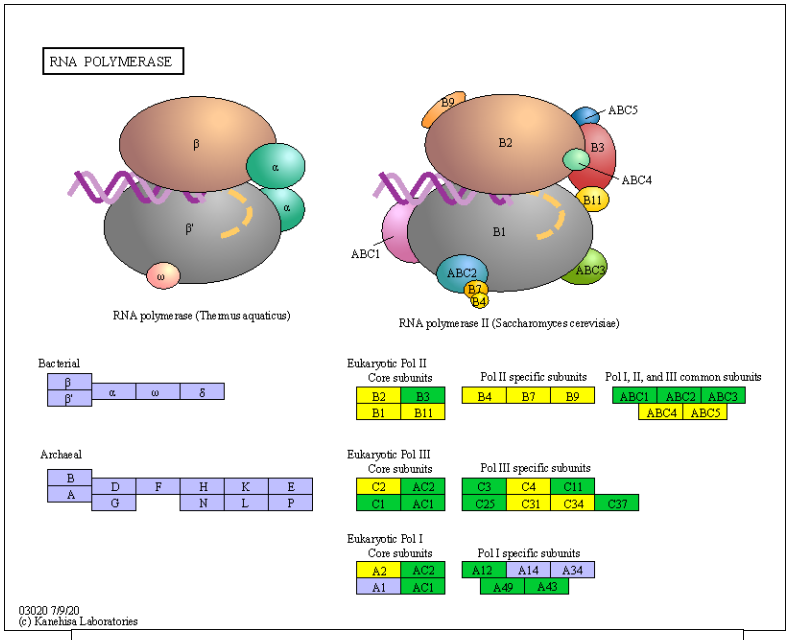


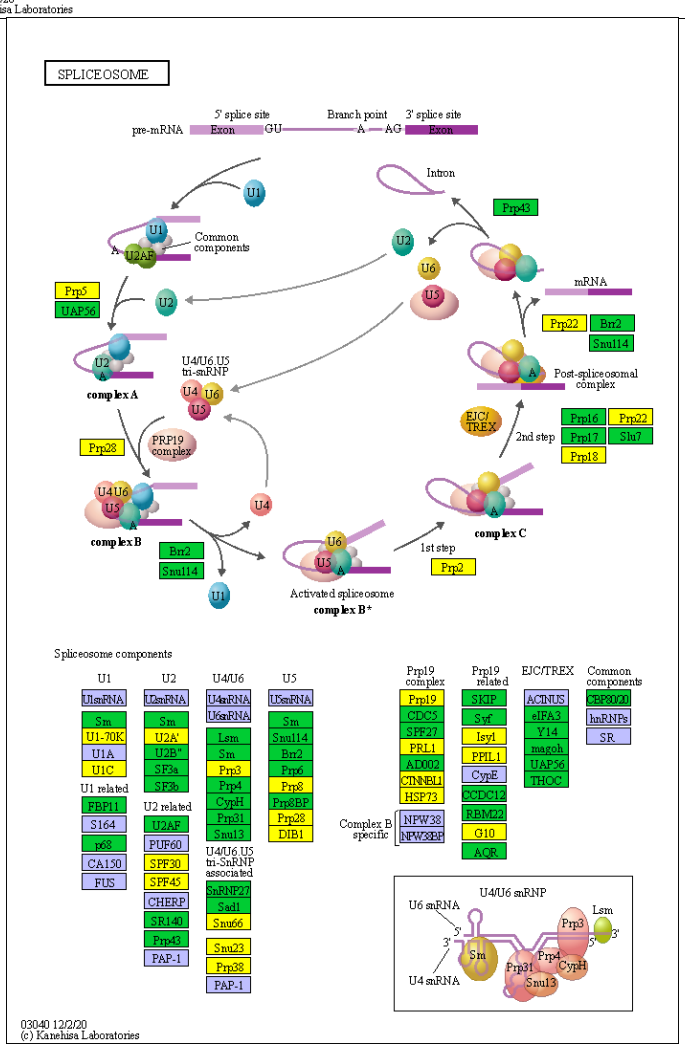

**Figure S6.3 Nucleotide biosynthesis is upregulated in IPO323_SSV**
*Z. tritici* KEGG pathways for the purine biosynthetic process (ko00230) and pyrimidine biosynthetic process (ko00240), with genes upregulated (green), downregulated (red) or not differentially expressed (yellow) in IPO323_SSV compared to IPO233. Pathway components with no annotated genes are displayed in blue.

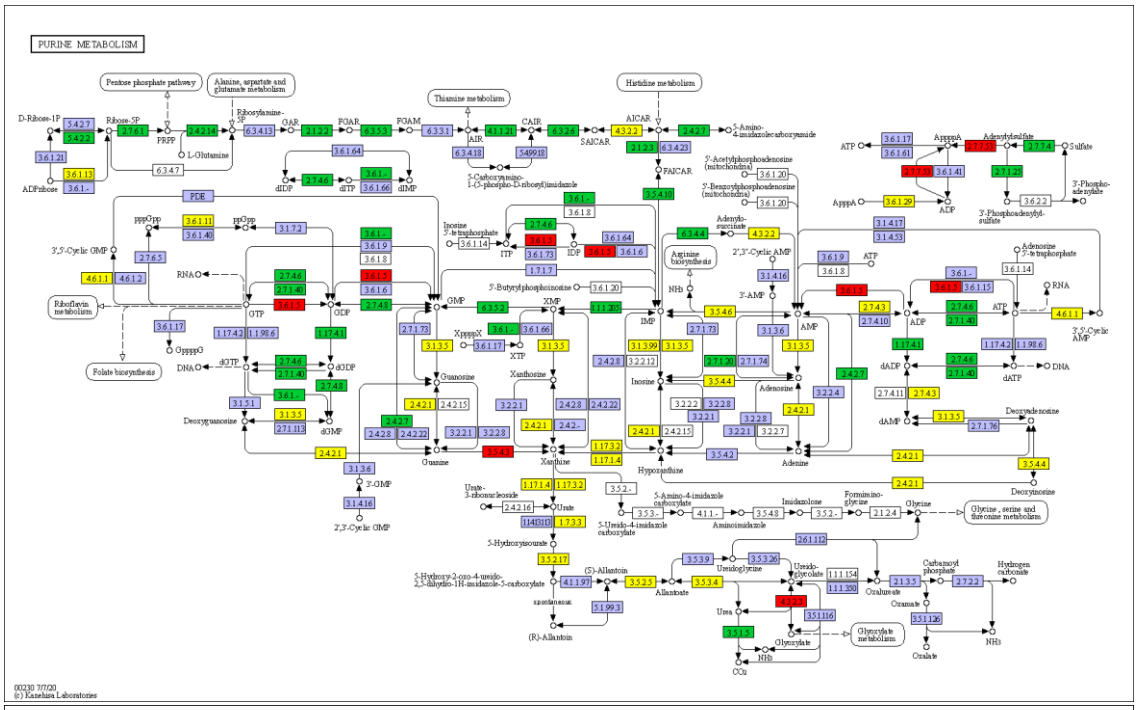


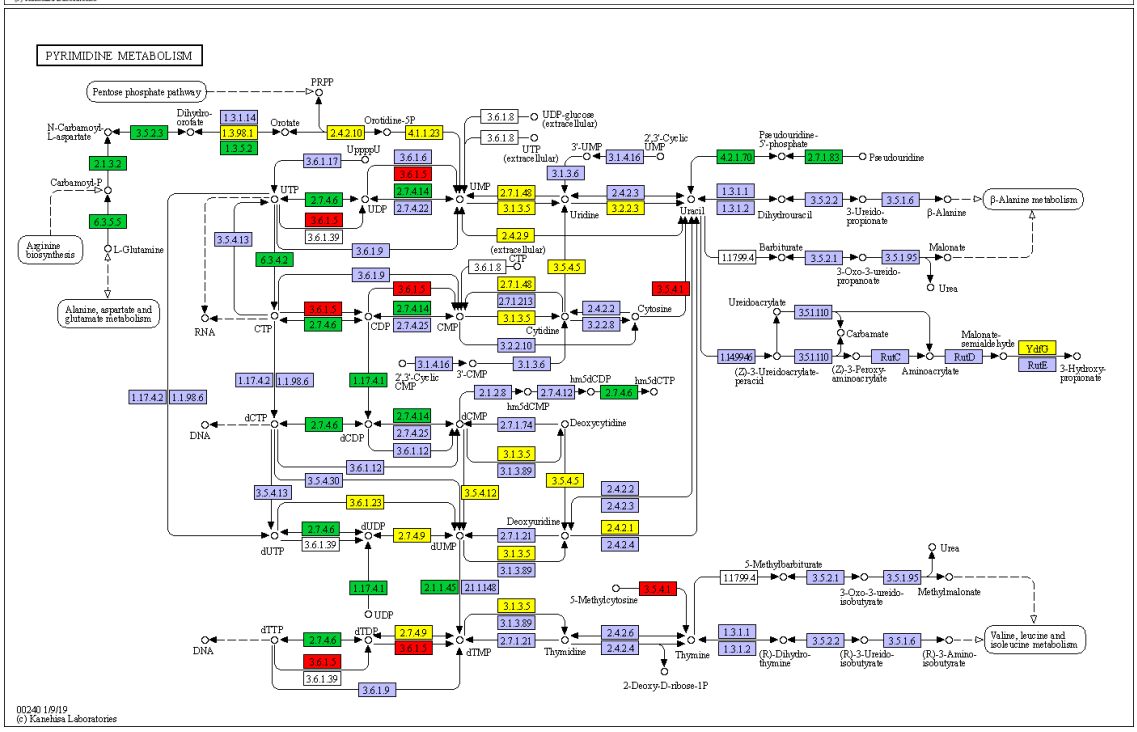

**Figure S6.4 The pentose phosphate pathway is upregulated in IPO323_SSV**

*Z. tritici* KEGG pathway for the pentose phosphate pathway (ko00030), with genes upregulated (green), downregulated (red) or not differentially expressed (yellow) in IPO323_SSV compared to IPO233. Pathway components with no annotated genes are displayed in blue.

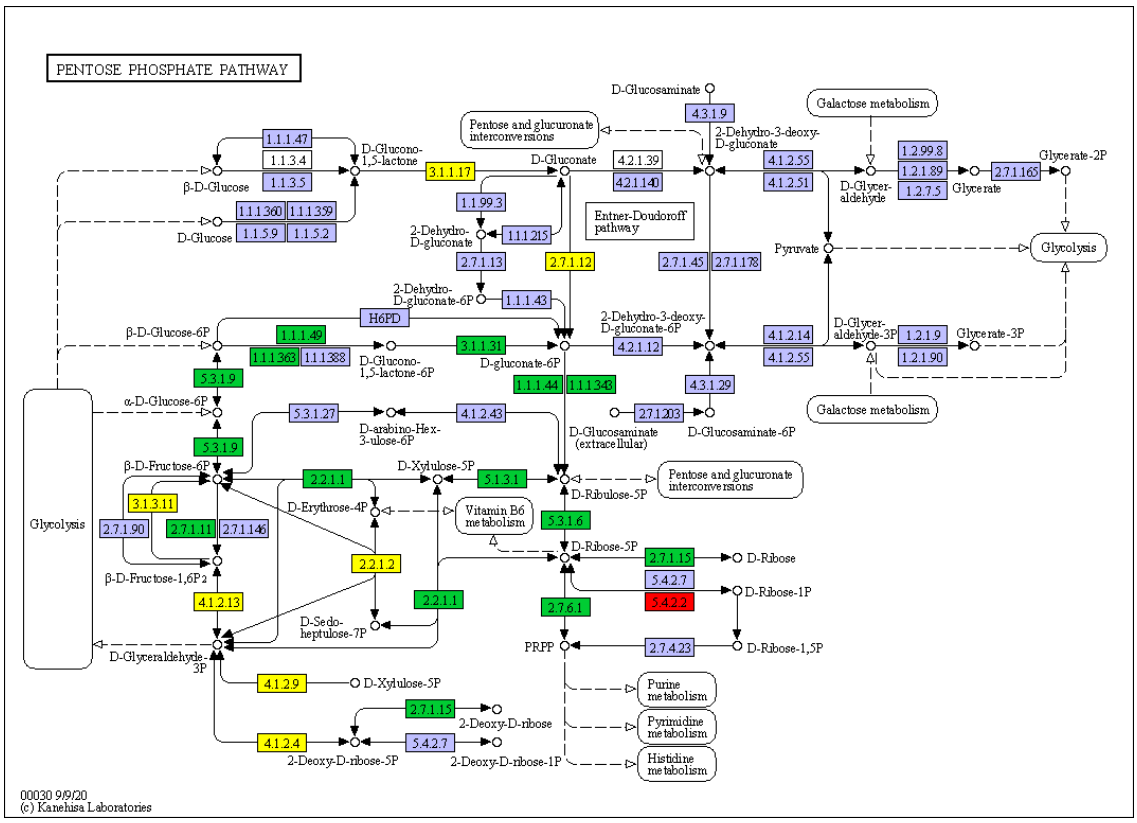

**Figure S6.5 DNA replication machinery is upregulated in IPO323_SSV**

*Z. tritici* KEGG pathway for the DNA replication (ko03030), with genes upregulated (green), downregulated (red) or not differentially expressed (yellow) in IPO323_SSV compared to IPO233. Pathway components with no annotated genes are displayed in blue.

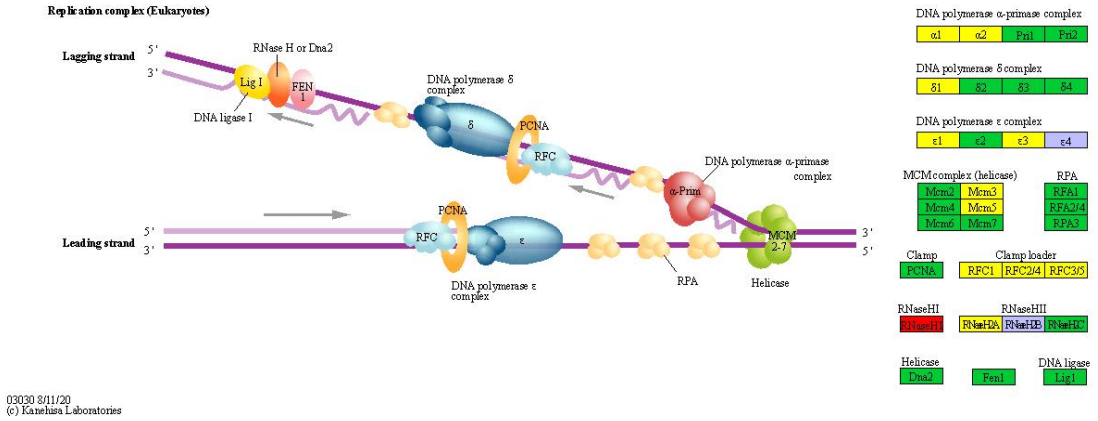

# Chapter 7
# **General Discussion**

## 7.1 Objectives of this thesis

At its outset, research for this thesis aimed to address questions surrounding the source of nutrition supporting germination and growth during symptomless infection of wheat by *Z. tritici* (Brennan et al., 2019; Sánchez-Vallet et al., 2015). Initially, this focused on autophagy (Chapter 3), the cellular recycling pathway that has become prominent as an important process in the development and virulence of fungal plant pathogens (Kershaw & Talbot, 2009; Lv et al., 2017; Ren et al., 2017). Additionally, detailed analysis of fatty acid β-oxidation was carried out (Chapter 4), in light of the proposed importance of utilising abundant lipid droplets within the *Z. tritici* spore for hyphal growth during early colonisation (Francisco et al., 2019; Rudd et al., 2015).

During these investigations, the unexpected identification of additional *Z. tritici* strains with attenuated virulence and altered growth morphology prompted the forward genetic characterisation of the cellular processes underlying these phenotypes. Whole genome resequencing of non-pathogenic T-DNA insertion strains identified disruption of genes within the cyclic adenosine monophosphate (cAMP)-protein kinase A (PKA) and cell wall integrity (CWI) signalling cascades, leading to further functional characterisation of these pathways during *Z. tritici* infection through transcriptomic analysis (Chapter 5). Furthermore, during early investigations of *Z. tritici* autophagy, a spontaneous mutant of the reference strain IPO323 was also identified, instigating exploration of the underlying genotypic and transcriptomic causes of this phenotype (Chapter 6).

The cumulative results obtained provide novel insights into the metabolic and signalling pathways involved in *Z. tritici* infection on wheat leaves.

## 7.2 Nutrient acquisition during the symptomless phase

One of the key remaining questions from the past decade of *Z. tritici* research is how the fungus gains nutrition during the symptomless phase of infection (Brennan et al., 2019). Researchers have posed the question of whether *Z. tritici* uses host-derived nutrients during epiphytic and apoplastic growth before the necrotrophic switch, and can therefore be defined as a hemibiotroph, or instead relies on stored lipids in the spore at this stage, favouring the term

‘latent necrotroph’ (Sánchez-Vallet et al., 2015). While previous transcriptome studies have identified the upregulation of putative lipid metabolism genes during early infection (Palma-Guerrero et al., 2017; Rudd et al., 2015), functional characterisation of these genes has not previously been reported.

### 7.2.1 Mitochondrial β-oxidation supports early colonisation

This thesis provides further evidence for the use of stored lipids by *Z. tritici* as a carbon source during early infection, through molecular characterisation of fatty acid β-oxidation (Chapter 4). Mitochondrial β-oxidation, through the enoyl-CoA hydratase enzyme ZtEch1, was shown to be crucial for the starvation-induced hyphal growth of *Z. tritici*, and hence the virulence of this pathogen. The germination of *Δztech1* blastospores was abolished on carbon-deficient medium, while hyphal growth on nitrogen-deficient medium was still observed. This suggests that defective epiphytic growth without mitochondrial β-oxidation is caused by an inability to remobilise stored carbon, rather than a defect in hyphal growth or the aberrant mitochondrial morphology in *Δztech1* spores. The continued contribution of ZtEch1 to symptomless colonisation of the mesophyll should be investigated by direct injection of *Δztech1* spores or hyphae into wheat leaves, or the conditional suppression of *ZtEch1* midway through the symptomless phase. Conditional gene expression at specific infection phases was recently achieved in *Ustilago maydis* by placing the target gene under the control of a promoter known to be regulated with the desired *in planta* transcription profile (Schmitz et al., 2020). This represents a powerful tool for studying the *in planta* function of genes whose deletion leads to inhibited germination or early invasive growth, such as FUS3 and HOG1 MAPKs in *Z. tritici* (Cousin et al., 2006; Mehrabi, Zwiers, et al., 2006).

Intriguingly, spontaneous rescue of germination in a subset of *Δztech1* cells indicates the potential for metabolic recovery in this background, and the possibility of redundancy with other enzymes or parallel β-oxidation pathways. Genomic and transcriptomic analysis of these *Δztech1Rev* strains is required to understand the cause of their phenotypic recovery. Although mitochondria and peroxisomes display division of labour in their β-oxidation functions in eukaryotes (Poirier et al., 2006), some overlap in function between these pathways has been identified in fungi (Kretschmer, Klose, et al., 2012;

Kretschmer, Wang, et al., 2012; Maggio-Hall & Keller, 2004). Furthermore, functional genomic analysis of putative peroxisomal β-oxidation genes and the apparent dispensability of MFP homologs, which are required for this pathway in other fungi (Hiltunen et al., 1992; Wang et al., 2007), provided preliminary evidence for the presence of a non-canonical peroxisomal β-oxidation pathway in *Z. tritici*. Characterisation of other putative peroxisomal β-oxidation enzymes, as well as the generation of peroxisome deficient *Z. tritici* strains, will help to investigate this pathway and uncover its function during infection.

These findings contribute to the growing evidence that lipid metabolism is crucial for the virulence of many plant pathogenic fungi, particularly during the early stages of infection by foliar pathogens (Solomon et al., 2004; Tang et al., 2019; Wang et al., 2007), raising its potential utility as an antifungal target. Further investigation of the enzymes that contribute to fatty acid metabolism in *Z. tritici* is necessary for developing inhibition of this process as a control strategy. In particular, elucidating the unique aspects of β-oxidation in these filamentous pathogens compared to mammalian and host plant cells is required to assess its suitability as a chemical target.

### 7.2.2 Autophagy is not required for lipid mobilisation or virulence

Despite the evidence presented here for the importance of lipid metabolism in early infection, questions still remain regarding the mechanisms used by *Z. tritici* to mobilise fatty acids from within lipid droplets. Disruption of autophagy in this thesis, through the deletion of *ZtATG1*, led to no defect in starvation-induced hyphal growth or virulence, suggesting that autophagy is dispensable for the recycling of stored lipids and cellular differentiation during infection (Chapter 3). However, these results do not rule out the contribution of autophagy to lipid droplet breakdown, as this may be complemented by the increased activity of cytosolic TAG lipases in *Δztatg1* mutants. Previous studies in *Saccharomyces cerevisiae* have identified both transcriptional and post-translational activation of these enzymes in autophagy-deficient strains (Maeda et al., 2015). The expression of candidate *Z. tritici* TAG lipases should therefore be analysed in wild type and *Δztatg1* backgrounds. Furthermore, targeted deletion of *Z. tritici* TAG lipase homologs could elucidate their importance to providing fatty acids

for β-oxidation during early infection, although functional redundancy between these enzymes is possible.

Evidence presented in this study suggests that *Z. tritici* undergoes active autophagy during blastosporulation on rich media. This is contrary to the inactivity of this processes during growth on rich media in *S. cerevisiae* (Cebollero & Reggiori, 2009). This discrepancy could be explained by the fact that blastosporulation is taken out of its natural context *in vitro*. Blastospores produced by lateral budding of epiphytic hyphae during early infection need to be filled with stored lipids, if they are to provide a viable secondary inoculum (Francisco et al., 2019). However, this occurs on the leaf surface where nutrients are scarce. In this context, autophagy may be involved in recycling intracellular membrane lipids for the formation of lipid droplets in developing blastospores, a function which has been demonstrated in starved mammalian cells (Rambold et al., 2015). This function may be maintained in *Z. tritici* during *in vitro* blastosporulation. Continued production of virulent blastospores in autophagy-deficient *Δztatg1* strains may be supported by the increased activity of fatty acid synthesis using the abundant carbon source available from rich medium. Indeed, fatty acid biosynthesis has been shown to be important for blastosporulation *in vitro*, as inhibition of FA synthase causes a switch to hyphal growth on rich media (Cairns et al. unpublished).

An autophagy-independent function of ZtATG8 was also suggested by the delay in symptoms development caused by *Δztatg8* strains. Discrepancy in the phenotypes of *Δatg1* and *Δatg8* strains of filamentous fungi have been reported (Nadal & Gold, 2010; Ying et al., 2016), although detailed characterisation of independent ATG8 functions are limited to model yeasts (Liu et al., 2018; Maeda et al., 2017). These studies have largely relied on strains lacking ATG8 conjugation to separate phenotypes from its functions in autophagy, which should be pursued in future investigation of *Z. tritici* autophagy.

### 7.2.3 *Z. tritici*: hemibiotroph or latent necrotroph?

Evidence to support the hypothesis that *Z. tritici* accesses significant nutrition from the host during epiphytic growth and early mesophyll colonisation is currently limited to the expression of a subset of secreted proteases, lipases and cell wall degrading enzymes at this stage (Palma-Guerrero et al., 2016;

Rudd et al., 2015). However, whether these enzymes function in accessing apoplastic nutrients is yet to be determined (Sánchez-Vallet et al., 2015). The appearance of chlorosis during late infection by *Δztcyr1* strains suggests that they continue to grow within the mesophyll, despite no evidence of induced necrosis (Chapter 5). Chlorosis in these leaves may be caused by stress resulting from the utilisation of apoplastic nutrients. This finding suggests that *Z. tritici* may be capable of accessing host nutrients to support growth without extensive cell lysis, and that infection by *Δztcyr1* may show characteristics of colonisation by biotrophic endophytes (Rasmussen et al., 2012). However, the induction of some genes associated with necrotrophic growth at 9 dpi in *Δztcyr1*, including secreted hydrolytic enzymes, means that late infection by this strain may not be a suitable proxy for symptomless infection by the wild type.

The inability of *Δztech1* to germinate on the leaf surface provides strong evidence that internal lipid stores are the primary source of energy during early epiphytic growth. Furthermore, the ability of *Z. tritici* hyphae to grow for at least three weeks on water agar, as observed here and in other studies (Kay, 2017), suggests that blastospores contain enough stored nutrients to support extensive hyphal growth. Indeed, the level of hyphal proliferation under starvation *in vitro* potentially exceeds that observed during the symptomless phase before induction of necrosis (Keon et al., 2007; Haueisen et al., 2019). Therefore, any contribution of apoplastic nutrients to *Z. tritici* mesophyll colonisation is likely to be minor and perhaps dispensable. Moreover, molecular characterisation of this contribution is likely to be hindered by functional redundancy between the enzymes required for breakdown and uptake of external nutrients. Overall, this thesis supports the definition of *Z. tritici* as a latent necrotroph.

Questions remain over use of the term hemibiotroph to define other apoplastic pathogens with prolonged asymptomatic phases during initial infection (Précigout et al., 2020). Along with *Z. tritici*, multiple other Dothideomycete fungi have long been defined as hemibiotrophic, including the devastating banana pathogen *Mycosphaerella fijisiensis* causing black sigatoka, the canola blackleg disease pathogen *Leptospheria maculans* and the pine needle blight fungus *Dothistroma septosporum* (Ohm et al., 2012). These pathogens also colonise the leaf tissue through stomata and inhabit the apoplast asymptomatically for extended periods before causing necrosis. Similar to *Z. tritici*, *D. septosporum*

encodes a reduced complement of predicted PCWDEs and displays higher expression of these genes during the necrotrophic phase (Bradshaw et al., 2016; de Wit et al., 2012). Furthermore, the glyoxylate cycle gene ICL1 was found to be essential for *L. maculans* pathogenicity through supporting hyphal growth during early infection, suggesting stored lipids may support early infection by this fungus (Idnurm & Howlett, 2002). Currently, evidence for biotrophic feeding by these pathogens before the induction of necrosis is unclear, raising the possibility that other 'hemibiotrophs' of this fungal class may be better described as latent necrotrophs. Analysis of *in planta* lipid metabolism gene expression and functional characterisation of fatty acid β-oxidation genes during infection by these pathogens is required to assess the importance of stored lipids to their pathogenicity.

## 7.3 Signalling pathways underpinning the *Z. tritici* infection cycle

Perception of external cues during host colonisation is crucial for controlling infection-related development, adaptation to the host environment and virulence in pathogenic organisms. For many plant pathogenic fungi, this involves host surface recognition to induce the differentiation of penetration structures, and sensing of the internal host environment to combat defence responses and control invasive growth (Sakulkoo et al., 2018; Turrà et al., 2014). Forward genetic investigation of virulence determinants in this thesis provided novel insights into the signalling pathways that control *Z. tritici* infection at various stages, including regulation of hyphal growth, adaptation to the host environment and the induction of necrosis (Chapters 5 and 6).

### 7.3.1 Light signalling in *Z. tritici* development and virulence

The defects in hyphal morphogenesis and virulence identified in the spontaneous mutant IPO323_SSV are potentially associated with a deletion in the putative light-responsive gene *ZtWC-1* (Chapter 6). If confirmed through complementation experiments, this indicates the possible function of light signalling during *Z. tritici* infection. The regulation of *Z. tritici* growth and morphology by light during invasion may be advantageous, considering the reliance of this pathogen on stomatal penetration (Kema, Yu, et al., 1996), and

the increased stomatal opening during the day in response to light (Shimazaki et al., 2007). If light signalling is inhibited in IPO323_SSV through ZtWC-1 disruption, reduced filamentation and preferential blastosporulation in this strain may represent a defect in adaptive control of development by light. Promoting hyphal growth during the day when stomata are open could enhance host penetration, while blastosporulation at night may generate secondary inoculum which could be dispersed by the formation of dew. To explore the influence of light on *Z. tritici* development, future studies should assess the effect of different light regimes on hyphal growth and blastosporulation during starvation *in vitro*. This would be complemented by investigating the impact of shading during early infection on virulence, similar to previous experiments demonstrating the role of light in the induction of necrosis by *Z. tritici* (Keon et al., 2007).

Furthermore, light exposure experienced by *Z. tritici* during epiphytic growth will likely lead to oxidative stress (Fuller et al., 2015), providing another potential *in planta* function of light regulation in this stress response. Blue light signalling through WC-1 has been shown to regulate resistance to UV-mediated oxidative stress in multiple fungal species (Canessa et al., 2013; Fuller et al., 2013; Idnurm & Heitman, 2005), suggesting visible light is used as a signal of more damaging shorter wavelengths (Fuller et al., 2015). IPO323_SSV displayed increased sensitivity to hydrogen peroxide, which provides preliminary evidence for the role of ZtWC-1 in the oxidative stress response. Assessing the effect of pre-exposure to light on *Z. tritici* sensitivity to oxidative will help investigate this putative function.

### 7.3.2 Cell wall integrity signalling during adaptation to the host environment

A recent study comparing *Z. tritici* gene expression during *in vitro* carbon starvation and early infection found some overlap in expression profiles, including several infection-associated genes (Francisco et al., 2019). However, the set of genes identified was relatively small compared to the number of genes identified as upregulated in *Z. tritici* during early leaf colonisation (Rudd et al., 2015), and did not include the LysM-domain effectors known to be crucial for evasion of host defences (Marshall et al., 2011; Tian et al., 2021). This

suggests that cues from the host environment other than nutrient starvation are important for regulating infection-related processes in *Z. tritici*.

Results in this thesis suggest that the CWI pathway is involved in regulating adaptation to the host apoplast by controlling the expression of secreted genes, including the essential LysM effectors (Chapter 5). This regulation is essential for suppression of the host immune response, explaining previous reports of CWI pathway disruption causing failure to colonise the mesophyll (Mehrabi, Van Der Lee, et al., 2006). Regulation of infection-related gene expression may therefore involve perception of signals in the apoplast that disrupt the *Z. tritici* cell wall upon invasion. Future studies should investigate gene expression in *Z. tritici* upon exposure to cell wall perturbation, to investigate the potential co-regulation of this response with virulence-associated genes. These findings contribute to a growing body of evidence that the CWI pathway is important for host defence evasion by fungal plant pathogens (Turrà et al., 2014).

### 7.3.3 Potential role of cAMP-PKA signalling in the transition to necrotrophy

Several crucial questions remain unanswered surrounding the switch to necrotrophic growth during *Z. tritici* infection (Brennan et al., 2019); what triggers this transition in feeding habit, how does the fungus induce host necrosis and what is the adaptive function (if any) of the latent phase? Previous studies have implicated *Z. tritici* manipulation of host mitogen-activated protein kinase (MAPK) signalling and chromatin remodelling in controlling the transcriptional changes seen in the plant during the transition to necrotrophy (Lee et al., 2015; Rudd et al., 2008). Furthermore, transcriptional studies have identified host defence suppression during the symptomless phase (Rudd et al., 2015), which is known to require *Z. tritici* effector proteins (Marshall et al., 2011). This has led to the hypothesis disease progression is governed by *Z. tritici* 'hi-jacking' host defence signalling, first through immune suppression and then activation of programmed cell death associated with the hypersensitive response (Hammond-Kosack & Rudd, 2008). However, the signalling pathways and secreted factors governing this switch in growth habit in the fungus remain largely uncharacterised.

After initial identification of a point mutation in the *Z. tritici* adenylate cyclase gene (*ZtCYR1)* associated with avirulence, targeted deletion provided evidence for the role of cAMP-PKA signalling in controlling the necrotrophic switch (Chapter 5). Despite evidence of continued growth of *Δztcyr1* in the host, this strain did not cause necrotic lesions or induce the associated wheat defence response seen during wild type infection. Differential regulation of secreted proteins associated with the transition to necrotrophy (Rudd et al., 2015), including putative effectors, identified in this strain could explain this defect in infection progression. These results not only implicate the cAMP-PKA pathway in regulating necrotrophic growth, but also provide leads into the potential *Z. tritici* virulence factors which induce the host hypersensitive response.

Further study is required to understand the upstream signals which regulate adenylate cyclase and PKA activity in *Z. tritici*, which could elucidate the triggers regulating the necrotrophic switch. This should include further analysis of the G-protein coupled receptor proteins previously found to influence *Z. tritici* cAMP production and virulence (Mehrabi et al., 2009). Although the cAMP-PKA signalling is well characterised to respond to environmental nutrient status in *S. cerevisiae*, this pathway has also been characterised to respond to a wide range of external stimuli in fungal pathogens to control morphology and virulence (Fuller & Rhodes, 2012). In fact, activation of PKA is induced in multiple plant pathogens during host penetration on the leaf surface where external nutrients are scarce (Choi & Dean, 1997; Z. Yang & Dickman, 1999), suggesting divergence from the activation of *S. cerevisiae* PKA by extracellular glucose (Tamaki, 2007). Induction of the necrotrophic switch could therefore be regulated by PKA after perception of changing conditions in the host during colonisation, or dwindling internal nutrient stores in the pathogen.

As previously mentioned, evidence for the continued growth of *Δztcyr1* without host necrosis suggests that infection by this strain may resemble endophyte colonisation. *Z. tritici* has been proposed to have evolved from a non-pathogenic endophyte ancestor, considering the lack of intracellular growth and reduced PCWDE content in its genome (Goodwin et al., 2011; Sánchez-Vallet et al., 2015). Considering these findings, the potential function of the cAMP-PKA pathway in controlling necrotrophic growth may provide a crucial link in the evolution of pathogenicity in *Z. tritici.* The latent period without feeding during *Z.*

*tritici* infection could be an artefact of an ancestral endophyte, which may have required an initial period of self-supported growth while establishing suppression of host defence. The maintenance of this latent phase could enhance *Z. tritici* fitness by helping the fungus to establish mesophyll colonisation before inducing necrosis, allowing access to more stomata required for asexual sporulation. Observations of reduced pycnidia production after truncation of the latent period provides some evidence to support this, with authors speculating that symptomless growth allows the fungus to reach a "critical internal biomass" before the necrotrophic switch (Lee et al., 2015).

### 7.3.4 Signalling pathways as targets for fungal pathogen control

There is an increasing body of evidence for the importance of MAPK and cAMP-PKA signalling to the virulence of fungal pathogens of plants and humans (Dichtl et al., 2016; Fuller & Rhodes, 2012; Turrà et al., 2014). These pathways therefore represent potentially useful targets for antifungal control strategies. This is particularly true considering the pleiotropic functions of these pathways in various cellular processes required for virulence, which reduces the potential for the development of antifungal resistance (Fuller & Rhodes, 2012). Furthermore, there is evidence for the synergistic enhancement of drug activity by inhibition of these signalling pathways, potentially due to their role in the resistance response to other antifungals (Bastidas et al., 2009; Dichtl et al., 2016). For example, PKC inhibition and deletion has been found to increase sensitivity to echinocandin and azole fungicides (LaFayette et al., 2010; Sussman et al., 2004).

The fungal cell wall has been widely recognised as a key potential target for the development of fungicides, given its specificity to this kingdom containing many pathogens of eukaryotic hosts (Hasim & Coleman, 2019; Odds et al., 2003). Inhibition of signal transduction pathways involved in regulating cell wall synthesis and remodelling, such as the CWI pathway, remain an as yet unexploited target for potential fungicides (Heinisch, 2005; Heinisch & Rodicio, 2018). The cAMP-PKA pathway also falls into this category, having also been implicated in regulating the cell wall stress response in multiple fungal pathogens (Fuller et al., 2011; Zhu et al., 2017), including in *Z. tritici* here (Chapter 5).

Further elucidation of the signalling components in the *Z. tritici* CWI and cAMP-PKA pathways, and the signals that they perceive, will be crucial for understanding their potential use as targets for disease control.

## 7.4 Perspectives on *Z. tritici* research

### 7.4.1 Is it time for a new reference strain?

The instability of the *Z. tritici* genome under laboratory culture conditions has been previously demonstrated, with large chromosomal polymorphisms appearing during *in vitro* subculture (Möller et al., 2018). As well as the loss of chromosome 18, genotypic analysis of the spontaneous IPO323 mutant IPO323_SSV identified large deletions in a conserved fungal transcription factor and the subtelomeric region of chromosome 5 (Chapter 6). These deletions were associated with reduced virulence and altered morphological development in this strain. Polymorphisms such as these are distinct from the chromosomal losses and rearrangements that have been previously characterised during asexual propagation of *Z. tritici* (Möller et al., 2018). Furthermore, a spontaneous SNP in the ZtCYR1, identified here, was associated with loss of necrotrophic growth and asexual development in the host, but no dramatic defect during *in vitro* growth (Chapter 5). This highlights the potential impact of polymorphisms on *Z. tritici* pathogenicity that may go unnoticed in laboratory strains without assessment of genotype and *in planta* phenotype.

Considering these findings, a study needs to be instigated to sequence IPO323 strains from different laboratories, in order to understand the genotypic variation in this ‘reference’ strain. Previous proposals of karyotyping IPO323 strains (discussed at the ‘*Zymoseptoria tritici* community meeting 2017’ in Kiel, Germany) should be extended to next generation sequencing. This is required to encompass more cryptic polymorphisms gained during *in vitro* subculture, such as those identified in this thesis. Such a study is crucial for the comparison of parallel research in different laboratories, including the interpretation of results in the published literature and the appraisal of new results in contrast with other studies.

The sequencing of the IPO323 genome, published 10 years ago (Goodwin et al., 2011), enabled rapid progress in the understanding of *Z. tritici* infection

through functional genomic and transcriptomic studies (Brunner et al., 2013; Mirzadi Gohari et al., 2015; Rudd et al., 2015). Moreover, this facilitated the omics analysis of other strains using short read sequencing and alignment to this high quality reference assembly (Palma-Guerrero et al., 2017; Stukenbrock et al., 2011). However, developments in next generation sequencing call into question the utility of studying one isolate, with the option of resequencing and assembly of new high quality genomes becoming increasingly available (Badet et al., 2020). This is especially true considering the increasing evidence for dramatic variation in *Z. tritici* strains at a genomic and transcriptomic level (Badet et al., 2020; Haueisen et al., 2019; Palma-Guerrero et al., 2017), which translates to diversity in morphology, development and infection strategy of this pathogen (Haueisen et al., 2019).

Perhaps a bank of strains with fully assembled genomes should be defined and disseminated to encompass the variation in traits such as aggressiveness, host cultivar specificity and infection-related development. This would enable the broadening of our understanding of molecular host-pathogen interactions beyond IPO323. At least, if the continued use of a 'reference' isolate is deemed to be required, the *Z. tritici* community should consider the selection of a new strain, in order to start afresh without the genotypic variation known to be present in global IPO323 population almost 40 years after its isolation. Furthermore, the rapid evolution of *Z. tritici* under the strong selection pressures of fungicide application and deployment of resistance genotypes may have led to dramatic changes in pathogen the pathogen genome over this time frame (McDonald & Stukenbrock, 2016). Indeed, the avirulence gene *AvrStb6*, recently discovered in IPO323 (Zhong et al., 2017), has undergone rapid selection in the *Z. tritici* population since this strain was isolated, leading to the complete loss of the avirulent isoform in modern field isolates with widespread use of the corresponding *Stb6* wheat genotype (Stephens et al., 2021).

### 7.4.2 Future identification of virulence determinants in *Z. tritici*

Transcriptomics using RNA sequencing has been invaluable in understanding the molecular basis of host-pathogen interactions, progressing the field from focus on individual genes of interest to global analysis of both host and pathogen factors across different stages of infection (Kawahara et al., 2012;

Westermann et al., 2017). This has been seen in studies of the *Z. tritici*-wheat interaction, starting with investigation of individual fungal strains (Kellner et al., 2014; Rudd et al., 2015; Yang et al., 2013), and progressing to comparative studies revealing variation in molecular strategies of different isolates (Haueisen et al., 2019; Palma-Guerrero et al., 2017). These studies have changed our understanding of the *Z. tritici* infection strategy (Sánchez-Vallet et al., 2015), and identified many genes which may be crucial to its virulence, providing leads for further characterisation using reverse genetic approaches. Indeed, the investigation of fatty acid β-oxidation in the present study was prompted by evidence of the upregulation of genes putatively involved in lipid metabolism during early infection (Rudd et al., 2015).

However, since these transcriptomic studies, only a handful of studies have characterised genes contributing to *Z. tritici* virulence (Choi et al., 2016; Francisco et al., 2020; Habig et al., 2020; King et al., 2017; Mohammadi et al., 2017; Poppe et al., 2015; Tiley et al., 2018). This may have resulted from the emergence of *Z. tritici* as a model system for the study of plant pathogen evolutionary genomics (Feurtey et al., 2019), which has become the focus of many groups working on the species. Understanding of the cellular processes contributing to *Z. tritici* infection is therefore far behind other model pathogen species, such as *Magnaporthe oryzae*, and requires significantly more attention. However, *Z. tritici* is well placed to become leading system in our understanding of infection by apoplastic Dothideomycete pathogens, which cause a number of economically important diseases (Ohm et al., 2012).

Future elucidation of *Z. tritici* virulence factors should utilise the recent advances in next generation sequencing technologies to streamline research. The efficiency of forward genetics techniques is greatly enhanced by cheap and rapid sequencing, and provides the advantage that investment of time and resources in detailed characterisation is done in the knowledge that the target is involved in virulence. However, forward genetics is not suitable for identifying essential genes as potential targets of control strategies, which is more amenable to reverse genetic techniques involving the introduction of inducible promoters. Implementation of these techniques will be invaluable in identifying novel targets for control of *Z. tritici*.

Furthermore, RNA sequencing is becoming a powerful tool for understanding the regulatory networks underlying pathogen infection, through analysis of transcriptomic changes upon disruption of signalling components by reverse genetics, as exemplified in this thesis (Chapter 5) and other studies (Sakulkoo et al., 2018). This technique should be deployed to further investigate the control of infection related-processes by the MAPKs HOG1 and FUS3, which could lead to identification of downstream processes involved in germination and host penetration previously identified as controlled by these pathways in *Z. tritici* (Cousin et al., 2006; Mehrabi, Zwiers, et al., 2006). Other regulatory networks that require investigation in *Z. tritici* include the SNF1 pathway, which has been found to regulate PCWDE expression in multiple plant pathogens (Feng et al., 2014; Lee et al., 2009), and may help reveal the importance of these hydrolytic enzymes to *Z. tritici* infection. Moreover, future studies should investigate the *Z. tritici* unfolded protein response, which is emerging as a promising potential target for fungal disease control with pleiotropic influences on processes required in all pathogens, including effector secretion, responses to stress and cellular development (Guillemette et al., 2014; Hampel et al., 2016; Krishnan & Askew, 2014; Pinter et al., 2019; Tang et al., 2015).

## 7.5 Summary

In summary, the present thesis reveals novel understanding of the cellular mechanisms contributing to infection of wheat by *Z. tritici*. The crucial role of mitochondrial β-oxidation during growth under starvation and virulence was elucidated. This provides strong evidence for the importance of stored lipids in supporting early infection, and that *Z. tritici* is a 'latent necrotroph'. Autophagy was found to be dispensable for virulence in *Z. tritici*, implicating the function of direct lipolysis in the breakdown of lipid droplets. Further insights into the role of intracellular signalling pathways in *Z. tritici* infection were also revealed. The CWI pathway was found to be involved in the regulation of secreted proteins required for the adaptation of *Z. tritici* to the host environment, while cAMP-PKA signalling was implicated in controlling the transition to necrotrophy. Finally, preliminary evidence was presented for the role of light signalling in *Z. tritici* development and virulence through the transcriptional regulator ZtWC-1. These findings provide numerous leads for future research into the molecular basis of

infection by this devastating pathogen, and identify potential targets for the development of new fungicides for use in its control.

## 8.1 References


Alexandratos, N., & Bruinsma, J. (2012). *World agriculture towards 2030/2050: the 2012 revision* (No. 12–03; ESA Working Paper).

Allen, A., Islamovic, E., Kaur, J., Gold, S., Shah, D., & Smith, T. J. (2013). The virally encoded killer proteins from Ustilago maydis. *Fungal Biology Reviews*, *26*(4), 166–173. https://doi.org/10.1016/j.fbr.2012.10.001

Allen, T. D., & Nuss, D. L. (2004). Specific and Common Alterations in Host Gene Transcript Accumulation following Infection of the Chestnut Blight Fungus by Mild and Severe Hypoviruses. *Journal of Virology*, *78*(8), 4145–4155. https://doi.org/10.1128/jvi.78.8.4145-4155.2004

Almagro Armenteros, J. J., Sønderby, C. K., Sønderby, S. K., Nielsen, H., & Winther, O. (2017). DeepLoc: prediction of protein subcellular localization using deep learning. *Bioinformatics*, *33*(21), 3387–3395. https://doi.org/10.1093/bioinformatics/btx431

Alnuaimi, A. D., O'Brien-Simpson, N. M., Reynolds, E. C., & Mccullough, M. J. (2013). Clinical isolates and laboratory reference Candida species and strains have varying abilities to form biofilms. *FEMS Yeast Research*, *13*(7), 689–699. https://doi.org/10.1111/1567-1364.12068

Appels, R., Eversole, K., Feuillet, C., Keller, B., Rogers, J., Stein, N., Pozniak, C. J., Choulet, F., Distelfeld, A., Poland, J., Ronen, G., Barad, O., Baruch, K., Keeble-Gagnère, G., Mascher, M., Ben-Zvi, G., Josselin, A. A., Himmelbach, A., Balfourier, F., … Wang, L. (2018). Shifting the limits in wheat research and breeding using a fully annotated reference genome. *Science*, *361*(6403), eaar7191. https://doi.org/10.1126/science.aar7191

Arraiano, L. S., & Brown, J. K. M. (2017). Sources of resistance and susceptibility to Septoria tritici blotch of wheat. *Molecular Plant Pathology*, *18*(2), 276–292. https://doi.org/10.1111/mpp.12482

Asakura, M., Ninomiya, S., Sugimoto, M., Oku, M., Yamashita, S. -i., Okuno, T., Sakai, Y., & Takano, Y. (2009). Atg26-Mediated Pexophagy Is Required for Host Invasion by the Plant Pathogenic Fungus Colletotrichum orbiculare. *The Plant Cell*, *21*(4), 1291–1304. https://doi.org/10.1105/tpc.108.060996

Asakura, M., Okuno, T., & Takano, Y. (2006). Multiple contributions of peroxisomal metabolic function to fungal pathogenicity in Colletotrichum lagenarium. *Applied and Environmental Microbiology*, *72*(9), 6345–6354. https://doi.org/10.1128/AEM.00988-06

Ashkani, S., Rafii, M. Y., Shabanimofrad, M., Miah, G., Sahebi, M., Azizi, P., Tanweer, F. A., Akhtar, M. S., & Nasehi, A. (2015). Molecular breeding strategy and challenges towards improvement of blast disease resistance in rice crop. *Frontiers in Plant Science*, *6*, 886. https://doi.org/10.3389/fpls.2015.00886

Badet, T., Oggenfuss, U., Abraham, L., McDonald, B. A., & Croll, D. (2020). A 19-isolate reference-quality global pangenome for the fungal wheat pathogen Zymoseptoria tritici. *BMC Biology*, *18*, 12. https://doi.org/10.1186/s12915-020-0744-3

Bailey, B. A. (1995). Purification of a protein from culture filtrates of Fusarium oxysporum that induces ethylene and necrosis in leaves of Erythroxylum coca. *Phytopathology*, *85*, 1250–1255. https://doi.org/10.1094/Phyto-85-1250

Baker, S. E., Kroken, S., Inderbitzin, P., Asvarak, T., Li, B., Shi, L., Yoder, O. C., & Turgeon, B. G. (2006). Two Polyketide Synthase-Encoding Genes Are Required for Biosynthesis of the Polyketide Virulence Factor , T-toxin , by Cochliobolus

heterostrophus. *Molecular Plant Microbe Interaction*, *19*(2), 139–149. https://doi.org/10.1094/MPMI-19-0139

Balestrini, R., & Bonfante, P. (2014). Cell wall remodeling in mycorrhizal symbiosis: A way towards biotrophism. *Frontiers in Plant Science*, *5*, 237. https://doi.org/10.3389/fpls.2014.00237

Balint-Kurti, P. (2019). The plant hypersensitive response : concepts , control and consequences. *Molecular Plant Pathology*, *20*(8), 1163–1178. https://doi.org/10.1111/mpp.12821

Ballou, E. R., Avelar, G. M., Childers, D. S., Mackie, J., Bain, J. M., Wagener, J., Kastora, S. L., Panea, M. D., Hardison, S. E., Walker, L. A., Erwig, L. P., Munro, C. A., Gow, N. A. R., Brown, G. D., MacCallum, D. M., & Brown, A. J. P. (2016). Lactate signalling regulates fungal β-glucan masking and immune evasion. *Nature Microbiology*, *2*, 16238. https://doi.org/10.1038/nmicrobiol.2016.238

Barre, A., Bourne, Y., & Van Damme, E. J. M. (2019). Overview of the Structure – Function Relationships of Mannose-Specific Lectins from Plants , Algae and Fungi. *International Journal of Molecular Sciences*, *20*, 254. https://doi.org/10.3390/ijms20020254

Bartlett, K., & Eaton, S. (2004). Mitochondrial β-oxidation. *European Journal of Biochemistry*, *271*(3), 462–469. https://doi.org/10.1046/j.1432-1033.2003.03947.x

Bastidas, R. J., Reedy, J. L., Morales-johansson, H., Heitman, J., & Cardenas, M. E. (2009). Signaling cascades as drug targets in model and pathogenic fungi. *Current Opinion in Investigational Drugs*, *9*(8), 856–864.

Beaufour, M., Godin, F., Vallée, B., Cadene, M., & Bénédetti, H. (2012). Interaction proteomics suggests a new role for the Tfs1 protein in yeast. *Journal of Proteome Research*, *11*(6), 3211–3218. https://doi.org/10.1021/pr201239t

Bebber, D. P., Ramotowski, M. A. T., & Gurr, S. J. (2013). Crop pests and pathogens move polewards in a warming world. *Nature Climate Change*, *3*(11), 985–988. https://doi.org/10.1038/nclimate1990

Behr, M. A. (2002). BCG - Different strains, different vaccines? *Lancet Infectious Diseases*, *2*(2), 86–92. https://doi.org/10.1016/S1473-3099(02)00182-2

Ben M'Barek, S., Cordewener, J. H. G., Tabib Ghaffary, S. M., van der Lee, T. A. J., Liu, Z., Mirzadi Gohari, A., Mehrabi, R., America, A. H. P., Robert, O., Friesen, T. L., Hamza, S., Stergiopoulos, I., de Wit, P. J. G. M., & Kema, G. H. J. (2015). FPLC and liquid-chromatography mass spectrometry identify candidate necrosis-inducing proteins from culture filtrates of the fungal wheat pathogen Zymoseptoria tritici. *Fungal Genetics and Biology*, *79*, 54–62. https://doi.org/10.1016/j.fgb.2015.03.015

Ben M'Barek, S., Karisto, P., Abdedayem, W., Laribi, M., Fakhfakh, M., Kouki, H., Mikaberidze, A., & Yahyaoui, A. (2020). Improved control of septoria tritici blotch in durum wheat using cultivar mixtures. *Plant Pathology*, *69*(9), 1655–1665. https://doi.org/10.1111/ppa.13247

Benghezal, M., Roubaty, C., Veepuri, V., Knudsen, J., & Conzelmann, A. (2007). SLC1 and SLC4 encode partially redundant acyl-coenzyme A 1-acylglycerol-3-phosphate O-acyltransferases of budding yeast. *Journal of Biological Chemistry*, *282*(42), 30845–30855. https://doi.org/10.1074/jbc.M702719200

Berraies, S., Gharbi, M. S., Rezgui, S., & Yahyaoui, A. (2014). Estimating grain yield losses caused by septoria leaf blotch on durum wheat in Tunisia. *Chilean Journal of Agricultural Research*, *74*(4), 432–437. https://doi.org/10.4067/S0718-58392014000400009

Blake, J. J., Gosling, P., Fraaije, B. A., Burnett, F. J., Knight, S. M., Kildea, S., & Paveley, N. D. (2018). Changes in field dose–response curves for demethylation inhibitor (DMI) and quinone outside inhibitor (QoI) fungicides against Zymoseptoria tritici, related to laboratory sensitivity phenotyping and genotyping assays. *Pest Management Science*, *74*(2), 302–313. https://doi.org/10.1002/ps.4725

Boller, T., & Felix, G. (2009). A Renaissance of Elicitors: Perception of Microbe-Associated Molecular Patterns and Danger Signals by Pattern-Recognition Receptors. *Annual Review of Plant Biology*, *60*(1), 379–406. https://doi.org/10.1146/annurev.arplant.57.032905.105346

Bormann, J., Boenisch, M. J., Brückner, E., Firat, D., & Schäfer, W. (2014). The adenylyl cyclase plays a regulatory role in the morphogenetic switch from vegetative to pathogenic lifestyle of Fusarium graminearum on wheat. *PLoS ONE*, *9*(3). https://doi.org/10.1371/journal.pone.0091135

Both, M., Csukai, M., Stumpf, M. P. H., & Spanua, P. D. (2005). Gene Expression Profiles of Blumeria graminis Indicate Dynamic Changes to Primary Metabolism during Development of an Obligate Biotrophic Pathogen. *The Plant Cell*, *17*, 2107–2122. https://doi.org/doi/10.1105/tpc.105.032631

Bourguet, D., Delmotte, F., Franck, P., Guillemaud, T., Reboud, X., Vacher, C., Bordeaux, U., & Walker, A. S. (2013). Heterogeneity of selection and the evolution of resistance. *Trends in Ecology and Evolution*, *28*(2), 110–118. https://doi.org/10.1016/j.tree.2012.09.001

Bourguet, D., Delmotte, F., Franck, P., Guillemaud, T., Reboud, X., Vacher, C., & Walker, A. S. (2016). Combining selective pressures to enhance the durability of disease resistance genes. *Frontiers in Plant Science*, *7*, 1916. https://doi.org/10.3389/fpls.2016.01916

Bowler, J., Scott, E., Tailor, R., Scalliet, G., Ray, J., & Csukai, M. (2010). New capabilities for Mycosphaerella graminicola research. *Molecular Plant Pathology*, *11*(5), 691–704. https://doi.org/10.1111/j.1364-3703.2010.00629.x

Bradshaw, R. E., Guo, Y., Sim, A. D., Kabir, M. S., Chettri, P., Ozturk, I. K., Hunziker, L., Ganley, R. J., & Cox, M. P. (2016). Genome-wide gene expression dynamics of the fungal pathogen Dothistroma septosporum throughout its infection cycle of the gymnosperm host Pinus radiata. *Molecular Plant Pathology*, *17*(2), 210–224. https://doi.org/10.1111/mpp.12273

Brand, A. (2012). Hyphal growth in human fungal pathogens and its role in virulence. *International Journal of Microbiology*, *2012*, 517529. https://doi.org/10.1155/2012/517529

Brand, A., & Gow, N. A. (2009). Mechanisms of hypha orientation of fungi. *Current Opinion in Microbiology*, *12*(4), 350–357. https://doi.org/10.1016/j.mib.2009.05.007

Breen, J., Mur, L. A. J., Sivakumaran, A., Akinyemi, A., Wilkinson, M. J., & Lopez, C. M. R. (2016). Botrytis cinerea loss and restoration of virulence during in vitro culture follows flux in global DNA methylation. *BioRxiv*. https://doi.org/10.1101/059477

Brennan, C. J., Benbow, H. R., Mullins, E., & Doohan, F. M. (2019). A review of the known unknowns in the early stages of septoria tritici blotch disease of wheat. *Plant Pathology*, *68*(8), 1427–1438. https://doi.org/10.1111/ppa.13077

Brown, J. K. M., Chartrain, L., Lasserre-Zuber, P., & Saintenac, C. (2015). Genetics of resistance to Zymoseptoria tritici and applications to wheat breeding. *Fungal Genetics and Biology*, *79*, 33–41. https://doi.org/10.1016/j.fgb.2015.04.017

Bruder Nascimento, A. C., dos Reis, T. F., de Castro, P. A., Hori, J. I., Bom, V. L. P., de Assis, L. J., Ramalho, L. N. Z., Rocha, M. C., Malavazi, I., Brown, N. A., Valiante, V., Brakhage, A. A., Hagiwara, D., & Goldman, G. H. (2016). Mitogen activated protein kinases SakA HOG1 and MpkC collaborate for Aspergillus fumigatus virulence. *Molecular Microbiology*, *100*(5), 841–859. https://doi.org/10.1111/mmi.13354

Brun, S., Malagnac, F., Bidard, F., Lalucque, H., & Silar, P. (2009). Functions and regulation of the Nox family in the filamentous fungus Podospora anserina : a new role in cellulose degradation. *Molecular Microbiology*, *74*(2), 480–496. https://doi.org/10.1111/j.1365-2958.2009.06878.x

Brundrett, M. (2004). Diversity and classification of mycorrhizal associations. *Biological Reviews*, *79*, 473–495. https://doi.org/10.1017/S1464793103006316

Brunner, P. C., & McDonald, B. A. (2018). Evolutionary analyses of the avirulence effector AvrStb6 in global populations of Zymoseptoria tritici identify candidate amino acids involved in recognition. *Molecular Plant Pathology*, *19*(8), 1836–1846. https://doi.org/10.1111/mpp.12662

Brunner, P. C., Torriani, S. F. F., Croll, D., Stukenbrock, E. H., & McDonald, B. A. (2013). Coevolution and life cycle specialization of plant cell wall degrading enzymes in a hemibiotrophic pathogen. *Molecular Biology and Evolution*, *30*(6), 1337–1347. https://doi.org/10.1093/molbev/mst041

Cabib, E., & Arroyo, J. (2013). How carbohydrates sculpt cells: Chemical control of morphogenesis in the yeast cell wall. *Nature Reviews Microbiology*, *11*(9), 648–655. https://doi.org/10.1038/nrmicro3090

Cagliari, D., Dias, N. P., Galdeano, D. M., dos Santos, E. Á., Smagghe, G., & Zotti, M. J. (2019). Management of Pest Insects and Plant Diseases by Non-Transformative RNAi. *Frontiers in Plant Science*, *10*(October). https://doi.org/10.3389/fpls.2019.01319

Cairns, T. C., Sidhu, Y. S., Chaudhari, Y. K., Talbot, N. J., Studholme, D. J., & Haynes, K. (2015). Construction and high-throughput phenotypic screening ofZymoseptoria tritici over-expression strains. *Fungal Genetics and Biology*, *79*, 110–117. https://doi.org/10.1016/j.fgb.2015.04.013

Camões, F., Islinger, M., Guimarães, S. C., Kilaru, S., Schuster, M., Godinho, L. F., Steinberg, G., & Schrader, M. (2015). New insights into the peroxisomal protein inventory: Acyl-CoA oxidases and -dehydrogenases are an ancient feature of peroxisomes. *Biochimica et Biophysica Acta - Molecular Cell Research*, *1853*(1), 111–125. https://doi.org/10.1016/j.bbamcr.2014.10.005

Canessa, P., Schumacher, J., Hevia, M. A., Tudzynski, P., & Larrondo, L. F. (2013). Assessing the effects of light on differentiation and virulence of the plant pathogen botrytis cinerea: Characterization of the white collar complex. *PLoS ONE*, *8*(12). https://doi.org/10.1371/journal.pone.0084223

Cassola, A., Parrot, M., Silberstein, S., Magee, B. B., Passeron, S., Giasson, L., & Cantore, M. L. (2004). Candida albicans Lacking the Gene Encoding the Regulatory Subunit of Protein Kinase A Displays a Defect in Hyphal Formation and an Altered Localization of the Catalytic Subunit. *Eukaryotic Cell*, *3*(1), 190–199. https://doi.org/10.1128/EC.3.1.190-199.2004

Castro, M., Kramer, K., Valdivia, L., Ortiz, S., & Castillo, A. (2003). A double-stranded RNA mycovirus confers hypovirulence-associated traits to Botrytis cinerea. *FEMS Microbiology Letters*, *228*(1), 87–91. https://doi.org/10.1016/S0378-1097(03)00755-9

Catanzariti, A. M., & Jones, D. A. (2010). Effector proteins of extracellular fungal plant pathogens that trigger host resistance. *Functional Plant Biology*, *37*(10), 901–906. https://doi.org/10.1071/FP10077

Caza, M., & Kronstad, J. W. (2019). The cAMP/protein kinase a pathway regulates virulence and adaptation to host conditions in cryptococcus neoformans. *Frontiers in Cellular and Infection Microbiology*, *9*(JUN), 1–15. https://doi.org/10.3389/fcimb.2019.00212

Cebollero, E., & Reggiori, F. (2009). Regulation of autophagy in yeast Saccharomyces cerevisiae. *Biochimica et Biophysica Acta - Molecular Cell Research*, *1793*(9), 1413–1421. https://doi.org/10.1016/j.bbamcr.2009.01.008

Chacko, L., & Ananthanarayanan, V. (2019). Quantification of Mitochondrial Dynamics in Fission Yeast. *Bio-Protocol*, *9*(23), 1–9. https://doi.org/10.21769/bioprotoc.3450

Chen, C.-H., Ringelberg, C. S., Gross, R. H., Dunlap, J. C., & Loros, J. J. (2009). Genome-wide analysis of light-inducible responses reveals hierarchical light signalling in Neurospora. *The EMBO Journal*, *28*(8), 1029–1042. https://doi.org/10.1038/emboj.2009.54

Chen, L., Hou, B., Lalonde, S., Takanaga, H., Hartung, M. L., Qu, X., Guo, W., Kim, J., Underwood, W., Chaudhuri, B., Chermak, D., Antony, G., White, F. F., Somerville, S. C., Mudgett, M. B., & Frommer, W. B. (2010). Sugar transporters for intercellular exchange and nutrition of pathogens. *Nature*, *468*, 527–532. https://doi.org/10.1038/nature09606

Chen, R. E., & Thorner, J. (2007). Function and Regulation in MAPK Signaling Pathways. *Biochimica et Biophysica Acta*, *1773*(8), 1311–1340. https://doi.org/10.1016/j.bbamcr.2007.05.003

Chen, S., Zhou, Y., Chen, Y., & Gu, J. (2018). Fastp: An ultra-fast all-in-one FASTQ preprocessor. *Bioinformatics*, *34*(17), i884–i890. https://doi.org/10.1093/bioinformatics/bty560

Cheong, H., Nair, U., Geng, J., & Klionsky, D. J. (2008). The Atg1 Kinase Complex Is Involved in the Regulation of Protein Recruitment to Initiate Sequestering Vesicle Formation for Nonspecific Autophagy in Saccharomyces cerevisiae. *Molecular Biology of the Cell*, *19*(2), 666–681. https://doi.org/10.1091/mbc.E07-08-0826

Cheval, P., Siah, A., Bomble, M., Popper, A. D., Reignault, P., & Halama, P. (2017). Evolution of QoI resistance of the wheat pathogen Zymoseptoria tritici in Northern France. *Crop Protection*, *92*, 131–133. https://doi.org/10.1016/j.cropro.2016.10.017

Cho, W. K., Yu, J., Lee, K. M., Son, M., Min, K., Lee, Y. W., & Kim, K. H. (2012). Genome-wide expression profiling shows transcriptional reprogramming in Fusarium graminearum by Fusarium graminearum virus 1-DK21 infection. *BMC Genomics*, *13*(1). https://doi.org/10.1186/1471-2164-13-173

Cho, Y., Kim, K. H., La Rota, M., Scott, D., Santopietro, G., Callihan, M., Mitchell, T. K., & Lawrence, C. B. (2009). Identification of novel virulence factors associated with signal transduction pathways in Alternaria brassicicola. *Molecular Microbiology*, *72*(6), 1316–1333. https://doi.org/10.1111/j.1365-2958.2009.06689.x

Choi, W., & Dean, R. A. (1997). The adenylate cyclase gene MAC1 of Magnaporthe grisea controls appressorium formation and other aspects of growth and development. *The Plant Cell*, *9*(11), 1973–1983. https://doi.org/10.1105/tpc.9.11.1973

Choi, Y. E., & Goodwin, S. B. (2011). MVE1, encoding the velvet gene product homolog in Mycosphaerella graminicola, is associated with aerial mycelium

formation, melanin biosynthesis, hyphal swelling, and light signaling. *Applied and Environmental Microbiology*, *77*(3), 942–953. https://doi.org/10.1128/AEM.01830-10

Choi, Y. E., Lee, C., & Goodwin, S. B. (2016). Generation of Reactive Oxygen Species via NOXa Is Important for Development and Pathogenicity of Mycosphaerella graminicola. *Mycobiology*, *44*(1), 38–47. https://doi.org/10.5941/MYCO.2016.44.1.38

Christensen, M. J., Bennett, R. J., Ansari, H. A., Koga, H., Johnson, R. D., Bryan, G. T., Simpson, W. R., Koolaard, J. P., Nickless, E. M., & Voisey, C. R. (2008). Epichloe endophytes grow by intercalary hyphal extension in elongating grass leaves. *Fungal Genetics and Biology*, *45*, 84–93. https://doi.org/10.1016/j.fgb.2007.07.013

Chu, Y., Jeon, J., Yea, S., Kim, Y., Yun, S., Lee, Y., & Kim, K. (2002). Double-Stranded RNA Mycovirus from Fusarium graminearum. *Applied and Environmental Microbiology*, *68*(5), 2529–2534. https://doi.org/10.1128/AEM.68.5.2529

Chungu, C., Gilbert, J., & Townley-Smith, F. (2001). Septoria tritici blotch development as affected by temperature, duration of leaf wetness, inoculum concentration, and host. *Plant Disease*, *85*(4), 430–435. https://doi.org/10.1094/PDIS.2001.85.4.430

Claret, S., Gatti, X., Thoraval, D., & Crouzet, M. (2005). The Rgd1p Rho GTPase-Activating Protein and the Mid2p Cell Wall Sensor Are Required at Low pH for Protein Kinase C Pathway Activation and Cell Survival in Saccharomyces cerevisiae. *Eukaryotic Cell*, *4*(8), 1375–1386. https://doi.org/10.1128/EC.4.8.1375

Cohen, L., & Eyal, Z. (1993). The histology of processes associated with the infection of resistant and susceptible wheat cultivars with Septoria tritici. *Plant Pathology*, *42*, 737–743. https://doi.org/10.1111/j.1365-3059.1993.tb01560.x

Collopy, P. D., Colot, H. V., Park, G., Ringelberg, C., Crew, C. M., Borkovich, K. A., & Dunlap, J. C. (2010). High-throughput construction of gene deletion cassettes for generation of Neurospora crassa knockout strains. *Methods in Molecular Biology (Clifton, N.J.)*, *638*, 33–40. https://doi.org/10.1007/978-1-60761-611-5_3

Colmenares, A. J., Aleu, J., Durán-Patrón, R., Collado, I. G., & Hernández-Galán, R. (2002). The putative role of botrydial and related metabolites in the infection mechanism of Botrytis cinerea. *Journal of Chemical Ecology*, *28*(5), 997–1005. https://doi.org/10.1023/A:1015209817830

Colot, H. V., Park, G., Turner, G. E., Ringelberg, C., Crew, C. M., Litvinkova, L., Weiss, R. L., Borkovich, K. A., & Dunlap, J. C. (2006). A high-throughput gene knockout procedure for Neurospora reveals functions for multiple transcription factors. *Proceedings of the National Academy of Sciences of the United States of America*, *103*(21), 10352–10357. https://doi.org/10.1073/pnas.0601456103

Cook, D. E., Mesarich, C. H., & Thomma, B. P. H. J. (2015). Understanding Plant Immunity as a Surveillance System to Detect Invasion. *Annual Review of Phytopathology*, *53*(1), 541–563. https://doi.org/10.1146/annurev-phyto-080614-120114

Cools, H. J., & Fraaije, B. A. (2013). Update on mechanisms of azole resistance in Mycosphaerella graminicola and implications for future control. *Pest Management Science*, *69*(2), 150–155. https://doi.org/10.1002/ps.3348

Cooper, T. F., Rozen, D. E., & Lenski, R. E. (2003). Parallel changes in gene expression after 20,000 generations of evolution in Escherichia coli. *Proceedings of the National Academy of Sciences of the United States of America*, *100*(3), 1072–1077. https://doi.org/10.1073/pnas.0334340100

Corral-Ramos, C., Roca, M. G., Di Pietro, A., Roncero, M. I. G., & Ruiz-Roldán, C. (2015). Autophagy contributes to regulation of nuclear dynamics during vegetative growth and hyphal fusion in fusarium oxysporum. *Autophagy*, *11*(1), 131–144. https://doi.org/10.4161/15548627.2014.994413

Cousin, A., Mehrabi, R., Guilleroux, M., Dufresne, M., Van Der Lee, T., Waalwijk, C., Langin, T., & Kema, G. H. J. (2006). The MAP kinase-encoding gene MgFus3 of the non-appressorium phytopathogen Mycosphaerella graminicola is required for penetration and in vitro pycnidia formation. *Molecular Plant Pathology*, *7*(4), 269–278. https://doi.org/10.1111/j.1364-3703.2006.00337.x

Cowger, C., Hoffer, M. E., & Mundt, C. C. (2000). Specific adaptation by Mycosphaerella graminicola to a resistant wheat cultivar. *Plant Pathology*, *49*(4), 445–451. https://doi.org/10.1046/j.1365-3059.2000.00472.x

Croll, D., Zala, M., & McDonald, B. A. (2013). Breakage-fusion-bridge Cycles and Large Insertions Contribute to the Rapid Evolution of Accessory Chromosomes in a Fungal Pathogen. *PLoS Genetics*, *9*(6). https://doi.org/10.1371/journal.pgen.1003567

Csorba, T., Kontra, L., & Burgyán, J. (2015). Viral silencing suppressors: Tools forged to fine-tune host-pathogen coexistence. *Virology*, *479–480*, 85–103. https://doi.org/10.1016/j.virol.2015.02.028

D'Souza, C. A., & Heitman, J. (2001). Conserved cAMP signaling cascades regulate fungal development and virulence. *FEMS Microbiology Reviews*, *25*(3), 349–364. https://doi.org/10.1016/S0168-6445(01)00058-4

de Assis, L. J., Manfiolli, A., Mattos, E., Fabri, J. H. T. M., Malavazi, I., Jacobsen, I. D., Brock, M., Cramer, R. A., Thammahong, A., Hagiwara, D., Ries, L. N. A., & Goldman, G. H. (2018). Protein Kinase A and High-Osmolarity Glycerol Response Pathways Cooperatively Control Cell Wall Carbohydrate Mobilization in Aspergillus fumigatus. *MBio*, *9*, e01952.

de Jonge, R., Esse, H. P. Van, Kombrink, A., Shinya, T., Desaki, Y., Bours, R., Krol, S. Van Der, Shibuya, N., Joosten, M. H. A. J., & Thomma, B. P. H. J. (2010). Conserved Fungal LysM Effector Ecp6 Prevents Chitin-Triggered Immunity in Plants. *Science*, *329*(5994), 953–955.

De Silva, D. D., Crous, P. W., Ades, P. K., Hyde, K. D., & Taylor, P. W. J. (2017). Life styles of Colletotrichum species and implications for plant biosecurity. *Fungal Biology Reviews*, *31*(3), 155–168. https://doi.org/10.1016/j.fbr.2017.05.001

de Wit, P. J. G. M., van der Burgt, A., Ökmen, B., Stergiopoulos, I., Abd-Elsalam, K. A., Aerts, A. L., Bahkali, A. H., Beenen, H. G., Chettri, P., Cox, M. P., Datema, E., de Vries, R. P., Dhillon, B., Ganley, A. R., Griffiths, S. A., Guo, Y., Hamelin, R. C., Henrissat, B., Kabir, M. S., … Bradshaw, R. E. (2012). The Genomes of the Fungal Plant Pathogens Cladosporium fulvum and Dothistroma septosporum Reveal Adaptation to Different Hosts and Lifestyles But Also Signatures of Common Ancestry. *PLoS Genetics*, *8*(11). https://doi.org/10.1371/journal.pgen.1003088

Dean, R., Van Kan, J. A. L., Pretorius, Z. A., Hammond-Kosack, K. E., Di Pietro, A., Spanu, P. D., Rudd, J. J., Dickman, M., Kahmann, R., Ellis, J., & Foster, G. D. (2012). The Top 10 fungal pathogens in molecular plant pathology. *Molecular Plant Pathology*, *13*(4), 414–430. https://doi.org/10.1111/j.1364-3703.2011.00783.x

Deising, H., Nicholson, R. L., Haug, M., Howard, R. J., & Mendgen, K. (1992). Adhesion pad formation and the involvement of cutinase and esterases in the attachment of uredospores to the host cuticle. *The Plant Cell*, *4*(9), 1101–1111.

https://doi.org/10.2307/3869478

Dekhang, R., Wu, C., Smith, K. M., Lamb, T. M., Peterson, M., Bredeweg, E. L., Ibarra, O., Emerson, J. M., Karunarathna, N., Lyubetskaya, A., Azizi, E., Hurley, J. M., Dunlap, J. C., Galagan, J. E., Freitag, M., Sachs, M. S., & Bell-Pedersen, D. (2017). The Neurospora transcription factor ADV-1 transduces light signals and temporal information to control rhythmic expression of genes involved in cell fusion. *G3: Genes, Genomes, Genetics*, *7*(1), 129–142. https://doi.org/10.1534/g3.116.034298

Demoor, A., Silar, P., & Brun, S. (2019). Appressorium: The breakthrough in Dikarya. *Journal of Fungi*, *5*(3). https://doi.org/10.3390/jof5030072

Deng, Y., Qu, Z., & Naqvi, N. I. (2013). The role of Snx41-based pexophagy in magnaporthe development. *PLoS ONE*, *8*(11), 1–10. https://doi.org/10.1371/journal.pone.0079128

Derbyshire, M., Denton-Giles, M., Hegedus, D., Seifbarghi, S., Rollins, J., Kan, J. Van, Seidl, M. F., Faino, L., Mbengue, M., Navaud, O., Raffaele, S., Hammond-Kosack, K., Heard, S., & Oliver, R. (2017). The complete genome sequence of the phytopathogenic fungus Sclerotinia sclerotiorum reveals insights into the genome architecture of broad host range pathogens. *Genome Biology and Evolution*, *9*(3), 593–618. https://doi.org/10.1093/gbe/evx030

Deschamps-Francoeur, G., Simoneau, J., & Scott, M. S. (2020). Handling multi-mapped reads in RNA-seq. *Computational and Structural Biotechnology Journal*, *18*, 1569–1576. https://doi.org/10.1016/j.csbj.2020.06.014

Di Pietro, A., Garcia-Maceira, F. I., Meglecz, E., & Roncero, M. I. G. (2001). A MAP kinase of the vascular wilt fungus Fusarium oxysporum is essential for root penetration and pathogenesis. *Molecular Microbiology*, *39*(5), 1140–1152.

Dichtl, K., Helmschrott, C., Dirr, F., & Wagener, J. (2012). Deciphering cell wall integrity signalling in Aspergillus fumigatus: Identification and functional characterization of cell wall stress sensors and relevant Rho GTPases. *Molecular Microbiology*, *83*(3), 506–519. https://doi.org/10.1111/j.1365-2958.2011.07946.x

Dichtl, K., Samantaray, S., & Wagener, J. (2016). Cell wall integrity signalling in human pathogenic fungi. *Cellular Microbiology*, *18*(9), 1228–1238. https://doi.org/10.1111/cmi.12612

Dita, M., Barquero, M., Heck, D., Mizubuti, E. S. G., & Staver, C. P. (2018). Fusarium wilt of banana: Current knowledge on epidemiology and research needs toward sustainable disease management. *Frontiers in Plant Science*, *871*(October), 1–21. https://doi.org/10.3389/fpls.2018.01468

Divon, H. H., & Fluhr, R. (2007). Nutrition acquisition strategies during fungal infection of plants. *FEMS Microbiology Letters*, *266*(1), 65–74. https://doi.org/10.1111/j.1574-6968.2006.00504.x

Djamei, A., Schipper, K., Rabe, F., Ghosh, A., Vincon, V., Kahnt, J., Osorio, S., Tohge, T., Fernie, A. R., Feussner, I., Feussner, K., Meinicke, P., Stierhof, Y. D., Schwarz, H., MacEk, B., Mann, M., & Kahmann, R. (2011). Metabolic priming by a secreted fungal effector. *Nature*, *478*(7369), 395–398. https://doi.org/10.1038/nature10454

Dobin, A., Davis, C. A., Schlesinger, F., Drenkow, J., Zaleski, C., Jha, S., Batut, P., Chaisson, M., & Gingeras, T. R. (2013). STAR: Ultrafast universal RNA-seq aligner. *Bioinformatics*, *29*(1), 15–21. https://doi.org/10.1093/bioinformatics/bts635

Dodds, P. N., & Rathjen, J. P. (2010). Plant immunity: Towards an integrated view of plantğ€" pathogen interactions. *Nature Reviews Genetics*, *11*(8), 539–548.

https://doi.org/10.1038/nrg2812

Doehlemann, G., Berndt, P., & Hahn, M. (2006). Different signalling pathways involving a Gα protein, cAMP and a MAP kinase control germination of Botrytis cinerea conidia. *Molecular Microbiology*, *59*(3), 821–835. https://doi.org/10.1111/j.1365-2958.2005.04991.x

Dong, S., Raffaele, S., & Kamoun, S. (2015). The two-speed genomes of filamentous pathogens: Waltz with plants. *Current Opinion in Genetics and Development*, *35*, 57–65. https://doi.org/10.1016/j.gde.2015.09.001

Donlin, M. J., Upadhya, R., Gerik, K. J., Lam, W., Vanarendonk, L. G., Specht, C. A., Sharma, N. K., & Lodge, J. K. (2014). Cross talk between the cell wall integrity and cyclic AMP/protein kinase a pathways in Cryptococcus neoformans. *MBio*, *5*(4), 1–10. https://doi.org/10.1128/mBio.01573-14

Duan, Z., Chen, Y., Huang, W., Shang, Y., Chen, P., & Wang, C. (2013). Linkage of autophagy to fungal development , lipid storage and virulence in Metarhizium robertsii. *Autophagy*, *9*(4), 538–549.

Duncan, K. E., & Howard, R. J. (2000). Cytological analysis of wheat infection by the leaf blotch pathogen Mycosphaerella graminicola. *Mycological Research*, *104*(9), 1074–1082. https://doi.org/10.1017/S0953756299002294

Dunn, M. F., Ramírez-Trujillo, J. A., & Hernández-Lucas, I. (2009). Major roles of isocitrate lyase and malate synthase in bacterial and fungal pathogenesis. *Microbiology*, *155*(10), 3166–3175. https://doi.org/10.1099/mic.0.030858-0

El Gueddari, N. E., Rauchhaus, U., Moerschbacher, B. M., & Deising, H. B. (2002). Developmentally regulated conversion of surface-exposed chitin to chitosan in cell walls of plant pathogenic fungi. *New Phytologist*, *156*(1), 103–112. https://doi.org/10.1046/j.1469-8137.2002.00487.x

Ellis, J. G., Lagudah, E. S., Spielmeyer, W., & Dodds, P. N. (2014). The past, Present and future of breeding rust resistant wheat. *Frontiers in Plant Science*, *5*(NOV), 1–13. https://doi.org/10.3389/fpls.2014.00641

Erdmann, R., Veenhuis, M., Mertens, D., & Kunau, W. H. (1989). Isolation of peroxisome-deficient mutants of Saccharomyces cerevisiae. *Proceedings of the National Academy of Sciences of the United States of America*, *86*(14), 5419–5423. https://doi.org/10.1073/pnas.86.14.5419

Eriksen, L., & Munk, L. (2003). The occurrence of Mycosphaerella graminicola and its anamorph Septoria tritici in winter wheat during the growing season. *European Journal of Plant Pathology*, *109*(3), 253–259. https://doi.org/10.1023/A:1022851502770

Eyal, Z., Schare, A. ., Prescott, J. M., & van Ginkel, M. (1987). *The Septoria diseases of wheat: Concepts and methods of disease management*. https://doi.org/10.1007/BF02858957

Fang, Y. L., Peng, Y. L., & Fan, J. (2017). The Nep1-like protein family of Magnaporthe oryzae is dispensable for the infection of rice plants. *Scientific Reports*, *7*(1), 1–10. https://doi.org/10.1038/s41598-017-04430-0

Farré, J. C., & Subramani, S. (2016). Mechanistic insights into selective autophagy pathways: Lessons from yeast. *Nature Reviews Molecular Cell Biology*, *17*(9), 537–552. https://doi.org/10.1038/nrm.2016.74

Feng, J., Zhang, H., Strelkov, S. E., & Hwang, S. (2014). The LmSNF1 Gene Is Required for Pathogenicity in the Canola Blackleg Pathogen Leptosphaeria maculans. *PLoS ONE*, *9*(3), e92503. https://doi.org/10.1371/journal.pone.0092503

Feng, Y., He, D., Yao, Z., & Klionsky, D. J. (2014). The machinery of macroautophagy. *Cell Research*, *24*(1), 24–41. https://doi.org/10.1038/cr.2013.168

Feron, G., Blin-Perrin, C., Krasniewski, I., Mauvais, G., & Lherminier, J. (2005). Metabolism of fatty acid in yeast: Characterisation of β-oxidation and ultrastructural changes in the genus Sporidiobolus sp. cultivated on ricinoleic acid methyl ester. *FEMS Microbiology Letters*, *250*(1), 63–69. https://doi.org/10.1016/j.femsle.2005.06.045

Feurtey, A., Lorrain, C., Croll, D., Eschenbrenner, C., Freitag, M., Habig, M., Haueisen, J., Möller, M., Schotanus, K., & Stukenbrock, E. H. (2019). Genome compartmentalization predates species divergence in the plant pathogen genus Zymoseptoria. *BioRxiv*, 1–15. https://doi.org/10.1101/864561

Filomeni, G., Zio, D. De, & Cecconi, F. (2015). Oxidative stress and autophagy : the clash between damage and metabolic needs. *Cell Death and Differentiation*, *22*, 377–388. https://doi.org/10.1038/cdd.2014.150

Fisher, M. C., Hawkins, N. J., Sanglard, D., & Gurr, S. J. (2018). Health and Food Security. *Science*, *360*, 739–742. https://doi.org/10.1126/science.aap7999

Fisher, M. C., Henk, D. A., Briggs, C. J., Brownstein, J. S., Madoff, L. C., McCraw, S. L., & Gurr, S. J. (2012). Emerging fungal threats to animal, plant and ecosystem health. *Nature*, *484*(7393), 186–194. https://doi.org/10.1038/nature10947

Fones, H., & Gurr, S. (2015). The impact of Septoria tritici Blotch disease on wheat: An EU perspective. *Fungal Genetics and Biology*, *79*, 3–7. https://doi.org/10.1016/j.fgb.2015.04.004

Fones, H. N., Eyles, C. J., Kay, W., Cowper, J., & Gurr, S. J. (2017). A role for random, humidity-dependent epiphytic growth prior to invasion of wheat by Zymoseptoria tritici. *Fungal Genetics and Biology*, *106*(May), 51–60. https://doi.org/10.1016/j.fgb.2017.07.002

Fortwendel, J. R., Juvvadi, P. R., Perfect, B. Z., Rogg, L. E., Perfect, J. R., & Steinbach, W. J. (2010). Transcriptional Regulation of Chitin Synthases by Calcineurin Controls Paradoxical Growth of Aspergillus fumigatus in Response to Caspofungin □. *Antimicrobial Agents and Chemotherapy*, *54*(4), 1555–1563. https://doi.org/10.1128/AAC.00854-09

Fouché, S., Badet, T., Oggenfuss, U., Plissonneau, C., Francisco, C. S., & Croll, D. (2020). Stress-Driven Transposable Element De-repression Dynamics and Virulence Evolution in a Fungal Pathogen. *Molecular Biology and Evolution*, *37*(1), 221–239. https://doi.org/10.1093/molbev/msz216

Fouché, S., Plissonneau, C., McDonald, B. A., & Croll, D. (2018). Meiosis leads to pervasive copy-number variation and distorted inheritance of accessory chromosomes of the wheat pathogen Zymoseptoria tritici. *Genome Biology and Evolution*, *10*(6), 1416–1429. https://doi.org/10.1093/gbe/evy100

Fraaije, B. A., Cools, H. J., Fountaine, J., Lovell, D. J., Motteram, J., West, J. S., & Lucas, J. A. (2005). Role of ascospores in further spread of QoI-resistant cytochrome b alleles (G143A) in field populations of Mycosphaerella graminicola. *Phytopathology*, *95*(8), 933–941. https://doi.org/10.1094/PHYTO-95-0933

Francisco, C. S., Ma, X., Zwyssig, M. M., McDonald, B. A., & Palma-Guerrero, J. (2019). Morphological changes in response to environmental stresses in the fungal plant pathogen Zymoseptoria tritici. *Scientific Reports*, *9*(1), 9642. https://doi.org/10.1038/s41598-019-45994-3

Francisco, C. S., Zwyssig, M. M., & Palma-Guerrero, J. (2020). The role of vegetative cell fusions in the development and asexual reproduction of the wheat fungal

pathogen Zymoseptoria tritici. *BMC Biology*, *18*(1), 1–16. https://doi.org/10.1186/s12915-020-00838-9

Fujikawa, T., Sakaguchi, A., Nishizawa, Y., Kouzai, Y., Minami, E., Yano, S., Koga, H., Meshi, T., & Nishimura, M. (2012). Surface α-1,3-Glucan Facilitates Fungal Stealth Infection by Interfering with Innate Immunity in Plants. *PLoS Pathogens*, *8*(8). https://doi.org/10.1371/journal.ppat.1002882

Fukasawa, Y., Tsuji, J., Fu, S. C., Tomii, K., Horton, P., & Imai, K. (2015). MitoFates: Improved prediction of mitochondrial targeting sequences and their cleavage sites. *Molecular and Cellular Proteomics*, *14*(4), 1113–1126. https://doi.org/10.1074/mcp.M114.043083

Fuller, K. K., Loros, J. J., & Dunlap, J. C. (2015). Fungal photobiology: visible light as a signal for stress, space and time. *Current Genetics*, *61*(3), 275–288. https://doi.org/10.1007/s00294-014-0451-0.Fungal

Fuller, K. K., & Rhodes, J. C. (2012). Protein kinase A and fungal virulence: A sinister side to a conserved nutrient sensing pathway. *Virulence*, *3*(2), 109–121. https://doi.org/10.4161/viru.19396

Fuller, K. K., Richie, D. L., Feng, X., Krishnan, K., Stephens, T. J., Wikenheiser-Brokamp, K. A., Askew, D. S., & Rhodes, J. C. (2011). Divergent Protein Kinase A isoforms co-ordinately regulate conidial germination, carbohydrate metabolism and virulence in Aspergillus fumigatus. *Molecular Microbiology*, *79*(4), 1045–1062. https://doi.org/10.1111/j.1365-2958.2010.07509.x.

Fuller, K. K., Ringelberg, C. S., Loros, J. J., & Dunlap, J. C. (2013). The fungal pathogen Aspergillus fumigatus regulates growth, metabolism, and stress resistance in response to light. *MBio*, *4*(2), e00142-13. https://doi.org/10.1128/mBio.00142-13

Futagami, T., & Goto, M. (2012). Putative cell wall integrity sensor proteins in Aspergillus nidulans . *Communicative & Integrative Biology*, *5*(2), 206–208. https://doi.org/10.4161/cib.18993

Futagami, T., Nakao, S., Kido, Y., Oka, T., Kajiwara, Y., Takashita, H., Omori, T., Furukawa, K., & Goto, M. (2011). Putative stress sensors WscA and WscB are involved in hypo-osmotic and acidic pH stress tolerance in aspergillus nidulans. *Eukaryotic Cell*, *10*(11), 1504–1515. https://doi.org/10.1128/EC.05080-11

Fux, C. A., Shirtliff, M., Stoodley, P., & Costerton, J. W. (2005). Can laboratory reference strains mirror “real-world” pathogenesis? *Trends in Microbiology*, *13*(2), 58–63. https://doi.org/10.1016/j.tim.2004.11.001

Gabaldón, T. (2014). Evolutionary considerations on the origin of peroxisomes from the endoplasmic reticulum, and their relationships with mitochondria. *Cellular and Molecular Life Sciences*, *71*(13), 2379–2382. https://doi.org/10.1007/s00018-014-1640-1

Gabriel, F., Accoceberry, I., Bessoule, J.-J., Salin, B., Lucas-Guerin, M., Manon, S., Dementhon, K., & Noel, T. (2014). A Fox2-Dependent Fatty Acid ß-Oxidation Pathway Coexists Both in Peroxisomes and Mitochondria of the Ascomycete Yeast Candida lusitaniae. *PLoS ONE*, *9*(12). https://doi.org/10.1371/journal.pone

Gallego-Hernandez, A. L., DePas, W. H., Park, J. H., Teschler, J. K., Hartmann, R., Jeckel, H., Drescher, K., Beyhan, S., Newman, D. K., & Yildiz, F. H. (2020). Upregulation of virulence genes promotes Vibrio cholerae biofilm hyperinfectivity. *Proceedings of the National Academy of Sciences of the United States of America*, *117*(20), 11010–11017. https://doi.org/10.1073/pnas.1916571117

García, R., Bravo, E., Diez-Muñiz, S., Nombela, C., Rodríguez-Peña, J. M., & Arroyo,

J. (2017). A novel connection between the Cell Wall Integrity and the PKA pathways regulates cell wall stress response in yeast. *Scientific Reports*, *7*(1), 1–15. https://doi.org/10.1038/s41598-017-06001-9

García, R., Pulido, V., Orellana-Muñoz, S., Nombela, C., Vázquez de Aldana, C. R., Rodríguez-Peña, J. M., & Arroyo, J. (2019). Signalling through the yeast MAPK Cell Wall Integrity pathway controls P-body assembly upon cell wall stress. *Scientific Reports*, *9*(1), 1–13. https://doi.org/10.1038/s41598-019-40112-9

Garcia, R., Rodríguez-Pena, J. M., Bermejo, C., & Arroyo, J. (2009). The High Osmotic Response and Cell Wall Integrity Pathways Cooperate to Regulate Transcriptional Responses to Zymolyase-induced Cell Wall Stress in Saccharomyces cerevisiae. *Journal of Biological Chemistry*, *284*(16), 10901–10911. https://doi.org/10.1074/jbc.M808693200

Garnault, M., Duplaix, C., Leroux, P., Couleaud, G., Carpentier, F., David, O., & Walker, A. S. (2019). Spatiotemporal dynamics of fungicide resistance in the wheat pathogen Zymoseptoria tritici in France. *Pest Management Science*, *75*(7), 1794–1807. https://doi.org/10.1002/ps.5360

Garrison, E., & Marth, G. (2012). Haplotype-based variant detection from short-read sequencing. *ArXiv12073907 Q-Bio*. http://arxiv.org/abs/1207.3907

Gauthier, G. M. (2015). Dimorphism in Fungal Pathogens of Mammals, Plants, and Insects. *PLoS Pathogens*, *11*(2), 1–7. https://doi.org/10.1371/journal.ppat.1004608

Geisbrecht, B. V., Zhu, D., Schulz, K., Nau, K., Morrell, J. C., Geraghty, M., Schulz, H., Erdmann, R., & Gould, S. J. (1998). Molecular characterization of Saccharomyces cerevisiae Δ3,Δ2-enoyl- CoA isomerase. *Journal of Biological Chemistry*, *273*(50), 33184–33191. https://doi.org/10.1074/jbc.273.50.33184

Geoghegan, I., Steinberg, G., & Gurr, S. (2017). The Role of the Fungal Cell Wall in the Infection of Plants. *Trends in Microbiology*, *25*(12), 957–967. https://doi.org/10.1016/j.tim.2017.05.015

Ghabrial, S. A., Castón, J. R., Jiang, D., Nibert, M. L., & Suzuki, N. (2015). 50-Plus Years of Fungal Viruses. *Virology*, *479–480*, 356–368. https://doi.org/10.1016/j.virol.2015.02.034

Gietz, R. D., & Woods, R. A. (2002). Transformation of yeast by lithium acetate/single-stranded carrier DNA/polyethylene glycol method. *Methods in Enzymology*, *350*(February 2002), 87–96. https://doi.org/10.1016/S0076-6879(02)50957-5

Gijzen, M., & Nürnberger, T. (2006). Nep1-like proteins from plant pathogens: Recruitment and diversification of the NPP1 domain across taxa. *Phytochemistry*, *67*(16), 1800–1807. https://doi.org/10.1016/j.phytochem.2005.12.008

Gilbert, K. B., Holcomb, E. E., Allscheid, R. L., & Carrington, J. C. (2019). Hiding in plain sight: New virus genomes discovered via a systematic analysis of fungal public transcriptomes. *PLoS ONE*, *14*(7), 1–51. https://doi.org/10.1371/journal.pone.0219207

Gilbert, R. D., Johnson, A. M., & Dean, R. A. (1996). Chemical signals responsible for appressorium formation in the rice blast fungus Magnaporthe grisea. *Physiological and Molecular Plant Pathology*, *48*(5), 335–346. https://doi.org/10.1006/pmpp.1996.0027

Godfray, H. C. J., Mason-D'Croz, D., & Robinson, S. (2016). Food system consequences of a fungal disease epidemic in a major crop. *Philosophical Transactions of the Royal Society B: Biological Sciences*, *371*, 20150467.

Goodwin, S. B., M'Barek, S. Ben, Dhillon, B., Wittenberg, A. H. J., Crane, C. F., Hane, J. K., Foster, A. J., van der Lee, T. A. J., Grimwood, J., Aerts, A., Antoniw, J., Bailey, A., Bluhm, B., Bowler, J., Bristow, J., van der Burgt, A., Canto-Canché, B., Churchill, A. C. L., Conde-Ferràez, L., … Kema, G. H. J. (2011). Finished genome of the fungal wheat pathogen Mycosphaerella graminicola reveals dispensome structure, chromosome plasticity, and stealth pathogenesis. *PLoS Genetics*, *7*(6). https://doi.org/10.1371/journal.pgen.1002070

Goyal, R. K., Tulpan, D., Chomistek, N., Fundora, D. G., West, C., Ellis, B. E., Frick, M., Laroche, A., & Foroud, N. A. (2018). Analysis of MAPK and MAPKK gene families in wheat and related Triticeae species. *BMC Genomics*, *19*, 178.

Griffioen, G., Branduardi, P., Ballarini, A., Anghileri, P., Norbeck, J., Baroni, M. D., & Ruis, H. (2001). Nucleocytoplasmic Distribution of Budding Yeast Protein Kinase A Regulatory Subunit Bcy1 Requires Zds1 and Is Regulated by Yak1-Dependent Phosphorylation of Its Targeting Domain. *Molecular and Cellular Biology*, *21*(2), 511–523. https://doi.org/10.1128/mcb.21.2.511-523.2001

Guillemette, T., Calmes, B., & Simoneau, P. (2014). Impact of the UPR on the virulence of the plant fungal pathogen A. brassicicola. *Virulence*, *5*(2), 357–364. https://doi.org/10.4161/viru.26772

Guillemette, T., van Peij, N. N. M. E., Goosen, T., Lanthaler, K., Robson, G. D., van den Hondel, C. A. M. J. J., Stam, H., & Archer, D. B. (2007). Genomic analysis of the secretion stress response in the enzyme-producing cell factory Aspergillus niger. *BMC Genomics*, *8*. https://doi.org/10.1186/1471-2164-8-158

Guo, J., Dai, X., Xu, J., Wang, Y., Bai, P., Liu, F., & Duan, Y. (2011). Molecular Characterization of a Fus3 / Kss1 Type MAPK from Puccinia striiformis f . sp . tritici , PsMAPK1. *PLoS ONE*, *6*(7), e21895. https://doi.org/10.1371/journal.pone.0021895

Guyon, K., Balagué, C., Roby, D., & Raffaele, S. (2014). Secretome analysis reveals effector candidates associated with broad host range necrotrophy in the fungal plant pathogen Sclerotinia sclerotiorum. *BMC Genomics*, *15*(1). https://doi.org/10.1186/1471-2164-15-336

Habig, M., Bahena-Garrido, S. M., Barkmann, F., Haueisen, J., & Stukenbrock, E. H. (2020). The transcription factor Zt107320 affects the dimorphic switch, growth and virulence of the fungal wheat pathogen Zymoseptoria tritici. *Molecular Plant Pathology*, *21*(1), 124–138. https://doi.org/10.1111/mpp.12886

Habig, M., Kema, G. H. J., & Stukenbrock, E. H. (2018). Meiotic drive of female-inherited supernumerary chromosomes in a pathogenic fungus. *ELife*, *7*, e40251. https://doi.org/10.7554/eLife.40251

Habig, M., Quade, J., & Stukenbrock, E. H. (2017). Forward genetics approach reveals host genotype-dependent importance of accessory chromosomes in the fungal wheat pathogen Zymoseptoria tritici. *MBio*, *8*(6), 1–16. https://doi.org/10.1128/mBio.01919-17

Haemmerle, G., Lass, A., Zimmermann, R., Gorkiewicz, G., Meyer, C., Rozman, J., Heldmaier, G., Maier, R., Theussl, C., Eder, S., Kratky, D., Wagner, E. F., Klingenspor, M., Hoefler, G., & Zechner, R. (2006). Defective Lipolysis and Altered Energy Metabolism in Mice Lacking Adipose Triglyceride Lipase. *Science*, *312*(5774), 734–738. https://doi.org/10.1126/science.1123965

Hammond-Kosack, K. E., & Rudd, J. J. (2008). Plant resistance signalling hijacked by a necrotrophic fungal pathogen. *Plant Signaling and Behavior*, *3*(11), 993–995. https://doi.org/10.4161/psb.6292

Hampel, M., Jakobi, M., Schmitz, L., Meyer, U., Finkernagel, F., Doehlemann, G., & Heimel, K. (2016). Unfolded protein response (UPR) regulator cib1 controls expression of genes encoding secreted virulence factors in Ustilago maydis. *PLoS ONE*, *11*(4), 1–16. https://doi.org/10.1371/journal.pone.0153861

Han, K.-H., Han, K.-Y., Yu, J.-H., Chae, K.-S., Kwang-Yeop, J., & Han, D.-M. (2001). The nsdD gene encodes a putative GATA-type transcription factor necessary for sexual development of Aspergillus nidulans. *Molecular Microbiology*, *41*(2), 299–309. https://doi.org/10.1046/j.1365-2958.2001.02472.x

Hao, F., Ding, T., Wu, M., Zhang, J., Yang, L., Chen, W., & Li, G. (2018). Two novel hypovirulence-associated mycoviruses in the phytopathogenic fungus Botrytis cinerea: Molecular characterization and suppression of infection cushion formation. *Viruses*, *10*(5). https://doi.org/10.3390/v10050254

Hartmann, F. E., & Croll, D. (2017). Distinct trajectories of massive recent gene gains and losses in populations of a microbial eukaryotic pathogen. *Molecular Biology and Evolution*, *34*(11), 2808–2822. https://doi.org/10.1093/molbev/msx208

Hartmann, F. E., Sánchez-Vallet, A., McDonald, B. A., & Croll, D. (2017). A fungal wheat pathogen evolved host specialization by extensive chromosomal rearrangements. *ISME Journal*, *11*(5), 1189–1204. https://doi.org/10.1038/ismej.2016.196

Hasim, S., & Coleman, J. J. (2019). Targeting the fungal cell wall: Current therapies and implications for development of alternative antifungal agents. *Future Medicinal Chemistry*, *11*(8), 869–883. https://doi.org/10.4155/fmc-2018-0465

Hatta, R., Ito, K., Hosaki, Y., Tanaka, T., Tanaka, A., Yamamoto, M., Akimitsu, K., & Tsuge, T. (2002). A conditionally dispensable chromosome controls host-specific pathogenicity in the fungal plant pathogen Alternaria alternata. *Genetics*, *161*(1), 59–70. https://doi.org/10.1093/genetics/161.1.59

Haueisen, J., Möller, M., Eschenbrenner, C. J., Grandaubert, J., Seybold, H., Adamiak, H., & Stukenbrock, E. H. (2019). Highly flexible infection programs in a specialized wheat pathogen. *Ecology and Evolution*, *9*(1), 275–294. https://doi.org/10.1002/ece3.4724

He, Q., Cheng, P., Yang, Y., Wang, L., Gardner, K. H., & Liu, Y. (2002). White collar-1, a DNA binding transcription factor and a light sensor. *Science*, *297*(5582), 840–843. https://doi.org/10.1126/science.1072795

Head, N. E., & Yu, H. (2004). Cross-Sectional Analysis of Clinical and Environmental Isolates of Pseudomonas aeruginosa: Biofilm Formation, Virulence, and Genome Diversity. *Infection and Immunity*, *72*(1), 133–144. https://doi.org/10.1128/IAI.72.1.133-144.2004

Heimel, K., Freitag, J., Hampel, M., Ast, J., Bölker, M., & Kämper, J. (2013). Crosstalk between the unfolded protein response and pathways that regulate pathogenic development in Ustilago maydis. *Plant Cell*, *25*(10), 4262–4277. https://doi.org/10.1105/tpc.113.115899

Heinisch, J. (2005). Baker's yeast as a tool for the development of antifungal kinase inhibitors - targeting protein kinase C and the cell integrity pathway. *Biochimica et Biophysica Acta*, *1754*, 171–182. https://doi.org/10.1016/j.bbapap.2005.07.032

Heinisch, J., & Rodicio, R. (2018). Protein kinase C in fungi - more than just cell wall integrity. *FEMS Microbiology Reviews*, *42*(1), 22–39. https://doi.org/10.1093/femsre/fux051

Helber, N., Wippel, K., Sauer, N., Schaarschmidt, S., Hause, B., & Requena, N. (2011). A versatile monosaccharide transporter that operates in the arbuscular

mycorrhizal fungus Glomus sp is crucial for the symbiotic relationship with plants. *Plant Cell*, *23*(10), 3812–3823. https://doi.org/10.1105/tpc.111.089813

Hellens, R., Mullineaux, P., & Klee, H. (2000). A guide to Agrobacterium binary Ti vectors. *Trends in Plant Science*, *5*(10), 446–451. https://doi.org/10.1016/S1360-1385(00)01740-4

Hemetsberger, C., Herrberger, C., Zechmann, B., Hillmer, M., & Doehlemann, G. (2012). The Ustilago maydis effector Pep1 suppresses plant immunity by inhibition of host peroxidase activity. *PLoS Pathogens*, *8*(5). https://doi.org/10.1371/journal.ppat.1002684

Hiltunen, J. K., Wenzel, B., Beyer, A., Erdmann, R., Fossa, A., & Kunau, W. H. (1992). Peroxisomal multifunctional β-oxidation protein of Saccharomyces cerevisiae. Molecular analysis of the FOX2 gene and gene product. *Journal of Biological Chemistry*, *267*(10), 6646–6653.

Hoch, H. C., Staples, R. C., Whitehead, B., Comeau, J., & Wolf, E. D. (1987). Signaling for growth orientation and cell differentiation by surface topography in Uromyces. *Science*, *235*(4796), 1659–1662. https://doi.org/10.1126/science.235.4796.1659

Hopke, A., Brown, A. J. P., Hall, R. A., & Wheeler, R. T. (2018). Dynamic Fungal Cell Wall Architecture in Stress Adaptation and Immune Evasion. *Trends in Microbiology*, *26*(4), 284–295. https://doi.org/10.1016/j.tim.2018.01.007

Horbach, R., Navarro-Quesada, A. R., Knogge, W., & Deising, H. B. (2011). When and how to kill a plant cell: Infection strategies of plant pathogenic fungi. *Journal of Plant Physiology*, *168*(1), 51–62. https://doi.org/10.1016/j.jplph.2010.06.014

Hou, Z., Xue, C., Peng, Y., Katan, T., Kistler, H. C., & Xu, J. R. (2002). A mitogen-activated protein kinase gene (MGV1) in Fusarium graminearum is required for female fertility, heterokaryon formation, and plant infection. *Molecular Plant-Microbe Interactions*, *15*(11), 1119–1127. https://doi.org/10.1094/MPMI.2002.15.11.1119

Howard, R. J., & Ferrari, M. A. (1989). Role of melanin in appressorium function. *Experimental Mycology*, *13*(4), 403–418. https://doi.org/10.1016/0147-5975(89)90036-4

Hu, S., Zhou, X., Gu, X., Cao, S., Wang, C., & Xu, J. R. (2014). The cAMP-PKA pathway regulates growth, sexual and asexual differentiation, and pathogenesis in fusarium graminearum. *Molecular Plant-Microbe Interactions*, *27*(6), 557–566. https://doi.org/10.1094/MPMI-10-13-0306-R

Hunter, T., Coker, R. R., & Royle, D. J. (1999). The teleomorph stage, Mycosphaerella graminicola, in epidemics of septoria tritici blotch on winter wheat in the UK. *Plant Pathology*, *48*(1), 51–57. https://doi.org/10.1046/j.1365-3059.1999.00310.x

Idnurm, A., Bailey, A. M., Cairns, T. C., Elliott, C. E., Foster, G. D., Ianiri, G., & Jeon, J. (2017). A silver bullet in a golden age of functional genomics: the impact of Agrobacterium-mediated transformation of fungi. *Fungal Biology and Biotechnology*, *4*(1), 6. https://doi.org/10.1186/s40694-017-0035-0

Idnurm, A., & Heitman, J. (2005). Light controls growth and development via a conserved pathway in the fungal kingdom. *PLoS Biology*, *3*(4), 0615–0626. https://doi.org/10.1371/journal.pbio.0030095

Idnurm, A., & Howlett, B. J. (2002). Isocitrate Lyase Is Essential for Pathogenicity of the Fungus Leptosphaeria maculans to Canola ( Brassica napus). *Eukaryotic Cell*, *1*(5), 719–724. https://doi.org/10.1128/EK.1.5.719

Irieda, H., Inoue, Y., Mori, M., Yamada, K., Oshikawa, Y., Saitoh, H., Uemura, A.,

Terauchi, R., Kitakura, S., Kosaka, A., Singkaravanit-Ogawa, S., & Takano, Y. (2019). Conserved fungal effector suppresses PAMP-triggered immunity by targeting plant immune kinases. *Proceedings of the National Academy of Sciences of the United States of America*, *116*(2), 496–505. https://doi.org/10.1073/pnas.1807297116

Islam, M. T., Kim, K. H., & Choi, J. (2019). Wheat blast in Bangladesh: The current situation and future impacts. *Plant Pathology Journal*, *35*(1), 1–10. https://doi.org/10.5423/PPJ.RW.08.2018.0168

Jashni, M. K., Dols, I. H. M., Iida, Y., Boeren, S., Beenen, H. G., & Mehrabi, R. (2015). Synergistic action of a metalloprotease and a serine protease from Fusarium oxysporum cleaves chitin-binding tomato chitinases. *Molecular Plant Microbes Interaction*, *28*(9), 996–1008. https://doi.org/http://dx.doi.org/10.1094/MPMI-04-15-0074-R Synergistic

Jeandet, P. (2015). Phytoalexins: Current progress and future prospects. *Molecules*, *20*(2), 2770–2774. https://doi.org/10.3390/molecules20022770

Jenczmionka, N. J., Maier, F. J., Lösch, A. P., & Schäfer, W. (2003). Mating, conidiation and pathogenicity of Fusarium graminearum, the main causal agent of the head-blight disease of wheat, are regulated by the MAP kinase gpmk1. *Current Genetics*, *43*(2), 87–95. https://doi.org/10.1007/s00294-003-0379-2

Jenczmionka, N. J., & Schäfer, W. (2005). The Gpmk1 MAP kinase of Fusarium graminearum regulates the induction of specific secreted enzymes. *Current Genetics*, *47*(1), 29–36. https://doi.org/10.1007/s00294-004-0547-z

Jiang, C., Zhang, X., Liu, H., & Xu, J. (2018). Mitogen-activated protein kinase signaling in plant pathogenic fungi. *PLoS Pathogens*, *14*(3), e1006875. https://doi.org/10.1371/journal.ppat.1006875

Jones, J. D. G., & Dangl, J. L. (2006). The plant immune system. *Nature*, *444*, 323–329.

Joosten, M. H. A. J., & De Wit, P. J. G. M. (1989). Identification of Several Pathogenesis-Related Proteins in Tomato Leaves Inoculated with Cladosporium fulvum ( syn . Fulvia fulva ) as 1 , 3-fl-Glucanases and Chitinases ’. *Plant Physiology*, *89*, 945–951.

Jørgensen, L. N., Hovmøller, M. S., Hansen, J. G., Lassen, P., Clark, B., Bayles, R., Rodemann, B., Flath, K., Jahn, M., Goral, T., Jerzy Czembor, J., Cheyron, P., Maumene, C., De Pope, C., Ban, R., Nielsen, G. C., & Berg, G. (2014). IPM Strategies and Their Dilemmas Including an Introduction to www.eurowheat.org. *Journal of Integrative Agriculture*, *13*(2), 265–281. https://doi.org/10.1016/S2095-3119(13)60646-2

Jørgensen, L. N., van den Bosch, F., Oliver, R. P., Heick, T. M., & Paveley, N. D. (2017). Targeting Fungicide Inputs According to Need. *Annual Review of Phytopathology*, *55*(1), 181–203. https://doi.org/10.1146/annurev-phyto-080516-035357

Josefsen, L., Droce, A., Sondergaard, T. E., Sørensen, J. L., Bormann, J., Schäfer, W., Giese, H., & Olsson, S. (2012). Autophagy provides nutrients for nonassimilating fungal structures and is necessary for plant colonization but not for infection in the necrotrophic plant pathogen Fusarium graminearum. *Autophagy*, *8*(3), 326–337. https://doi.org/10.4161/auto.18705

Joubert, A., Bataille-Simoneau, N., Campion, C., Guillemette, T., Hudhomme, P., Iacomi-Vasilescu, B., Leroy, T., Pochon, S., Poupard, P., & Simoneau, P. (2011). Cell wall integrity and high osmolarity glycerol pathways are required for

adaptation of Alternaria brassicicola to cell wall stress caused by brassicaceous indolic phytoalexins. *Cellular Microbiology*, *13*(1), 62–80. https://doi.org/10.1111/j.1462-5822.2010.01520.x

Jugé, R., Breugnot, J., Da Silva, C., Bordes, S., Closs, B., & Aouacheria, A. (2016). Quantification and characterization of UVB-induced mitochondrial fragmentation in normal primary human keratinocytes. *Scientific Reports*, *6*, 35065. https://doi.org/10.1038/srep35065

Kabbage, M., Williams, B., & Dickman, M. B. (2013). Cell Death Control: The Interplay of Apoptosis and Autophagy in the Pathogenicity of Sclerotinia sclerotiorum. *PLoS Pathogens*, *9*(4). https://doi.org/10.1371/journal.ppat.1003287

Kabbage, M., Yarden, O., & Dickman, M. B. (2015). Pathogenic attributes of Sclerotinia sclerotiorum: Switching from a biotrophic to necrotrophic lifestyle. *Plant Science*, *233*, 53–60. https://doi.org/10.1016/j.plantsci.2014.12.018

Kabeya, Y., Noda, N. N., Fujioka, Y., Suzuki, K., Inagaki, F., & Ohsumi, Y. (2009). Characterization of the Atg17-Atg29-Atg31 complex specifically required for starvation-induced autophagy in Saccharomyces cerevisiae. *Biochemical and Biophysical Research Communications*, *389*(4), 612–615. https://doi.org/10.1016/j.bbrc.2009.09.034

Kaffarnik, F., Müller, P., Leibundgut, M., Kahmann, R., & Feldbrügge, M. (2003). PKA and MAPK phosphorylation of Prf1 allows promoter discrimination in Ustilago maydis. *EMBO Journal*, *22*(21), 5817–5826. https://doi.org/10.1093/emboj/cdg554

Kamada, Y., Jung, U. S., Piotrowski, J., & Levin, D. E. (1995). The protein kinase C-activated MAP kinase pathway of Saccharomyces cerevisiae mediates a novel aspect of the heat shock response. *Genes and Development*, *9*, 1559–1571.

Kanehisa, M., & Sato, Y. (2020). KEGG Mapper for inferring cellular functions from protein sequences. *Protein Science*, *29*(1), 28–35. https://doi.org/10.1002/pro.3711

Kanehisa, M., Sato, Y., & Morishima, K. (2016). BlastKOALA and GhostKOALA: KEGG Tools for Functional Characterization of Genome and Metagenome Sequences. *Journal of Molecular Biology*, *428*(4), 726–731. https://doi.org/10.1016/j.jmb.2015.11.006

Kankanala, P., Czymmek, K., & Valent, B. (2007). Roles for rice membrane dynamics and plasmodesmata during biotrophic invasion by the blast fungus. *Plant Cell*, *19*(2), 706–724. https://doi.org/10.1105/tpc.106.046300

Kanki, T., Wang, K., Cao, Y., Baba, M., & Klionsky, D. J. (2009). Atg32 Is a Mitochondrial Protein that Confers Selectivity during Mitophagy. *Developmental Cell*, *17*(1), 98–109. https://doi.org/10.1016/j.devcel.2009.06.014

Kanyuka, K., & Rudd, J. J. (2019). Cell surface immune receptors: the guardians of the plant's extracellular spaces. *Current Opinion in Plant Biology*, *50*, 1–8. https://doi.org/10.1016/j.pbi.2019.02.005

Kawahara, Y., Oono, Y., Kanamori, H., Matsumoto, T., Itoh, T., & Minami, E. (2012). Simultaneous RNA-seq analysis of a mixed transcriptome of rice and blast fungus interaction. *PloS One*, *7*(11), 1–15. https://doi.org/10.1371/journal.pone.0049423

Kay, W. T. (2017). *Novel insights into the asexual life-cycle of the wheat-leaf pathogen Zymoseptoria tritici* [University of Exeter]. http://hdl.handle.net/10871/31538

Kellner, R., Bhattacharyya, A., Poppe, S., Hsu, T. Y., Brem, R. B., & Stukenbrock, E. H. (2014). Expression profiling of the wheat pathogen Zymoseptoria tritici reveals genomic patterns of transcription and host-specific regulatory programs. *Genome*

*Biology and Evolution*, *6*(6), 1353–1365. https://doi.org/10.1093/gbe/evu101

Kema, Gerrit H.J., Mirzadi Gohari, A., Aouini, L., Gibriel, H. A. Y., Ware, S. B., Van Den Bosch, F., Manning-Smith, R., Alonso-Chavez, V., Helps, J., Ben M'Barek, S., Mehrabi, R., Diaz-Trujillo, C., Zamani, E., Schouten, H. J., Van Der Lee, T. A. J., Waalwijk, C., De Waard, M. A., De Wit, P. J. G. M., Verstappen, E. C. P., … Seidl, M. F. (2018). Stress and sexual reproduction affect the dynamics of the wheat pathogen effector AvrStb6 and strobilurin resistance. *Nature Genetics*, *50*(3), 375–380. https://doi.org/10.1038/s41588-018-0052-9

Kema, Gert H. J., van der Lee, T. A. J., Mendes, O., Verstappen, E. C. P., Lankhorst, R. K., Sandbrink, H., van der Burgt, A., Zwiers, L.-H., Csukai, M., & Waalwijk, C. (2008). Large-Scale Gene Discovery in the Septoria Tritici Blotch Fungus *Mycosphaerella graminicola* with a Focus on In Planta Expression. *Molecular Plant-Microbe Interactions*, *21*(9), 1249–1260. https://doi.org/10.1094/MPMI-21-9-1249

Kema, Gert H.J., Verstappen, E. C. P., Todorova, M., & Waalwijk, C. (1996). Successful crosses and molecular tetrad and progeny analyses demonstrate heterothallism in Mycosphaerella graminicola. *Current Genetics*, *30*(3), 251–258. https://doi.org/10.1007/s002940050129

Kema, Gert H.J., Yu, D. Z., Rijkenberg, F. H. J., Shaw, M. W., & Baayen, R. P. (1996). Histology of the pathogenesis of Mycosphaerella graminicola in wheat. *Phytopathology*, *86*(7), 777–786. https://doi.org/10.1094/Phyto-86-777

Keon, J., Antoniw, J., Carzaniga, R., Deller, S., Ward, J. L., Baker, J. M., Beale, M. H., Hammond-Kosack, K., & Rudd, J. J. (2007). Transcriptional adaptation of Mycosphaerella graminicola to programmed cell death (PCD) of its susceptible wheat host. *Molecular Plant-Microbe Interactions*, *20*(2), 178–193. https://doi.org/10.1094/MPMI-20-2-0178

Kerdraon, L., Barret, M., Laval, V., & Suffert, F. (2019). Differential dynamics of microbial community networks help identify microorganisms interacting with residue-borne pathogens: The case of Zymoseptoria tritici in wheat. *Microbiome*, *7*(1), 1–17. https://doi.org/10.1186/s40168-019-0736-0

Kershaw, M. J., & Talbot, N. J. (2009). Genome-wide functional analysis reveals that infection-associated fungal autophagy is necessary for rice blast disease. *Proceedings of the National Academy of Sciences of the United States of America*, *106*(37), 15967–15972. https://doi.org/10.1073/pnas.0901477106

Kettles, G. J., Bayon, C., Canning, G., Rudd, J. J., & Kanyuka, K. (2017). Apoplastic recognition of multiple candidate effectors from the wheat pathogen Zymoseptoria tritici in the nonhost plant Nicotiana benthamiana. *New Phytologist*, *213*(1), 338–350. https://doi.org/10.1111/nph.14215

Kettles, G. J., Bayon, C., Sparks, C. A., Canning, G., Kanyuka, K., & Rudd, J. J. (2018). Characterization of an antimicrobial and phytotoxic ribonuclease secreted by the fungal wheat pathogen Zymoseptoria tritici. *New Phytologist*, *217*(1), 320–331. https://doi.org/10.1111/nph.14786

Kettles, G. J., Hofinger, B. J., Hu, P., Bayon, C., Rudd, J. J., Balmer, D., Courbot, M., Hammond-Kosack, K. E., Scalliet, G., & Kanyuka, K. (2019). sRNA Profiling Combined With Gene Function Analysis Reveals a Lack of Evidence for Cross-Kingdom RNAi in the Wheat – Zymoseptoria tritici Pathosystem. *Frontiers in Plant Science*, *10*(July). https://doi.org/10.3389/fpls.2019.00892

Kettles, G. J., & Kanyuka, K. (2016). Dissecting the Molecular Interactions between Wheat and the Fungal Pathogen Zymoseptoria tritici. *Frontiers in Plant Science*, *7*(April), 1–7. https://doi.org/10.3389/fpls.2016.00508

Khan, I. A., Lu, J. P., Liu, X. H., Rehman, A., & Lin, F. C. (2012). Multifunction of autophagy-related genes in filamentous fungi. *Microbiological Research*, *167*(6), 339–345. https://doi.org/10.1016/j.micres.2012.01.004

Khoza, T. G., Dubery, I. A., & Piater, L. A. (2019). Identification of Candidate Ergosterol-Responsive Proteins Associated with the Plasma Membrane of Arabidopsis thaliana. *International Journal of Molecular Sciences*, *20*, 1302. https://doi.org/10.3390/ijms20061302

Kilaru, S., Ma, W., Schuster, M., Courbot, M., & Steinberg, G. (2015). Conditional promoters for analysis of essential genes in Zymoseptoria tritici. *Fungal Genetics and Biology*, *79*, 166–173. https://doi.org/10.1016/j.fgb.2015.03.024

Kilaru, S., Schuster, M., Ma, W., & Steinberg, G. (2017). Fluorescent markers of various organelles in the wheat pathogen Zymoseptoria tritici. *Fungal Genetics and Biology*, *105*(March), 16–27. https://doi.org/10.1016/j.fgb.2017.05.001

Kilaru, S., Schuster, M., Studholme, D., Soanes, D., Lin, C., Talbot, N. J., & Steinberg, G. (2015). A codon-optimized green fluorescent protein for live cell imaging in Zymoseptoria tritici. *Fungal Genetics and Biology*, *79*, 125–131. https://doi.org/10.1016/j.fgb.2015.03.022

Kildea, S., Marten-Heick, T., Grant, J., Mehenni-Ciz, J., & Dooley, H. (2019). A combination of target-site alterations, overexpression and enhanced efflux activity contribute to reduced azole sensitivity present in the Irish Zymoseptoria tritici population. *European Journal of Plant Pathology*, *154*(3), 529–540. https://doi.org/10.1007/s10658-019-01676-4

Kildea, S., Ransbotyn, V., Khan, M. R., Fagan, B., Leonard, G., Mullins, E., & Doohan, F. M. (2008). Bacillus megaterium shows potential for the biocontrol of septoria tritici blotch of wheat. *Biological Control*, *47*(1), 37–45. https://doi.org/10.1016/j.biocontrol.2008.07.001

Kim, H., Ridenour, J. B., Dunkle, L. D., & Bluhm, B. H. (2011). Regulation of stomatal tropism and infection by light in cercospora zeae-maydis: Evidence for coordinated host/pathogen responses to photoperiod? *PLoS Pathogens*, *7*(7). https://doi.org/10.1371/journal.ppat.1002113

Kim, K. S., Min, J., & Dickman, M. B. (2008). Oxalic Acid Is an Elicitor of Plant Programmed Cell Death during Sclerotinia sclerotiorum Disease Development. *Molecular Plant Microbe Interaction*, *21*(5), 605–612. https://doi.org/10.1094/MPMI-21-5-0605

King, R., Urban, M., Lauder, R. P., Hawkins, N., Evans, M., Plummer, A., Halsey, K., Lovegrove, A., Hammond-Kosack, K., & Rudd, J. J. (2017). A conserved fungal glycosyltransferase facilitates pathogenesis of plants by enabling hyphal growth on solid surfaces. *PLoS Pathogens*, *13*(10), 1–26. https://doi.org/10.1371/journal.ppat.1006672

Kiššová, I. B., Salin, B., Schaeffer, J., Bhatia, S., Manon, S., Camougrand, N., Kiššová, I., Salin, B., & Camougrand, N. (2007). Selective and Non-Selective Autophagic Degradation of Mitochondria in Yeast ND ES RIB. *Autophagy*, *4*(3), 329–336. https://doi.org/10.4161/auto.4034

Kitagaki, H., Wu, H., Shimoi, H., & Ito, K. (2002). Two homologous genes, DCW1 (YKL046c) and DFG5, are essential for cell growth and encode glycosylphosphatidylinositol (GPI)-anchored membrane proteins required for cell wall biogenesis in Saccharomyces cerevisiae. *Molecular Microbiology*, *46*(4), 1011–1022. https://doi.org/10.1046/j.1365-2958.2002.03244.x

Klionsky, D. J., Baehrecke, E. H., Brumell, J. H., Chu, C. T., Codogno, P., Cuervo, A.

M., Debnath, J., Deretic, V., Elazar, Z., Eskelinen, E., Finkbeiner, S., & Fueyo-margareto, J. (2011). A comprehensive glossary of autophagy-related molecules and processes (2nd edition). *Autophagy*, *7*(11), 1273–1294. https://doi.org/10.4161/auto.7.11.17661

Klockgether, J., Munder, A., Neugebauer, J., Davenport, C. F., Stanke, F., Larbig, K. D., Heeb, S., Schöck, U., Pohl, T. M., Wiehlmann, L., & Tümmler, B. (2010). Genome diversity of Pseudomonas aeruginosa PAO1 laboratory strains. *Journal of Bacteriology*, *192*(4), 1113–1121. https://doi.org/10.1128/JB.01515-09

Klose, J., & Kronstad, J. W. (2006). The multifunctional β-oxidation enzyme is required for full symptom development by the biotrophic maize pathogen Ustilago maydis. *Eukaryotic Cell*, *5*(12), 2047–2061. https://doi.org/10.1128/EC.00231-06

Koch, C., Moll, T., Neuberg, M., Ahorn, H., & Nasmyth, K. (1993). A role for the transcription factors Mbp1 and Swi4 in progression from G1 to S phase. *Science*, *261*(5128), 1551–1557. https://doi.org/10.1126/science.8372350

Köffel, R., Tiwari, R., & Falquet, L. (2005). The Saccharomyces cerevisiae YLL012/YEH1, YLR020/YEH2, and TGL1 Genes Encode a Novel Family of Membrane-Anchored Lipases That Are Required for Steryl Ester Hydrolysis TGL1 Genes Encode a Novel Family of Membrane-Anchored Lipases That Are Required for Ster. *Molecular and Cellular Biology*, *25*(5), 1655–1668. https://doi.org/10.1128/MCB.25.5.1655

Kojima, K., Kikuchi, T., Takano, Y., Oshiro, E., & Okuno, T. (2002). The mitogen-activated protein kinase gene MAF1 is essential for the early differentiation phase of appressorium formation in Colletotrichum lagenarium. *Molecular Plant-Microbe Interactions*, *15*(12), 1268–1276. https://doi.org/10.1094/MPMI.2002.15.12.1268

Konopka, J., Casadevall, A., Taylor, J., Heitman, J., & Cowen, L. (2019). *One health: fungal pathogens of humans, animals, and plants*.

Kramer, B., Thines, E., & Foster, A. J. (2009). MAP kinase signalling pathway components and targets conserved between the distantly related plant pathogenic fungi Mycosphaerella graminicola and Magnaporthe grisea. *Fungal Genetics and Biology*, *46*(9), 667–681. https://doi.org/10.1016/j.fgb.2009.06.001

Kretschmer, M., Croll, D., & Kronstad, J. W. (2017). Maize susceptibility to Ustilago maydis is influenced by genetic and chemical perturbation of carbohydrate allocation. *Molecular Plant Pathology*, *18*(9), 1222–1237. https://doi.org/10.1111/mpp.12486

Kretschmer, M., Klose, J., & Kronstad, J. W. (2012). Defects in mitochondrial and peroxisomal β-oxidation influence virulence in the maize pathogen Ustilago maydis. *Eukaryotic Cell*, *11*(8), 1055–1066. https://doi.org/10.1128/EC.00129-12

Kretschmer, M., Wang, J., & Kronstad, J. W. (2012). Peroxisomal and Mitochondrial β-Oxidation Pathways Influence the Virulence of the Pathogenic Fungus Cryptococcus neoformans. *Eukaryotic Cell*, *11*(8), 1042–1054. https://doi.org/10.1128/ec.00128-12

Krishnan, K., & Askew, D. S. (2014). The fungal UPR: A regulatory hub for virulence traits in the mold pathogen Aspergillus fumigatus. *Virulence*, *5*(2), 334–340. https://doi.org/10.4161/viru.26571

Kunze, M., Kragler, F., Binder, M., Hartig, A., & Gurvitz, A. (2002). Targeting of malate synthase 1 to the peroxisomes of Saccharomyces cerevisiae cells depends on growth on oleic acid medium. *European Journal of Biochemistry*, *269*(3), 915–922. https://doi.org/10.1046/j.0014-2956.2001.02727.x

Kunze, M., Pracharoenwattana, I., Smith, S. M., & Hartig, A. (2006). A central role for

the peroxisomal membrane in glyoxylate cycle function. *Biochimica et Biophysica Acta - Molecular Cell Research*, *1763*(12), 1441–1452. https://doi.org/10.1016/j.bbamcr.2006.09.009

Kurat, C. F., Natter, K., Petschnigg, J., Wolinski, H., Scheuringer, K., Scholz, H., Zimmermann, R., Leber, R., Zechner, R., & Kohlwein, S. D. (2006). Obese yeast: Triglyceride lipolysis is functionally conserved from mammals to yeast. *Journal of Biological Chemistry*, *281*(1), 491–500. https://doi.org/10.1074/jbc.M508414200

LaFayette, S. L., Collins, C., Zaas, A. K., Schell, W. A., Betancourt-Quiroz, M., Gunatilaka, A. A. L., Perfect, J. R., & Cowen, L. E. (2010). PKC Signaling Regulates Drug Resistance of the Fungal Pathogen Candida albicans via Circuitry Comprised of Mkc1, Calcineurin, and Hsp90. *PLoS Pathogens*, *6*(8), e1001069. https://doi.org/10.1371/journal.ppat.1001069

Lambou, K., Malagnac, F., Barbisan, C., Tharreau, D., Lebrun, M. H., & Silar, P. (2008). The crucial role of the Pls1 tetraspanin during ascospore germination in Podospora anserina provides an example of the convergent evolution of morphogenetic processes in fungal plant pathogens and saprobes. *Eukaryotic Cell*, *7*(10), 1809–1818. https://doi.org/10.1128/EC.00149-08

Langmead, B., & Salzberg, S. L. (2012). Fast gapped-read alignment with Bowtie 2. *Nature Methods*, *9*(4), 357–359. https://doi.org/10.1038/nmeth.1923

Latz, M. A. C., Jensen, B., Collinge, D. B., & Lyngs Jørgensen, H. J. (2020). Identification of two endophytic fungi that control Septoria tritici blotch in the field, using a structured screening approach. *Biological Control*, *141*(September 2019), 104128. https://doi.org/10.1016/j.biocontrol.2019.104128

Lee, J., Orosa, B., Millyard, L., Edwards, M., Kanyuka, K., Gatehouse, A., Rudd, J., Hammond-Kosack, K., Pain, N., & Sadanandom, A. (2015). Functional analysis of a Wheat Homeodomain protein, TaR1, reveals that host chromatin remodelling influences the dynamics of the switch to necrotrophic growth in the phytopathogenic fungus Zymoseptoria tritici. *New Phytologist*, *206*(2), 598–605. https://doi.org/10.1111/nph.13323

Lee, K. S., Levin, D. E., & Eg, M. (1992). Dominant Mutations in a Gene Encoding a Putative Protein Kinase (BCKI) Bypass the Requirement for a Saccharomyces cerevisiae Protein Kinase C Homolog. *Molecular and Cellular Biology*, *12*(1), 172–182.

Lee, S., Lee, J., Lee, S., Park, E., Kim, K., Kim, M., Yun, S., & Lee, Y. (2009). GzSNF1 Is Required for Normal Sexual and Asexual Development in the Ascomycete Gibberella zeae. *Eukaryotic Cell*, *8*(1), 116–127. https://doi.org/10.1128/EC.00176-08

Lee, W. S., Rudd, J. J., Hammond-Kosack, K. E., & Kanyuka, K. (2014). Mycosphaerella graminicola LysM effector-mediated stealth pathogenesis subverts recognition through both CERK1 and CEBiP homologues in wheat. *Molecular Plant-Microbe Interactions*, *27*(3), 236–243. https://doi.org/10.1094/MPMI-07-13-0201-R

Lehti-Shiu, M. D., Zou, C., Hanada, K., & Shiu, S.-H. (2009). Evolutionary History and Stress Regulation of Plant Receptor-Like Kinase/Pelle Genes. *Plant Physiology*, *150*, 12–26. https://doi.org/10.1104/pp.108.134353

Lendenmann, M. H., Croll, D., & McDonald, B. A. (2015). QTL mapping of fungicide sensitivity reveals novel genes and pleiotropy with melanization in the pathogen Zymoseptoria tritici. *Fungal Genetics and Biology*, *80*, 53–67. https://doi.org/10.1016/j.fgb.2015.05.001

Levin, D. E. (2011). Regulation of cell wall biogenesis in Saccharomyces cerevisiae: The cell wall integrity signaling pathway. *Genetics*, *189*(4), 1145–1175. https://doi.org/10.1534/genetics.111.128264

Lewis, C. M., Persoons, A., Bebber, D. P., Kigathi, R. N., Maintz, J., Findlay, K., Bueno-Sancho, V., Corredor-Moreno, P., Harrington, S. A., Kangara, N., Berlin, A., García, R., Germán, S. E., Hanzalová, A., Hodson, D. P., Hovmøller, M. S., Huerta-Espino, J., Imtiaz, M., Mirza, J. I., … Saunders, D. G. O. (2018). Potential for re-emergence of wheat stem rust in the United Kingdom. *Communications Biology*, *1*(1), 1–9. https://doi.org/10.1038/s42003-018-0013-y

Li, B., & Dewey, C. N. (2011). RSEM: accurate transcript quantification from RNA-Seq data with or without a reference genome. *BMC Bioinformatics*, *12*(323). https://doi.org/10.1186/1471-2105-12-323

Li, H., Handsaker, B., Wysoker, A., Fennell, T., Ruan, J., Homer, N., Marth, G., Abecasis, G., & Durbin, R. (2009). The Sequence Alignment/Map format and SAMtools. *Bioinformatics*, *25*(16), 2078–2079. https://doi.org/10.1093/bioinformatics/btp352

Li, W. W., Li, J., & Bao, J. K. (2012). Microautophagy: Lesser-known self-eating. *Cellular and Molecular Life Sciences*, *69*(7), 1125–1136. https://doi.org/10.1007/s00018-011-0865-5

Li, Yang, Zhang, X., Hu, S., Liu, H., & Xu, J. R. (2017). PKA activity is essential for relieving the suppression of hyphal growth and appressorium formation by MoSfl1 in Magnaporthe oryzae. *PLoS Genetics*, *13*(8), 1–28. https://doi.org/10.1371/journal.pgen.1006954

Li, Yanjie, Zhang, L., Wang, D., Zhou, H., Ouyang, H., Ming, J., & Jin, C. (2008). Deletion of the msdS/AfmsdC gene induces abnormal polarity and septation in Aspergillus fumigatus. *Microbiology*, *154*(7), 1960–1972. https://doi.org/10.1099/mic.0.2008/017525-0

Lin, X., Andrew Alspaugh, J., Liu, H., & Harris, S. (2015). Fungal morphogenesis. *Cold Spring Harbor Perspectives in Medicine*, *5*(2), 1–26. https://doi.org/10.1101/cshperspect.a019679

Liu, D., Coloe, S., Baird, R., & Pedersen, J. (2000). Rapid Mini-Preparation of Fungal DNA for PCR. *Journal of Clinical Microbiology*, *38*(1), 471.

Liu, W., Zhou, X., Li, G., Li, L., Kong, L., Wang, C., Zhang, H., & Xu, J. R. (2011). Multiple plant surface signals are sensed by different mechanisms in the rice blast fungus for appressorium formation. *PLoS Pathogens*, *7*(1), e1001261. https://doi.org/10.1371/journal.ppat.1001261

Liu, X. H., Lu, J. P., Zhang, L., Dong, B., Min, H., & Lin, F. C. (2007). Involvement of a Magnaporthe grisea serine/threonine kinase gene, MgATG1, in Appressorium turgor and pathogenesis. *Eukaryotic Cell*, *6*(6), 997–1005. https://doi.org/10.1128/EC.00011-07

Liu, Xiao-hong, Zhao, Y., Zhu, X., Zeng, X., Huang, L., & Dong, B. (2017). Autophagy-related protein MoAtg14 is involved in differentiation , development and pathogenicity in the rice blast fungus Magnaporthe oryzae. *Scientific Reports*, *7*, 40018. https://doi.org/10.1038/srep40018

Liu, Xiao-man, Yamasaki, A., Du, X., Coffman, V. C., Ohsumi, Y., Nakatogawa, H., Wu, J., & Noda, N. N. (2018). Lipidation-independent vacuolar functions of Atg8 rely on its noncanonical interaction with a vacuole membrane protein. *ELife*, *7*, e41237. https://doi.org/10.7554/eLife.41237

Liu, Zhaohui, Zhang, Z., Faris, J. D., Oliver, R. P., Syme, R., McDonald, M. C.,

McDonald, B. A., Solomon, P. S., Lu, S., Shelver, W. L., Xu, S., & Friesen, T. L. (2012). The cysteine rich necrotrophic effector SnTox1 produced by Stagonospora nodorum triggers susceptibility of wheat lines harboring Snn1. *PLoS Pathogens*, *8*(1). https://doi.org/10.1371/journal.ppat.1002467

Liu, Zixu, Wu, Y., Yang, F., Zhang, Y., Chen, S., Xie, Q., Tian, X., & Zhou, J. (2013). BIK1 interacts with PEPRs to mediate ethylene-induced immunity. *Proceedings of the National Academy of Sciences of the United States of America*, *110*(15), 6205–6210. https://doi.org/10.1073/pnas.1215543110

Lo Presti, L., Lanver, D., Schweizer, G., Tanaka, S., Liang, L., Tollot, M., Zuccaro, A., Reissmann, S., & Kahmann, R. (2015). Fungal effectors and plant susceptibility. *Annual Review of Plant Biology*, *66*(May), 513–545. https://doi.org/10.1146/annurev-arplant-043014-114623

Lockshon, D., Surface, L. E., Kerr, E. O., Kaeberlein, M., & Kennedy, B. K. (2007). The sensitivity of yeast mutants to oleic acid implicates the peroxisome and other processes in membrane function. *Genetics*, *175*(1), 77–91. https://doi.org/10.1534/genetics.106.064428

Loesch, A., Hutwimmer, S., & Strasser, H. (2010). Carbon utilization pattern as a potential quality control criterion for virulence of Beauveria brongniartii. *Journal of Invertebrate Pathology*, *104*(1), 58–65. https://doi.org/10.1016/j.jip.2010.01.007

Lofgren, L. A., LeBlanc, N. R., Certano, A. K., Nachtigall, J., LaBine, K. M., Riddle, J., Broz, K., Dong, Y., Bethan, B., Kafer, C. W., & Kistler, H. C. (2018). Fusarium graminearum: pathogen or endophyte of North American grasses? *New Phytologist*, *217*(3), 1203–1212. https://doi.org/10.1111/nph.14894

Lorang, J., Kidarsa, T., Bradford, C. S., Gilbert, B., Curtis, M., Tzeng, S.-C., Maier, C. S., & Wolpert, T. J. (2012). Tricking the Guard : Exploiting Plant. *Science*, *338*(November), 659–662.

Lorang, J. M., Sweat, T. A., & Wolpert, T. J. (2007). Plant disease susceptibility conferred by a “resistance” gene. *Proceedings of the National Academy of Sciences of the United States of America*, *104*(37), 14861–14866. https://doi.org/10.1073/pnas.0702572104

Lorenz, M. C., & Fink, G. R. (2002). Life and death in a macrophage: Role of the glyoxylate cycle in virulence. *Eukaryotic Cell*, *1*(5), 657–662. https://doi.org/10.1128/EC.1.5.657-662.2002

Lotze, M. T., Zeh, H. J., Rubartelli, A., Sparvero, L. J., Amoscato, A. A., Washburn, N. R., DeVera, M. E., Liang, X., Tör, M., & Billiar, T. (2007). The grateful dead: Damage-associated molecular pattern molecules and reduction/oxidation regulate immunity. *Immunological Reviews*, *220*(1), 60–81. https://doi.org/10.1111/j.1600-065X.2007.00579.x

Love, M. I., Huber, W., & Anders, S. (2014). Moderated estimation of fold change and dispersion for RNA-seq data with DESeq2. *Genome Biology*, *15*(12), 1–21. https://doi.org/10.1186/s13059-014-0550-8

Lowndes, N. F., Johnson, A. L., Breeden, L., & Johnston, L. H. (1992). SWI6 protein is required for transcription of the periodically expressed DNA synthesis genes in budding yeast. *Nature*, *357*, 505–508. https://doi.org/10.1038/357505a0

Lucas, J. A., Hawkins, N. J., & Fraaije, B. A. (2015). The Evolution of Fungicide Resistance. In *Advances in Applied Microbiology* (Vol. 90, pp. 29–92). Elsevier Ltd. https://doi.org/10.1016/bs.aambs.2014.09.001

Lv, W., Wang, C., Yang, N., Que, Y., Talbot, N. J., & Wang, Z. (2017). Genome-wide functional analysis reveals that autophagy is necessary for growth, sporulation,

deoxynivalenol production and virulence in Fusarium graminearum. *Scientific Reports*, *7*, 11062. https://doi.org/10.1038/s41598-017-11640-z

Lv, W., Xu, Z., Talbot, N. J., & Wang, Z. (2020). The sorting nexin FgAtg20 is involved in the Cvt pathway, non-selective macroautophagy, pexophagy and pathogenesis in Fusarium graminearum. *Cellular Microbiology*, *22*, e13208. https://doi.org/10.1111/cmi.13208

Lynch-Day, M. A., & Klionsky, D. J. (2010). The Cvt pathway as a model for selective autophagy. *FEBS Letters*, *584*(7), 1359–1366. https://doi.org/10.1016/j.febslet.2010.02.013

Lynch, K. M., Zannini, E., Guo, J., Axel, C., Arendt, E. K., Kildea, S., & Coffey, A. (2016). Control of Zymoseptoria tritici cause of septoria tritici blotch of wheat using antifungal Lactobacillus strains. *Journal of Applied Microbiology*, *121*(2), 485–494. https://doi.org/10.1111/jam.13171

Ma, L. J., Van Der Does, H. C., Borkovich, K. A., Coleman, J. J., Daboussi, M. J., Di Pietro, A., Dufresne, M., Freitag, M., Grabherr, M., Henrissat, B., Houterman, P. M., Kang, S., Shim, W. B., Woloshuk, C., Xie, X., Xu, J. R., Antoniw, J., Baker, S. E., Bluhm, B. H., … Rep, M. (2010). Comparative genomics reveals mobile pathogenicity chromosomes in Fusarium. *Nature*, *464*(7287), 367–373. https://doi.org/10.1038/nature08850

Ma, X., Keller, B., McDonald, B. A., Palma-Guerrero, J., & Wicker, T. (2018). Comparative Transcriptomics Reveals How Wheat Responds to Infection by *Zymoseptoria tritici*. *Molecular Plant-Microbe Interactions*, *31*(4), 420–431. https://doi.org/10.1094/MPMI-10-17-0245-R

Ma, Z., Song, T., Zhu, L., Ye, W., Wang, Y., Shao, Y., Dong, S., Zhang, Z., Dou, D., Zheng, X., Tyler, B. M., & Wang, Y. (2015). A Phytophthora sojae Glycoside Hydrolase 12 Protein Is a Major Virulence Factor during Soybean Infection and Is Recognized as a PAMP. *The Plant Cell*, *27*, 2057–2072. https://doi.org/10.1105/tpc.15.00390

Madeira, F., Park, Y. M., Lee, J., Buso, N., Gur, T., Madhusoodanan, N., Basutkar, P., Tivey, A. R. N., Potter, S. C., Finn, R. D., & Lopez, R. (2019). The EMBL-EBI search and sequence analysis tools APIs in 2019. *Nucleic Acids Research*, *47*(W1), W636–W641. https://doi.org/10.1093/nar/gkz268

Maeda, Y., Oku, M., & Sakai, Y. (2017). Autophagy-independent function of Atg8 in lipid droplet dynamics in yeast. *Journal of Biochemistry*, *161*(4), 339–348. https://doi.org/10.1093/jb/mvw078

Maeda, Y., Oku, M., Sakai, Y., Maeda, Y., Oku, M., & Sakai, Y. (2015). A defect of the vacuolar putative lipase Atg15 accelerates degradation of lipid droplets through lipolysis A defect of the vacuolar putative lipase Atg15 accelerates degradation of lipid droplets through lipolysis. *Autophagy*, *11*(8), 1247–1258. https://doi.org/10.1080/15548627.2015.1056969

Maggio-Hall, L. A., & Keller, N. P. (2004). Mitochondrial β-oxidation in Aspergillus nidulans. *Molecular Microbiology*, *54*(5), 1173–1185. https://doi.org/10.1111/j.1365-2958.2004.04340.x

Maggio-Hall, L. A., Lyne, P., Wolff, J. A., & Keller, N. P. (2008). A single acyl-CoA dehydrogenase is required for catabolism of isoleucine, valine and short-chain fatty acids in Aspergillus nidulans. *Fungal Genetics and Biology*, *45*(3), 180–189. https://doi.org/10.1016/j.fgb.2007.06.004

Malavazi, I., Goldmanm, G. H., & Brown, N. A. (2014). The importance of connections between the cell wall integrity pathway and the unfolded protein response in

filamentous fungi. *Briefings in Functional Genomics*, *13*(6), 456–470. https://doi.org/10.1093/bfgp/elu027

Malinovsky, F. G., Fangel, J. U., & Willats, W. G. T. (2014). The role of the cell wall in plant immunity. *Frontiers in Plant Science*, *5*, 178. https://doi.org/10.3389/fpls.2014.00178

Manente, M., & Ghislain, M. (2009). The lipid-translocating exporter family and membrane phospholipid homeostasis in yeast. *FEMS Yeast Research*, *9*(5), 673–687. https://doi.org/10.1111/j.1567-1364.2009.00513.x

Marshall, R., Kombrink, A., Motteram, J., Loza-Reyes, E., Lucas, J., Hammond-Kosack, K. E., Thomma, B. P. H. J., & Rudd, J. J. (2011). Analysis of two in planta expressed LysM effector homologs from the fungus mycosphaerella graminicola reveals novel functional properties and varying contributions to virulence on wheat. *Plant Physiology*, *156*(2), 756–769. https://doi.org/10.1104/pp.111.176347

Marzano, S.-Y. L., Hobbs, H. A., Nelson, B. D., Hartman, G. L., Eastburn, D. M., McCoppin, N. K., & Domier, L. L. (2015). Transfection of Sclerotinia sclerotiorum with In Vitro Transcripts of a Naturally Occurring Interspecific Recombinant of Sclerotinia sclerotiorum Hypovirus 2 Significantly Reduces Virulence of the Fungus . *Journal of Virology*, *89*(9), 5060–5071. https://doi.org/10.1128/jvi.03199-14

Marzano, S.-Y. L., Nelson, B. D., Ajayi-oyetunde, O., Bradley, C. A., Hughes, T. J., Hartman, G. L., Eastburn, D. M., & Domier, L. L. (2016). Identification of Diverse Mycoviruses through Metatranscriptomics Characterization of the Viromes of Five Major Fungal Plant Pathogens Shin-Yi. *Journal of Virology*, *90*, 6846–6863. https://doi.org/10.1128/JVI.00357-16

Masloff, S., Pöggeler, S., & Kück, U. (1999). The pro1+ gene from Sordaria macrospora encodes a C6 zinc finger transcription factor required for fruiting body development. *Genetics*, *152*(1), 191–199. https://doi.org/10.1093/genetics/152.1.191

Mattiazzi Ušaj, M., Brložnik, M., Kaferle, P., Žitnik, M., Wolinski, H., Leitner, F., Kohlwein, S. D., Zupan, B., & Petrovič, U. (2015). Genome-wide localization study of yeast pex11 identifies peroxisome-mitochondria interactions through the ERMES complex. *Journal of Molecular Biology*, *427*(11), 2072–2087. https://doi.org/10.1016/j.jmb.2015.03.004

McCorison, C. B., & Goodwin, S. B. (2020). The wheat pathogen Zymoseptoria tritici senses and responds to different wavelengths of light. *BMC Genomics*, *21*(1), 1–15. https://doi.org/10.1186/s12864-020-06899-y

McDonald, B. A., & Stukenbrock, E. H. (2016). Rapid emergence of pathogens in agro-ecosystems : global threats to agricultural sustainability and food security. *Philosophical Transactions of the Royal Society B: Biological Sciences*, *371*, 20160026. https://doi.org/10.1098/rstb.2016.0026

McDonald, M. C., McDonald, B. A., & Solomon, P. S. (2015). Recent advances in the Zymoseptoria tritici–wheat interaction: Insights from pathogenomics. *Frontiers in Plant Science*, *6*(FEB), 1–5. https://doi.org/10.3389/fpls.2015.00102

McEwen, J. E., Hong, K. H., Park, S., & Preciado, G. T. (1993). Sequence and chromosomal localization of two PET genes required for cytochrome c oxidase assembly in Saccharomyces cerevisiae. *Current Genetics*, *23*(1), 9–14. https://doi.org/10.1007/BF00336742

Mcintosh, R. A., & Pretorius, Z. A. (2011). Borlaug Global Rust Initiative provides momentum for wheat rust research. *Euphytica*, *179*, 1–2.

https://doi.org/10.1007/s10681-011-0389-y

McKinney, J. D., Zu Bentrup, K. H., Munoz-Elias, E. J., Miczak, A., Chen, B., Chan, W. T., Swenson, D., Sacchettini, J. C., Jacobs Jr., W. R., & Russel, D. G. (2000). Persistence of Mycobacterium tuberculosis in macrophages and mice requires the glyoxylate shunt enzyme isocitrate lyase. *Nature*, *406*, 735–738. https://doi.org/10.1038/35021074

Mehrabi, R., Ding, S., & Xu, J. R. (2008). MADS-box transcription factor Mig1 is required for infectious growth in Magnaporthe grisea. *Eukaryotic Cell*, *7*(5), 791–799. https://doi.org/10.1128/EC.00009-08

Mehrabi, R., & Kema, G. H. J. (2006). Protein kinase a subunits of the ascomycete pathogen Mycosphaerella graminicola regulate asexual fructification, filamentation, melanization and osmosensing. *Molecular Plant Pathology*, *7*(6), 565–577. https://doi.org/10.1111/j.1364-3703.2006.00361.x

Mehrabi, R., M'Barek, S. Ben, Van Der Lee, T. A. J., Waalwijk, C., De Wit, P. J. G. M., & Kema, G. H. J. (2009). Gα and Gβ proteins regulate the cyclic AMP pathway that is required for development and pathogenicity of the phytopathogen mycosphaerella graminicola. *Eukaryotic Cell*, *8*(7), 1001–1013. https://doi.org/10.1128/EC.00258-08

Mehrabi, R., Van Der Lee, T., Waalwijk, C., & Kema, G. H. J. (2006). MgSlt2, a cellular integrity MAP kinase gene of the fungal wheat pathogen Mycosphaerella graminicola, is dispensable for penetration but essential for invasive growth. *Molecular Plant-Microbe Interactions*, *19*(4), 389–398. https://doi.org/10.1094/MPMI-19-0389

Mehrabi, R., Zwiers, L.-H., De Waard, M. A., & Kema, G. H. J. (2006). MgHog1 Regulates Dimorphism and Pathogenicity in the Fungal Wheat Pathogen Mycosphaerella graminicola. *Molecular Plant-Microbe Interactions*, *19*(11), 1262–1269. https://doi.org/10.1094/MPMI-19-1262

Meile, L., Croll, D., Brunner, P. C., Plissonneau, C., Hartmann, F. E., McDonald, B. A., & Sánchez-Vallet, A. (2018). A fungal avirulence factor encoded in a highly plastic genomic region triggers partial resistance to septoria tritici blotch. *New Phytologist*, *219*(3), 1048–1061. https://doi.org/10.1111/nph.15180

Meile, L., Peter, J., Puccetti, G., Alassimone, J., McDonald, B. A., & Sánchez-Vallet, A. (2020). Chromatin dynamics contribute to the spatiotemporal expression pattern of virulence genes in a fungal plant pathogen. *MBio*, *11*(5), 1–18. https://doi.org/10.1128/mBio.02343-20

Mejri, S., Siah, A., Coutte, F., Magnin-Robert, M., Randoux, B., Tisserant, B., Krier, F., Jacques, P., Reignault, P., & Halama, P. (2018). Biocontrol of the wheat pathogen Zymoseptoria tritici using cyclic lipopeptides from Bacillus subtilis. *Environmental Science and Pollution Research*, *25*(30), 29822–29833. https://doi.org/10.1007/s11356-017-9241-9

Mendgen, K., Hahn, M., & Deising, H. (1996). Morphogenesis and Mechanisms of Penetration By Plant Pathogenic Fungi. *Annual Review of Phytopathology*, *34*(1), 367–386. https://doi.org/10.1146/annurev.phyto.34.1.367

Meng, S., Xiong, M., Jagernath, J. S., Wang, C., Qiu, J., Shi, H., & Kou, Y. (2020). UvAtg8-Mediated Autophagy Regulates Fungal Growth, Stress Responses, Conidiation, and Pathogenesis in Ustilaginoidea virens. *Rice*, *13*(1). https://doi.org/10.1186/s12284-020-00418-z

Mey, G., Held, K., Scheffer, J., Tenberge, K. B., & Tudzynski, P. (2002). CPMK2, an SLT2-homologous mitogen-activated protein (MAP) kinase, is essential for

pathogenesis of Claviceps purpurea on rye: Evidence for a second conserved pathogenesis-related MAP kinase cascade in phytopathogenic fungi. *Molecular Microbiology*, *46*(2), 305–318. https://doi.org/10.1046/j.1365-2958.2002.03133.x

Mikawa, T., Kanoh, J., & Ishikawa, F. (2010). Fission yeast Vps1 and Atg8 contribute to oxidative stress resistance. *Genes to Cells*, *15*, 229–242. https://doi.org/10.1111/j.1365-2443.2009.01376.x

Minina, E. A., Bozhkov, P. V., & Hofius, D. (2014). Autophagy as initiator or executioner of cell death. *Trends in Plant Science*, *19*(11), 692–697. https://doi.org/10.1016/j.tplants.2014.07.007

Mirzadi Gohari, A., Ware, S. B., Wittenberg, A. H. J., Mehrabi, R., Ben M'Barek, S., Verstappen, E. C. P., van der Lee, T. A. J., Robert, O., Schouten, H. J., de Wit, P. P. J. G. M., & Kema, G. H. J. (2015). Effector discovery in the fungal wheat pathogen Zymoseptoria tritici. *Molecular Plant Pathology*, *16*(9), 931–945. https://doi.org/10.1111/mpp.12251

Mizushima, N., & Komatsu, M. (2011). Autophagy: Renovation of cells and tissues. *Cell*, *147*(4), 728–741. https://doi.org/10.1016/j.cell.2011.10.026

Mizushima, N., & Levine, B. (2010). Autophagy in mammalian development and differentiation. *Nature Cell Biology*, *12*(9), 823–830. https://doi.org/10.1038/ncb0910-823

Mohammadi, N., Mehrabi, R., Mirzadi Gohari, A., Mohammadi Goltapeh, E., Safaie, N., & Kema, G. H. J. (2017). The ZtVf1 transcription factor regulates development and virulence in the foliar wheat pathogen Zymoseptoria tritici. *Fungal Genetics and Biology*, *109*(October), 26–35. https://doi.org/10.1016/j.fgb.2017.10.003

Möller, M., Habig, M., Freitag, M., & Stukenbrock, E. H. (2018). Extraordinary Genome Instability and Widespread Chromosome Rearrangements During Vegetative Growth. *Genetics*, *210*, 517–529. https://doi.org/10.1534/genetics.118.301050

Morais do Amaral, A., Antoniw, J., Rudd, J. J., & Hammond-Kosack, K. E. (2012). Defining the Predicted Protein Secretome of the Fungal Wheat Leaf Pathogen Mycosphaerella graminicola. *PLoS ONE*, *7*(12), e49904. https://doi.org/10.1371/journal.pone.0049904

Mösch, H. U., & Fink, G. R. (1997). Dissection of filamentous growth by transposon mutagenesis in Sacchromyces cerevisiae. *Genetics*, *145*(3), 671–684. https://doi.org/10.1093/genetics/145.3.671

Mösch, H. U., Kübler, E., Krappmann, S., Fink, G. R., & Braus, G. H. (1999). Crosstalk between the Ras2p-controlled mitogen-activated protein kinase and cAMP pathways during invasive growth of Saccharomyces cerevisiae. *Molecular Biology of the Cell*, *10*(5), 1325–1335. https://doi.org/10.1091/mbc.10.5.1325

Motteram, J., Küfner, I., Deller, S., Brunner, F., Hammond-Kosack, K. E., Nürnberger, T., & Rudd, J. J. (2009). Molecular characterization and functional analysis of MgNLP, the sole NPP1 domain-containing protein, from the fungal wheat leaf pathogen mycosphaerella graminicola. *Molecular Plant-Microbe Interactions*, *22*(7), 790–799. https://doi.org/10.1094/MPMI-22-7-0790

Motteram, J., Lovegrove, A., Pirie, E., Marsh, J., Devonshire, J., van de Meene, A., Hammond-Kosack, K., & Rudd, J. J. (2011). Aberrant protein N-glycosylation impacts upon infection-related growth transitions of the haploid plant-pathogenic fungus Mycosphaerella graminicola. *Molecular Microbiology*. https://doi.org/10.1111/j.1365-2958.2011.07701.x

Mouyna, I., Morelle, W., Vai, M., Monod, M., Léchenne, B., Fontaine, T., Beauvais, A., Sarfati, J., Prévost, M. C., Henry, C., & Latgé, J. P. (2005). Deletion of GEL2

encoding for a β(1-3)glucanosyltransferase affects morphogenesis and virulence in Aspergillus fumigatus. *Molecular Microbiology*, *56*(6), 1675–1688. https://doi.org/10.1111/j.1365-2958.2005.04654.x

Mueller, A. N., Ziemann, S., Treitschke, S., Aßmann, D., & Doehlemann, G. (2013). Compatibility in the Ustilago maydis-Maize Interaction Requires Inhibition of Host Cysteine Proteases by the Fungal Effector Pit2. *PLoS Pathogens*, *9*(2). https://doi.org/10.1371/journal.ppat.1003177

Muñoz-Adalia, E. J., Flores-Pacheco, J. A., Martínez-Álvarez, P., Martín-García, J., Fernández, M., & Diez, J. J. (2016). Effect of mycoviruses on the virulence of Fusarium circinatum and laccase activity. *Physiological and Molecular Plant Pathology*, *94*, 8–15. https://doi.org/10.1016/j.pmpp.2016.03.002

Munro, C. A., Selvaggini, S., Bruijn, I. De, Walker, L., Lenardon, M. D., Gerssen, B., Milne, S., Brown, A. J. P., & Gow, N. A. R. (2007). The PKC , HOG and Ca 2 + signalling pathways co-ordinately regulate chitin synthesis in Candida albicans. *Molecular Microbiology*, *63*(5), 1399–1413. https://doi.org/10.1111/j.1365-2958.2007.05588.x

Nadal, M., García-Pedrajas, M. D., & Gold, S. E. (2008). Dimorphism in fungal plant pathogens. *FEMS Microbiology Letters*, *284*(2), 127–134. https://doi.org/10.1111/j.1574-6968.2008.01173.x

Nadal, M., & Gold, S. E. (2010). The autophagy genes atg8 and atg1 affect morphogenesis and pathogenicity in Ustilago maydis. *Molecular Plant Pathology*, *11*(4), 463–478. https://doi.org/10.1111/j.1364-3703.2010.00620.x

Nakagawa, J., Waldner, H., Meyer-Monard, S., Hofsteenge, J., Jenö, P., & Moroni, C. (1995). AUH, a gene encoding an AU-specific RNA binding protein with intrinsic enoyl-CoA hydratase activity. *Proceedings of the National Academy of Sciences of the United States of America*, *92*(6), 2051–2055. https://doi.org/10.1073/pnas.92.6.2051

Nakatogawa, H., Suzuki, K., Kamada, Y., & Ohsumi, Y. (2009). Dynamics and diversity in autophagy mechanisms: Lessons from yeast. *Nature Reviews Molecular Cell Biology*, *10*(7), 458–467. https://doi.org/10.1038/nrm2708

Naranjo-Ortiz, M. A., & Gabaldon, T. (2019). Fungal evolution : major ecological adaptations and evolutionary transitions. *Biological Reviews*, *94*, 1443–1476. https://doi.org/10.1111/brv.12510

Naumann, T. A., Wicklow, D. T., & Price, N. P. J. (2011). Identification of a chitinase-modifying protein from Fsarium verticillioides: Truncation of a host resistance protein by a fungalysin metalloprotease. *Journal of Biological Chemistry*, *286*(41), 35358–35366. https://doi.org/10.1074/jbc.M111.279646

Nguyen, L. N., Bormann, J., Le, G. T. T., Stärkel, C., Olsson, S., Nosanchuk, J. D., Giese, H., & Schäfer, W. (2011). Autophagy-related lipase FgATG15 of Fusarium graminearum is important for lipid turnover and plant infection. *Fungal Genetics and Biology*, *48*(3), 217–224. https://doi.org/10.1016/j.fgb.2010.11.004

Nguyen, T. Van, Schäfer, W., & Bormann, J. (2012). The Stress-Activated Protein Kinase FgOS-2 Is a Key Regulator in the Life Cycle of the Cereal Pathogen Fusarium graminearum. *Molecular Plant Microbe Interaction*, *25*(9), 1142–1156. https://doi.org/10.1094/MPMI-02-12-0047-R

Nitsche, B. M., Burggraaf-Van Welzen, A. M., Lamers, G., Meyer, V., & Ram, A. F. J. (2013). Autophagy promotes survival in aging submerged cultures of the filamentous fungus Aspergillus niger. *Applied Microbiology and Biotechnology*, *97*(18), 8205–8218. https://doi.org/10.1007/s00253-013-4971-1

Odds, F. C., Brown, A. J. P., & Gow, N. A. R. (2003). Antifungal agents: Mechanisms of action. *Trends in Microbiology*, *11*(6), 272–279. https://doi.org/10.1016/S0966-842X(03)00117-3

Odilbekov, F., Armoniené, R., Koc, A., Svensson, J., & Chawade, A. (2019). GWAS-Assisted Genomic Prediction to Predict Resistance to Septoria Tritici Blotch in Nordic Winter Wheat at Seedling Stage. *Frontiers in Genetics*, *10*(November), 1–10. https://doi.org/10.3389/fgene.2019.01224

Oerke, E. C. (2006). Crop losses to pests. *Journal of Agricultural Science*, *144*(1), 31–43. https://doi.org/10.1017/S0021859605005708

Ohm, R. A., Feau, N., Henrissat, B., Schoch, C. L., Horwitz, B. A., Barry, K. W., Condon, B. J., Copeland, A. C., Dhillon, B., Glaser, F., Hesse, C. N., Kosti, I., LaButti, K., Lindquist, E. A., Lucas, S., Salamov, A. A., Bradshaw, R. E., Ciuffetti, L., Hamelin, R. C., … Grigoriev, I. V. (2012). Diverse Lifestyles and Strategies of Plant Pathogenesis Encoded in the Genomes of Eighteen Dothideomycetes Fungi. *PLoS Pathogens*, *8*(12). https://doi.org/10.1371/journal.ppat.1003037

Ökmen, B., Etalo, D. W., Joosten, M. H. A. J., Bouwmeester, H. J., de Vos, R. C. H., Collemare, J., & De Wit, P. J. G. M. (2013). Detoxification of α-tomatine by Cladosporium fulvum is required for full virulence on tomato. *New Phytologist*, *198*(4), 1203–1214. https://doi.org/10.1111/nph.12208

Oliveira-Garcia, E., & Deising, H. B. (2013). Infection Structure – Speci fi c Expression of b-1,3-Glucan Synthase Is Essential for Pathogenicity of Colletotrichum graminicola and Evasion of b-Glucan–Triggered Immunity in Maize. *The Plant Cell*, *25*, 2356–2378. https://doi.org/10.1105/tpc.112.103499

Oliver, R. P., & Solomon, P. S. (2010). New developments in pathogenicity and virulence of necrotrophs. *Current Opinion in Plant Biology*, *13*(4), 415–419. https://doi.org/10.1016/j.pbi.2010.05.003

Orton, E. S., & Brown, J. K. M. (2016). Reduction of growth and reproduction of the biotrophic fungus Blumeria graminis in the presence of a necrotrophic pathogen. *Frontiers in Plant Science*, *7*, 742. https://doi.org/10.3389/fpls.2016.00742

Orvedahl, A., & Levine, B. (2009). Eating the enemy within: Autophagy in infectious diseases. *Cell Death and Differentiation*, *16*(1), 57–69. https://doi.org/10.1038/cdd.2008.130

Osés-Ruiz, M., & Talbot, N. J. (2017). Cell cycle-dependent regulation of plant infection by the rice blast fungus Magnaporthe oryzae. *Communicative and Integrative Biology*, *10*(5–6), 0–5. https://doi.org/10.1080/19420889.2017.1372067

Owen, W. J., Yao, C., Myung, K., Kemmitt, G., Leader, A., Meyer, K. G., Bowling, A. J., Slanec, T., & Kramer, V. J. (2017). Biological characterization of fenpicoxamid, a new fungicide with utility in cereals and other crops. *Pest Management Science*, *73*(10), 2005–2016. https://doi.org/10.1002/ps.4588

Pakula, T. M., Laxell, M., Huuskonen, A., Uusitalo, J., Saloheimo, M., & Penttilä, M. (2003). The effects of drugs inhibiting protein secretion in the filamentous fungus Trichoderma reesei. Evidence for down-regulation of genes that encode secreted proteins in the stressed cells. *Journal of Biological Chemistry*, *278*(45), 45011–45020. https://doi.org/10.1074/jbc.M302372200

Palma-Guerrero, J., Ma, X., Torriani, S. F. F., Zala, M., Francisco, C. S., Hartmann, F. E., Croll, D., & McDonald, B. A. (2017). Comparative transcriptome analyses in zymoseptoria tritici reveal significant differences in gene expression among strains during plant infection. *Molecular Plant-Microbe Interactions*, *30*(3), 231–244. https://doi.org/10.1094/MPMI-07-16-0146-R

Palma-Guerrero, J., Torriani, S. F. F., Zala, M., Carter, D., Courbot, M., Rudd, J. J., McDonald, B. A., & Croll, D. (2016). Comparative transcriptomic analyses of Zymoseptoria tritici strains show complex lifestyle transitions and intraspecific variability in transcription profiles. *Molecular Plant Pathology*, *17*(6), 845–859. https://doi.org/10.1111/mpp.12333

Panwar, V., McCallum, B., & Bakkeren, G. (2013). Endogenous silencing of Puccinia triticina pathogenicity genes through in planta-expressed sequences leads to the suppression of rust diseases on wheat. *Plant Journal*, *73*(3), 521–532. https://doi.org/10.1111/tpj.12047

Parniske, M. (2000). Intracellular accommodation of microbes by plants : a common developmental program for symbiosis and disease ? *Current Opinion in Plant Biology*, *3*, 320–328.

Parzych, K. R., Ariosa, A., Mari, M., & Klionsky, D. J. (2018). A newly characterized vacuolar serine carboxypeptidase, Atg42/Ybr139w, is required for normal vacuole function and the terminal steps of autophagy in the yeast Saccharomyces cerevisiae. *Molecular Biology of the Cell*, *29*(9), 1089–1099. https://doi.org/10.1091/mbc.E17-08-0516

Patkar, R. N., Ramos-Pamplona, M., Gupta, A. P., Fan, Y., & Naqvi, N. I. (2012). Mitochondrial β-oxidation regulates organellar integrity and is necessary for conidial germination and invasive growth in Magnaporthe oryzae. *Molecular Microbiology*, *86*(6), 1345–1363. https://doi.org/10.1111/mmi.12060

Pearson, M. N., Beever, R. E., Boine, B., & Arthur, K. (2009). Mycoviruses of filamentous fungi and their relevance to plant pathology. *Molecular Plant Pathology*, *10*(1), 115–128. https://doi.org/10.1111/j.1364-3703.2008.00503.x

Person, C., Samborski, D. J., & Rohringer, R. (1962). The Gene-For-Gene Concept. *Nature*, *194*, 561–562.

Pham, T. A. T., Schwerdt, J. G., Shirley, N. J., Xing, X., Hsieh, Y. S. Y., Srivastava, V., Bulone, V., & Little, A. (2019). Analysis of cell wall synthesis and metabolism during early germination of Blumeria graminis f. sp. hordei conidial cells induced in vitro. *Cell Surface*, *5*(August), 100030. https://doi.org/10.1016/j.tcsw.2019.100030

Piekarska, K., Hardy, G., Mol, E., van den Burg, J., Strijbis, K., van Roermund, C., van den Berg, M., & Distel, B. (2008). The activity of the glyoxylate cycle in peroxisomes of Candida albicans depends on a functional β-oxidation pathway: Evidence for reduced metabolite transport across the peroxisomal membrane. *Microbiology*, *154*(10), 3061–3072. https://doi.org/10.1099/mic.0.2008/020289-0

Piekarska, K., Mol, E., van den Berg, M., Hardy, G., van den Burg, J., van Roermund, C., MacCallum, D., Odds, F., & Distel, B. (2006). Peroxisomal Fatty Acid β-Oxidation Is Not Essential for Virulence of Candida albicans . *Eukaryotic Cell*, *5*(11), 1847–1856. https://doi.org/10.1128/ec.00093-06

Pilet-Nayel, M. L., Moury, B., Caffier, V., Montarry, J., Kerlan, M. C., Fournet, S., Durel, C. E., & Delourme, R. (2017). Quantitative resistance to plant pathogens in pyramiding strategies for durable crop protection. *Frontiers in Plant Science*, *8*(October), 1–9. https://doi.org/10.3389/fpls.2017.01838

Pinan-Lucarré, B., Balguerie, A., & Clavé, C. (2005). Accelerated cell death in Podospora autophagy mutants. *Eukaryotic Cell*, *4*(11), 1765–1774. https://doi.org/10.1128/EC.4.11.1765

Pinan-Lucarré, B., Paoletti, M., Dementhon, K., Coulary-Salin, B., & Clavé, C. (2003). Autophagy is induced during cell death by incompatibility and is essential for differentiation in the filamentous fungus Podospora anserina. *Molecular*

*Microbiology*, *47*(2), 321–333. https://doi.org/10.1046/j.1365-2958.2003.03208.x

Pinter, N., Hach, C. A., Hampel, M., Rekhter, D., Zienkiewicz, K., Feussner, I., Poehlein, A., Daniel, R., Finkernagel, F., & Heimel, K. (2019). Signal peptide peptidase activity connects the unfolded protein response to plant defense suppression by Ustilago maydis. In *PLoS Pathogens* (Vol. 15, Issue 4). https://doi.org/10.1371/journal.ppat.1007734

Plaumann, P. L., Schmidpeter, J., Dahl, M., Taher, L., & Koch, C. (2018). A dispensable chromosome is required for virulence in the hemibiotrophic plant pathogen Colletotrichum higginsianum. *Frontiers in Microbiology*, *9*, 1005. https://doi.org/10.3389/fmicb.2018.01005

Plissonneau, C., Hartmann, F. E., & Croll, D. (2018). Pangenome analyses of the wheat pathogen Zymoseptoria tritici reveal the structural basis of a highly plastic eukaryotic genome. *BMC Biology*, *16*(1), 1–16. https://doi.org/10.1186/s12915-017-0457-4

Poirier, Y., Antonenkov, V. D., Glumoff, T., & Hiltunen, J. K. (2006). Peroxisomal β-oxidation-A metabolic pathway with multiple functions. *Biochimica et Biophysica Acta - Molecular Cell Research*, *1763*(12), 1413–1426. https://doi.org/10.1016/j.bbamcr.2006.08.034

Pollack, J. K., Harris, S. D., & Marten, M. R. (2009). Autophagy in filamentous fungi. *Fungal Genetics and Biology*, *46*(1), 1–8. https://doi.org/10.1016/j.fgb.2008.10.010

Pomraning, K. R., Bredeweg, E. L., Kerkhoven, E. J., Barry, K., Haridas, S., Hundley, H., LaButti, K., Lipzen, A., Yan, M., Magnuson, J. K., Simmons, B. A., Grigoriev, I. V., Nielsen, J., & Baker, S. E. (2018). Regulation of Yeast-to-Hyphae Transition in Yarrowia lipolytica . *MSphere*, *3*(6), 1–18. https://doi.org/10.1128/msphere.00541-18

Ponomarenko, A., Goodwin, S. B., & Kema, G. H. J. (2011). *Septoria tritici blotch (STB) of wheat*. Plant Health Instructor. https://doi.org/10.1094/PHI-I-2011-0407-01

Poppe, S., Dorsheimer, L., Happel, P., & Stukenbrock, E. H. (2015). Rapidly Evolving Genes Are Key Players in Host Specialization and Virulence of the Fungal Wheat Pathogen Zymoseptoria tritici (Mycosphaerella graminicola). *PLoS Pathogens*, *11*(7), 1–21. https://doi.org/10.1371/journal.ppat.1005055

Précigout, P. A., Claessen, D., Makowski, D., & Robert, C. (2020). Does the latent period of leaf fungal pathogens reflect their trophic type? A meta-analysis of biotrophs, hemibiotrophs, and necrotrophs. *Phytopathology*, *110*(2), 345–361. https://doi.org/10.1094/PHYTO-04-19-0144-R

Qi, T., Guo, J., Peng, H., Liu, P., Kang, Z., & Guo, J. (2019). Host-induced gene silencing: A powerful strategy to control diseases of wheat and barley. *International Journal of Molecular Sciences*, *20*(1). https://doi.org/10.3390/ijms20010206

Quarantin, A., Hadeler, B., Kröger, C., Schäfer, W., Favaron, F., Sella, L., & Martínez-Rocha, A. L. (2019). Different hydrophobins of fusarium graminearumare involved in hyphal growth, attachment, water-air interface penetration and plant infection. *Frontiers in Microbiology*, *10*(APR), 1–19. https://doi.org/10.3389/fmicb.2019.00751

R4P Network. (2016). Trends and Challenges in Pesticide Resistance Detection. *Trends in Plant Science*, *21*(10), 834–853. https://doi.org/10.1016/j.tplants.2016.06.006

Rabe, F., Ajami-rashidi, Z., Doehlemann, G., Kahmann, R., & Djamei, A. (2013). Degradation of the plant defence hormone salicylic acid by the biotrophic fungus

Ustilago maydis. *Molecular Microbiology*, *89*(1), 179–188. https://doi.org/10.1111/mmi.12269

Ramamoorthy, V., Zhao, X., Snyder, A. K., Xu, J. R., & Shah, D. M. (2007). Two mitogen-activated protein kinase signalling cascades mediate basal resistance to antifungal plant defensins in Fusarium graminearum. *Cellular Microbiology*, *9*(6), 1491–1506. https://doi.org/10.1111/j.1462-5822.2006.00887.x

Rambold, A. S., Cohen, S., Lippincott-schwartz, J., Rambold, A. S., Cohen, S., & Lippincott-schwartz, J. (2015). Fatty Acid Trafficking in Starved Cells : Regulation by Lipid Droplet Lipolysis , Autophagy , and Article Fatty Acid Trafficking in Starved Cells : Regulation by Lipid Droplet Lipolysis , Autophagy , and Mitochondrial Fusion Dynamics. *Developmental Cell*, *32*(6), 678–692. https://doi.org/10.1016/j.devcel.2015.01.029

Rasmussen, S., Liu, Q., Parsons, A. J., Xue, H., Sinclair, B., & Newman, J. A. (2012). Grass-endophyte interactions : a note on the role of monosaccharide transport in the Neotyphodium lolii-Lolium perenne symbiosis. *New Phytologist*, *196*, 7–12. https://doi.org/10.1111/j.1469-8137.2012.04250.x

Ray, S., Anderson, J. M., Urmeev, F. I., & Goodwin, S. B. (2003). Rapid induction of a protein disulfide isomerase and defense-related genes in wheat in response to the hemibiotrophic fungal pathogen Mycosphaerella graminicola. *Plant Molecular Biology*, *53*(5), 701–714. https://doi.org/10.1023/b:plan.0000019120.74610.52

Reggiori, F., & Klionsky, D. J. (2013). Autophagic processes in yeast: Mechanism, machinery and regulation. *Genetics*, *194*(2), 341–361. https://doi.org/10.1534/genetics.112.149013

Rehfus, A., Strobel, D., Bryson, R., & Stammler, G. (2018). Mutations in sdh genes in field isolates of Zymoseptoria tritici and impact on the sensitivity to various succinate dehydrogenase inhibitors. *Plant Pathology*, *67*(1), 175–180. https://doi.org/10.1111/ppa.12715

Reina-Pinto, J. J., & Yephremov, A. (2009). Surface lipids and plant defenses. *Plant Physiology and Biochemistry*, *47*(6), 540–549. https://doi.org/10.1016/j.plaphy.2009.01.004

Reino, J. L., Hernández-Galán, R., Durán-Patrón, R., & Collado, I. G. (2004). Virulence - Toxin production relationship in isolates of the plant pathogenic fungus Botrytis cinerea. *Journal of Phytopathology*, *152*(10), 563–566. https://doi.org/10.1111/j.1439-0434.2004.00896.x

Reinoso-Martín, C., Schu, C., Schuetzer-muehlbauer, M., & Kuchler, K. (2003). The Yeast Protein Kinase C Cell Integrity Pathway Mediates Tolerance to the Antifungal Drug Caspofungin through Activation of Slt2p Mitogen-Activated Protein Kinase Signaling †. *Eukaryotic Cell*, *2*(6), 1200–1210. https://doi.org/10.1128/EC.2.6.1200

Ren, W., Zhang, Z., Shao, W., Yang, Y., Zhou, M., & Chen, C. (2017). The autophagy-related gene BcATG1 is involved in fungal development and pathogenesis in Botrytis cinerea. *Molecular Plant Pathology*, *18*(2), 238–248. https://doi.org/10.1111/mpp.12396

Richie, D. L., Fuller, K. K., Fortwendel, J., Miley, M. D., McCarthy, J. W., Feldmesser, M., Rhodes, J. C., & Askew, D. S. (2007). Unexpected link between metal ion deficiency and autophagy in Aspergillus fumigatus. *Eukaryotic Cell*, *6*(12), 2437–2447. https://doi.org/10.1128/EC.00224-07

Richie, D. L., Hartl, L., Aimanianda, V., Winters, M. S., Fuller, K. K., Miley, M. D., White, S., McCarthy, J. W., Latgé, J. P., Feldmesser, M., Rhodes, J. C., & Askew,

D. S. (2009). A role for the unfolded protein response (UPR) in virulence and antifungal susceptibility in Aspergillus fumigatus. *PLoS Pathogens*, *5*(1). https://doi.org/10.1371/journal.ppat.1000258

Riquelme, M., Aguirre, J., Bartnicki-García, S., Braus, G. H., Feldbrügge, M., Fleig, U., Hansberg, W., Herrera-Estrella, A., Kämper, J., Kück, U., Mouriño-Pérez, R. R., Takeshita, N., & Fischer, R. (2018). Fungal Morphogenesis, from the Polarized Growth of Hyphae to Complex Reproduction and Infection Structures. *Microbiology and Molecular Biology Reviews*, *82*(2), 1–47. https://doi.org/10.1128/mmbr.00068-17

Ritchie, M. E., Phipson, B., Wu, D., Hu, Y., Law, C. W., Shi, W., & Smyth, G. K. (2015). Limma powers differential expression analyses for RNA-sequencing and microarray studies. *Nucleic Acids Research*, *43*(7), e47. https://doi.org/10.1093/nar/gkv007

Robinson, M. D., McCarthy, D. J., & Smyth, G. K. (2010). edgeR: A Bioconductor package for differential expression analysis of digital gene expression data. *Bioinformatics*, *26*(1), 139–140. https://doi.org/10.1093/bioinformatics/btp616

Robinson, M. D., & Oshlack, A. (2010). A scaling normalization method for differential expression analysis of RNA-seq data. *Genome Biology*, *11*(3). https://doi.org/10.1186/gb-2010-11-3-r25

Rocha, M. C., De Godoy, K. F., De Castro, P. A., Hori, J. I., Pedro Bom, V. L., Brown, N. A., Da Cunha, A. F., Goldman, G. H., Malavazi, I., & Yu, J. H. (2015). The Aspergillus fumigatus pkcAG579R mutant is defective in the activation of the cell wall integrity pathway but is dispensable for virulence in a neutropenic mouse infection model. *PLoS ONE*, *10*(8), 1–34. https://doi.org/10.1371/journal.pone.0135195

Rodriguez-Moreno, L., Ebert, M. K., Bolton, M. D., & Thomma, B. P. H. J. (2018). Tools of the crook- infection strategies of fungal plant pathogens. *The Plant Journal*, *93*(4), 664–674. https://doi.org/10.1111/tpj.13810

Rodriguez, R. J., Jr, J. F. W., Arnold, A. E., & Redman, R. S. (2009). Fungal endophytes: diversity and functional roles. *New Phytologist*, *182*, 314–330. https://doi.org/10.1111/j.1469-8137.2009.02773.x

Rohel, E. A., Payne, A. C., Fraaije, B. A., & Hollomon, D. W. (2001). Exploring infection of wheat and carbohydrate metabolism in Mycosphaerella graminicola transformants with differentially regulated green fluorescent protein expression. *Molecular Plant-Microbe Interactions*, *14*(2), 156–163. https://doi.org/10.1094/MPMI.2001.14.2.156

Rovenich, H., Boshoven, J. C., & Thomma, B. P. H. J. (2014). Filamentous pathogen effector functions: Of pathogens, hosts and microbiomes. *Current Opinion in Plant Biology*, *20*, 96–103. https://doi.org/10.1016/j.pbi.2014.05.001

Rudd, J. J., Kanyuka, K., Hassani-Pak, K., Derbyshire, M., Andongabo, A., Devonshire, J., Lysenko, A., Saqi, M., Desai, N. M., Powers, S. J., Hooper, J., Ambroso, L., Bharti, A., Farmer, A., Hammond-Kosack, K. E., Dietrich, R. A., & Courbot, M. (2015). Transcriptome and Metabolite Profiling of the Infection Cycle of *Zymoseptoria tritici* on Wheat Reveals a Biphasic Interaction with Plant Immunity Involving Differential Pathogen Chromosomal Contributions and a Variation on the Hemibiotrophic Lifest. *Plant Physiology*, *167*(3), 1158–1185. https://doi.org/10.1104/pp.114.255927

Rudd, J. J., Keon, J., & Hammond-Kosack, K. E. (2008). The wheat mitogen-activated protein kinases TaMPK3 and TaMPK6 are differentially regulated at multiple levels during compatible disease interactions with Mycosphaerella graminicola. *Plant*

*Physiology*, *147*(2), 802–815. https://doi.org/10.1104/pp.108.119511

Rui, O., & Hahn, M. (2007). The Slt2-type MAP kinase Bmp3 of Botrytis cinerea is required for normal saprotrophic growth, conidiation, plant surface sensing and host tissue colonization. *Molecular Plant Pathology*, *8*(2), 173–184. https://doi.org/10.1111/j.1364-3703.2007.00383.x

Ryder, L. S., & Talbot, N. J. (2015). Regulation of appressorium development in pathogenic fungi. *Current Opinion in Plant Biology*, *26*, 8–13. https://doi.org/10.1016/j.pbi.2015.05.013

Sakulkoo, W., Osés-Ruiz, M., Garcia, E. O., Soanes, D. M., Littlejohn, G. R., Hacker, C., Correia, A., Valent, B., & Talbot, N. J. (2018). A single fungal MAP kinase controls plant cell-to-cell invasion by the rice blast fungus. *Science*, *359*(6382), 1399–1403. https://doi.org/10.1126/science.aaq0892

Sánchez-Vallet, A., McDonald, M. C., Solomon, P. S., & McDonald, B. A. (2015). Is Zymoseptoria tritici a hemibiotroph? *Fungal Genetics and Biology*, *79*, 29–32. https://doi.org/10.1016/j.fgb.2015.04.001

Sanchez-Vallet, A., Mesters, J. R., & Thomma, B. P. H. J. (2014). The battle for chitin recognition in plant-microbe interactions. *FEMS Microbiology Letters*, *39*, 171–183. https://doi.org/10.1093/femsre/fuu003

Savary, S., Stetkiewicz, S., Brun, F., & Willocquet, L. (2015). Modelling and mapping potential epidemics of wheat diseases—examples on leaf rust and Septoria tritici blotch using EPIWHEAT. *European Journal of Plant Pathology*, *142*(4), 771–790. https://doi.org/10.1007/s10658-015-0650-7

Savary, S., Willocquet, L., Pethybridge, S. J., Esker, P., McRoberts, N., & Nelson, A. (2019). The global burden of pathogens and pests on major food crops. *Nature Ecology and Evolution*, *3*(3), 430–439. https://doi.org/10.1038/s41559-018-0793-y

Scheerer, L., Pemsl, D., Dita, M., Perez Vicente, L., & Staver, C. (2018). A quantified approach to projecting losses caused by Fusarium wilt Tropical race 4. *Acta Horticulturae*, *1196*(March), 211–218. https://doi.org/10.17660/ActaHortic.2018.1196.26

Schellenberger, R., Touchard, M., Clément, C., Baillieul, F., Cordelier, S., Crouzet, J., & Dorey, S. (2019). Apoplastic invasion patterns triggering plant immunity: plasma membrane sensing at the frontline. *Molecular Plant Pathology*, *20*(11), 1602–1616. https://doi.org/10.1111/mpp.12857

Schmidt, S. P., Corydon, T. J., Pedersen, C. B., Bross, P., & Gregersen, N. (2010). Misfolding of short-chain acyl-CoA dehydrogenase leads to mitochondrial fission and oxidative stress. *Molecular Genetics and Metabolism*, *100*(2), 155–162. https://doi.org/10.1016/j.ymgme.2010.03.009

Schmitt, K., Smolinski, N., Neumann, P., Schmaul, S., Hofer-pretz, V., Braus, G. H., & Valerius, O. (2017). Asc1p/RACK1 Connects Ribosomes to Eukaryotic Phosphosignaling. *Molecular and Cellular Biology*, *37*(3), e00279-16. https://doi.org/10.1128/ MCB.00279-16

Schmitz, L., Kronstad, J. W., & Heimel, K. (2020). Conditional gene expression reveals stage-specific functions of the unfolded protein response in the Ustilago maydis–maize pathosystem. *Molecular Plant Pathology*, *21*(2), 258–271. https://doi.org/10.1111/mpp.12893

Schrader, M., Godinho, L. F., Costello, J. L., & Islinger, M. (2015). The different facets of organelle interplay-An overview of organelle interactions. *Frontiers in Cell and Developmental Biology*, *3*, 1–22. https://doi.org/10.3389/fcell.2015.00056

Schrader, M., & Yoon, Y. (2007). Mitochondria and peroxisomes: Are the “Big Brother” and the “Little Sister” closer than assumed? *BioEssays*, *29*(11), 1105–1114. https://doi.org/10.1002/bies.20659

Schurch, N. J., Schofield, P., Gierliński, M., Cole, C., Sherstnev, A., Singh, V., Wrobel, N., Gharbi, K., Simpson, G. G., Owen-Hughes, T., Blaxter, M., & Barton, G. J. (2016). How many biological replicates are needed in an RNA-seq experiment and which differential expression tool should you use? *RNA*, *22*(6), 839–851. https://doi.org/10.1261/rna.053959.115

Scrimale, T., Didone, L., de Mesy Bentley, K. L., & Krysan, D. J. (2009). The Unfolded Protein Response Is Induced by the Cell Wall Integrity Mitogen-activated Protein Kinase Signaling Cascade and Is Required for Cell Wall Integrity in Saccharomyces cerevisiae. *Molecular Biology of the Cell*, *20*, 164–175. https://doi.org/10.1091/mbc.E08–08–0809

Segers, G. C., Van Wezel, R., Zhang, X., Hong, Y., & Nuss, D. L. (2006). Hypovirus papain-like protease p29 suppresses RNA silencing in the natural fungal host and in a heterologous plant system. *Eukaryotic Cell*, *5*(6), 896–904. https://doi.org/10.1128/EC.00373-05

Selvaraj, P., Shen, Q., Yang, F., & Naqvi, N. I. (2017). Cpk 2, a catalytic subunit of cyclic AMP-PKA, regulates growth and pathogenesis in rice blast. *Frontiers in Microbiology*, *8*(NOV), 1–17. https://doi.org/10.3389/fmicb.2017.02289

Selvaraj, P., Tham, H. F., Ramanujam, R., & Naqvi, N. I. (2017). Subcellular compartmentation, interdependency and dynamics of the cyclic AMP-dependent PKA subunits during pathogenic differentiation in rice blast. *Molecular Microbiology*, *105*(3), 484–504. https://doi.org/10.1111/mmi.13713

Sexton, A. C., Minic, Z., Cozijnsen, A. J., Pedras, M. S. C., & Howlett, B. J. (2009). Cloning, purification and characterisation of brassinin glucosyltransferase, a phytoalexin-detoxifying enzyme from the plant pathogen Sclerotinia sclerotiorum. *Fungal Genetics and Biology*, *46*(2), 201–209. https://doi.org/10.1016/j.fgb.2008.10.014

Shaw, M. W., & Royle, D. J. (1989). Airborne inoculum as a major source of Septoria tritici (Mycosphaerella graminicola) infections in winter wheat crops in the UK. *Plant Pathology*, *38*(1), 35–43. https://doi.org/10.1111/j.1365-3059.1989.tb01425.x

Shaw, Michael W., Emmanuel, C. J., Emilda, D., Terhem, R. B., Shafia, A., Tsamaidi, D., Emblow, M., & van Kan, J. A. L. (2016). Analysis of Cryptic, Systemic Botrytis Infections in Symptomless Hosts. *Frontiers in Plant Science*, *7*(May). https://doi.org/10.3389/fpls.2016.00625

Shen, Y. Q., & Burger, G. (2009). Plasticity of a key metabolic pathway in fungi. *Functional and Integrative Genomics*, *9*(2), 145–151. https://doi.org/10.1007/s10142-008-0095-6

Shetty, N. P., Kristensen, B. K., Newmana, M. A., Møller, K., Gregersen, P. L., & Jørgensen, H. J. L. (2003). Association of hydrogen peroxide with restriction of Septoria tritici in resistant wheat. *Physiological and Molecular Plant Pathology*, *62*(6), 333–346. https://doi.org/10.1016/S0885-5765(03)00079-1

Shi, G., Zhang, Z., Friesen, T. L., Raats, D., Fahima, T., Brueggeman, R. S., Lu, S., Trick, H. N., Liu, Z., Chao, W., Frenkel, Z., Xu, S. S., Rasmussen, J. B., & Faris, J. D. (2016). The hijacking of a receptor kinase-driven pathway by a wheat fungal pathogen leads to disease. *Science Advances*, *2*(10). https://doi.org/10.1126/sciadv.1600822

Shi, L., Wang, J., Quan, R., Yang, F., Shang, J., & Chen, B. (2019). CpATG8, a

homolog of yeast autophagy protein ATG8, is required for pathogenesis and hypovirus accumulation in the chest blight fungus. *Frontiers in Cellular and Infection Microbiology*, *9*(JUL), 1–8. https://doi.org/10.3389/fcimb.2019.00222

Shimazaki, K., Doi, M., Assmann, S. M., & Kinoshita, T. (2007). Light Regulation of Stomatal Movement. *Annual Review of Plant Biology*, *58*, 219–247. https://doi.org/10.1146/annurev.arplant.57.032905.105434

Shimizu, S., Kanaseki, T., Mizushima, N., Mizuta, T., Arakawa-Kobayashi, S., Thompson, C. B., & Tsujimoto, Y. (2004). Role of Bcl-2 family proteins in a non-apoptopic programmed cell death dependent on autophagy genes. *Nature Cell Biology*, *6*(12), 1221–1228. https://doi.org/10.1038/ncb1192

Shoji, J. Y., Arioka, M., & Kitamoto, K. (2006). Vacuolar membrane dynamics in the filamentous fungus Aspergillus oryzae. *Eukaryotic Cell*, *5*(2), 411–421. https://doi.org/10.1128/EC.5.2.411-421.2006

Shoji, J. Y., & Craven, K. D. (2011). Autophagy in basal hyphal compartments: A green strategy of great recyclers. *Fungal Biology Reviews*, *25*(2), 79–83. https://doi.org/10.1016/j.fbr.2011.04.001

Shoji, J. Y., Kikuma, T., Arioka, M., & Kitamoto, K. (2010). Macroautophagy-mediated degradation of whole nuclei in the filamentous fungus Aspergillus oryzae. *PLoS ONE*, *5*(12). https://doi.org/10.1371/journal.pone.0015650

Shpilka, T., & Elazar, Z. (2015). Lipid droplets regulate autophagosome biogenesis. *Autophagy*, *11*(11), 2130–2131. https://doi.org/10.1080/15548627.2015.1093719

Shumayla, Sharma, S., Kumar, R., Mendu, V., & Singh, K. (2016). Genomic Dissection and Expression Profiling Revealed Functional Divergence in Triticum aestivum Leucine Rich Repeat Receptor Like Kinases ( TaLRRKs ). *Frontiers in Plant Science*, *7*, 1374. https://doi.org/10.3389/fpls.2016.01374

Shumayla, Sharma, S., Pandey, A. K., & Singh, K. (2016). Molecular Characterization and Global Expression Analysis of Lectin Receptor Kinases in Bread Wheat ( Triticum aestivum ). *PLoS ONE*, *11*(4), e0153925. https://doi.org/10.1371/journal.pone.0153925

Shwab, E. K., Juvvadi, P. R., Waitt, G., Soderblom, E. J., Moseley, M. A., Nicely, N. I., & Steinbach, W. J. (2017). Phosphorylation of Aspergillus fumigatus PkaR Impacts Growth and Cell Wall Integrity Through Novel Mechanisms. *FEBS Letters*, *591*(22), 3730–3744. https://doi.org/10.1002/1873-3468.12886

Siah, A., Deweer, C., Duyme, F., Sanssené, J., Durand, R., Halama, P., & Reignault, P. (2010). Correlation of in planta endo-beta-1,4-xylanase activity with the necrotrophic phase of the hemibiotrophic fungus Mycosphaerella graminicola. *Plant Pathology*, *59*(4), 661–670. https://doi.org/10.1111/j.1365-3059.2010.02303.x

Sidhu, Y. S. (2015). *Molecular tools for functional genomic analyses of the stealth pathogenesis of wheat by Zymoseptoria tritici* [University of Exeter]. https://ore.exeter.ac.uk/repository/handle/10871/20219

Sidhu, Y. S., Cairns, T. C., Chaudhari, Y. K., Usher, J., Talbot, N. J., Studholme, D. J., Csukai, M., & Haynes, K. (2015). Exploitation of sulfonylurea resistance marker and non-homologous end joining mutants for functional analysis in Zymoseptoria tritici. *Fungal Genetics and Biology*, *79*, 102–109. https://doi.org/10.1016/j.fgb.2015.04.015

Sidhu, Y. S., Chaudhari, Y. K., Usher, J., Cairns, T. C., Csukai, M., & Haynes, K. (2015). A suite of Gateway® compatible ternary expression vectors for functional analysis in Zymoseptoria tritici. *Fungal Genetics and Biology*, *79*, 180–185.

https://doi.org/10.1016/j.fgb.2015.03.021

Singh, R., Kaushik, S., Wang, Y., Xiang, Y., Novak, I., Komatsu, M., Tanaka, K., Cuervo, A. M., & Czaja, M. J. (2009). Autophagy regulates lipid metabolism. *Nature*, *458*(7242), 1131–1135. https://doi.org/10.1038/nature07976

Singh, R. P., Hodson, D. P., Huerta-espino, J., Jin, Y., Njau, P., Wanyera, R., Herrera-foessel, S. A., & Ward, R. W. (2008). Will Stem Rust Destroy the World's Wheat Crop? In *Advance in Agronomy* (Vol. 98, pp. 271–309). https://doi.org/10.1016/S0065-2113(08)00205-8

Singh, R. P., Singh, P. K., Rutkoski, J., Hodson, D. P., He, X., Jørgensen, L. N., Hovmøller, M. S., & Huerta-Espino, J. (2016). Disease Impact on Wheat Yield Potential and Prospects of Genetic Control. *Annual Review of Phytopathology*, *54*(1), 303–322. https://doi.org/10.1146/annurev-phyto-080615-095835

Skamnioti, P., & Gurr, S. J. (2007). Magnaporthe grisea Cutinase2 Mediates Appressorium Differentiation and Host Penetration and Is Required for Full Virulence. *The Plant Cell Online*, *19*(8), 2674–2689. https://doi.org/10.1105/tpc.107.051219

Slim, A., Piarulli, L., Kourda, H. C., Rouaissi, M., Robbana, C., Chaabane, R., Pignone, D., Montemurro, C., & Mangini, G. (2019). Genetic structure analysis of a collection of Tunisian durum wheat germplasm. *International Journal of Molecular Sciences*, *20*(13), 1–14. https://doi.org/10.3390/ijms20133362

Smith, K. M., Sancar, G., Dekhang, R., Sullivan, C. M., Li, S., Tag, A. G., Sancar, C., Bredeweg, E. L., Priest, H. D., McCormick, R. F., Thomas, T. L., Carrington, J. C., Stajich, J. E., Bell-Pedersen, D., Brunner, M., & Freitag, M. (2010). Transcription factors in light and circadian clock signaling networks revealed by genomewide mapping of direct targets for neurospora white collar complex. *Eukaryotic Cell*, *9*(10), 1549–1556. https://doi.org/10.1128/EC.00154-10

Snelders, N. C., Kettles, G. J., Rudd, J. J., & Thomma, B. P. H. J. (2018). Plant pathogen effector proteins as manipulators of host microbiomes? *Molecular Plant Pathology*, *19*(2), 257–259. https://doi.org/10.1111/mpp.12628

Snelders, N. C., Rovenich, H., Petti, G. C., Rocafort, M., van den Berg, G. C. M., Vorholt, J. A., Mesters, J. R., Seidl, M. F., Nijland, R., & Thomma, B. P. H. J. (2020). Microbiome manipulation by a soil-borne fungal plant pathogen using effector proteins. *Nature Plants*, *6*, 1365–1374. https://doi.org/10.1038/s41477-020-00799-5

Soanes, D. M., Chakrabarti, A., Paszkiewicz, K. H., Dawe, A. L., & Talbot, N. J. (2012). Genome-wide transcriptional profiling of appressorium development by the rice blast fungus Magnaporthe oryzae. *PLoS Pathogens*, *8*(2). https://doi.org/10.1371/journal.ppat.1002514

Soledade, M., Pedras, C., & Yaya, E. E. (2015). Plant chemical defenses: Are all constitutive antimicrobial metabolites phytoanticipins? *Natural Product Communications*, *10*(1), 209–218. https://doi.org/10.1177/1934578x1501000142

Solomon, P. S., Lee, R. C., Wilson, T. J. G., & Oliver, R. P. (2004). Pathogenicity of Stagonospora nodorum requires malate synthase. *Molecular Microbiology*, *53*(4), 1065–1073. https://doi.org/10.1111/j.1365-2958.2004.04178.x

Songe, M. M., Thoen, E., Evensen, O., & Skaar, I. (2014). In vitro passages impact on virulence of Saprolegnia parasitica to Atlantic salmon, Salmo salar L. parr. *Journal of Fish Diseases*, *37*(9), 825–834. https://doi.org/10.1111/jfd.12175

Soukup, A. A., Farnoodian, M., Berthier, E., & Keller, N. P. (2012). NosA, a transcription factor important in Aspergillus fumigatus stress and developmental

response, rescues the germination defect of a laeA deletion. *Fungal Genetics and Biology*, *49*(11), 857–865. https://doi.org/10.1016/j.fgb.2012.09.005

Soyer, J. L., Grandaubert, J., Haueisen, J., Schontanus, K., & Stukenbrock, E. H. (2019). In planta chromatin immunoprecipitation in Zymoseptoria tritici reveals chromatin-based regulation of putative effector gene expression. *BioRxiv*. https://doi.org/10.1101/544627

Spanu, P. D., & Panstruga, R. (2017). Editorial : Biotrophic Plant-Microbe Interactions. *Frontiers in Plant Science*, *8*, 1–4. https://doi.org/10.3389/fpls.2017.00192

Spanu, P., & Kämper, J. (2010). Genomics of biotrophy in fungi and oomycetes-emerging patterns. *Current Opinion in Plant Biology*, *13*(4), 409–414. https://doi.org/10.1016/j.pbi.2010.03.004

Speijer, D. (2011). Oxygen radicals shaping evolution: Why fatty acid catabolism leads to peroxisomes while neurons do without it: FADH2/NADH flux ratios determining mitochondrial radical formation were crucial for the eukaryotic invention of peroxisomes and catabolic tissue. *BioEssays*, *33*(2), 88–94. https://doi.org/10.1002/bies.201000097

Sperschneider, J., Dodds, P. N., Gardiner, D. M., Singh, K. B., & Taylor, J. M. (2018). Improved prediction of fungal effector proteins from secretomes with EffectorP 2.0. *Molecular Plant Pathology*, *19*(9), 2094–2110. https://doi.org/10.1111/mpp.12682

Spreghini, E., Davis, D. A., Subaran, R., Kim, M., & Mitchell, A. P. (2003). Roles of Candida albicans Dfg5p and Dcw1p cell surface proteins in growth and hypha formation. *Eukaryotic Cell*, *2*(4), 746–755. https://doi.org/10.1128/EC.2.4.746-755.2003

Steffens, E. K., Becker, K., Krevet, S., Teichert, I., & Kück, U. (2016). Transcription factor PRO1 targets genes encoding conserved components of fungal developmental signaling pathways. *Molecular Microbiology*, *102*(5), 792–809. https://doi.org/10.1111/mmi.13491

Steinberg, G. (2015). Cell biology of Zymoseptoria tritici: Pathogen cell organization and wheat infection. *Fungal Genetics and Biology*, *79*, 17–23. https://doi.org/10.1016/j.fgb.2015.04.002

Steinhauer, D., Salat, M., Frey, R., Mosbach, A., Luksch, T., Balmer, D., Hansen, R., Widdison, S., Logan, G., Dietrich, R. A., Kema, G. H. J., Bieri, S., Sierotzki, H., Torriani, S. F. F., & Scalliet, G. (2019). A dispensable paralog of succinate dehydrogenase subunit C mediates standing resistance towards a subclass of SDHI fungicides in Zymoseptoria tritici. In *PLoS Pathogens* (Vol. 15, Issue 12). https://doi.org/10.1371/journal.ppat.1007780

Stephens, C., Ölmez, F., Blyth, H., McDonald, M., Bansal, A., Turgay, E. B., Hahn, F., Saintenac, C., Nekrasov, V., Solomon, P., Milgate, A., Fraaije, B., Rudd, J., & Kanyuka, K. (2021). Remarkable recent changes in the genetic diversity of the avirulence gene AvrStb6 in global populations of the wheat pathogen Zymoseptoria tritici. *Molecular Plant Pathology*, *22*(9), 1121-1133. https://doi.org/10.1111/mpp.13101

Stergiopoulos, I., & de Wit, P. J. G. M. (2009). Fungal Effector Proteins. *Annual Review of Phytopathology*, *47*(1), 233–263. https://doi.org/10.1146/annurev.phyto.112408.132637

Stergiopoulos, I., Zwiers, L. H., & De Waard, M. A. (2003). The ABC transporter MgAtr4 is a virulence factor of Mycosphaerella graminicola that affects colonization of substomatal cavities in wheat leaves. *Molecular Plant-Microbe Interactions*, *16*(8), 689–698. https://doi.org/10.1094/MPMI.2003.16.8.689

Stewart, E. L., Croll, D., Lendenmann, M. H., Sanchez-Vallet, A., Hartmann, F. E., Palma-Guerrero, J., Ma, X., & Mcdonald, B. A. (2018). Quantitative trait locus mapping reveals complex genetic architecture of quantitative virulence in the wheat pathogen Zymoseptoria tritici. *Molecular Plant Pathology*, *9*(1), 201–216. https://doi.org/10.1111/mpp.12515

Stewart, E. L., & McDonald, B. A. (2014). Measuring quantitative virulence in the wheat pathogen zymoseptoria tritici using high-throughput automated image analysis. *Phytopathology*, *104*(9), 985–992. https://doi.org/10.1094/PHYTO-11-13-0328-R

Stotz, H. U., Mitrousia, G. K., de Wit, P. J. G. M., & Fitt, B. D. L. (2014). Effector-triggered defence against apoplastic fungal pathogens. *Trends in Plant Science*, *19*(8), 491–500. https://doi.org/10.1016/j.tplants.2014.04.009

Strateva, T., & Mitov, I. (2011). Contribution of an arsenal of virulence factors to pathogenesis of Pseudomonas aeruginosa infections. *Annals of Microbiology*, *61*(4), 717–732. https://doi.org/10.1007/s13213-011-0273-y

Studt, L., Humpf, H. U., & Tudzynski, B. (2013). Signaling Governed by G Proteins and cAMP Is Crucial for Growth, Secondary Metabolism and Sexual Development in Fusarium fujikuroi. *PLoS ONE*, *8*(2). https://doi.org/10.1371/journal.pone.0058185

Stukenbrock, E. H., Bataillon, T., Dutheil, J. Y., Stukenbrock, E. H., Bataillon, T., Dutheil, J. Y., Hansen, T. T., Li, R., Zala, M., Mcdonald, B. A., Wang, J., & Schierup, M. H. (2011). The making of a new pathogen : Insights from comparative population genomics of the domesticated wheat pathogen Mycosphaerella graminicola and its wild sister species The making of a new pathogen : Insights from comparative population genomics of the dome. *Genome Research*, *21*, 2157–2166. https://doi.org/10.1101/gr.118851.110

Stukenbrock, E. H., & Dutheil, J. Y. (2018). Fine-Scale Recombination Maps of Fungal Plant. *Genetics*, *208*, 1209–1229. https://doi.org/10.1534/genetics.117.300502/-/DC1.1

Suemoto, H., Matsuzaki, Y., & Iwahashi, F. (2019). Metyltetraprole, a novel putative complex III inhibitor, targets known QoI-resistant strains of Zymoseptoria tritici and Pyrenophora teres. *Pest Management Science*, *75*(4), 1181–1189. https://doi.org/10.1002/ps.5288

Suffert, F., & Sache, I. (2011). Relative importance of different types of inoculum to the establishment of Mycosphaerella graminicola in wheat crops in north-west Europe. *Plant Pathology*, *60*(5), 878–889. https://doi.org/10.1111/j.1365-3059.2011.02455.x

Suffert, F., & Thompson, R. N. (2018). Some reasons why the latent period should not always be considered constant over the course of a plant disease epidemic. *Plant Pathology*, *67*(9), 1831–1840. https://doi.org/10.1111/ppa.12894

Suffert, Frédéric, Delestre, G., & Gélisse, S. (2019). Sexual Reproduction in the Fungal Foliar Pathogen Zymoseptoria tritici Is Driven by Antagonistic Density Dependence Mechanisms. *Microbial Ecology*, *77*, 110–123. https://doi.org/10.1007/s00248-018-1211-3

Suffert, Frédéric, Goyeau, H., Sache, I., Carpentier, F., Gélisse, S., Morais, D., & Delestre, G. (2018). Epidemiological trade-off between intra- and interannual scales in the evolution of aggressiveness in a local plant pathogen population. *Evolutionary Applications*, *11*(5), 768–780. https://doi.org/10.1111/eva.12588

Sumita, T., Izumitsu, K., & Tanaka, C. (2017). Characterization of the autophagy-related gene BmATG8 in Bipolaris maydis. *Fungal Biology*, *121*(9), 785–797. https://doi.org/10.1016/j.funbio.2017.05.008

Summers, R. W., & Brown, J. K. M. (2013). Constraints on breeding for disease resistance in commercially competitive wheat cultivars. *Plant Pathology*, *62*, 115–121. https://doi.org/10.1111/ppa.12165

Sun, Q., Choi, G. H., & Nuss, D. L. (2009). Hypovirus-responsive transcription factor gene pro1 of the chestnut blight fungus Cryphonectria parasitica is required for female fertility, asexual spore development, and stable maintenance of hypovirus infection. *Eukaryotic Cell*, *8*(3), 262–270. https://doi.org/10.1128/EC.00338-08

Sussman, A., Huss, K., Chio, L., Heidler, S., Shaw, M., Ma, D., Zhu, G., Campbell, R. M., Park, T., Kulanthaivel, P., Scott, J. E., Carpenter, J. W., Strege, M. A., Belvo, M. D., Swartling, J. R., Fischl, A., Yeh, W., Shih, C., & Ye, X. S. (2004). Discovery of Cercosporamide , a Known Antifungal Natural Product , as a Selective Pkc1 Kinase Inhibitor through High-Throughput Screening †. *Eukaryotic Cell*, *3*(4), 932–943. https://doi.org/10.1128/EC.3.4.932

Sutton, P. N., Gilbert, M. J., Williams, L. E., & Hall, J. L. (2007). Powdery mildew infection of wheat leaves changes host solute transport and invertase activity. *Physiologia Plantarum*, *129*, 787–795. https://doi.org/10.1111/j.1399-3054.2007.00863.x

Suzuki, K., Kirisako, T., Kamada, Y., Mizushima, N., Noda, T., & Ohsumi, Y. (2001). The pre-autophagosomal structure organized by concerted functions of APG genes is essential for autophagosome formation. *The EMBO Journal*, *20*(21), 5971–5981.

Takano, Y., Kikuchi, T., Kubo, Y., Hamer, J. E., & Mise, K. (2000). The Colletotrichum lagenarium MAP Kinase Gene CMK1 Regulates Diverse Aspects of Fungal Pathogenesis. *Molecular Plant Microbe Interaction*, *13*(4), 374–383.

Talbot, N. J., Kershaw, M. J., Wakley, G. E., De Vries, O. M. H., Wessels, J. G. H., & Hamer, J. E. (1996). MPG1 encodes a fungal hydrophobin involved in surface interactions during infection-related development of Magnaporthe grisea. *The Plant Cell*, *8*(6), 985–999. https://doi.org/10.1105/tpc.8.6.985

Tamaki, H. (2007). Glucose-stimulated cAMP-protein kinase a pathway in yeast Saccharomyces cerevisiae. *Journal of Bioscience and Bioengineering*, *104*(4), 245–250. https://doi.org/10.1263/jbb.104.245

Tamura, N., Oku, M., & Sakai, Y. (2010). Atg8 regulates vacuolar membrane dynamics in a lipidation-independent manner in Pichia pastoris . *Journal of Cell Science*, *123*(23), 4107–4116. https://doi.org/10.1242/jcs.070045

Tanaka, A., Cartwright, G. M., Saikia, S., Kayano, Y., Takemoto, D., Kato, M., Tsuge, T., & Scott, B. (2013). ProA, a transcriptional regulator of fungal fruiting body development, regulates leaf hyphal network development in the Epichloë festucae-Lolium perenne symbiosis. *Molecular Microbiology*, *90*(3), 551–568. https://doi.org/10.1111/mmi.12385

Tang, L., Yu, X., Zhang, L., Zhang, L., Chen, L., Zou, S., Liang, Y., Yu, J., & Dong, H. (2019). Mitochondrial FgEch1 is responsible for conidiation and full virulence in Fusarium graminearum. *Current Genetics*, *66*(2), 361–371. https://doi.org/10.1007/s00294-019-01028-z

Tang, W., Ru, Y., Hong, L., Zhu, Q., Zuo, R., Guo, X., Wang, J., Zhang, H., Zheng, X., Wang, P., & Zhang, Z. (2015). System-wide characterization of bZIP transcription factor proteins involved in infection-related morphogenesis of Magnaporthe oryzae. *Environmental Microbiology*, *17*(4), 1377–1396. https://doi.org/10.1111/1462-2920.12618

Tauchi-Sato, K., Ozeki, S., Houjou, T., Taguchi, R., & Fujimoto, T. (2002). The surface

of lipid droplets is a phospholipid monolayer with a unique fatty acid composition. *Journal of Biological Chemistry*, *277*(46), 44507–44512. https://doi.org/10.1074/jbc.M207712200

Teter, S. A., Eggerton, K. P., Scott, S. V., Kim, J., Fischer, A. M., & Klionsky, D. J. (2001). Degradation of lipid vesicles in the yeast vacuole requires function of Cvt17, a putative lipase. *Journal of Biological Chemistry*, *276*(3), 2083–2087. https://doi.org/10.1074/jbc.C000739200

Thiam, A. R., Farese, R. V., & Walther, T. C. (2013). The biophysics and cell biology of lipid droplets. *Nature Reviews Molecular Cell Biology*, *14*(12), 775–786. https://doi.org/10.1038/nrm3699

Thines, E., Weber, R. W. S., & Talbot, N. J. (2000). MAP kinase and protein kinase A-dependent mobilization of triacylglycerol and glycogen during appressorium turgor generation by Magnaporthe grisea. *Plant Cell*, *12*(9), 1703–1718. https://doi.org/10.1105/tpc.12.9.1703

Thomma, B. P. H. J., Nürnberger, T., & Joosten, M. H. A. J. (2011). Of PAMPs and effectors: The blurred PTI-ETI dichotomy. *Plant Cell*, *23*(1), 4–15. https://doi.org/10.1105/tpc.110.082602

Thorvaldsdóttir, H., Robinson, J. T., & Mesirov, J. P. (2013). Integrative Genomics Viewer (IGV): High-performance genomics data visualization and exploration. *Briefings in Bioinformatics*, *14*(2), 178–192. https://doi.org/10.1093/bib/bbs017

Tian, H., MacKenzie, C. I., Rodriguez-Moreno, L., van den Berg, G. C. M., Chen, H., Rudd, J. J., Mesters, J. R., & Thomma, B. P. H. J. (2021). Three LysM effectors of Zymoseptoria tritici collectively disarm chitin-triggered plant immunity. *Molecular Plant Pathology, 22*(6), 683-693. https://doi.org/10.1111/mpp.13055

Tiley, A. M. M., Foster, G. D., & Bailey, A. M. (2018). Exploring the genetic regulation of asexual sporulation in Zymoseptoria tritici. *Frontiers in Microbiology*, *9*. https://doi.org/10.3389/fmicb.2018.01859

Tiley, A. M. M., White, H. J., Foster, G. D., & Bailey, A. M. (2019). The ZtvelB gene is required for vegetative growth and sporulation in the wheat pathogen Zymoseptoria tritici. *Frontiers in Microbiology*, *10*(October), 2210. https://doi.org/10.3389/FMICB.2019.02210

Till, A., Lakhani, R., Burnett, S. F., & Subramani, S. (2012). Pexophagy: The selective degradation of peroxisomes. *International Journal of Cell Biology*, *2012*. https://doi.org/10.1155/2012/512721

Toda, T., Cameron, S., Sass, P., Zoller, M., & Wigler, M. (1987). Three different genes in S. cerevisiae encode the catalytic subunits of the cAMP-dependent protein kinase. *Cell*, *50*(2), 277–287. https://doi.org/10.1016/0092-8674(87)90223-6

Torggler, R., Papinski, D., & Kraft, C. (2017). Assays to Monitor Autophagy in Saccharomyces cerevisiae. *Cells*, *6*(3), 23. https://doi.org/10.3390/cells6030023

Torriani, S. F. F., Melichar, J. P. E., Mills, C., Pain, N., Sierotzki, H., & Courbot, M. (2015). Zymoseptoria tritici: A major threat to wheat production, integrated approaches to control. *Fungal Genetics and Biology*, *79*, 8–12. https://doi.org/10.1016/j.fgb.2015.04.010

Toyama, E. Q., Herzig, S., Courchet, J., Lewis Jr., T. L., Losón, O. C., Hellberg, K., Young, N. P., Chen, H., Polleux, F., Chan, D. C., & Shaw, R. J. (2016). AMP-activated protein kinase mediates mitochondrial fission in response to energy stress. *Science*, *351*(6270), 275–282. https://doi.org/10.1126/science.aab4138

Turrà, D., & Di Pietro, A. (2015). Chemotropic sensing in fungus-plant interactions.

*Current Opinion in Plant Biology*, *26*, 135–140. https://doi.org/10.1016/j.pbi.2015.07.004

Turrà, D., El Ghalid, M., Rossi, F., & Di Pietro, A. (2015). Fungal pathogen uses sex pheromone receptor for chemotropic sensing of host plant signals. *Nature*, *527*(7579), 521–524. https://doi.org/10.1038/nature15516

Turrà, D., Segorbe, D., & Di Pietro, A. (2014). Protein Kinases in Plant-Pathogenic Fungi: Conserved Regulators of Infection. *Annual Review of Phytopathology*, *52*(1), 267–288. https://doi.org/10.1146/annurev-phyto-102313-050143

Underwood, W. (2012). The plant cell wall: A dynamic barrier against pathogen invasion. *Frontiers in Plant Science*, *3*(MAY), 1–6. https://doi.org/10.3389/fpls.2012.00085

Van De Sande, W. W. J., & Vonk, A. G. (2019). Mycovirus therapy for invasive pulmonary aspergillosis? *Medical Mycology*, *57*, S179–S188. https://doi.org/10.1093/mmy/myy073

van de Wouw, M., Kik, C., Van Hintum, T., Van Treuren, R., & Visser, B. (2009). Genetic erosion in crops: Concept, research results and challenges. *Plant Genetic Resources: Characterisation and Utilisation*, *8*(1), 1–15. https://doi.org/10.1017/S1479262109990062

van den Berg, F., Paveley, N. D., & van den Bosch, F. (2016). Dose and number of applications that maximize fungicide effective life exemplified by Zymoseptoria tritici on wheat – a model analysis. *Plant Pathology*, *65*(8), 1380–1389. https://doi.org/10.1111/ppa.12558

van den Berg, F., van den Bosch, F., & Paveley, N. D. (2013). Optimal fungicide application timings for disease control are also an effective anti-resistance strategy: A case study for zymoseptoria tritici (mycosphaerella graminicola) on wheat. *Phytopathology*, *103*(12), 1209–1219. https://doi.org/10.1094/PHYTO-03-13-0061-R

Van Esse, H. P., Bolton, M. D., Stergiopoulos, I., De Wit, P. J. G. M., & Thomma, B. P. H. J. (2007). The chitin-binding Cladosporium fulvum effector protein Avr4 is a virulence factor. *Molecular Plant-Microbe Interactions*, *20*(9), 1092–1101. https://doi.org/10.1094/MPMI-20-9-1092

Van Kan, J. A. L., Shaw, M. W., & Grant-Downton, R. T. (2014). Botrytis species: Relentless necrotrophic thugs or endophytes gone rogue? *Molecular Plant Pathology*, *15*(9), 957–961. https://doi.org/10.1111/mpp.12148

Van Kan, J. A. L., Stassen, J. H. M., Mosbach, A., Van Der Lee, T. A. J., Faino, L., Farmer, A. D., Papasotiriou, D. G., Zhou, S., Seidl, M. F., Cottam, E., Edel, D., Hahn, M., Schwartz, D. C., Dietrich, R. A., Widdison, S., & Scalliet, G. (2017). A gapless genome sequence of the fungus Botrytis cinerea. *Molecular Plant Pathology*, *18*(1), 75–89. https://doi.org/10.1111/mpp.12384

van Zutphen, T., Todde, V., de Boer, R., Kreim, M., Hofbauer, H. F., Wolinski, H., Veenhuis, M., van der Klei, I. J., & Kohlwein, S. D. (2014). Lipid droplet autophagy in the yeast Saccharomyces cerevisiae. *Molecular Biology of the Cell*, *25*(2), 290–301. https://doi.org/10.1091/mbc.E13-08-0448

VanEtten, H. D., Mansfield, J. W., Bailey, J. A., & Farmer, E. E. (1994). Two Classes of Plant Antibiotics: Phytoalexins versus “Phytoanticipins.” *The Plant Cell*, *6*(9), 1191. https://doi.org/10.2307/3869817

Vaz Patto, M. C., & Niks, R. E. (2001). Leaf wax layer may prevent appressorium differentiation but does not influence orientation of the leaf rust fungus Puccinia hordei on Hordeum chilense leaves. *European Journal of Plant Pathology*, *107*(8),

795–803. https://doi.org/10.1023/A:1012410330287

Veneault-Fourrey, C., Barooah, M., Egan, M., Wakley, G., & Talbot, N. J. (2006). Autophagic Fungal Cell Death Is Necessary for Infection by the Rice Rice Blast Fungus. *Science*, *312*(5773), 580–583.

Veronese, P., Nakagami, H., Bluhm, B., AbuQamar, S., Chen, X., Salmeron, J., Dietrich, R. A., Hirt, H., & Mengiste, T. (2006). The Membrane-Anchored BOTRYTIS-INDUCED KINASE1 Plays Distinct Roles in Arabidopsis Resistance to Necrotrophic and Biotrophic Pathogens. *The Plant Cell*, *18*, 257–273. https://doi.org/10.1105/tpc.105.035576.1

Vienken, K., & Fischer, R. (2006). The Zn(II)2Cys6 putative transcription factor NosA controls fruiting body formation in Aspergillus nidulans. *Molecular Microbiology*, *61*(2), 544–554. https://doi.org/10.1111/j.1365-2958.2006.05257.x

Vlaardingerbroek, I., Beerens, B., Schmidt, S. M., Cornelissen, B. J. C., & Rep, M. (2016). Dispensable chromosomes in Fusarium oxysporum f. sp lycopersici. *Molecular Plant Pathology*, *17*(9), 1455–1466. https://doi.org/10.1111/mpp.12440

Voegele, R. T., & Mendgen, K. (2003). Rust haustoria: Nutrient uptake and beyond. *New Phytologist*, *159*(1), 93–100. https://doi.org/10.1046/j.1469-8137.2003.00761.x

Voegele, R. T., Struck, C., Hahn, M., & Mendgen, K. (2001). The role of haustoria in sugar supply during infection of broad bean by the rust fungus Uromyces fabae. *Proceedings of the National Academy of Sciences of the United States of America*, *98*(14), 8133–8138. https://doi.org/10.1073/pnas.131186798

Voigt, O., & Pöggeler, S. (2013). Autophagy genes Smatg8 and Smatg4 are required for fruiting-body development, vegetative growth and ascospore germination in the filamentous ascomycete Sordaria macrospora. *Autophagy*, *9*(1), 33–49. https://doi.org/10.4161/auto.22398

Wan, J., Zhang, X., Neece, D., Ramonell, K. M., Clough, S., Kim, S., Stacey, M. G., & Stacey, G. (2008). A LysM Receptor-Like Kinase Plays a Critical Role in Chitin Signaling and Fungal Resistance in Arabidopsis. *The Plant Cell*, *20*, 471–481. https://doi.org/10.1105/tpc.107.056754

Wanders, R. J. A., Waterham, H. R., & Ferdinandusse, S. (2016). Metabolic interplay between peroxisomes and other subcellular organelles including mitochondria and the endoplasmic reticulum. *Frontiers in Cell and Developmental Biology*, *3*, 1–15. https://doi.org/10.3389/fcell.2015.00083

Wang, L., & Lin, X. (2012). Morphogenesis in Fungal Pathogenicity: Shape, Size, and Surface. *PLoS Pathogens*, *8*(12), 8–11. https://doi.org/10.1371/journal.ppat.1003027

Wang, Q., Liu, H., Xu, H., Hei, R., Zhang, S., Jiang, C., & Xu, J. R. (2019). Independent losses and duplications of autophagy-related genes in fungal tree of life. *Environmental Microbiology*, *21*(1), 226–243. https://doi.org/10.1111/1462-2920.14451

Wang, Y., Mohsen, A. W., Mihalik, S. J., Goetzman, E. S., & Vockley, J. (2010). Evidence for physical association of mitochondrial fatty acid oxidation and oxidative phosphorylation complexes. *Journal of Biological Chemistry*, *285*(39), 29834–29841. https://doi.org/10.1074/jbc.M110.139493

Wang, Z.-Y., Soanes, D. M., Kershaw, M. J., & Talbot, N. J. (2007). Functional analysis of lipid metabolism in Magnaporthe grisea reveals a requirement for peroxisomal fatty acid b-oxidation during appressorium-mediated plant infection. *Molecular Plant Microbe Interaction*, *20*(5), 475–491. https://doi.org/doi:10.1094/MPMI-20-5-

0475

Wang, Z.-Y., Thornton, C. R., Kershaw, M. J., Debao, L., & Talbot, N. J. (2003). The glyoxylate cycle is required for temporal regulation of virulence by the plant pathogenic fungus Magnaporthe grisea. *Molecular Microbiology*, *47*(6), 1601–1612. https://doi.org/10.1046/j.1365-2958.2003.03412.x

Weber, R. W. S., Wakley, G. E., Thines, E., & Talbot, N. J. (2001). The vacuole as central element of the lytic system and sink for lipid droplets in maturing appressoria of Magnaporthe grisea. *Protoplasma*, *216*(1–2), 101–112. https://doi.org/10.1007/BF02680137

Weiberg, A., Wang, M., Lin, F. M., Zhao, H., Zhang, Z., Kaloshian, I., Huang, H. Da, & Jin, H. (2013). Fungal small RNAs suppress plant immunity by hijacking host RNA interference pathways. *Science*, *342*(6154), 118–123. https://doi.org/10.1126/science.1239705

Westermann, A. J., Barquist, L., & Vogel, J. (2017). Resolving host–pathogen interactions by dual RNA-seq. *PLoS Pathogens*, *13*(2), 1–19. https://doi.org/10.1371/journal.ppat.1006033

Williams, B., Kabbage, M., Kim, H. J., Britt, R., & Dickman, M. B. (2011). Tipping the balance: Sclerotinia sclerotiorum secreted oxalic acid suppresses host defenses by manipulating the host redox environment. *PLoS Pathogens*, *7*(6). https://doi.org/10.1371/journal.ppat.1002107

Wu, C., Yang, F., Smith, K. M., Peterson, M., Dekhang, R., Zhang, Y., Zucker, J., Bredeweg, E. L., Mallappa, C., Zhou, X., Lyubetskaya, A., Townsend, J. P., Galagan, J. E., Freitag, M., Dunlap, J. C., Bell-Pedersen, D., & Sachs, M. S. (2014). Genome-wide characterization of light-regulated genes in Neurospora crassa. *G3: Genes, Genomes, Genetics*, *4*(9), 1731–1745. https://doi.org/10.1534/g3.114.012617

Wynn, W. K. (1976). Appressorium Formation over Stomates by the Bean Rust Fungus: Response to a Surface Contact Stimulus. In *Phytopathology* (Vol. 66, Issue 2, p. 136). https://doi.org/10.1094/phyto-66-136

Xie, Z., & Klionsky, D. J. (2007). Autophagosome formation: Core machinery and adaptations. *Nature Cell Biology*, *9*(10), 1102–1109. https://doi.org/10.1038/ncb1007-1102

Xu, J. R., & Hamer, J. E. (1996). MAP kinase and cAMP signaling regulate infection structure formation and pathogenic growth in the rice blast fungus Magnaporthe grisea. *Genes and Development*, *10*(21), 2696–2706. https://doi.org/10.1101/gad.10.21.2696

Xu, J. R., Staiger, C. J., & Hamer, J. E. (1998). Inactivation of the mitogen-activated protein kinase Mps1 from the rice blast fungus prevents penetration of host cells but allows activation of plant defense responses. *Proceedings of the National Academy of Sciences of the United States of America*, *95*(21), 12713–12718. https://doi.org/10.1073/pnas.95.21.12713

Xu, J. R., Urban, M., Sweigard, J. A., & Hamer, J. E. (1997). The CPKA gene of Magnaporthe grisea is essential for appressorial penetration. *Molecular Plant-Microbe Interactions*, *10*(2), 187–194. https://doi.org/10.1094/MPMI.1997.10.2.187

Xu, L., & Chen, W. (2013). Random T-DNA mutagenesis identifies a Cu/Zn superoxide dismutase gene as a virulence factor of Sclerotinia sclerotiorum. *Molecular Plant-Microbe Interactions*, *26*(4), 431–441. https://doi.org/10.1094/MPMI-07-12-0177-R

Yamauchi, J., Takayanagi, N., Komeda, K., Takano, Y., & Okuno, T. (2004). cAMP-PKA signaling regulates multiple steps of fungal infection cooperatively with Cmk1

MAP kinase in Colletotrichum lagenarium. *Molecular Plant-Microbe Interactions*, *17*(12), 1355–1365. https://doi.org/10.1094/MPMI.2004.17.12.1355

Yamazaki, H., Tanaka, A., Kaneko, J. ichi, Ohta, A., & Horiuchi, H. (2008). Aspergillus nidulans ChiA is a glycosylphosphatidylinositol (GPI)-anchored chitinase specifically localized at polarized growth sites. *Fungal Genetics and Biology*, *45*(6), 963–972. https://doi.org/10.1016/j.fgb.2008.02.008

Yanagisawa, S., Kikuma, T., & Kitamoto, K. (2013). Functional analysis of Aoatg1 and detection of the Cvt pathway in Aspergillus oryzae. *FEMS Microbiology Letters*, *338*(2), 168–176. https://doi.org/10.1111/1574-6968.12047

Yang, F., Li, W., & Jørgensen, H. J. L. (2013). Transcriptional reprogramming of wheat and the hemibiotrophic pathogen Septoria tritici during two phases of the compatible interaction. *PLoS ONE*, *8*(11), 1–15. https://doi.org/10.1371/journal.pone.0081606

Yang, N., McDonald, M. C., Solomon, P. S., & Milgate, A. W. (2018). Genetic mapping of Stb19, a new resistance gene to Zymoseptoria tritici in wheat. *Theoretical and Applied Genetics*, *131*(12), 2765–2773. https://doi.org/10.1007/s00122-018-3189-0

Yang, Z., & Dickman, M. B. (1999). Colletotrichum trifolii mutants disrupted in the catalytic subunit of cAMP-dependent protein kinase are nonpathogenic. *Molecular Plant-Microbe Interactions*, *12*(5), 430–439. https://doi.org/10.1094/MPMI.1999.12.5.430

Yates, S., Mikaberidze, A., Krattinger, S. G., Abrouk, M., Hund, A., Yu, K., Studer, B., Fouche, S., Meile, L., Pereira, D., Karisto, P., & McDonald, B. A. (2019). Precision Phenotyping Reveals Novel Loci for Quantitative Resistance to Septoria Tritici Blotch. *Plant Phenomics*, *2019*, 1–11. https://doi.org/10.34133/2019/3285904

Yemelin, A., Brauchler, A., Jacob, S., Laufer, J., Heck, L., Foster, A. J., Antelo, L., Andresen, K., & Thines, E. (2017). Identification of factors involved in dimorphism and pathogenicity of Zymoseptoria tritici. In *PLoS ONE* (Vol. 12, Issue 8). https://doi.org/10.1371/journal.pone.0183065

Yesbolatova, A., Saito, Y., Kitamoto, N., Makino-Itou, H., Ajima, R., Nakano, R., Nakaoka, H., Fukui, K., Gamo, K., Tominari, Y., Takeuchi, H., Saga, Y., Hayashi, K. ichiro, & Kanemaki, M. T. (2020). The auxin-inducible degron 2 technology provides sharp degradation control in yeast, mammalian cells, and mice. *Nature Communications*, *11*(1). https://doi.org/10.1038/s41467-020-19532-z

Ying, S. H., Liu, J., Chu, X. L., Xie, X. Q., & Feng, M. G. (2016). The autophagy-related genes BbATG1 and BbATG8 have different functions in differentiation, stress resistance and virulence of mycopathogen Beauveria bassiana. *Scientific Reports*, *6*(January), 1–12. https://doi.org/10.1038/srep26376

Yu, J., Park, J. Y., Heo, J. I., & Kim, K. H. (2020). The ORF2 protein of Fusarium graminearum virus 1 suppresses the transcription of FgDICER2 and FgAGO1 to limit host antiviral defences. *Molecular Plant Pathology*, *21*(2), 230–243. https://doi.org/10.1111/mpp.12895

Zaman, S., Lippman, S. I., Zhao, X., & Broach, J. R. (2008). How Saccharomyces responds to nutrients. *Annual Review of Genetics*, *42*, 27–81. https://doi.org/10.1146/annurev.genet.41.110306.130206

Zeller, C. E., Parnell, S. C., & Dohlman, H. G. (2007). The RACK1 ortholog Asc1 functions as a G-protein β subunit coupled to glucose responsiveness in yeast. *Journal of Biological Chemistry*, *282*(34), 25168–25176. https://doi.org/10.1074/jbc.M702569200

Zhan, H., Yue, H., Zhao, X., Wang, M., Song, W., & Nie, X. (2017). Genome-Wide Identification and Analysis of MAPK and MAPKK Gene Families in Bread Wheat (Triticum aestivum L.). *Genes*, *8*, 284. https://doi.org/10.3390/genes8100284

Zhan, J., Pettway, R. E., & McDonald, B. A. (2003). The global genetic structure of the wheat pathogen Mycosphaerella graminicola is characterized by high nuclear diversity, low mitochondrial diversity, regular recombination, and gene flow. *Fungal Genetics and Biology*, *38*(3), 286–297. https://doi.org/10.1016/S1087-1845(02)00538-8

Zhang, L., Kars, I., Essenstam, B., Liebrand, T. W. H., Wagemakers, L., Elberse, J., Tagkalaki, P., Tjoitang, D., van den Ackerveken, G., & van Kan, J. A. L. (2014). Fungal endopolygalacturonases are recognized as microbe-associated molecular patterns by the arabidopsis receptor-like protein RESPONSIVENESS TO BOTRYTIS POLYGALACTURONASES. *Plant Physiology*, *164*(1), 352–364. https://doi.org/10.1104/pp.113.230698

Zhang, W., Fraiture, M., Kolb, D., Löffelhardt, B., Desaki, Y., Boutrot, F. F. G., Tör, M., Zipfel, C., Gust, A. A., & Brunner, F. (2013). Arabidopsis RECEPTOR-LIKE PROTEIN30 and Receptor-Like Kinase SUPPRESSOR OF BIR1-1 / EVERSHED Mediate Innate Immunity to Necrotrophic Fungi. *The Plant Cell*, *25*, 4227–4241. https://doi.org/10.1105/tpc.113.117010

Zhang, Y., Qi, H., Taylor, R., Xu, W., Liu, L. F., & Jin, S. (2007). The role of autophagy in mitochondria maintenance: Characterization of mitochondrial functions in autophagy-deficient S. cerevisiae strains. *Autophagy*, *3*(4), 337–346. https://doi.org/10.4161/auto.4127

Zhao, Z., Liu, H., Wang, C., & Xu, J. J.-R. (2013). Comparative analysis of fungal genomes reveals different plant cell wall degrading capacity in fungi. *BMC Genomics*, *14*(1), 274. https://doi.org/10.1186/1471-2164-14-274

Zhong, J., Chen, D., Zhu, H. J., Gao, B. D., & Zhou, Q. (2016). Hypovirulence of Sclerotium rolfsii caused by associated RNA mycovirus. *Frontiers in Microbiology*, *7*, 1–18. https://doi.org/10.3389/fmicb.2016.01798

Zhong, Z., Marcel, T. C., Hartmann, F. E., Ma, X., Plissonneau, C., Zala, M., Ducasse, A., Confais, J., Compain, J., Lapalu, N., Amselem, J., McDonald, B. A., Croll, D., & Palma-Guerrero, J. (2017). A small secreted protein in Zymoseptoria tritici is responsible for avirulence on wheat cultivars carrying the Stb6 resistance gene. *New Phytologist*, *214*(2), 619–631. https://doi.org/10.1111/nph.14434

Zhou, X., & Ballou, E. R. (2018). The Cryptococcus neoformans Titan Cell: From In Vivo Phenomenon to In Vitro Model. *Current Clinical Microbiology Reports*, *5*(4), 252–260. https://doi.org/10.1007/s40588-018-0107-9

Zhu, W., Wei, W., Fu, Y., Cheng, J., Xie, J., Li, G., Yi, X., Kang, Z., Dickman, M. B., & Jiang, D. (2013). A Secretory Protein of Necrotrophic Fungus Sclerotinia sclerotiorum That Suppresses Host Resistance. *PLoS ONE*, *8*(1). https://doi.org/10.1371/journal.pone.0053901

Zhu, W., Zhou, M., Xiong, Z., Peng, F., & Wei, W. (2017). The cAMP-PKA signaling pathway regulates pathogenicity, hyphal growth, appressorial formation, conidiation, and stress tolerance in Colletotrichum higginsianum. *Frontiers in Microbiology*, *8*, 1416. https://doi.org/10.3389/fmicb.2017.01416

Zientara-Rytter, K., & Subramani, S. (2020). Mechanistic Insights into the Role of Atg11 in Selective Autophagy. *Journal of Molecular Biology*, *432*(1), 104–122. https://doi.org/10.1016/j.jmb.2019.06.017

Ziv, C., Zhao, Z., Gao, Y. G., & Xia, Y. (2018). Multifunctional roles of plant cuticle

during plant-pathogen interactions. *Frontiers in Plant Science*, *9*(July), 1–8. https://doi.org/10.3389/fpls.2018.01088

Zwiers, L. H., & De Waard, M. A. (2001). Efficient Agrobacterium tumefaciens-mediated gene disruption in the phytopathogen Mycosphaerella graminicola. *Current Genetics*, *39*(5–6), 388–393. https://doi.org/10.1007/s002940100216